UNIVERSITY OF IOANNINA
SCHOOL OF SCIENCES
DEPARTMENT OF PHYSICS
DIVISION OF THEORETICAL PHYSICS

Effective Theory Models from String Theory: Implications in Particle Physics and Cosmology

Vasileios Basiouris

PHD Thesis

IOANNINA 2025

Πανεπιστήμιο Ιωαννίνων
Σχολή Θετικών Επιστημών
Τμήμα Φυσικής
Τομέας Θεωρητικής Φυσικής

Πρότυπα Ενεργών Θεωριών από τη Θεωρία Υπερχορδών: επιπτώσεις στη Σωματιδιακή Φυσική και Κοσμολογία

Βασίλειος Μπασιούρης

Διδακτορική Διατριβή

Ιωάννινα 2025

Three-member advisory committee:

- George Leontaris – Emeritus Professor, Physics Department, University of Ioannina, Ioannina, Greece.
- Panagiota Kanti – Professor, Physics Department, University of Ioannina, Ioannina, Greece.
- Leandros Perivolaropoulos – Professor, Physics Department, University of Ioannina, Ioannina, Greece.

Seven-member PhD examination committee:

- George Leontaris (Supervisor) – Emeritus Professor, Physics Department, University of Ioannina, Greece.
- Panagiota Kanti – Professor, Physics Department, University of Ioannina, Greece.
- Leandros Perivolaropoulos – Professor, Physics Department, University of Ioannina, Greece.
- Ignatios Antoniadis, Professor, Directeur de recherche, Laboratory of Theoretical Physics and High Energies LPTHE, Sorbonne University, France
- Kyriakos Tamvakis – Emeritus Professor, Physics Department, University of Ioannina, Greece.
- Athanasios Dedes – Professor, Physics Department, University of Ioannina, Greece.
- Ioannis Florakis - Assistant Professor, Physics Department, University of Ioannina, Greece.

Acknowledgments

First of all, I would like to express my deep gratitude to my supervisor, Emeritus Professor George Leontaris, for his continuous academic and moral support, as well as the guidance and motivation he has provided me throughout these years of my graduate studies.

I am especially grateful to Emeritus Professor Kyriakos Tamvakis and Professor Panagiota Kanti for their support throughout my studies and for supporting my applications for postdoctoral positions with recommendation letters. It is also important to mention my collaborators in the last project of my PhD. Professor Stephen F. King and Dr. Miguel Crispim Romão gave me a new perspective on how to approach a research problem through many online meetings and discussions, and for that I am deeply grateful.

A special mention goes to all the faculty members of the Theoretical Physics section of the Physics Department, who gave me an opportunity to learn about the fascinating world of particle physics and cosmology–ideas I never imagined I would encounter. My sincere gratitude to all of them.

List of Publications

The current Ph.D. dissertation is mainly based on the following articles which are listed below:

1. V. Basiouris, "**A string loop origin for dark radiation and superheavy dark matter in type IIB compactifications**", [arXiv: 2411.18737 [hep-th]].

2. V. Basiouris, M. Crispim Romão, S. F. King and G. K. Leontaris, "**Modular Family Symmetry in fluxed GUTs**", Phys. Rev. D **111** (2025) no.1, 015012, [arXiv:2407.06618 [hep-ph]].

3. V. Basiouris and G. K. Leontaris, "**Sterile neutrinos, $0\nu\beta\beta$ decay and the W-boson mass anomaly in a flipped SU(5) from F-theory**", Eur. Phys. J. C **82** (2022) no.11, 1041 [arXiv:2205.00758 [hep-ph]].

4. V. Basiouris and G. K. Leontaris, "**Remarks on the Effects of Quantum Corrections on Moduli Stabilization and de Sitter Vacua in Type IIB String Theory**", Fortsch. Phys. **70** (2022) no.2-3, 2100181, [arXiv:2109.08421 [hep-th]].

5. V. Basiouris and G. K. Leontaris, "**Note on de Sitter vacua from perturbative and non-perturbative dynamics in type IIB/F-theory compactifications**", Phys. Lett. B **810** (2020), 135809, [arXiv:2007.15423 [hep-th]].

I also worked in parallel on the following article:

1. V. Basiouris and D. Chakraborty, **"Three-Field String Inflation with Perturbative Corrections: Dynamics and Implications,"** [arXiv:2502.06958 [hep-th]].

Abstract

This thesis aims to provide a better understanding of the moduli stabilization mechanisms in string theory and the phenomenological consequences of Grand Unified Theories (GUTs) in the framework of F-theory. In the first section, a review of the Standard Model is provided along with the open problems in high energy physics and cosmology. Moreover, the most promising solutions for the Kähler moduli stabilization problem are analyzed, along with the basic geometric tools for constructing local F-theory GUTs. In the next chapter, the analysis of perturbative moduli stabilization with D_7 is presented, where the logarithmic string loop corrections are added to the Kähler potential complementing the contributions of non-perturbative corrections to the superpotential. We show that de Sitter (dS) vacua are accessible to the low-energy effective theory due to the uplifting effects of the D-terms, emerging from the magnetic fluxes in the D_7 branes context. In addition, more complex geometric compactifications are discussed exhibiting the universal effect of the loop corrections to the search for dS vacua beyond the simple toroidal-like volumes. Apart from the stabilization conditions, a model of dark radiation and dark matter is suggested, where the moduli decay into closed string axions, comprising the dark radiation of the universe. Additionally, moduli decays to the dark sector degrees of freedom could in principle produce the correct dark matter abundance. From the F-theory perspective, two different GUTs are presented. In the first attempt, a flipped $SU(5)$ is constructed in the spectral cover approach, where right handed and sterile neutrinos are augmented to explain the tiny mass of the left handed partners. Furthermore, phenomenological issues like proton decay, $0\nu\beta\beta$ decay and $g_\mu - 2$ are explained, in light of the new symmetry breaking scales introduced in the model. Finally, an F-theory $SU(5)$ model is examined, pointing towards the emergence of a flavor family symmetry from internal fluxes. The complex structure moduli of the geometry's tori are laid stabilized to specific non-linear paths due to G_3 fluxes, resulting in the breaking of the $SL(2,Z)$ symmetry down to a congruence subgroup Γ_N. Based on the above, an $SU(5) \times S_4$ is utilized to explain the Yukawa matrices in both the quark and the neutrino sector, where the whole setup is parametrized by the values of the moduli. In the last chapter, a conclusion is outlined sketching the prospects for future expansions.

Περίληψη στα Ελληνικά

Η σύγχρονη εποχή της Φυσικής Υψηλών Ενεργειών βασίζεται στις ανακαλύψεις του Καθιερωμένου Προτύπου Θεμελιωδών Αλληλεπιδράσεων (ΚΠ) και της Γενικής Θεωρίας της Σχετικότητας κατά τον περασμένο αιώνα. Παρά τις πολλαπλές προσπάθειες ερευνητών δεν έχει επιτευχθεί η πλήρης ενοποίηση των θεμελιωδών δυνάμεων της φύσης, καθώς το ΚΠ περιγράφει τις πυρηνικές δυνάμεις (ισχυρή και ασθενής πυρηνική) και την ηλεκτρομαγνητική δύναμη, αγνοώντας τη βαρύτητα. Το ΚΠ βασίζεται στην κβαντική θεωρία πεδίου για να περιγράψει τις συμμετρίες βαθμίδας $SU(3) \times SU(2)_L \times U(1)$, οι οποίες χαρακτηρίζουν όλες τις αλληλεπιδράσεις των υποατομικών σωματιδίων σε πειραματικά επαληθευμένο επίπεδο. Η πρόσφατη ανακάλυψη του μποζονίου *Higgs* από τον μεγάλο επιταχυντή αδρονίων (*LHC*) στο Ευρωπαϊκό Πυρηνικό Κέντρο Ερευνών (*CERN*) ολοκλήρωσε εν πολλοίς το ΚΠ, όμως διάφορα ερωτήματα παραμένουν αναπάντητα εντός του πλαισίου του. Αναφέροντας ενδεικτικά μερικά από αυτά: α) την κβάντωση του φορτίου και την ενοποίηση των ζεύξεων βαθμίδας β) η προέλευση της μάζας των νετρίνων γ) η παρατηρούμενη ιεραρχία στις μάζες των σωματιδίων ε) η ένταξη της βαρύτητας σε κβαντικό επίπεδο. Παράλληλα με τις εξελίξεις στην σωματιδιακή φυσική, κοσμολογικές έρευνες υποδεικνύουν την διάρθρωση στην δομή της μάζας του σύμπαντος, από την οποία το 85% δεν ακτινοβολεί. Η φύση της σκοτεινής ύλης παραμένει άγνωστη και πιστεύεται πως αποτελείται από σωματίδια που εδρεύουν σε σκοτεινούς τομείς της γεωμετρίας του σύμπαντος, αλληλεπιδρώντας αμιδρώς με τα σωματίδια του ΚΠ.

Καταδεικνύεται, λοιπόν, ως επιτακτική ανάγκη η προέκταση του ΚΠ σε μία περισσότερο ολοκληρωμένη θεωρία για την ορθότερη περιγραφή των σωματιδίων σε όλες τις ενεργειακές βαθμίδες. Οι θεωρίες πέραν του ΚΠ ονομάζονται Μεγαλοενοποιημένες Θεωρίες Βαθμίδας ($Grand\ Unified\ Theories,\ GUTs$), οι οποίες περιγράφονται από μεγαλύτερης συμμετρίας αλγεβρικές ομάδες που έχουν ώς υποομάδες το ΚΠ. Ενιδεικτικά κάποιες από τις ομάδες αυτές είναι $SU(5), SO(10)$ καθώς επίσης και οι ειδικές ομάδες E_6, E_7, E_8. Χαρακτηριστικότερο παράδειγμα πρόβλεψης αυτών των θεωριών αποτελεί το Ελάχιστο Υπερσυμμετρικό Μοντέλο, που με την εισαγωγή της Υπερσυμμετρίας, καταφέρει να επιτύχει την σύζευξη των ζεύξεων σε κλίμακα $\sim 10^{16}\ GeV$. Ακόμη, η ύπαρξη μεγαλύτερης διάστασης αναπαραστάσεων στις *GUTs* μπορούν να εξηγήσουν την προέλευση της μάζας των νετρίνων, μέσω της εισαγωγής νέων σωματιδίων και πρωτότυπων μηχανισμών. Παρόλα αυτά, τα προβλήματα στην προέλευση της ιεραρχίας των μαζών, καθώς και η ελλειπής περιγραφή των αλληπιδράσεων σε αρκετά υψηλές ενέργειες οδήγησε στην μελέτη της Θεωρίας των Υπερχορδών. Η συγκεκριμένη θεωρία επιτυγχάνει σε μαθηματικό επίπεδο να εντάξει και την βαρύτητα σε κβαντικό επίπεδο σε ενεργειακές κλίμακες, όμως, πολύ υψηλότερες από των προαναφερθέντων θεωρίων $M_{Planck} \cong 2.4 \times 10^{18}\ GeV$. Βαρύνουσας σημασίας στην θεμελίωσης της θεωρίας υπερχορδών παίζουν εκτεταμένα αντικείμενα, οι μεμβράνες *D-branes*, οι οποίες εκτείνονται πέραν των τριών χωρικών διαστάσεων. Η ύπαρξη περισσοτέρων χωρικών διαστάσεων στο σύμπαν αποτελεί εφαλτήριο για την πρόταση καινοτόμων λύσεων, αλλά προϋποθέτει τις κατάλληλες συνθήκες συμπαγοποίησης (*compactification*) της θεωρίας. Η θεωρία χορδών διαχωρίζεται σε πέντε διαφορετικές θεωρίες: η τύπου I, οι θεωρίες τύπου II (IIA και IIB) και οι ετεροτικές χορδές ($SO(32), E_8 \times E_8$).

Η παρούσα διατριβή εστιάζει στις θεωρίες τύπου IIB και στην μη-διαταρακτική ολοκλήρωση αυτής την *F*-θεωρία. Όσον αφορά την πρώτη, η παρούσα μελέτη ασχολείται με τις συνθήκες σταθερότητας του συμπαγοποιημένου χώρου. Πιο συγκεκριμένα, η γεωμετρία του χώρου καθορίζεται από τις τιμές ορισμένων βαθμωτών πεδίων, των *moduli*, τα οποία χωρίζονται σε δυο κατηγορίες: τα *Kähler* και τα μιγαδικής δομής. Επικεντρώνοντας την προσοχή μας στην κατηγορία των *Kähler*, μελετήθηκε η συνεισφορά των κβαντικών διαταρακτικών διορθώσεων στο δυναμικό *Kähler*. Η μορφή αυτών των διορθώσεων είναι λογαριθμικής μορφής και η προέλευση τους οφείλεται σε σκεδάσεις βαρυτονίων μεταξύ των μεμβρανών και εντοπισμένων κορυφών της τετραδιάστατης δράσης *Einstein-Hilbert* στον κάθετο χώρο των μεμβρανών. Ακόμη, η συνέργεια μεταξύ των προαναφερθέντων κβαντικών διορθώσεων και των μη διαταρακτικών διορθώσεων στο υπερδυναμικό οδήγησε σε ένα βαθμωτό δυναμικό με *Anti de-Sitter*(*AdS*) ελάχιστο. Όμως, η παρατήρηση του συνεχώς επιταχυνόμενου σύμπαντος ευνοεί τις *de-Sitter*(*dS*) λύσεις με θετική κοσμολογική σταθερά, γεγονός που οδηγεί στην εισαγωγή των *D*-όρων που προσέφερουν την ανύψωση του δυναμικού στους θεμιτούς χώρους. Επιπρόσθετα, μέσω αυτής της μελέτης ερευνώνται οι επιτρεπόμενες τιμές και τα όρια που πρέπει να ικανοποιούν οι ελεύθερες παράμετροι της θεωρίας στην περίπτωση όπου ο συμπαγοποιημένος χώρος είναι τοροειδούς μορφής, αλλά και σε πιο γενεικευμένες γεωμετρίες υποβάθρου. Σε ένα δεύτερο βαθμό, εξετάζεται η προέλευση της σκοτεινής ακτινοβολίας και της σκοτεινής ύλης υπό το πρίσμα των νέων λογαριθμικών διορθώσεων. Ειδικότερα, μελετήθηκαν οι μεταπτώσεις των *moduli* σε αξιονικούς βαθμούς ελευθερίας, που εμπεριέχονται στην τύπου IIB θεωρία, ώστε αυτοί να αποτελέσουν την σωματιδιακή φύση της σκοτεινής ακτινοβολίας. Παράλληλα, οι επιπτώσεις αυτών των σωματιδιών περιορίζονται από κοσμολογικά όρια, όπως ο αριθμός των γενιών στα νετρίνα και οι μάζες των βαθμωτών *moduli*. Όσον αφορά την σκοτεινή ύλη, οι μεταπτώσεις των *moduli* σε σωματίδια των σκοτεινών τομέων, που δεν αλληλεπιδρούν με τα σωματίδια του ΚΠ, οδήγησε στην μελέτη των μεθόδων παραγωγής τους καθώς και της εναπομείνουσας ποσότητας τους στο σύμπαν. Οι δύο κυριότεροι μηχανισμοί παραγωγής αποδεικνύεται πως σχετίζονται με δύο διαφορετικές κλιμακές ενέργειας για την θερμοκρασία επαναθέρμανσης του σύμπαντος, καταλήγοντας να υπάρχει η πιθανότητα για ύπαρξη σωμάτων σκοτεινής ύλης με μάζα από μερικά GeV μέχρι και 10^{11} GeV.

Στο δεύτερο μέρος, η διατριβή εστιάζει στην F-θεωρία και στην κατασκευή $GUTs$ με σκοπό την επεξήγηση φαινομενολογικών ζητημάτων. Κατά πρώτον μελετήθηκε το μοντέλο $flipped\ SU(5)$ στο πλαίσιο του *spectral cover*, που γεωμετρικά σχετίζει τις ιδιότητες της ύλης με τοπολογικές ιδιότητες και την προέλευση της συμμετρίας βαθμίδος με τις ρίζες της εξίσωσης του. Στο συγκεκριμένο μοντέλο εξετάσθηκε το μοντέλο *seesaw* για την αναζήτηση μάζας των νετρίνων, καθώς επίσης καθορίστηκε το ενδιάμεσο σπάσιμο της συμμετρίας για την αποφυγή παρατήρησης διάσπασης πρωτονίου. Ακόμη, μέσω των νέων διανυσματικού τύπου σωματιδίων προτείνεται μία λύση για το πρόβλημα του $g_\mu - 2$, ενώ η πρόσφατη διαφορά στην μάζα του μποζονίου W μπορεί να εξηγηθεί λόγω παραβιάσεων της μοναδικότητας στον λεπτονικό τομέα. Αναφορικά με την εργασία στο τελευταίο κεφάλαιο της διατριβής, αυτή εξετάζει την *modular* συμμετρία και τις συνέπειες της στην μελέτη του προβλήματος της γεύσης των σωματιδίων. Η προέλευσης αυτής της διακριτής συμμετρίας εντοπίζεται στην γεωμετρία, όπου η συμπαγοποίηση γίνεται σε τόρους. Αυτοί χαρακτηρίζονται από την $SL(2,Z)$ συμμετρία, συνεπώς η εισαγωγή εσωτερικών ροών προκαλεί το σπάσιμο της συμμετρίας οθώντας τα μιγαδικής δομής *moduli* σε συγκεριμένες διαδρομές. Οι υποομάδες που παράγονται από το προανεφερθέν σπάσιμο ορίζουν πίνακες Γ_N διάστασης 2×2 με ακέραια στοιχεία και βαθμό N. Ο βαθμός N εμπλέκεται στον υπολογισμό του σπασίματος συμμετρίας και καθορίζεται από τις ακέραιες ροές οδηγώντας σε πιθανές συμμετρίες γεύσης όπως η S_4 για $N = 4$. Με βάση τα παραπάνω, η τελική συμμετρία του F-θεωρητικού μοντέλου είναι η $SU(5) \times S_4$, όπου μελετήθηκε η δομή των $Yukawa$ πινάκων που στην συγκεριμένη εικόνα αποτελούν *modular* σχήματα. Το πλεονέκτημα της πρόσεγγισης αυτής έγκειται στο γεγονός πως η ιεραρχία μαζών (κουαρκς και νετρίνων) και οι γωνίες μίξης επέρχονται φυσιολογικά, μιας και τα διαφορετικά *modular* βάρη των πεδίων μπορούν να δομήσουν ευνοϊκότερα τις ζεύξεις του μοντέλου. Ακόμη, τα συγκεκριμένα *modular* σχήματα καθορίζονται πλήρως από τις τιμές των γεωμετρικών *moduli* γεγονός που είναι επιθυμητό για μια θεωρία που εξάγει από πρώτες αρχές τις προβλέψεις.

Contents

List of Figures

List of Tables

1 Theories beyond the Standard Model

1.1 Overview of the Standard model

The Standard Model of particle physics describes the fundamental interactions (excluding gravity) of particle physics as a quantum field theory [7; 8; 9; 10; 11]. This theory formulates the aforementioned interactions under gauge symmetries, where the forces are mediated by the corresponding gauge bosons. All of nature's particle content can be separated into two categories: the fermions and the bosons. Fermions have half integer spin and bosons have integer spin. The fermionic sector of the theory forms the matter, while bosons operate as force mediators. The fundamental forces, which are contained in this framework, are the electromagnetic force, the electroweak force and the strong force. All the ingredients above are based on the SM gauge group:

$$G_{SM} = SU(3)_C \times SU(2)_L \times U(1)_Y \ . \tag{1.1.1}$$

The first part $SU(3)_C$ is associated with the strong nuclear force, providing an explanation of the forces between the quarks inside the nucleus. The quarks consist the fundamental matter components, while the force mediators are labeled as gluons. These quarks come in three generations due to their assigned quantum number and are confined inside the hadrons (composed of three quarks) and mesons (composed of quark and anti-quark). The remaining part of the SM gauge group $SU(2)_L \times U(1)_Y$ refers to the unified electro-weak sector of the theory. Apart form the quarks, matter also contains some fermionic degrees of freedom called leptons. This category contains three families with the electron being the lightest (e, μ, τ), and their corresponding neutrinos $(\nu_e, \nu_\mu, \nu_\tau)$. The $SU(2)_L$ group refers to the weak isospin, acting on the left handed fermions, while the $U(1)_Y$ is the hypercharge group. Quarks (u, d, c, s, t, b) transform as a triplet under the color group $SU(3)_C$ and as doublet under the $SU(2)_L$. Leptons are neutral under the $SU(3)_C$ and are embedded in a doublet under the $SU(2)_L$. Regarding the gauge bosons of the $SU(2)_L \times U(1)_Y$, there are four different degrees of freedom: the three electroweak bosons ($W^{\pm}, Z$) and the photon γ.

The missing part of all the above is the Higgs mechanism that provides mass to the particles through the Yukawa couplings. Its discovery by the LHC experiment in CERN [12; 13] has almost completed the puzzle of the SM. The vital contribution of the Higgs mechanism is to explain the spontaneously broken symmetry of $SU(2)_L \times U(1)_Y$ down to the electromagnetic $U(1)_{EM}$ around the scale of $\sim$ 100 GeV. In Table 1., all matter content is shown collectively with respect to the transformation properties under the SM gauge group.

Name	Fields	$SU(3)_C \times SU(2)_L \times U(1)_Y$
Gauge bosons	G	$(8,1)_0$
	W	$(1,3)_0$
	B	$(1,1)_0$
Quarks	$\begin{pmatrix} u \\ d \end{pmatrix}_L, \begin{pmatrix} c \\ s \end{pmatrix}_L, \begin{pmatrix} t \\ b \end{pmatrix}_L$	$(3,2)_{\frac{1}{6}}$
	$\bar{u}_R^{\dagger}, \ \bar{c}_R^{\dagger}, \ \bar{t}_R^{\dagger}$	$(\bar{3},1)_{-\frac{2}{3}}$
	$\bar{d}_R^{\dagger}, \ \bar{s}_R^{\dagger}, \ \bar{b}_R^{\dagger}$	$(\bar{3},1)_{\frac{1}{3}}$
Leptons	$\begin{pmatrix} \nu_e \\ e \end{pmatrix}_L, \begin{pmatrix} \nu_\mu \\ \mu \end{pmatrix}_L, \begin{pmatrix} \nu_\tau \\ \tau \end{pmatrix}_L$	$(1,2)_{-\frac{1}{2}}$
	$e_R^{\dagger}, \ \mu_R^{\dagger}, \ \tau_R^{\dagger}$	$(1,1)_1$
Higgs	H	$(1,2)_{\frac{1}{2}}$

Table 1.1: Transformation properties of the elementary particles of the Standard Model.

The Standard model's Lagrangian could be separated as below:

$$\mathcal{L} = \mathcal{L}_G + \mathcal{L}_F + \mathcal{L}_H + \mathcal{L}_Y, \tag{1.1.2}$$

where the above terms stand for: $\mathcal{L}_G$ for the gauge sector, $\mathcal{L}_G$ for the fermions sector, $\mathcal{L}_G$ for the Higgs sector and $\mathcal{L}_Y$ for the Yukawa sector. We will describe in detail the terms of each sector and provide the explanation of the Higgs mechanism. Starting with the gauge sector, the relevant Lagrangian terms can be expanded to be:

$$\mathcal{L}_G = -\frac{1}{4}G^A_{\mu\nu}G^{A\mu\nu} - \frac{1}{4}W^I_{\mu\nu}W^{I\mu\nu} - \frac{1}{4}B_{\mu\nu}B^{\mu\nu}, \tag{1.1.3}$$

where the above field tensors of the SM gauge fields are defined as:

$$SU(3)_C: \quad G^A_{\mu\nu} = \partial_\mu G^A_\nu - \partial_\nu G^A_\mu + g_3 f^{ABC} G^{B,\mu} G^{C,\nu}, \tag{1.1.4}$$

$$SU(2)_L: \quad W^I_{\mu\nu} = \partial_\mu W^A_\nu - \partial_\nu W^A_\mu + g_e \epsilon^{ABC} W^{B,\mu} W^{C,\nu}, \tag{1.1.5}$$

$$U(1)_Y: \quad B_{\mu\nu} = \partial_\mu B_\nu - \partial_\nu B_\mu \,. \tag{1.1.6}$$

In these definitions, we have used the gauge coupling constants g_3, g_2 of the $SU(3)_C, SU(2)_L$ correspondingly. In addition, the structure constants f^{ABC}, ϵ^{ABC} have derived through the commutation relations of the group generators

$$SU(3)_C: \quad [T^a, T^b] = i f^{abc} T^c, \tag{1.1.7}$$

$$SU(2)_L: \quad [r^a, r^b] = i \epsilon^{abc} r^c, \tag{1.1.8}$$

where the T matrices are related to the Gell-Matrices $T^i = \lambda^i/2$ and the r are associated to Pauli matrices $r^i = \sigma^i/2$. As for the fermionic sector, we need to introduce the covariant derivative:

$$D_\mu = \partial_\mu + i g_1 Y B_\mu + i g_2 W_\mu S^I + i g_3 G^A_\mu T^A, \tag{1.1.9}$$

where the S, T are the fundamental representation's generators of the $SU(2), SU(3)$, while Y is the hypercharge generator of each field. The electric charge q of the theory is given by the $q = T^3 + Y$, where the T^3 is the third generator of the weak isospin. Furthermore, we need to introduce the fields definition as:

$$Q_{iL} = \begin{pmatrix} u_{iL} \\ d_{iL} \end{pmatrix}, \quad L_{iL} = \begin{pmatrix} \nu_{iL} \\ e_{iL} \end{pmatrix}, \quad \bar{u}_{iR}, \quad \bar{d}_{iR}, \quad e_{iR} \,. \tag{1.1.10}$$

$$\mathcal{L}_F = i(\bar{L}\not{D}L + \bar{e}_R\not{D}e_R + \bar{Q}\not{D}Q + \bar{u}_R\not{D}u_R + \bar{d}_R\not{D}d_R) \ . \tag{1.1.11}$$

The most interesting part of the SM's Lagrangian is related to the Higgs field. During the formulation of the theory, the research community had no definite answer on how to include mass terms to the Lagrangian. The problem was that SM treated the fields as massless particles, before the introduction of the notion of Spontaneous Symmetry Breaking of gauge symmetries. The mechanism states that a gauge symmetry could be spontaneously broken if the Lagrangian respects the symmetry, but the vacuum state is not invariant under the relevant transformations. The Higgs sector of the Lagrangian is written as:

$$\mathcal{L}_H = (D_\mu H)^\dagger (D^\mu H) - \mu^2 H^\dagger H - \lambda (H^\dagger H)^2 \ . \tag{1.1.12}$$

The above potential is invariant under the $SU(2)_L \times U(1)_Y$, although the vacuum state is not. The signs of the parameters μ, λ will determine the structure of the vacua. It is proved that for $\mu^2 < 0$ and $\lambda > 0$, there exists a plethora of vacua where once a single one is picked, then the symmetry is broken. More precisely, we can write:

$$\langle H \rangle = \frac{1}{\sqrt{2}} \begin{pmatrix} 0 \\ v \end{pmatrix}, \tag{1.1.13}$$

where v is the vacuum expectation value (vev) $v = \sqrt{-\mu^2/\lambda}$. Furthermore, we can expand the Higgs field around the minimum as:

$$H = \frac{1}{\sqrt{2}} \begin{pmatrix} G^+ \\ v + h^0 + G^- \end{pmatrix}, \tag{1.1.14}$$

where the h^0 is a real scalar field, v is the vev and G^+, G^- are the Goldstone bosons [14; 15]. These degrees of freedom are absorbed in the definitions of W^+ and Z^0. Substituting in the equation (1.1.12) the vev of the Higgs fields, we can derive four different tree level masses for the fields W^I_μ, B_μ, where these masses can be written as:

$$M^2_{W^\pm} = \frac{g_2^2 v^2}{4}, \quad M^2_Z = \frac{v^2(g_1^2+g_2^2)}{4}, \quad M^2_A = 0\ . \tag{1.1.15}$$

The new fields Z, A are the mass eigenstates of the W^3_μ, B_μ, corresponding to massless photon and the neutral gauge boson Z of the weak interactions. The observed inequality between the charged bosons $W^\pm$ and the Z boson leads to the so called Weinberg angle, which is defined as:

$$\sin\theta_W = \frac{M_W}{M_Z}, \quad \tan\theta_W = \frac{g_1}{g_2}\ . \tag{1.1.16}$$

According to the experimental measurements, the strength of the forces render that the vev of the Higgs fields must lie at $v \cong 246$ GeV. The next step is to define the mass terms for the fields, i.e. the Yukawa sector of the theory.

$$\mathcal{L}_Y = -\sum_{i,j} Y^u_{ij} Q^\dagger_i i\sigma_2 H^* u_{jR} - \sum_{i,j} Y^d_{ij} Q^\dagger_i H d_{jR} - \sum_{i,j} Y^e_{ij} L^\dagger_i H e_{jR} + \text{h.c.} \tag{1.1.17}$$

where the Y_{ij} matrices are 3×3 complex-valued matrices. It is important to highlight the fact that the mass matrices are not diagonal, so we need to perform a rotation of the basis. This rotation can be specified to the following unitary transformation:

$$Y^u_{diag} = V^u Y^u_{ij} V^{u\dagger}, \quad Y^d_{diag} = V^d Y^d_{ij} V^{d\dagger}, \quad Y^e_{diag} = V^e Y^e_{ij} V^{e\dagger}\ . \tag{1.1.18}$$

One important implication of the above discussion is that one can write down the weak interaction vertex between fermions and $W^\pm$ bosons as:

$$\mathcal{L} \supset g u^\dagger_i d_j W^+ + \text{h.c.} \supset g u^\dagger_i (V^\dagger_u V_d)_{ij} d_j W^+ + \text{h.c.} \tag{1.1.19}$$

The new matrix obtained parametrizes the mixing angles between the fermions and the weak interactions gauge bosons. The name of the matrix is denoted as the Cabibbo-Kobayashi-Maskawa (CKM) mixing matrix [16; 17]

$$V_{CKM} = V_u^\dagger V_d \ . \tag{1.1.20}$$

The CKM matrix has a standard parametrization, containing four degrees of freedom. This parametrization is summarized below:

$$V_{CKM} = \begin{pmatrix} c_{12}c_{13} & s_{12}c_{13} & c_{13}e^{-i\delta} \\ -s_{12}c_{23} - c_{12}s_{23}s_{13}e^{i\delta} & c_{12}c_{23} - s_{12}s_{23}s_{13}e^{i\delta} & s_{23}c_{13} \\ s_{12}s_{23} - c_{12}c_{23}s_{13}e^{i\delta} & -c_{12}s_{23} - s_{12}c_{23}s_{13}e^{i\delta} & c_{23}c_{13} \end{pmatrix} , \tag{1.1.21}$$

where the above matrix contains the definitions: $\cos(\theta_{ij}) = c_{ij}, \ \sin(\theta_{ij}) = s_{ij}$ and δ stands for a phase.
As for the open problems of the SM, there are several phenomenona that cannot be explained within its context. In this paragraph, we will try to refer in short to some of them, before proceeding to a more complete theory of SM, string theory. From the particle physics point of view, some of them are:

- Dark Matter: This unknown matter comprise almost 30% of the mass-energy content of the universe. Its characteristic effect is that it cannot radiate, while we assume that it has to be electrically neutral in order to be stable. In addition, none of the SM particles can match the observations due to the assumed dark matter, thus there is a necessity to introduce new degrees of freedom.

- Neutrinos: According to the SM, neutrinos have to massless. Although, an observed phenomenon known as Neutrino Oscillations [18], has proved that they do have a tiny mass. The transitions between their different flavors cannot be explained without some small mass differences among these particles. In the quantum field theory language, the flavor eigenstates are expressed as a linear combination of the mass eigenstates $\nu_{1,2,3}$.

$$\nu_{iL} = \sum_{i,j} U_{ij}\nu_{Lj}, \quad \nu_{iL} = (\nu_e, \nu_\mu, \nu_\tau) \ . \tag{1.1.22}$$

  In the above definition, we have included a unitary mixing matrix U, which measures the mixing between the states and it is an analogue to the CKM matrix. This matrix is called

Pontecorvo-Maki-Nakagawa-Sakata (PMNS) matrix. AS for the upper bound on neutrinos mass, cosmological bound place it around [19]:

$$\sum_i m_i < 0.12 \text{ eV} . \tag{1.1.23}$$

Despite the shortcomings with respect to the particle nature of high energy physics, there are additional open questions regarding the cosmological evolution.

- Cosmological Constant: Recent observations of supernovae imply that an accelerated phase of the universe is taking place. This fact would require for the equations of motion to have some specific form. Starting from the Friedmann-Robertson-Walker (FRW) metric:

$$ds^2 = -dt^2 + \alpha(t)(\frac{dr^2}{1-kr^2} + r^2(d\theta^2 + \sin^2\theta d\phi^2)), \tag{1.1.24}$$

  where the scale factor parametrizes the radial size of the universe. This factor is determined by the Einstein equations, where a source of negative pressure has been added, the cosmological constant Λ.

$$G_{\mu\nu} = R_{\mu\nu} - \frac{1}{2}g_{\mu\nu}R = 8\pi G T_{\mu\nu} - \Lambda g_{\mu\nu} . \tag{1.1.25}$$

  The above equations lead to the Friedmann equations of motion, which are summarized to:

$$(\frac{\dot{\alpha}}{\alpha})^2 = \frac{1}{3M_p^2}\rho_{tot} - \frac{k}{\alpha^2} + \frac{\Lambda}{3} \tag{1.1.26}$$

$$\frac{\ddot{\alpha}}{\alpha} = -\frac{1}{6M_p^2}(\rho_{tot} + 3p_{tot}) + \frac{\Lambda}{3}, \tag{1.1.27}$$

  where for the correct explanation of an accelerated universe, a positive contribution for the $\Lambda > 0$ is required. This cosmological constant lay at the scale of $\Lambda \cong 10^{-120}M_p^4$, since recent astronomical observations indicate that it has a positive (non vanishing) value [20].

- Baryon Asymmetry: Within the context of standard cosmology, matter and anti-matter should have been equally produced during the Big Bang. Nevertheless, current observation tend to point towards that universe's matter mainly consists of matter. Several solutions has been provided through the years [21; 22; 23], where this question remains an open problem yet.

1.2 Basic notions of type IIB flux compactifications and F-theory

1.2.1 String compactifications

The most interesting formulation of string theory is in a ten dimensional flat Minkowski space. There are many representations of string theories, which are summarized to : type IIA and IIB closed string theories, type I theory, heterotic string theory, M-theory and the non-perturbative formulation of type IIB theory, the F-theory. The main problem of the above theories is that we have to correctly compactify the additional six spatial dimensions, since the the living world is a four dimensional space. Working in this direction, the ten dimensions are a product of four-dimensional space with six internal dimensions compactified. Mathematically speaking, this is translated to:

$$ds_{10}^2 = e^{-2A(y)} ds_4^2 + e^{2A(y)} g_{mn} dy^m dy^n, \tag{1.2.1}$$

where the y^m parametrize the internal coordinates and $A(y)$ stands for the wrap factor. Variations of the wrap factor may result into interesting physical implications, where a separation between the branes could address the hierarchy problem. This scenario was formulated as Randall-Sundrum model [24; 25]. The notion of fluxes in warped geometries are given by the background values for certain tensor fields, which wrap the internal cycles of the manifold. Focusing more in the type IIB superstring theory in ten dimensions [26; 27; 28; 29], we have to write down its action in Einstein frame:

$$S_{IIB} = \frac{1}{2k_{10}^2} \int d^{10}x \sqrt{-G} (R - \frac{1}{2} |\frac{\partial \tau}{Im\tau}|^2 - \frac{|G_3|^2}{2Im\tau} - \frac{1}{4} |\tilde{F}_5|^2) + \frac{1}{8ik_{10}^2} \int \frac{C_4 \wedge G_3 \wedge \bar{G}_3}{Im\tau}, \tag{1.2.2}$$

where the three-form parametrized the field strengths $G_3 = F_3 - \tau H_3$ with the axio-dilaton $\tau = C_0 + ie^{-\phi}$. The field strengths are defined through the following relations:

$$H_3 = dB_2, \quad F_3 = dC_2, \quad \tilde{F}_5 = dC_4 - \frac{1}{2} dC_2 \wedge dB_2 + \frac{1}{2} B_2 \wedge dC_2\ . \tag{1.2.3}$$

Moreover, type IIB string theory has an additional $SL(2, R)$ symmetry, which leaves invariant the metric and the C_4 axion. The transformation properties of the remaining fields are given by:

$$\tau \longrightarrow \frac{a\tau + b}{c\tau + d}, \quad \begin{pmatrix} C_2 \\ B_2 \end{pmatrix} \longrightarrow \begin{pmatrix} a & b \\ c & d \end{pmatrix} \begin{pmatrix} C_2 \\ B_2 \end{pmatrix}, \quad ad - bc = 1 \; . \tag{1.2.4}$$

At the quantum level, the above symmetry is broken to the subgroup $SL(2, Z)$, which symmetry is manifestly apparent in the F-theory. Additionally, the fluxes of both RR and NSNS sector of the compactification could take discrete values, i.e. they are quantized, leading to:

$$\frac{1}{(2\pi)^2\alpha'} \int F \in \mathbb{Z}, \quad \frac{1}{(2\pi)^2\alpha'} \int H \in \mathbb{Z} \; . \tag{1.2.5}$$

All the above are formulated in background with $\mathcal{N} = 2$ supersymmetry with 32 supercharges. In order to discuss about four dimensional theories, someone has to find a consistent solution of equations of motion in ten dimensions, which admits a Ricci-flat manifold. These manifolds are called Calabi-Yau and we are going to provide a small summary of this type of manifold properties regarding its moduli space.

First of all, a manifold M of three complex dimensions is equipped with an important quantity, the Kähler form J, which contains the information of the metric $g_{m\bar{n}}$ and the internal complex coordinates z^m.

$$J = ig_{m\bar{n}} dz^m \wedge d\bar{z}^{\bar{n}} \; . \tag{1.2.6}$$

We are looking for Kähler manifolds, since we ould like to express the metric in terms of the internal coordinates, i.e. we would like the Kähler form to be closed $dJ = 0$. We will introduce the definition of the Kähler potential K, where the metric and the (1-1) form are expressed with respect to this potential as:

$$g_{m\bar{n}} = \partial_m \partial_{\bar{n}} K(z, \bar{z}), \quad J = i\partial\partial K \; . \tag{1.2.7}$$

The additional property of flatness of this manifold imposes an additional restriction to the Ricci tensor. This tensor can expressed in term so of the metric as:

$$R = -i\partial\bar{\partial} \log(\det g) \tag{1.2.8}$$

The flatness of the manifold is encoded, now, in the vanishing order of the geometric quantity the Chern class $c_n(M)$. If the first class of this quantity is vanished, we deduce that the internal geometry is flat. Apart form the aforementioned objects, we need to introduce the holomorphic three-form Ω, which will be used on later purposes for the definition of the moduli space.

$$\Omega = \Omega_{pqr} dz^p \wedge dz^q \wedge dz^r, \tag{1.2.9}$$

where the tensor Ω_{pqr} contains the information of the transformation of the spinors inside the geometry. The connection between the holomorphic three form and the Kähler form is given by:

$$J \wedge J \wedge J = \frac{3i}{4} \Omega \wedge \Omega, \quad J \wedge \Omega = 0 \, . \tag{1.2.10}$$

Based on the fact, we need to end up with a four dimensional space, the correct manifold to compactify the extra dimensions has to be a threefold. Besides, the correct preserved supersymmetry of the 4d space is $\mathcal{N} = 1$, which fact can be safely obtained in a threefold. The next step we have to make is to examine whether infinitesimal deformations of the metric preserve the flatness of the space.

$$\delta g = \delta g_{m\bar{n}} dz^m d\bar{z}^{\bar{n}} + \delta g_{mn} dz^m dz^n + c.c. \, . \tag{1.2.11}$$

In addition to the above, we have to choose the gauge $\nabla(\delta g) = 0$, where by this particular choice the two conditions on $\delta g_{m\bar{n}}$ and δg_{mn} are separated. For the first deformation, the constraint implies that the $\delta g_{m\bar{n}}$ has to an (1,1)-form. The Kähler form is expanded in this basis, used the harmonic forms ω_i, $i = 1, .., h^{1,1}$, as $J = t^i \omega_i$. The $h^{1,1}$ is topological quantity called Hodge number, which specifies the dimension of the cohomology group $H^{p,q}(M) = h^{p,q}$. The scalar fields t^i are named Kähler moduli. The positivity of the Kähler form in the background geometry, also, leads to additional comstraints on the 2-cycle $\Sigma^{(2)}$ and the 4-cycle $\Sigma^{(4)}$ of the manifold

$$\int_{\Sigma^{(2)}} J > 0, \quad \int_{\Sigma^{(4)}} J \wedge J > 0 \, . \tag{1.2.12}$$

The intersection number between these moduli fields is given by the triple intersection

$$k_{ijk} = \int_M \omega_i \wedge \omega_j \wedge \omega_k, \tag{1.2.13}$$

where the volume of the compactified space $\mathcal{V}$ in term of the 2-cycles is written as:

$$\mathcal{V} = \frac{1}{6} k_{ijk} t^i t^j t^k \, . \tag{1.2.14}$$

All the above are encoded in the Kähler metric, which resembles a known formula.

$$K = -2\ln(\mathcal{V}) \ . \tag{1.2.15}$$

Going to the other sector of the deformation δg_{mn}, it is proved that it is required to be a (2,0)-form. In order to go to the $H^{2,1}$ group, we have to perform a rescaling of the deformations as:

$$\chi = \Omega^{\bar{r}}_{pq}\delta g_{\bar{r}\bar{s}} dz^p dz^q d\bar{z}^{\bar{s}}, \tag{1.2.16}$$

where a basis for the 3-form could be defined as $(a^i, b_i),\ i = 0, ..., h^{2,1}$. The basis has to be complete, which fact can be written as:

$$\int_M a^i \wedge b_j = \delta^i_j \ . \tag{1.2.17}$$

The above ingredients come in handy, as long as we define the complex structure moduli space, where there exist $h^{2,1} + 1$ complex coordinates. The two quantities that are going to be used for the explicit computation of the holomorphic three form Ω are the coordinates z^i and the periods $F_i(z)$

$$z^i = \int_{A_i} \Omega, \quad F_i = \int_{B_i} \Omega \tag{1.2.18}$$

with A_i, B_i being the cycles of the homology group. Now, the holomorphic form can be expressed as:

$$\Omega = z^i a_i - F_i b^i \tag{1.2.19}$$

and the metric of the complex structure's moduli space [30; 31]

$$g_{i\bar{j}} = \frac{\partial^2 K_{cs}}{\partial z^i \partial \bar{z}^{\bar{j}}}, \quad K_{cs} = -\ln(i\int_M \Omega \wedge \Omega) \ . \tag{1.2.20}$$

An additional interesting topological quantity is the Euler characteristic χ, which parametrizes the only independent Hodge numbers $(h^{1,1}, h^{2,1})$ of a simply connected manifold

$$\chi = 2(h^{1,1} - h^{2,1}) \ . \tag{1.2.21}$$

The rest of the fields are written as an expansion of the harmonic forms in ten dimensions.

$$B_2 = b_0 + b_i\omega^i, \quad C_2 = c_0 + c_i\omega^i, \quad C_4 = d^i\tilde{\omega}_i + d_i'\omega^i + V^j \wedge a_j + A_j' \wedge b^j, \tag{1.2.22}$$

where the indices run as $i = 1, ..., h^{1,1}$, $j = 1, ..., h^{2,1}$. The b_0, c_0 are two axions, the b_i, c_i stand for model dependent axions, where the C_4 consists of an axion d^i along with its dual $\tilde{d}_i$ and the q-form V^j contained in the vector multiplet.

If the theory contains fixed points in the manifold due to O_3/O_7 orientifolds, some degrees of freedom are projected out. This leads to a different parametrization of the internal coordinates, since the supersymmetry is reduced to $\mathcal{N} = 1$. The reformed definitions for the moduli (Kähler T_i and cs z^j) and the axio-dilaton S, in this case, are given by:

$$S = C_0 + ie^{-i\phi}, \quad T_i = \tau_i + id_i + \frac{ik_{inn}}{2(S - \bar{S})}G^m(G - \bar{G})^n, \quad G_j = c_j - Sb_j \ . \tag{1.2.23}$$

Below, two figurative tables are presented depicting the four dimensional spectrum of the compactification both in $\mathcal{N} = 1, 2$ supersymmetry.

Multiplets	Multiplicity	Fields
gravity multiplet	1	$g_{\mu\nu}, V_0$
vector multiplet	$h^{2,1}$	z^j, V^j
Kähler hypermultiplet	$h^{1,1}$	t_i, b_i, c_i, d^i
universal hypermultiplet	1	S, b_0, c_0

Table 1.2: $\mathcal{N} = 2$ multiplets along with the spectrum's fields [30].

Multiplets	Multiplicity	Fields
gravity multiplet	1	$g_{\mu\nu}$
chiral multiplet	1	S
Kähler chiral multiplets	$h_+^{1,1}$	t_i, d^i
chiral multiplet	$h_-^{1,1}$	b_i, c_i
vector multiplet	$h_+^{2,1}$	V_+^j
c.s. chiral multiplets	$h_-^{2,1}$	z_-^j, b_0, c_0

Table 1.3: $\mathcal{N} = 1$ multiplets along with the spectrum's fields [30].

The resulting low energy $\mathcal{N} = 1$ supergravity formula for the scalar potential is written in terms of the Kähler potential and superpotential $\mathcal{W}$ as:

$$K = -2\ln(\mathcal{V}(T)) - \ln(S - \bar{S}) - \ln(i\int_M \Omega(z) \wedge \Omega(\bar{z})), \tag{1.2.24}$$

$$V = e^K \left[K^{I\bar{J}}\mathcal{D}_i\mathcal{W}\mathcal{D}_{\bar{j}}\bar{\mathcal{W}} - 3|\mathcal{W}|^2\right], \quad \mathcal{W} = \int_M G_3 \wedge \Omega\,, \tag{1.2.25}$$

where the indices I, J run over all moduli fields.

1.2.2 GUTs from F-theory

Despite the great success of the SM theory in describing various low energy phenomena, there are still mysteries regrading their origin. One of the central questions is a missing explanation on why the gauge group has this particular structure and whether we could explore the possibility of a unified more fundamental group. Hints point toward this direction, since the exploitation of the the gauge couplings at high energies renders unification to a certain value. The most promising candidate is string theory, which has managed to combine supersymmetry, extra dimensions and coupling unification at string scales in order to provide solutions to various problems of the SM. In this chapter, a brief discuss is going to presented about F-theory, the non-perturbative manifestation of type IIB string theory on Calabi-Yau manifolds. F-theory was constructed in the late 90's by Vafa [32] as twelve dimensional string theory. Recalling from the previous section the action of the type IIB theory and the definition of the axio-dilaton, we are going to sketch the fundamentals of the F-theory constructions. The invariance of the axio-dilaton under $SL(2, Z)$

from a mathematical point of view is identical to the transformation of an elliptic curve E_τ, more specifically of its complex structure under modular transformation.

$$\tau \longrightarrow \frac{a\tau + b}{c\tau + d}, \quad \tau = C_0 + \frac{i}{g_s}, \quad ad - bc = 1 \ . \tag{1.2.26}$$

The idea was that someone could embed the type IIB string theory on a torus, parametrized by the value of the value of the axio-dilaton. This means that the geometry corresponds to a complex fourfold, generated by the elliptic curve, which is actually the elliptic fibration over the threefold. The non-perturbative nature of the theory is manifested through the fact that the elliptic curve is correlated to the motion of the string coupling g_s. The total space of F-theory, them, can be described by the four dimensional $R^{3,1}$ space augmented by a X complex fourfold with the threefold base B_3.
In mathematics, elliptic curves are points that satisfy the Weierstrass equation:

$$y^2 = x^3 + f(z)x + g(z), \tag{1.2.27}$$

where x, y, z are the complex coordinates and $f(z), g(z)$ are polynomials of eight and twelfth degree in z. Each point on the base B_3 through this equation is translated as a torus labeled by the coordinate z. The two most important quantities of an elliptic fibration are the discriminant Δ of the Weierstrass equation and the j-invariant modular function. Starting from the discriminant, the singularities could be classified by

$$\Delta = 4f^3 + 27g^2 \ . \tag{1.2.28}$$

If $\Delta \neq 0$, the elliptic curve is non-singular. On the other hand, the vanishing discriminant leads to the degeneration of the fibration, where 24 roots z_i can be identified. These roots correspond to extended objects, the 7-branes, where their location in the fibration is related to the z coordinate. In addition, from the definition of the j-function, the existence of 7-branes will emerge more naturally. This function connect the modular of the torus to the roots through:

$$j(\tau) = \frac{4(24f)^3}{\Delta} = \frac{4(24f)^3}{4f^3 + 27g^2}, \quad j(\tau) = e^{-2\pi i\tau} + 744 + \dots \ . \tag{1.2.29}$$

If this is the case of a vanishing discriminant, then, in the small vicinity of z_i one can expand the j function

$$j(\tau(z)) \cong \frac{1}{z-\bar{z}_i} \longrightarrow \tau(z) \cong \frac{1}{2\pi i}\ln(z-z_i)\ . \tag{1.2.30}$$

The above equation has some severe consequences in the understanding the various limits of the theory. If $z \longrightarrow z_i$, then $\tau \longrightarrow i\infty$, which in practice means that the theory resides in the weak coupling regime. This observation was first noticed by Sen [33]. Proceeding further one can notice that $\ln(z-z_i) = \ln|z-z_i| + i\theta$, where as the root is encirled, the τ undergoes a monodromy $\tau \longrightarrow \tau + 1$

$$\oint_{z_i} F_1 = \oint_{z_i} dC_0 = 1\ . \tag{1.2.31}$$

The existence of a monodromy implies the emergence of 7-branes at the location of z_i in the transverse space. The elliptic fiber is not a real physical object, but it is used to track down the variation of the axio-dilaton along the base B_3. The implication of the presence of 7-branes in the spectrum is that gauge symmetries could possibly emerge from F-theory. In type II string theories, D-branes are associated to $U(1)$ symmetries, where a stack of N D-branes lead to $U(N)$ gauge symmetries. Similarly, when 7-branes coincide, at the intersection point, a symmetry enhancement is achieved leading to gauge symmetries. The classification of the correspondence between singularities and gauge symmetries are given by Kodaira [34]. According to his work, there is a systematic classification of the different ADE algebras descending from the vanishing order of the discriminant in the Weierstrass equation. More recent works have proceeded the previous analysis and explored the physical properties of these constructions [35; 36; 37; 38].

Of particular interest is the local F-theory constructions. This approach is related to the Tate algorithm [39] for the singularities of the Weierstrass equation. A redefinition of the Weierstrass equation into an equation of local coordinates can be recasted as:

$$y^2 + a_1xy + a_3y = x^3 + a_2x^2 + a4x + a_6\ . \tag{1.2.32}$$

The a functions are functions depending in the complex coordinate z of the base B_3, while they are related to the previous functions f, g.

$$f = -\frac{1}{48}(\beta_2^2 - 24\beta_4), \quad g = -\frac{1}{864}(-\beta_2^2 + 36\beta_2\beta_4 - 216\beta_6) \tag{1.2.33}$$

$$\Delta = \frac{1}{8}(\beta_8\beta_2^2 - 9\beta_2\beta_4\beta_6 + 8\beta_4^3 + 27\beta_6^2), \tag{1.2.34}$$

where the new β functions are given by:

$$\beta_2 = a_1^2 + 4a_2, \quad \beta_4 = a_1 a_3 + 2a_4, \tag{1.2.35}$$

$$\beta_6 = a_3^2 + 4a_6, \quad \beta_8 = \frac{1}{4}(\beta_2\beta_6 - \beta_4^2)\ . \tag{1.2.36}$$

Based on the above, the resulting gauge group is associated to the vanishing order of each a function, since their definition is $a_i \sim b_i z^n$. A geometric origin is that the elliptic fiber is factorized at the location of the 7-branes on a particular divisor in B_3. In Table 4., the complete classification of the various gauge groups with respect to the singularity type is presented.

It would be illustrative to discuss local F-theory constructions such as a $SU(5)$ model. Assuming

$$a_1 = -b_5, a_2 = b_4 z, a_3 = -b_3 z^2, a_4 = b_2 z^3, a_6 = z^5 b_0, \tag{1.2.37}$$

where if we substitute these factors in the Tate formula, it results to :

$$y^2 = x^3 + b_0 z^5 + b_2 x z^3 + b_3 y z^2 + b_4 x^2 z + b_5 x y. \tag{1.2.38}$$

Type	**Group**	a_1	a_2	a_3	a_4	a_6	Δ
I_0	0	0	0	0	0	0	0
I_1	-	0	0	1	1	1	1
I_2	$SU(2)$	0	0	1	1	2	2
I_3^{ns}	-	0	0	2	2	3	3
I_3^s	-	0	1	1	2	3	3
I_{2n}^{ns}	$Sp(n)$	0	0	n	n	$2n$	$2n$
I_{2n}^s	$SU(2n)$	0	1	n	n	$2n$	$2n$
I_{2n}^{ns}	-	0	1	$n+1$	$n+1$	$2n+1$	$2n+1$
I_{2n+1}^s	$SU(2n+1)$	0	1	n	$n+1$	$2n+1$	$2n+1$
II	-	1	1	1	1	1	2
III	$SU(2)$	1	1	1	1	2	3
IV^{ns}	-	1	1	1	2	2	4
IV^s	$SU(3)$	1	1	1	2	3	4
I_0^{*ns}	G_2	1	1	1	2	3	6
I_0^{*ss}	$SO(7)$	1	1	2	2	4	6
I_0^{*s}	$SO(8)$	1	1	2	2	4	6
I_1^{*ns}	$SO(9)$	1	1	2	3	4	7
I_1^{*s}	$SO(10)$	1	1	2	3	5	7
I_2^{*ns}	$SO(11)$	1	1	3	3	5	8
I_2^{*s}	$SO(12)$	1	1	3	3	5	8
IV^{*ns}	F_4	1	2	2	3	4	8
IV^{*s}	E_6	1	2	3	3	5	8
III^{*s}	E_7	1	2	3	3	5	9
II^s	E_8	1	2	3	4	5	10

Table 1.4: Results from Tate's algorithm.

The above equation leads to an $SU(5)$ singularity. Now, the b coefficients can be understood as sections of the line-bundle in the divisor S_{GUT}. In order to perform an anomaly cancellation analysis, we have to define c_1 as the first Chern class of the tangent bundle of S_{GUT}, while $-t$ as the first Chern class of the normal bundle. The homology classes are written as:

$$\eta = 6c_1 - t \ . \tag{1.2.39}$$

Based on this definition, we can attribute to each coordinate a specific homology class, the same goes to the coefficients b_i.

$$x : \quad 2(c_1 - t) \tag{1.2.40}$$
$$y : \quad 3(c_1 - t) \tag{1.2.41}$$
$$z : \quad -t \tag{1.2.42}$$
$$b_k : \quad \eta - kc_1 \ . \tag{1.2.43}$$

Each term in (1.2.38) has the same homology class, e.g.

$$b_2xz^3 : \eta - 2c_1 + 2(c_1 - t) - 3t = 6(c_1 - t) \ . \tag{1.2.44}$$

Now, we have to translate the β functions in terms of the b sections.

$$\beta_2 = b_5^2 + 4b_4z, \tag{1.2.45}$$
$$\beta_4 = b_3b_5z^2 + 2b_2z^3, \tag{1.2.46}$$
$$\beta_6 = b_3^2z^4 + 4b_0z^5, \tag{1.2.47}$$
$$\beta_8 = z^5(R + z(4b_0b_4 - b_2^2)), \quad R = b_3^2b_4 - b_2b_3b_5 + b_0b_5 \ . \tag{1.2.48}$$

It is a good point to define the matter representations in the F-theory GUTs. These degrees of freedom lay at the intersection of two 7-branes, where from a mathematical scope they are Riemann surfaces where some symmetry enhancement is achieved. For instance, by choosing that the $b_5 = 0$, the discriminant becomes $\Delta \sim z^7$. According to the Tate's classification, this singularity returns an $SO(10)$ symmetry. Thus, we can deduce that a matter curve is laying along the intersection of two 7-branes at the singularity, leading to the 10 representation of $SU(5)$. This matter curve Σ can be written as:

$$\Sigma_{10} = \{b_5 = 0\} \ . \tag{1.2.49}$$

In a similar fashion, one can also obtain the 5 representation of the $SU(5)$ by considering $R = 0$, leading to $\Delta \sim z^6$. This is an $SU(6)$ singularity, where in the adjoint decomposition of $SU(6)$ there is the 5-plet. Again, the matter curve could be expressed as:

$$\Sigma_5 = \{R = 0 = b_3^2 b_4 - b_2 b_3 b_5 + b_0 b_5^2 = 0\} \ . \tag{1.2.50}$$

Finally, the notion of Yukawa couplings in the semi-local approach of F-theory is given by the triple intersections of 7-branes. For instance the top and bottom Yukawa couplings are given by:

$$Y_t \longrightarrow \{b_5 = 0, b_4 = 0\}, \quad \Delta \sim z^8 \longrightarrow E_6 \text{ singularity} \tag{1.2.51}$$

$$Y_b \longrightarrow \{b_3 = 0, b_5 = 0\}, \quad \Delta \sim z^8 \longrightarrow SO(12) \text{ singularity} \tag{1.2.52}$$

Based on this short introduction, one can extract a very useful machinery for the construction of GUTs in the close vicinity of an geometric singularity. It is also worth mentioning that an extensive amount of work have been done towards the computation of Yukawa couplings in F-theory [40; 41; 42; 43; 44; 45; 46; 47; 48; 49; 50; 51; 52; 53], since the geometric separation of the matter curves and their distinctive position in the GUT divisor allows for a natural explanation to the problem of mass hierarchical structure.

An important ingredient in the engineering of F-theory GUTs is the semi-local approach, mainly studied by [54]. In this picture the maximal symmetry is the E_8 gauge group, which is broken by geometric Higgs mechanism in resulting a G_S group (a surface for the GUT model), augmented by a commutant group described by the spectral cover surface.

$$E_8 \supset G_S \times SU(N)_\perp, \tag{1.2.53}$$

where the symmetries related to particle physics are

$$E_8 \longrightarrow E_6 \times SU(3)_\perp, \tag{1.2.54}$$
$$E_8 \longrightarrow SO(10) \times SU(4)_\perp, \tag{1.2.55}$$
$$E_8 \longrightarrow SU(5) \times SU(5)_\perp \ . \tag{1.2.56}$$

We will study an example to deeply understand the properties of the spectral cover. Starting from $G_S = SU(5)$, the matter representation are decomposed as:

$$248 \longrightarrow (24,1) + (1,24) + (5,10) + (\bar{5},\bar{10}) + (10,\bar{5}) \ . \tag{1.2.57}$$

The spectral cover equation are defined by the internal coordinates

$$z \longrightarrow U, x \longrightarrow V^2, y \longrightarrow V^3, \tag{1.2.58}$$

where based on this redefinition the Tate formula can be recasted to:

$$0 = b_0 U^5 + b_2 V^2 U^3 + b_3 V^3 U^2 + b_4 V^4 U + b_5 V^5. \tag{1.2.59}$$

In order to rewrite the above formula as a polynomial, we use the new variable $s = U/V$:

$$C_5 = b_5 + b_4 s + b_3 s^2 + b_2 s^3 + b_1 s^4 + b_0 s^5 \tag{1.2.60}$$

The roots of this fifth degree polynomial are characterized as weights t_i of the perpendicular group $SU(5)_\perp$ [55].

$$0 = b_5 + b_4 s + b_3 s^2 + b_2 s^3 + b_1 s^4 + b_0 s^5 = \Pi_{i=1}^{5}(s + t_i) \ . \tag{1.2.61}$$

To "charge" the matter fields with the new charges, one has to entangle the charges with the sections b_i, which sections define the matter curves. One can see that the sum and the product of the roots are given by:

$$b_1 = \sum_i t_i = 0, \quad b_5 = t_1 t_2 t_3 t_4 t_5 \ . \tag{1.2.62}$$

The above sections define the matter curves, as mentioned in (1.2.49), where the multiplicity of the representations are numbered by the number of different charges. For instance, there are five 10plets given by:

$$\Sigma_{10_i} : \ \ \mathcal{P}_{10} = b_5 \longrightarrow t_i = 0, \quad i = 1, 2, 3, 4, 5 \ . \tag{1.2.63}$$

In a similar manner, the 10 different 5plets are defined by:

$$\Sigma_{\bar{5}_{ij}} : \ \ \mathcal{P}_5 = R = \Pi_{i \neq j}(t_i + t_j) = 0 \ . \tag{1.2.64}$$

As for the singlets, their degrees of freedom are, also, defined by charges t_i, but they parametrize the space transverse to the matter curves.

$$\Sigma_{1_{ij}} : \ \ \mathcal{P}_0 = \Pi(\pm(t_i - t_j)) = 0, \tag{1.2.65}$$

whose polynomial match the discriminant of the spectral cover equation. The effective theory of this model is given by $SU(5) \times U(1)^4$, where the superpotential for the up quark masses

$$\mathcal{W} \supset 10_{t_i} 10_{t_i} 5_{-t_i - t_j} \ . \tag{1.2.66}$$

The above coupling contains the interactions for two different generations, although phenomenological reasons favor rank-1 mass matrix. Consequently, an additional symmetry would be required. To introduce this kind of symmetry, we need to understand the relation between the sections b_i and the roots t_i.

$$b_i = b_i(t_i) \ . \tag{1.2.67}$$

The inversion of this equation leads to branches due to the fact that there exists monodromies

$t_i = t_i(b_i)$ [55; 56; 57]. Considering the Z_2 monodromy, it means that two roots of the spectral cover equation (1.2.61) do not factorize, leadin to second degree polynomial

$$a_1 + a_2 s + a_3 s^2 = 0 \Rightarrow \tag{1.2.68}$$

$$s_1 = \frac{-a_2 + \sqrt{w}}{2a_3}, \quad s_2 = \frac{-a_2 + \sqrt{w}}{2a_3}, \quad w = a_2^2 - 4a_1 a_3. \tag{1.2.69}$$

The branchcuts are viewed as

$$\sqrt{w} = e^{i\theta/2}\sqrt{|w|} \Rightarrow \tag{1.2.70}$$

$$\theta \to -\theta, \quad \sqrt{w} \to -\sqrt{w}, \quad s_1 \leftrightarrow s_2 \ . \tag{1.2.71}$$

These branchcut provide an identification $t_1 \leftrightarrow t_2$, where the coupling constant for the up quark is modified to:

$$\mathcal{W} \supset 10_{t_1} 10_{t_1} 5_{-2t_1} \ . \tag{1.2.72}$$

The $SU(5)$ spectral cover provide the geometry with a 5-degree polynomial C_5, where some possible different monodromies can be introduced. All possible indentifications/factorizations of the polynomial are given below:

$$C_2 \times C_1 \times C_1 \times C_1 : (a_1 + a_2 s + a_3 s^2)(a_4 + a_5 s)(a_6 + a_7 s)(a_8 + a_9 s), \tag{1.2.73}$$

$$C_2 \times C_2 \times C_1 : (a_1 + a_2 s + a_3 s^2)(a_4 + a_5 s + a_6 s^2)(a_7 + a_8 s), \tag{1.2.74}$$

$$C_3 \times C_1 \times C_1 : (a_1 + a_2 s + a_3 s^2 + a_4 s^3)(a_5 + a_6 s)(a_7 + a_8 s), \tag{1.2.75}$$

$$C_3 \times C_2 : (a_1 + a_2 s + a_3 s^2 + a_4 s^3)(a_5 + a_6 s + a_7 s^2), \tag{1.2.76}$$

$$C_4 \times C_1 : (a_1 + a_2 s + a_3 s^2 + a_4 s^3 + a_5 s^4)(a_6 + a_7 s) \ . \tag{1.2.77}$$

1.3 Towards string phenomenology

1.3.1 Moduli stabilization

Most compactifications share a unique feature regarding their stability conditions. As it can seen by equation (2.1.67), fluxes can generate a non-trivial scalar potential depending on the various moduli fields of the theory. Up to the late 90's, no model had managed to find a consistent solution for describing the lat-time cosmology, since the allowed vacua were of Anti de-Sitter type. In order to explain the accelerated phase of the universe, one should derive a de-Sitter (dS) vacuum, where supersymmetry must be broken in a controllable way and higher derivative corrections to the vacuum should be subleading. Despite the no-go theorems [58; 59], stating that such solutions are forbidden in the context of superstring theory, a plethora of attempts point towards some available dS vacua.

The moduli space in string vacua is characterized by: the Kähler moduli, the complex structrue moduli and the axio-dilaton. Since these scalar fields are parametrizing the size and the shaoe of the interanl geometry and remain massless at tree-level, one should generate an 4d effective potential in order to generate masses for them. The intention to do so is that if they remain massless, new long range forces should be detected. The existence of extensive objects, like D-branes, have identified the warped compactifications as a bypass to the no-go theorems. One should start from the scalr potential (2.1.67), and try to understand the dynamics in the presence of fluxes. In the seminal work of Giddings at al. [60], they probed that complex structure moduli and axio-dilaton could be stabilized in the presence of integer fluxes. Starting from the metric of the type IIB string theory, we can associate the wrap factor $A(y)$ to the self-dual 5-form fluxes $\tilde{F}_5$.

$$ds_{10}^2 = e^{-2A(y)} ds_4^2 + e^{2A(y)} g_{mn} dy^m dy^n, \tag{1.3.1}$$

$$\tilde{F}_5 = (1 + *)[da \wedge dx^0 \wedge dx^1 \wedge dx^2 \wedge dx^3], \quad a = e^{4A(y)} \ . \tag{1.3.2}$$

Now, the 3-form fluxes defined by $G_3 = F_3 - \tau H_3$ are imaginary self dual, satisfying the relation

$$G_3 = i *_6 G_3, \tag{1.3.3}$$

where we have properly defined the Hogde dual $*_6$ in the internal geometry. The preservation of supersymmetry at the $\mathcal{N} = 1$ level leads to the constraint that the fluxes has to be primitive and of (2,1) type. The condition (1.3.3) erase the (0,3) part of the fluxes, since this part would attribute a non supersymmetric vacuum with $\mathcal{W} = \mathcal{W}_0$. Moreover, the above condition fixes the complex structure moduli and the axio-dilaton at high scales

$$m \sim \frac{\alpha'}{R^3}, \tag{1.3.4}$$

where R is the radius of the manifold. One last that should be addressed is the fluxes and the presence of D-branes serve as localized sources that could potentially raise some tadpoles. It is proved in [60] that fluxes generate a tadpole the C_4 axion. The D_7-branes provide some negative D3 charge in the geometry, where this charge can related in the language of F-theory to the Euler characteristic $\chi(M)$.

$$Q_3^{D_7} = -\frac{\chi}{24}\,. \tag{1.3.5}$$

The resulting tadpole which every type IIB/F-theory compactification must satisfy in the presence of integer fluxes is

$$\frac{1}{(2\pi)^4\alpha'^2}\int H_3 \wedge F_3 + N_{D_3} - N_{\bar{D}_3} = \frac{\chi}{24}\,. \tag{1.3.6}$$

Having managed to provide the mechanism for the stabilization of the cs moduli and axio-dilaton, the Kähler sector remains undetermined. Two different approaches, KKLT model [61] and Large Volume Scenario [62], lead to dS vacua have been proposed the last twenty years. We are going to briefly describe both of them in the rest of the section.

KKLT model

Focusing in the Kähler moduli sector, this proposal argues that non-perturabtive corrections to the no-scale scalar potential could in principle stabilize the compactification's volume. In string theory, there are two types of non-perturabtive corrections: i) Euclidean D_3 branes ii) Gaugino condensations. The first one can be written as:

$$\mathcal{W}_{D_3} = T(z)\exp(2\pi i\rho), \tag{1.3.7}$$

where $T(z)$ is a prefactor depending in the complex structure moduli and ρ stands for the volume modulus. The latter correction's form is summarized:

$$\mathcal{W}_{\text{gaugino}} = \Lambda^3_{N_c} = Ae^{\frac{2\pi i\rho}{N_c}}, \tag{1.3.8}$$

where the A parameter is determined by the scale of the gaugino condensation and N_c is the number of branes in the corresponding stack of branes. Taking into account these corrections, KKLT scenario achieved an AdS vacuum, with the Kähler potential and the superpotential given by:

$$K = -3\ln(-i(\rho - \bar{\rho})), \quad \mathcal{W} = \mathcal{W}_0 + Ae^{ia\rho} \ . \tag{1.3.9}$$

Imposing the flatness condition of superpotential $D\mathcal{W} = 0$, it leads to:

$$D\mathcal{W} = 0 \Rightarrow \mathcal{W}_0 = -Ae^{a\sigma_{cr}}(1 + \frac{2}{3}a\sigma_{cr}), \quad \rho = i\sigma \ . \tag{1.3.10}$$

The value of the potential at the vacuum can be found to be:

$$V_{AdS} = -\frac{a^2A^2e^{-2a\sigma_{cr}}}{6\sigma_{cr}} \ . \tag{1.3.11}$$

This vacuum has be found taking into account that $\sigma \gg 1$, in order to have controllable corrections. Additionally, $a\sigma > 1$ is imposed since the superpotential corrections have to be reliable. Nevertheless, the resulting vacuum is an AdS vacuum, so a mechanism should be included in order to uplift the model. The problem can be solved through introducing anti-branes $\bar{D}_3$, whose effect is to add a positive term in the scalar potential.

$$\delta V_{D_3} = \frac{d}{(\text{Im}\rho)^3}, \quad d > 0 \ . \tag{1.3.12}$$

AS for the scalar potential, substituting Kähler potential and superpotential of equation (1.3.9) in the formula for the scalar potential (2.1.67), one can derive:

$$V = \frac{aAe^{-a\sigma}}{2\sigma^2}(\frac{1}{3}a\sigma Ae^{-a\sigma} + \mathcal{W}_0 + ae^{-a\sigma}) + \frac{d}{\sigma^3} \ . \tag{1.3.13}$$

In the above potential, fine-tuning of D parameter would suffice to uplift the AdS vacuum to dS vacuum. In the following plot, the two vacua are shown for a specific values of the free parameters of the theory.

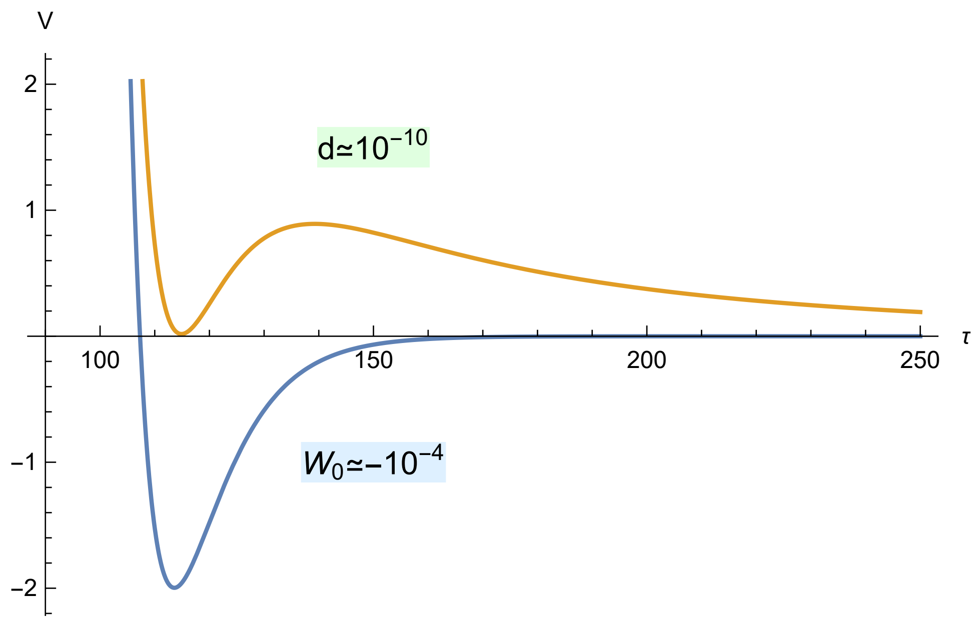

Figure 1.1: KKLT's vacua (1.3.13) for suppressed fluxes and a tiny uplift parameter d.

The next step for ensuring that the dS vacuum is stable, would be to explore the decay rate of the vacuum. The goal is to achieve a decay time, which is shorter than the recurrence time $t_r \sim e^{S_0},\ S_0 = \frac{24\pi^2}{V_0}$. Within the thin-wall approximation approach [63], the possibility of vacuum's decay rate is related to the dS entropy and can be computed from:

$$P = \exp(-\frac{S(\phi)}{(1+4V_0/3T^2)^2}), \tag{1.3.14}$$

where the temperature of the bubble wall is given by:

$$T = \int_{\phi_0}^{\infty} d\phi\sqrt{2V(\phi)}\ . \tag{1.3.15}$$

In the limit of considering the inclusion of gravitational effects $T^2 \gg V_0$, the approximated result is given by:

$$P \cong \exp(-S(\phi)) \cong \exp(-\frac{24\pi^2}{V_0}) \sim \exp(-10^{-120}) \ . \tag{1.3.16}$$

One could easily observe that the dS vacuum is practically stable during the cosmological timeline.

Large Volume Scenario

An alternative to the above scenario was proposed on the basis that there is decompactification direction in the moduli space along which:

- $\tau_i \equiv \mathrm{Im}(\rho_i) \longrightarrow \infty$.
- $V < 0$ for $\mathcal{V} \gg 1$.

The leading order (α'^3) corrections to the Kähler potential has been studied in [64], where this modification leads to the potential as:

$$K = -2\ln(\mathcal{V} + \frac{\xi}{2} + \text{world sheet instantons}) \ . \tag{1.3.17}$$

As for the superpotential, non-perturbative corrections need to added along each direction τ_i of the internal space:

$$\mathcal{W} = \mathcal{W}_0 + \sum_n A_n e^{ia_n\rho_n} \ . \tag{1.3.18}$$

The generic formula for the scalar potential can obtained from the following formula:

$$\begin{aligned} V = e^K \big[& G^{\rho_j\bar{\rho}_k}(a_jA_ja_k\bar{A}_k e^{i(a_j\rho_j - a_k\bar{\rho}_k)} + i(a_jA_je^{ia_j\rho_j}\bar{W}\partial_{\bar{\rho}_k}K - a_k\bar{A}_ke^{-ia_k\bar{\rho}_k}W\partial_jK)) + \\ & + 3\xi\frac{(\xi^2 + 7\xi\mathcal{V} + \mathcal{V}^2)}{(\mathcal{V}-\xi)(2\mathcal{V}+\xi)^2}|W|^2\big] \ . \end{aligned} \tag{1.3.19}$$

It is worth mentioning, also, that the constant ξ controls the strength of the α' corrections and its value is given by:

$$\xi = -\frac{\chi(X)\zeta(3)}{2(2\pi)^3}, \quad \hat{\xi} = \frac{\xi}{g_s^2} \ . \tag{1.3.20}$$

The above scalar potential can be split into three sperate terms:

$$V = V_{np_1} + V_{np_2} + V_{\alpha'}, \tag{1.3.21}$$

where it's term formula is summarized below:

$$V_{np_1} \sim \frac{(-k_{ssk}t^k)a_s^2|A_s|^2 e^{-2a_s\tau_s} e^{K_{cs}}}{\mathcal{V}} + O(\frac{1}{\mathcal{V}^2}), \tag{1.3.22}$$

where the index s stands for a modulus τ_s, which stays to smaller values than $\tau_i \to \infty$. The second non-perturtabive term is written as:

$$V_{np_2} \sim -\frac{a_s\tau_s e^{-a_s\tau_2}}{\mathcal{V}^2}|A_s\mathcal{W}_0|e^{K_{cs}} + O(\frac{1}{\mathcal{V}^3}) \ . \tag{1.3.23}$$

As for the perturbative part of the scalar potential, this is computed from the simple formula by:

$$V_{\alpha'} \sim \frac{3\xi}{16\mathcal{V}^3} + O(\frac{1}{\mathcal{V}^4}) \ . \tag{1.3.24}$$

Summing all the contributions, the scalar potential to the leading order in the large volume scenario could be read by the following derived formula:

$$V \sim \left[a_s^2 A_s^2 \frac{-k_{ssk}t^k}{\mathcal{V}} e^{-2a_s\tau_s} - |A_s\mathcal{W}|\frac{a_s\tau_s}{\mathcal{V}^2}e^{-a_s\tau_s} + \frac{\xi}{\mathcal{V}^3}|\mathcal{W}|^2\right] + O(\frac{1}{\mathcal{V}^4}) \ . \tag{1.3.25}$$

Given the above limit, the overall potential scale as

$$V \sim -e^{K_{cs}}|A_s W_0|\frac{\ln\mathcal{V}}{\mathcal{V}^3}, \tag{1.3.26}$$

where this potential reaches zero from the negative at large volumes.

1.3.2 Origin of right handed neutrinos and modular flavor symmetry

The SM theory included only left-handed neutrinos in the leptonic sector. Despite their presence, these degrees of freedom cannot acquire mass from any mechanism, since the mass terms are not allowed in the Lagrangian. Moreover, neutrinos are the only charge neutral particles of the SM, so there is a possibility for them to be of Majorana type. Assuming the Majorana case, we can introduce right-handed neutrinos ν_R, so the additional terms are:

$$\mathcal{L} = m_D \bar{\nu}_L \nu_R + M_R \bar{\nu}_R \nu_R + h.c. \tag{1.3.27}$$

where m_D and M_R are 3x3 matrices. The two terms have a different interpretation: the first one stands for the Dirac type operator, descending from $(Y_\nu)_{ij} \bar{L}_i \bar{H} \nu_{R_j}$. As for the latter term , there are various model dependent origins, where the simplest one is given by Weinberg [65], who introduced a dimension 5 operator.

$$\mathcal{L} = \lambda_\nu^{ij} \frac{L_i \bar{H} \bar{H} L_j}{\Lambda} \ . \tag{1.3.28}$$

The Λ energy scale denotes the scale of new physics, where one can observe that these terms are violating the total lepton number by $\Delta L = 2$. However, dimension 5 operators can be derived by a mechanism, named seesaw mechanism, where it can embedded easily in GUTs. Seesaw mechanism is classified into three different types: type I [66], type II [67] and type III [68].

Type I seesaw is the easiest to analyze, since the right handed neutrinos are singlets and no constraints can be imposed on them with respect to their mass. Given the Lagrangian in equation (1.3.27), the general mass matrix of both Dirac and Majorana type can be written as:

$$M_\nu = \begin{pmatrix} 0 & m_D \\ m_D^T & M_R \end{pmatrix}, \tag{1.3.29}$$

where the light neutrino masses could be obtained by:

$$m_\nu = m_D M_R^{-1} m_D^T \ . \tag{1.3.30}$$

In a similar fashion to the quark mixing, there is still missing an explanation for the lepton mixing [69]. Considering the Lagrangian for the leptons in the SM, we can write:

$$\mathcal{L} = -v_d Y^e_{ij} \bar{e}^i_L e^j_R - \frac{1}{2} M^\nu_{ij} \bar{\nu}^i_L \nu^{cj}_L + h.c. \tag{1.3.31}$$

Now, the mass matrices can be diagonalized by unitary matrices:

$$U^\dagger_{e_L} Y^e U_{e_R} = \begin{pmatrix} y_e & 0 & 0 \\ 0 & y_\mu & 0 \\ 0 & 0 & y_\tau \end{pmatrix}, \quad U^\dagger_{\nu_L} M^\nu U^*_{\nu_R} = \begin{pmatrix} m_1 & 0 & 0 \\ 0 & m_2 & 0 \\ 0 & 0 & m_3 \end{pmatrix} \tag{1.3.32}$$

The charged current (CC) couplings to W boson in the flavor basis is given by:

$$\mathcal{L} \supset -\frac{g}{\sqrt{2}} \bar{e}^i_L \gamma^\mu W^-_\mu \nu^i_L \Rightarrow \mathcal{L} \supset \frac{g}{\sqrt{2}} \begin{pmatrix} \bar{e}_L & \bar{\mu}_L & \bar{\tau}_L \end{pmatrix} U_{PMNS} \gamma^\mu W^-_\mu \begin{pmatrix} \nu_{1L} \\ \nu_{2L} \\ \nu_{3L} \end{pmatrix} + h.c.\,. \tag{1.3.33}$$

The above matrix can identified as Pontecorvo-Maki-Nakagawa-Sakata (PMNS) lepton mixing matrix

$$U_{PMNS} = U^\dagger_{e_L} U_{\nu_L}\ . \tag{1.3.34}$$

This matrix can be parametrized as:

$$U_{PMNS} = \begin{pmatrix} c_{12}c_{13} & s_{12}c_{13} & c_{13}e^{-i\delta} \\ -s_{12}c_{23} - c_{12}s_{23}s_{13}e^{i\delta} & c_{12}c_{23} - s_{12}s_{23}s_{13}e^{i\delta} & s_{23}c_{13} \\ s_{12}s_{23} - c_{12}c_{23}s_{13}e^{i\delta} & -c_{12}s_{23} - s_{12}c_{23}s_{13}e^{i\delta} & c_{23}c_{13} \end{pmatrix} \begin{pmatrix} 1 & 0 & 0 \\ 0 & e^{i\frac{a_{21}}{2}} & 0 \\ 0 & 0 & e^{i\frac{a_{31}}{2}} \end{pmatrix}, \tag{1.3.35}$$

where the a_{21}, a_{31} are Majorana phases. These phases can be constrained after observing neutrinoless double beta decay in experiments [70].

Despite the fact that the seesaw mechanism has provided an explanation for the origin of the neutrino masses, SM does not give any insight into the origin of fermion masses and the mixing parameters. The idea of a family symmetry may provide a solution to the above problem, which symmetry may be discrete or continuous, Abelian or non-Abelian (for some instructive reviews see [71; 72]). Recently, an interesting class of symmetries descending from the modular group $SL(2, Z)$ has dragged some attention. From a mathematical point of view, this symmetry describes a torus whose flat geometry can be viewed as it is cut open. The two dimensional space of the torus could be identified as the real and the imaginary axis of a complex plane spanning the upper half plane. The principal congruence subgroup of level N corresponds to a subset of matrices $\Gamma(N)$, whose determinant equals to unit and contains positive and negative integers. The connection between particle physics and modular symmetry lays at the understanding that extra dimensions in string theory are compactified in tori. Although the subgroups of $SL(2, Z)$ are infinite, finite symmetries can rendered by removing the infinite matrices, leaving only the quotient group:

$$\Gamma_N = PSL(2, Z)/\bar{\Gamma}(N) \ . \tag{1.3.36}$$

$$SL(2, Z) = \{\begin{pmatrix} a & b \\ c & d \end{pmatrix} | a, b, c, d \in Z, \ \det = 1\} \ . \tag{1.3.37}$$

Furthermore, the quoetients groups

$$\Gamma'_N \equiv SL(2, z)/\Gamma(N) \tag{1.3.38}$$

are denoted by the homogeneous finite modular groups. These matrices are two by two matrices with entries integers modulo N. The connections between the Γ_N and Γ'_N is given by:

$$\Gamma_N \cong \frac{\Gamma'_N}{\{\mathbf{1}, -\mathbf{1}\}} \tag{1.3.39}$$

The modular group can be generated by two elements S, T. Its transformation properties or the its action on the torus modulus τ are summarized below:

$$S = \begin{pmatrix} 0 & 1 \\ -1 & 0 \end{pmatrix}, \quad T = \begin{pmatrix} 1 & 1 \\ 0 & 1 \end{pmatrix}. \tag{1.3.40}$$

$$S : \tau \longrightarrow -\frac{1}{\tau}, \quad T : \tau \longrightarrow \tau + 1 \tag{1.3.41}$$

$$S^4 = (ST)^3 = 1, \quad S^2 T = T S^2 \, . \tag{1.3.42}$$

Additionally, the transformation properties of the modulus τ under the $SL(2, Z)$ is obtained by:

$$\tau \longrightarrow \gamma\tau = \gamma(\tau) = \frac{a\tau + b}{c\tau + d} \, . \tag{1.3.43}$$

In the rest of this section, we will describe how superymmetric theories include the notions of modular family symmetries on how to describe the Yukawa matrices depending only in a single modulus τ [73]. But, before proceeding in the following Table, the finite modular groups Γ_N up to order $N = 7$ are depicted.

N	Γ_N	$\lvert\Gamma_N\rvert$
2	S_3	6
3	A_4	12
4	S_4	24
5	A_5	60
6	$S_3 \times A_4$	72
7	$PSL(2, 7)$	168

Table 1.5: Finite modular groups of $SL(2, Z)$.

27 In the context of $\mathcal{N} = 1$ supersymmetry, the modular invariant supersymmetric theories [73; 74; 75] has the following action:

$$S = \int d^4x d^2\theta d^2\bar{\theta} K(\Phi_I, \bar{\Phi}_I, \tau, \bar{\tau}) + \Big(\int d^4x d^2\theta \mathcal{W}(\Phi_I, \tau) + h.c. \Big), \tag{1.3.44}$$

where K is the Kähler potential, where it is a real gauge invariant function of the superfields Φ_I. This action has to respect both the modular symmetry as well as the gauge symmetry of the SM or some GUT. The transformation properties of Φ_I are specified by the modular weight k_I and the corresponding representation r_I of Γ_N

$$\tau \longrightarrow \gamma\tau = \frac{a\tau + b}{c\tau + d}, \quad \Phi_I \longrightarrow (c\tau + d)^{-k_I} \rho_{r_I}(\gamma)\Phi_I \; . \tag{1.3.45}$$

AS for the Kähler potential, it takes the form

$$K(\Phi_i, \bar{\Phi}_I, \tau, \bar{\tau}) = -h\Lambda^2 \log(-i\tau + i\bar{\tau}) + \sum_I (-i\tau + i\bar{\tau})^{-k_I} |\Phi_I|^2, \quad h > 0 \; . \tag{1.3.46}$$

The above equation is invariant under the Kähler transformations, given the modular transformation of the moduli

$$\tau - \bar{\tau} \longrightarrow \frac{\tau - \bar{\tau}}{|c\tau + d|^2}, \tag{1.3.47}$$

$$K \longrightarrow K + h\Lambda^2 \log(c\tau + d) + h\Lambda^2 \log(c\bar{\tau} + d), \tag{1.3.48}$$

where the last two terms give null contribution after integrating the Grassmann coordinates θ [76; 77; 78; 79]. Regarding the superpotential $\mathcal{W}$, this can expanded into powers of the fields Φ_I

$$\mathcal{W} = \sum_n Y_{I_1..I_n}(\tau)\Phi_{I_1}...\Phi_{I_n}. \tag{1.3.49}$$

The functions Y_n are called modular forms of weight k_Y of level N are given by:

$$Y(\tau) \longrightarrow Y(\gamma\tau) = (c\tau + d)^{k_Y} \rho_{r_Y}(\gamma) Y(\tau), \tag{1.3.50}$$

where the important constraints imposed in the theory are:

$$k_Y = k_1 + ... + k_n, \quad \rho_{r_Y} \otimes ... \otimes \rho_{r_n} \ni \mathbf{1} \ . \tag{1.3.51}$$

The modular forms are defined as a holomorphic function of a variable τ

$$f(h\tau) = (c\tau + d)^k f(\tau), \quad h = \begin{pmatrix} a & b \\ c & d \end{pmatrix} \in \Gamma(N), \quad k > 0. \tag{1.3.52}$$

The linear space of these forms are denoted by $M_k(\Gamma(N))$ and its dimension is given by:

$$\dim M_k(\Gamma(N)) = \frac{(k-1)N + 6}{24} N^2 \Pi_p (1 - \frac{1}{p^2}), \quad N > 2, k \geq 2 \ . \tag{1.3.53}$$

Moreover, the automorphy factor $J(\gamma, \tau)$ is given by:

$$J(\gamma, \tau) = c\tau + d, \tag{1.3.54}$$

where the generic modular functions $F_{i\gamma} \equiv J^{-k} f_i(\gamma\tau)$ are transforming by

$$F_{i\gamma}(h\tau) = J^k(h, \tau) F_{i\gamma}(\tau), \quad F_{i\gamma}(\tau) = \rho_{ij}(\gamma) f_j(\tau) \ . \tag{1.3.55}$$

Observing the above equation, the ρ matrices are the representation matrices if the γ element is in the quotient group Γ_N. Consequently, there is always a basis of the modular form space, so that the $Y_r(\tau)$ are given:

$$Y_r(\gamma\tau) = (c\tau + d)^k \rho_r(\gamma) Y_r(\tau), \quad \gamma \in \Gamma, \quad \rho_r \in \Gamma_N \ . \tag{1.3.56}$$

2 Moduli Stabilization in type IIB string theory

Recent swampland conjectures [80; 81; 82] have sparked an interesting discussion regarding the nature of string theory vacua [1]. This hypothesis states that the string landscape does not contain stable dS vacua, although allow the possibility of metastable vacua. However, studies, by various researchers, have shown that dS minima are in principle accessible in string theory, when perturbative and non-perturbative dynamics are taken into account. Apparently, quantum corrections in string theory are of significant importance in shaping the scalar potential of the effective theory. As mentioned in section 1.3.1, during the past decades efforts have been focused on a solution to the moduli stabilization and dS vacua problems through introducing non-perturbative corrections and objects like D-branes [85; 86] [2]. The uplifting to dS space of the derived vacua can be attributed to a mechanism utilizing anti-D_3 branes ($\overline{D_3}$ for short), mainly used to the KKLT scenario, or by D-terms as explained in [93], where the leading order α'perturbative corrections [64] are also included in the Kähler potential dominating the small volume regime. [3]

The present work will be in the framework of type IIB string and F-theory compactifications with D_7-branes and fluxes, where the contributions from perturbative string-loop corrections [95] will be taken into account. Their origin can be traced back to higher derivative terms in the string action, whose effect is to generate a localized Einstein-Hilbert term. In the geometry of three intersecting D_7-branes, these contributions emerging as logarithmic corrections to the Kähler potential. Quantum corrections of this type are standard in the presence of D-branes and were also studied in the past [96; 97] although in different contexts. Also, in [98] it was shown that invariance of the effective classical action under $SL(2,R)$ transformations implies logarithmic corrections to the Kähler potential which depend on the untwisted Kähler moduli. Such contributions, break the no-scale structure of the Kähler potential and lead to an effective theory with

[1]For related reviews and further references see [83] and [84].

[2]For recent work on KKLT see [87]-[88] and for earlier contributions see [89; 90].For cases suggesting small $\mathcal{W}_0$ values see [91; 92].

[3]For a general review regarding four-dimensional compactifications with D-branes and fluxes see [94].

all Kähler moduli stabilised. Furthermore, D-term contributions related to the Abelian symmetries of the intersecting D_7- branes, work as an uplift mechanism and ensure the existence of dS vacua. This chapter features the combination of both the perturbative logarithmic corrections in the Kähler potential as well as non-perturbative contributions to the superpotential in the derivation of stable dS vacua in the four dimensional effective theory. Investigations will be focused on scenarios where the non-tivial non-perturbative corrections are only involving a subset of the available moduli, leaving the remaining scalar fields to be stabilized by the new quantum effects, where an additional implication is that they break the no-scale structure of the Kähler potential. Various string models favor such examples where some of the non-perturbative corrections in the superpotential are prohibited by Euclidean instanton contributions as described in [99] (see also[100]), where the world-volume fluxes lift fermionic zero modes preventing their generation. The following section contains the analysis of the previous mentioned approach. At first, the string quantum corrections are going to be presented and analyzed and the new contributions to the Kähler potential are going to be highlighted, in order to differentiate our methodology from previous studies. Moreover, two scenarios are investigated: the first one contains only one non-perturbative correction to the superpotential, while the latter studies the more complex case of multiple corrections. In both examples, the supersymmetric flatness conditions are scrutinized leading to various bounds on the internal fluxes and the free parameters of the theory. Moreover, an analysis of the aforementioned quantum corrections in fibred compactifications are summarized, pointing towards the effectiveness of those contributions to a broader spectrum of geometries. The uplifting of the AdS vacua will be performed by D-terms, resulting to completely stable dS vacua available for cosmological applications [101; 102]. In the last part of this chapter, the cosmological implications of these type of stabilized vacua are examined where logarithmic effects in the off-diagonal elements of the Kähler metric are taken into account. New contributions to the decays of moduli to axions are explored, which axions could comprise the particle nature of universe's dark radiation. Furthermore, a dark matter scenario is proposed based on the fact that moduli fields could also decay to degrees of freedom of the geometry's dark sector. These decays could potentially result into WIMPs where their mass lay in the range of order $\sim \mathcal{O}(10^3, 10^{11})\ GeV$.

2.1 Perturbative moduli stabilization

2.1.1 Quantum corrections in the Kähler potential

The notation for various fields used in the subsequent analysis is as follows: The dilaton and Kalb-Ramond fields are denoted with ϕ and B_2 respectively while the various p-form potentials with C_p, $p = 0, 2, 4$. The C_0 potential and the dilaton field ϕ are combined in the usual axion-dilaton combination:

$$S = C_0 + i\, e^{-\phi} \equiv C_0 + \frac{i}{g_s} \cdot$$

Finally, z_a, $a = 1, 2, 3, ...$ stand for the complex structure (CS) moduli and T_i, $i = 1, 2, 3, \ldots$ for the Kähler fields. The fluxed induced superpotential, $\mathcal{W}_0$, at the classical level is [103]

$$\mathcal{W}_0 = \int G_3 \wedge \Omega(z_a)\,, \tag{2.1.1}$$

with $\Omega(z_a)$ being the holomorphic (3,0)-form and $G_3 := F_3 - S\, H_3$, where the field strengths are $F_p := d\, C_{p-1}, H_3 := dB_2$. The perturbative superpotential $\mathcal{W}_0$ is a holomorphic function and depends on the axion-dilaton modulus S, and the CS moduli z_a. Thus, at the classical level, the supersymmetric conditions, $\mathcal{D}_{z_a}\mathcal{W}_0 = 0$ and $\mathcal{D}_S\mathcal{W}_0 = 0$ fix the moduli z_a, S, however, the Kähler moduli remain completely undetermined. At the same order, the Kähler potential depends logarithmically on the various fields, including the Kähler moduli

$$\mathcal{K}_0 = -\sum_{i=1}^{3} \ln(-i(T_i - \bar{T}_i)) - \ln(-i(S - \bar{S})) - \ln(-i \int \Omega \wedge \bar{\Omega}) \cdot \tag{2.1.2}$$

Then, the effective potential is computed using the standard formula

$$V_{\text{eff}} \;=\; e^{\mathcal{K}} \left(\sum_{I,J} \mathcal{D}_I \mathcal{W}_0 \mathcal{K}^{I\bar{J}} \mathcal{D}_{\bar{J}} \overline{\mathcal{W}}_0 - 3|\mathcal{W}_0|^2 \right) \cdot \tag{2.1.3}$$

In the absence of any radiative corrections, the latter vanishes identically due to supersymmetric conditions and the no scale structure of the Kähler potential. Hence, it is readily inferred that in order to stabilise the Kähler moduli it is necessary to go beyond the classical level. In fact, when quantum corrections are included they break the no-scale structure of the Kähler potential and presumably a non-vanishing contribution in the scalar potential, i.e. $V_{\text{eff}} \neq 0$, is feasible.

As already stated, in the quest for a stable dS minimum in effective string theories, the rôle of perturbative as well as non-perturbative corrections will be analysed. Furthermore it should be mentioned that this work takes place in the framework of type IIB string theory compactified on a 6-d Calabi-Yau (CY) manifold $\mathcal{X}_6$, and the 10-d space is $\mathcal{M}_4 \times \mathcal{X}_6$. The subsequent computations are assumed in the context of type IIB string theory compactified on the T^6/Z_N orbifold limit of the CY space. Furthermore, a geometric configuration consisting of three intersecting $D7$ branes is considered, while the internal volume $\mathcal{V}$ is expressed in terms of the imaginary parts v^i (the two-cycle volumes) of the Kähler moduli

$$\mathcal{V} = \frac{1}{6}k_{ijk}v^i v^j v^k, \; v^i = -\mathrm{Im}(T^i) \,, \tag{2.1.4}$$

where k_{ijk} are intersection numbers. The v^i are related to 4-cycle volumes τ_i as follows:

$$\tau_i = \frac{1}{2}k_{ijk}v^j v^k \,. \tag{2.1.5}$$

In the present case it is simply assumed that $\mathcal{V} = v^1 v^2 v^3$ or, in terms of the 4-cycle volumes τ_i's:

$$\mathcal{V} = \sqrt{\tau_1\tau_2\tau_3} \,. \tag{2.1.6}$$

After these preliminaries, in the remaining of this section the various types of corrections will be presented.

Starting with non-perturbative corrections of the superpotential, in principle, all three Kähler moduli considered in this model may contribute. In this case the superpotential takes the form

$$\mathcal{W} = \mathcal{W}_0 + \sum_{k=1}^{3} A_k e^{i a_k \rho_k} \,, \tag{2.1.7}$$

In the above formula, $\rho_k = b_k + i\tau_k$ where b_k is associated with the RR C_4 form, τ_k is given by (2.1.5) and $\mathcal{W}_0 = \int G_3 \wedge \Omega$ is the tree-level superpotential in (2.1.1). The second term in the right-hand side of (2.1.7) is the non-perturbative part [104]. The constants A_i in general depend on the complex structure moduli and the a_i parameters are assumed to be small (for example in the case of gaugino condensation in an $SU(N)$, they are of the form $\frac{2\pi}{N}$). However, it maybe possible that the choice of world-volume fluxes [99] allow only some of the Kähler moduli fields to have non-vanishing non-perturbative (NP) contributions. Before proceeding to the next step, some comments are due with respect to (w.r.t.) the reliability of the instanton correction and the specific choices in the subsequent analysis. This type of corrections originates from the presence of Euclidean D3-branes wrapping four-cycles in the base of the compactification [104]. First of all, in order the supergravity approximation to be valid, the condition $\tau_1 \geq 1$ should be fulfilled. Two main reasons are in favor of this argument. First, shrinking one direction to small volume

leads to highly curved Kähler cones or orbilfolds where the effective approximation is at stake. Second, the logarithmic correction [96] that has been added in the Kähler potential requires large transverse directions τ_i. We come back to this issue in section 3.2.
Next, quantum corrections to the Kähler potential will be discussed, starting with the $\alpha^{'3}$ contributions, which, in the large volume limit imply a redefinition of the dilaton field [64]

$$e^{-2\phi_4} \quad = \quad e^{-2\phi_{10}}(\mathcal{V}+\xi) = e^{-\frac{1}{2}\phi_{10}}\,(\hat{\mathcal{V}}+\hat{\xi})\,\cdot \tag{2.1.8}$$

The last expression on the right-hand side of (2.1.8) holds in the Einstein frame and the volume is written in terms of the imaginary parts of the Kähler deformations T^k as follows

$$\mathcal{V} = \frac{1}{3!}\kappa_{ijk}v^i v^j v^k,\ v^k = -\mathrm{Im}(T^k) = \hat{v}^k\, e^{\frac{1}{2}\phi_{10}}\,\cdot \tag{2.1.9}$$

The modifications in the Kähler potential correspond to a shift of the volume by a constant ξ which is determined in terms of the Euler characteristic $\xi = -\frac{\zeta(3)}{4(2\pi)^3}\chi$.
The origin of the second type of corrections comes from higher derivative terms which give rise to multigraviton scattering in string theory. In type IIB theories, the leading terms appearing in the 10-dimensional effective action are proportional to R^4, where R is the Riemann curvature. In theories with $\mathcal{N}=1$ sypersymmetry in 10 dimensions, the leading corrections already appear at order R^2. Here, the terms of interest to us are the R^4 couplings, which, after compactification to four dimensions $\mathcal{X}_{10}\to\mathcal{M}_4\times\mathcal{X}_6$, they induce a new Einstein-Hilbert (EH) term, multiplied by the Euler characteristic of the manifold. The one-loop amplitude of the on-shell scattering involving four gravitons has been worked out in [105; 106; 107; 108; 109; 110; 111; 112] where it has been shown that the ten-dimensional action reduces to

$$\mathcal{S}_{\rm grav} \quad = \quad \frac{1}{(2\pi)^7\alpha'^4}\int\limits_{M_4\times\mathcal{X}_6} e^{-2\phi}\mathcal{R}_{(10)} - \frac{\chi}{(2\pi)^4\alpha'}\int\limits_{M_4}\Big(-2\zeta(3)e^{-2\phi}\pm 4\zeta(2)\Big)\,R_{(4)}\,, \tag{2.1.10}$$

where $R_{(4)}$ denotes the ‘reduced’ Riemann tensor in four dimensions, the $\pm$ signs refer to the type IIA/B theory respectively, and the Euler characteristic is defined as

$$\chi = \frac{3}{4\pi^3}\int\limits_{\mathcal{X}_6} R\wedge R\wedge R\,\cdot \tag{2.1.11}$$

From (2.1.10), it is observed that a localised EH term [4] is generated with a coefficient propor-

[4]The computations have been performed in the orbifold limit [95] and localisation occurs at the orbifold fixed points p_i. These points correspond to the singularities where the Euler number is non-vanishing and in general

tional to χ defined in (2.1.11). Consequently it is inferred that this term is possible only in four dimensions. In the geometry of the bulk space, the $R_{(4)}$ EH terms of (2.1.10) correspond to vertices at points where $\chi \neq 0$, and as such, they emit gravitons and Kaluza-Klein (KK) excitations in the six-dimensional space. Furthermore, in the presence of $D7$ branes which are an essential ingredient of the internal space configurations in type IIB and F-theory, new types of quantum contributions emerge. It is found thereby that the exchange of closed string modes between the EH-vertices and $D7$ branes and $O7$-planes give rise to logarithmic corrections. These take the form [95]

$$\frac{4\zeta(2)}{(2\pi)^3}\chi\int_{M_4}\left(1-\sum_k e^{2\phi}T_k\ln(R_\perp^k/\mathtt{w})\right)R_{(4)}\ . \tag{2.1.12}$$

In the above, T_k is the tension of the k^{th} 7-brane, $R_\perp$ stands for the size of the two-dimensional space transverse to the brane, and $\mathtt{w}$ is a 'width' related to an effective ultraviolet cutoff for the graviton KK modes propagating in the bulk [109].

2.1.2 Effective potential

In this section, we are going to present two examples of scalar potentials augmented by both perturbative and non-perturabtive corrections. The stability conditions will be presented in parallel with the flatness conditions of the superpotential, whose ffect is to provide an insight to the scale of the internal fluxes. In the first example, we assume that only the τ_1 modulus induces a non-vanishing contribution in the NP part of the superpotential, thus

$$\mathcal{W}=\mathcal{W}_0+Ae^{ia\rho_1}\ . \tag{2.1.13}$$

As for the quantum corrections, they are parametrizing all the Kähler moduli of the geometric configuration and they are given by

$$\delta=\xi+\sum_{k=1}^{3}\eta_k\ln(\tau_k), \tag{2.1.14}$$

where an additional assumption is that all the D_7-branes have the same sting tension. This will lead to a more compact description of the logarithmic factor. The coefficients η_k and ξ are defined by

$\chi=\sum_i\chi_{p_i}$. In this sense, the existence of the term $\mathcal{R}_{(4)}$ is associated with these points, hence the term "localised gravity".

$$\eta_k \equiv \eta = -\frac{1}{2} g_s T_0 \quad ; \quad \xi = -\frac{\chi}{4} \times \begin{cases} \frac{\pi^2}{3} g_s^2 & \text{for orbifolds} \\ \zeta(3) & \text{for smooth CY} \end{cases} . \tag{2.1.15}$$

Taking into account the above corrections, the Kähler potential takes the form

$$\mathcal{K} = -2\ln\left(\sqrt{\tau_1\tau_2\tau_3} + \xi + \eta\ln(\tau_1\tau_2\tau_3)\right) \equiv -2\ln(\mathcal{V} + \xi + \eta\ln\mathcal{V}) \ \cdot \tag{2.1.16}$$

The covariant derivative of the superpotential w.r.t. the Kähler modulus ρ_1 is defined in the usual manner, i.e., $D_{\rho_1} W = \partial_{\rho_1}\mathcal{W} + \mathcal{W}\partial_{\rho_1}\mathcal{K}$. Working in the large volume limit, terms proportional to ξ and η coefficients compared to the volume $\mathcal{V}$ are ignored. Writing the Kähler potential as

$$\mathcal{K} = -2\log(\sqrt{(\rho_1-\bar\rho_1)(\rho_2-\bar\rho_2)(\rho_3-\bar\rho_3)} + O(\eta,\xi)) \tag{2.1.17}$$

and taking the derivatives [5]

$$\partial_{\rho_1}\mathcal{W} = i\alpha A e^{i\alpha\rho_1}, \quad \partial_{\rho_1}\mathcal{K} = -\frac{1}{\rho_1-\bar\rho_1} \tag{2.1.18}$$

it is readily found that

$$D_{\rho_1}\mathcal{W}\Big|_{\rho_1=i\tau_1} = i e^{-\alpha\tau_1}\left(\alpha A + \frac{A+\mathcal{W}_0 e^{\alpha\tau_1}}{2\tau_1}\right) \cdot \tag{2.1.19}$$

The corresponding supersymmetric condition, $D_{\rho_1}\mathcal{W} = 0$, fixes the value of the modulus $\tau_1 = \mathrm{Im}\rho_1$ in terms of the tree-level superpotential $\mathcal{W}_0$ (determined by the choice of the fluxes) and the coefficients α, A - related to non-perturbative contributions. Thus, the vanishing of the derivative (2.1.19) yields

$$\tau_1 = -\frac{1+2w}{2\alpha}\,, \tag{2.1.20}$$

where w represents either of the two branches W_0, W_{-1}, of the Lambert W-function

$$w = W_{0/-1}\left(\frac{\gamma}{2\sqrt{e}}\right)\,. \tag{2.1.21}$$

In (2.1.21), the convenient definition has been introduced

$$\gamma = \frac{\mathcal{W}_0}{A} \cdot \tag{2.1.22}$$

[5]We denote with calligraphic letters $\mathcal{W}_0, \mathcal{W}$ the tree-level and corrected superpotential and reserve the symbols W, W_0, W_{-1} for the Lambert W-function.

Real values of the solution are compatible with the bound $\gamma \geqslant -2e^{-1/2} \approx -1.213$ for both branches. For the "lower" branch W_0, equation (2.1.20) implies the constraint $\alpha\tau_1 \leqslant 1/2$. Requiring also $\alpha\tau_1 > 0$ it is found that the ratio $\gamma = \mathcal{W}_0/A$ is confined in the region:

$$-1.213 \leq \gamma \leq -1 \cdot \tag{2.1.23}$$

This solution is depicted with the blue curve in figure 2.1. The corresponding regions for the "higher" branch W_{-1}, depicted with the orange curve in figure 2.1, are

$$-1.213 \leq \gamma \leq 0\,, \tag{2.1.24}$$

and $\alpha\tau_1 \in [\frac{1}{2}, \infty]$.

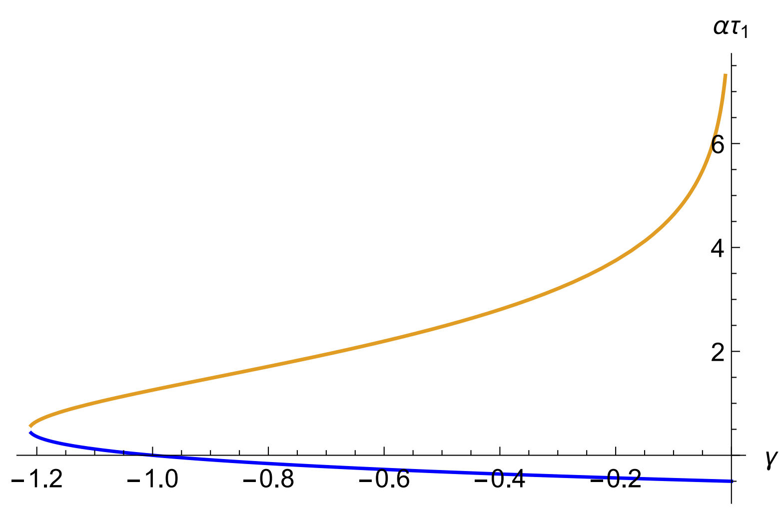

Figure 2.1: Plot of solution (2.1.20) for $\alpha\tau_1$ as a function of the ratio $\gamma = \frac{\mathcal{W}_0}{A}$. The orange (upper) and blue (lower) curves represent the W_{-1} and W_0 branches, respectively. Acceptable values ($\alpha\tau_1 > 0$) for the blue curve are compatible only with its section satisfying $\gamma < -1$.

The F-term scalar potential is computed by inserting (2.1.2) into (2.1.3). This yields a rather complicated formula which is not very illuminating, however, in the large volume limit it suffices to expand it w.r.t. the small parameters η and $\xi/\mathcal{V}$ and obtain a simplified form. Thus, without loosing its essential features, in this approximation the potential is written as a sum of three parts, as follows:

$$V_F \approx V_{F_1} + V_{F_2} + V_{F_3} \cdot \tag{2.1.25}$$

The various parts of the RHS in (2.1.25) are given by

$$\begin{aligned}
V_{F_1} &= \frac{3}{2}\mathcal{W}_0^2\,\frac{\xi - 2\eta(4-\ln\mathcal{V})}{\mathcal{V}^3} - 9\mathcal{W}_0^2\frac{\xi\eta\log(\mathcal{V})}{\mathcal{V}^4}\,,\\
V_{F_2} &= 4\frac{\alpha\tau_1}{\mathcal{V}^2}\tilde{A}(\tilde{A} + a\tau_1\tilde{A} + \mathcal{W}_0)\,,\\
V_{F_3} &= \tilde{A}(\tilde{A}\,f + \mathcal{W}_0\,g)\,\cdot
\end{aligned} \tag{2.1.26}$$

where $\tilde{A} = e^{-\alpha\tau_1}A$ and $O(\frac{1}{\mathcal{V}^5})$ or higher terms in the expansion are ignored. Also

$$\begin{aligned}
f =& \frac{3\xi - 8\eta(2\alpha\tau_1(2\alpha\tau_1+3)+3) - 4\xi\alpha\tau_1(\alpha\tau_1+1) - 2\eta(2\alpha\tau_1-1)(2\alpha\tau_1+3)\log\mathcal{V}}{2\mathcal{V}^3}\\
&+ \frac{\eta\xi(2\alpha\tau_1+3)((6\alpha\tau_1-3)\log\mathcal{V} - 4\alpha\tau_1)}{\mathcal{V}^4},\\
g =& \frac{(3-2\alpha\tau_1)\,(\xi + 2\eta\log(\mathcal{V})) - 24\eta(1+\alpha\tau_1)}{\mathcal{V}^3} - 6\eta\xi\frac{(3-2\alpha\tau_1)\log\mathcal{V} + 2\alpha\tau_1}{\mathcal{V}^4}\,\cdot
\end{aligned}$$

In the above all three Kähler moduli τ_i are expressed in terms of the volume $\mathcal{V}$ with τ_1 being considered at its critical value τ_1^{cr} given in (2.1.20), fixed from the supersymmetric conditions imposed on the superpotential. Therefore, only the two of them, namely τ_2 and τ_3 are left undetermined which appear only in the combination $\tau_2\tau_3 = \mathcal{V}/\tau_1^{cr}$ [6]. It is to be noted that, since there are regions of solutions $D_{\rho_1}\mathcal{W} = 0$, where τ_1 is hierarchically smaller than the rest of the moduli and $\alpha\tau_1$ receives relatively moderate values, (see figure 2.1), terms involving $\tilde{A}^2$ have also been retained. It should be further pointed out that, in principle, there are regions of the parameter space (in particular those with large values of τ_1^{cr}) where such terms are comparable to $\mathcal{V}^{-5}$, the latter being omitted in the large volume expansion. Then, $\tilde{A}^2$ terms could be safely neglected too. In this case non-perturbative corrections are suppressed and the perturbative logarithmic corrections prevail. One of the objectives of this work, however, is to also probe regions where all terms of (2.1.26) have comparable contributions to the total potential in (2.1.25).

At this point, it is worth clarifying the origin of the components (2.1.26). The term V_{F_1} is derived from the α' and perturbative string loop corrections due to the localised EH terms, both entering in the Kähler potential (2.1.16). Indeed, switching off the non-perturbative corrections, i.e. setting $A = 0$, the only term remaining in (2.1.26) is the V_{F_1} component which is identified with the one given in [113] where only perturbative corrections are studied. Setting η and ξ equal to zero, the only term that remains is the second component, V_{F_2}. This contribution comes exclusively from the non-perturbative corrections which were included in the superpotential. Finally, the third component V_{F_3} is a mixing term and it is non-vanishing only when both perturbative and non-

[6] From now on, we drop "cr" from τ_1^{cr} and write just τ_1 for simplicity.

perturbative corrections are present. As an additional check with regard to the non-perturbative part, the appropriate limit of (2.1.26) is taken to reproduce the already known results in the literature [85]. Indeed, for $\eta = \xi = 0$ the scalar potential becomes

$$V_{F_2} = \frac{4e^{-2\alpha\tau_1}\alpha A}{\tau_2\tau_3}(e^{\alpha\tau_1}\mathcal{W}_0 + A + \alpha\tau_1 A) \cdot \tag{2.1.27}$$

Solving (2.1.19) w.r.t. the $\mathcal{W}_0$, it is found that:

$$\mathcal{W}_0 = -Ae^{-\alpha\tau_1}(1 + 2\alpha\tau_1) \cdot \tag{2.1.28}$$

Substituting in (2.1.27) while putting $\tau_3 \longrightarrow \tau, \tau_2 \longrightarrow \tau, \tau_1 \longrightarrow \tau$ the result is

$$V_{min} = -\frac{4e^{-2\alpha\tau}\alpha^2A^2}{\tau}\,, \tag{2.1.29}$$

which (up to numerical factor related to the multiplicity of the Käher moduli) coincides with the solution of [85]. To proceed with the minimisation of the scalar potential (2.1.26), a more convenient form will be worked out. To this end, the following parameter is introduced

$$\epsilon = \frac{2w + 1}{w} \cdot \tag{2.1.30}$$

Furthermore, for later convenience, the range of the various parameters defined up to this point for the two branches of the solution are shown in Table 2.1. As already noted, in the LVS regime it would be more suitable to have large directions given by the lower branch W_{-1}. However, these solutions represent instanton corrections, and as it is obvious, the W_0 branch is a strongly coupled region, where higher order corrections should be taken into account. For the reasons discussed above and for the correctness of the effective approach, from now on only the W_{-1} branch will be considered as the solution for the τ_1 modulus. [7]

Using the above definitions, and the identities $2w = \gamma e^{\alpha\tau_1} = -(2\alpha\tau_1 + 1)$ resulting from (2.1.20-2.1.22) the F-term potential (2.1.25) can be cast in a convenient compact form. Considering the V_{F_2} piece in particular, under successive substitutions of $\gamma = \frac{\mathcal{W}_0}{A}$, $2\alpha\tau_1 = -(1+2w)$ and $\gamma e^{\alpha\tau_1} = 2w$ its third term gives

$$\frac{4\alpha\tau_1 A\mathcal{W}_0 e^{-\alpha\tau_1}}{\mathcal{V}^2} = -2\frac{\mathcal{W}_0^2(1 + 2w)}{\gamma e^{\alpha\tau_1}\mathcal{V}^2} = -\frac{\mathcal{W}_0^2(1 + 2w)}{w\mathcal{V}^2} \tag{2.1.31}$$

[7] The current understanding of the non-perturbative physics prevent a complete study of the other branch. A way of treating instanton corrections from $D3$-branes is presented in [114].

Branch	$a\tau$	γ	w	ϵ
$w = W_0(\frac{\gamma}{2\sqrt{e}})$	0	-1	$-\frac{1}{2}$	0
	$\frac{1}{2}$	$-\frac{2}{\sqrt{e}}$	-1	1
$w = W_{-1}(\frac{\gamma}{2\sqrt{e}})$	∞	0	$-\infty$	2
	$\frac{1}{2}$	$-\frac{2}{\sqrt{e}}$	-1	1

Table 2.1: The range of the various parameters used in the analysis.

Continuing as above, it is found that all three terms of V_{F_2} add up to:

$$V_{F_2} = -\frac{\mathcal{W}_0^2}{\mathcal{V}^2}\frac{(1+2w)^2}{4w^2} = -\frac{(\varepsilon \mathcal{W}_0)^2}{4\mathcal{V}^2} \,.$$

Finally, the following compact form of the whole V_F potential is obtained

$$V_F \approx (\epsilon \mathcal{W}_0)^2 \left(\frac{2\xi - \mathcal{V} + 4\eta(\log(\mathcal{V}) - 1)}{4\mathcal{V}^3} - \eta\xi\frac{3\log(\mathcal{V}) - 1}{\mathcal{V}^4}\right) + \mathcal{O}\left(\frac{1}{\mathcal{V}^5}\right) \,. \tag{2.1.32}$$

In the present approximation, valid in the large volume limit, it is observed that the parameters associated with the non-perturbative effects appear in the F-term potential as an overall positive-definite factor ϵ^2 where ϵ is defined in (2.1.30). Thus, the shape of V_F is controlled by the second factor which exhibits the volume dependence and involves the parameters ξ and η coming from the perturbative corrections in the Kähler potential. Indisputably, the properties of the potential depend decisively on the signs of ξ, η given in (2.1.15) which convey topological and geometric information of the compactification manifold. For closed orientable smooth manifolds and the particular D7-branes set up [95] in the present study the choice $\chi < 0, \xi > 0$ will be adopted. Then, dropping the subleading terms of order $\propto \frac{1}{\mathcal{V}^4}$ and higher in the large volume regime, and requiring the vanishing of the first derivative, it is found that the volume at the minimum of the potential is given by

$$\mathcal{V}_{\min} = -6\eta\, W_0\left(-\frac{1}{6\eta}e^{\frac{4}{3}-\frac{\xi}{2\eta}}\right) \,, \tag{2.1.33}$$

where W_0 is the Lambert W-function. Substituting $\mathcal{V}_{\min}$ into the second derivative yields:

$$\frac{d^2 V_F}{d\mathcal{V}^2} = (\epsilon \mathcal{W}_0)^2 \frac{\mathcal{V} - 6\eta}{2\mathcal{V}^5} \,. \tag{2.1.34}$$

Hence, a minimum exists as long as $\mathcal{V} \geqslant 6\eta$ which is obviously true in the large volume regime, although this corresponds to an AdS vacuum. Nonetheless, this can be naturally uplifted to a dS minimum, when D-term contributions are taken into account. It should be pointed out too, that minimisation of V_F w.r.t. $\mathcal{V}$ stabilises only the combination $\tau_2\tau_3 = \mathcal{V}/\tau_1$ leaving another independent combination of τ_2, τ_3 moduli undetermined. This will also be rendered with the inclusion of the D-terms in the next section.

In the next paradigm, we will examine the case where the flux induced superpotential $\mathcal{W}_0$, receives non-perturbative corrections from two Kähler moduli, ρ_1 and ρ_2. In this case, the superpotential takes the form:

$$\mathcal{W} = \mathcal{W}_0 + Ae^{ia\rho_1} + Be^{ib\rho_2}\ , \ \text{with } a > 0 \text{ and } b > 0\ . \tag{2.1.35}$$

Cases with two exponentials capture many new features and have been discussed in the literature in particular constructions. The racetrack form [115] suitable for cosmological applications could be considered as a particular case when both exponents of (2.1.35) involve the same modulus, i.e., when ρ_2 in replaced with ρ_1 in the second exponential. In general, two or more exponential terms imply a richer structure for the shape of V_{eff} which could exhibit saddle points between different vacua of the theory, so that successful types of inflationary scenarios can be realized [116]. Despite the vast literature devoted on such issues, the combined effects of (2.1.35) with perturbative logarithmic corrections to the Kähler potential have not been investigated so far. These ingredients are a generic feature of the effective theories derived from the 10-dimensional superstring action and thence it is the main subject of the subsequent analysis. In the present setup, the contribution of the moduli ρ_1, ρ_2 in the superpotential enters through the non-perturbative corrections, and thus, the appropriate flatness conditions must be imposed. The latter imply the vanishing of the corresponding covariant derivatives $D_{\rho_i}W = \partial_{\rho_i}\mathcal{W} + \mathcal{W}\partial_{\rho_i}\mathcal{K}$. Introducing the expansions with respect to $\eta/\mathcal{V}$ and $\xi/\mathcal{V}$ in the large volume limit, it is readily found that

$$D_{\rho_1}\mathcal{W}|^{\rho_2=i\tau_2}_{\rho_1=i\tau_1} = -\frac{A(e^{-a\tau_1}(1+2a\tau_1)+\beta e^{-b\tau_2}+\gamma)}{2\tau_1} + \mathcal{O}(\eta,\xi) = 0, \tag{2.1.36}$$

$$D_{\rho_2}\mathcal{W}|^{\rho_2=i\tau_2}_{\rho_1=i\tau_1} = -\frac{A(e^{-a\tau_1}+e^{-b\tau_2}(1+2b\tau_2)\beta+\gamma)}{2\tau_2} + \mathcal{O}(\eta,\xi) = 0\ , \tag{2.1.37}$$

where β, γ, stand for the following ratios :

$$\beta = \frac{B}{A},\ \gamma = \frac{\mathcal{W}_0}{A}\ . \tag{2.1.38}$$

If some reasonable assumptions concerning the various flux parameters and the range of moduli fields are made, the solutions of the above transcendental equations can be expressed in closed form with good accuracy, in terms of known functions. A possible choice of the approximations can be better perceptible as follows: The two equations (2.1.36) and (2.1.37) are combined to give

$$a\tau_1\, e^{-a\tau_1} = \beta\, b\tau_2\, e^{-b\tau_2}\ . \tag{2.1.39}$$

Since a, b are positive constants, it turns out that $\beta > 0$, while real solutions of (2.1.36,2.1.37) exist as long as $\gamma < 0$. The equation (2.1.39) is plotted in figure (2.2) for several values of β in the parametric space defined by the pair $(a\tau_1, b\tau_2)$. The curves of the left panel correspond to values $\beta < 1$ and the ones on the right, to $\beta > 1$. (For $\beta = 1$ a trivial solution exists $a\tau_1 = b\tau_2$ represented by the diagonal, not shown in the figure). The parametric space has been split into four regions I, II, III, IV with respect to the ranges of $a\tau_1$ and $b\tau_2$. Region I corresponds to large values of $a\tau_1, b\tau_2$ and thus, both terms of the non-perturbative contributions in (2.1.35) are suppressed. In general, in the large volume regime, perturbative logarithmic corrections are expected to prevail. In the opposite limit, region III corresponds to small values of $a\tau_1, b\tau_2$, and both NP-contributions become sizable, however, in this case large $\mathcal{V}$ requires τ_3-values much bigger than τ_1, τ_2. A drawback of this region is that non-perturbative corrections correspond to the large coupling regime and as such they are not fully controllable. Nevertheless, for the sake of completeness a short analysis will be presented in a subsequent section. Finally, the regions II and IV, for typical values of the gaugino condensation parameters $a = \frac{2\pi}{M} \sim b = \frac{2\pi}{N}$, can be associated with cases where there could be a milder hierarchy between the moduli fields $\tau_{1,2,3}$. Then, at least one NP-term in (2.1.35) could makesignificant contribution to the superpotential and it would be interesting to investigate its implications.

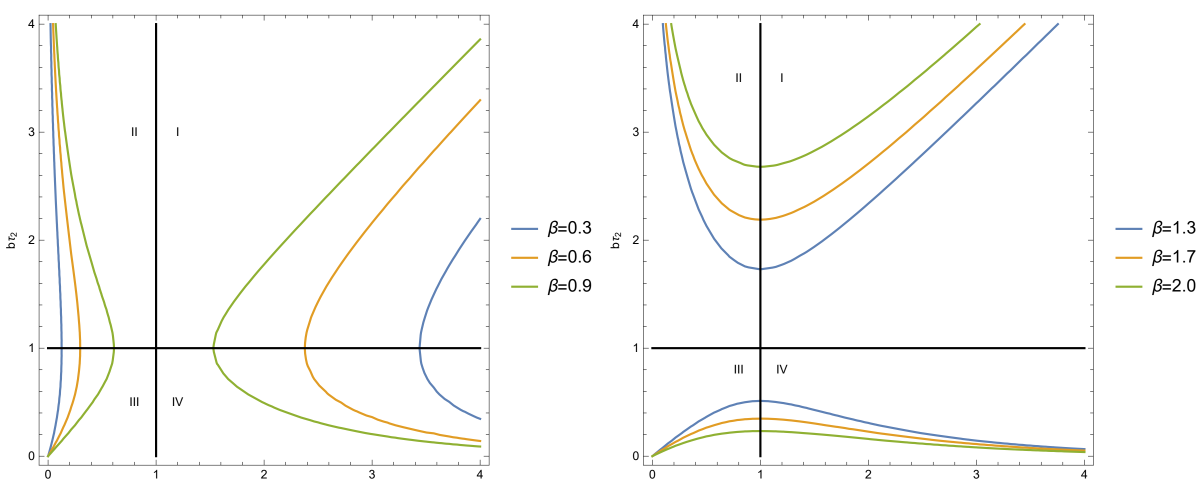

Figure 2.2: Graphical solution of Eq (2.1.39) for various values of the parameter $\beta = B/A$ defined in (2.1.38). The left panel shows curves for three values of $\beta < 1$ and the right panel for $\beta > 1$.

The present study will proceed with the investigation of the properties of V_{eff} in reasonable parts of the regions defined in figure 2.2, that is, regions with $a\tau_1 \ll 1$ and $b\tau_2 \ll 1$ will be excluded from the analysis. In the present section the F-term scalar potential will be analyzed and as a first approach, the restriction

$$\beta e^{-b\tau_2} \ll |\gamma| \leftrightarrow Be^{-b\tau_2} \ll |\mathcal{W}_0| \,, \tag{2.1.40}$$

will be imposed which entails a non-perturbative part $Be^{-b\tau_2}$ much smaller than the flux induced tree-level superpotential $|\mathcal{W}_0|$. It should be noted that in the large volume regime small fluxes discussed in recent works [91; 117; 118; 119], are not excluded by the assumption imposed above. For example, for $\mathcal{W}_0 \sim 10^{-8}$, condition (2.1.40) is satisfied[8], for $\beta \sim O(1)$ and $b\tau_2 > 20$. As it will be seen in the subsequent analysis, in this limiting case it is possible to present sufficiently accurate analytic formulae for the flatness solutions and achieve a compact form of V_{eff}. A different approach where this condition is relaxed will be presented in a subsequent section.

From (2.1.39) the first term of (2.1.40) is $\beta\, e^{-b\tau_2} = \frac{a\tau_1}{b\tau_2}\, e^{-a\tau_1}$. Hence, the approximation is valid for small fluxes associated with the coefficient B and/or large hierarchies $b\tau_2 \gg a\tau_1$. Thus, the focus of the analysis in the present section will be on the appropriate sections of the regions *I* and *II* where the hierarchy $a\tau_1 \ll b\tau_2$ holds (a similar analysis for region *IV* is appropriate for $a\tau_1 \gg b\tau_2$). The case of region *III* will be analyzed using a different parametrization.

In addition, the energy scale and the coefficients a, b related to gaugino condensations on each brane can differ. Under these assumptions, the equations (2.1.36,2.1.37) reduce to:

$$\begin{aligned} D_{\rho_1}\mathcal{W}|^{\rho_2=i\tau_2}_{\rho_1=i\tau_1} &= -A\frac{e^{-a\tau_1}(1+2a\tau_1)+\gamma}{2\tau_1} \approx 0, \\ D_{\rho_2}\mathcal{W}|^{\rho_2=i\tau_2}_{\rho_1=i\tau_1} &= -A\frac{e^{-a\tau_1}+2b\tau_2\beta\, e^{-b\tau_2}+\gamma}{2\tau_2} \approx 0\,. \end{aligned} \tag{2.1.41}$$

It is convenient to solve the above with respect to the moduli fields τ_1, τ_2. Defining the new variables w, u

$$w = -\frac{1+2a\tau_1}{2}, \;\; u = -b\tau_2\,, \tag{2.1.42}$$

[8]Considering the recent activity for the quest of vacua with exponentially small $\mathcal{W}_0$, it would be worth commenting on this parametric region. According to [120], the plethora of flux vacua could be described as a statistical ensemble where the value of $\mathcal{W}_0$ plays a significant rôle. Models with $\overline{D3}$ uplift, such as [85], are based on the conifold geometry for the D-brane configurations [26; 121], since the dilaton and the CS moduli are parametrically heavier than the Kähler fields and could be effectively integrated out. A large amount of CS moduli (which is the case for the most well studied CY manifolds) requires big D_3 charges in order to satisfy the tadpole cancellation. Consequently, this implies small values for $\mathcal{W}_0$ at the weak coupling regime as it is also predicted by the statistical analysis.

the solutions are expressed as follows [9]

$$\begin{aligned} w \equiv w(\gamma) &= W(\frac{\gamma}{2\sqrt{e}}), \\ u \equiv u(\gamma) &= W\left(\frac{\sqrt{e}\; e^{w} + \gamma}{2\beta}\right) \\ &\equiv W\left(\frac{\gamma}{\beta}\frac{1+2w}{4w}\right) . \end{aligned} \tag{2.1.43}$$

In the above solution, W stands for either of the two branches W_0, W_{-1} of the Lambert-W function. For large τ_2 values however, the function W in (2.1.43) should be identified with the branch W_{-1}. For later convenience, the following parameters are also introduced:

$$\varepsilon = \frac{1+2w}{w}, \quad \tilde{\varepsilon} = \frac{\varepsilon}{u} . \tag{2.1.44}$$

The restriction to real values of the two branches W_0, W_{-1} imposes the bounds on the various new parameters shown in Table 2.2. The approximation (2.1.40) is valid only for regions I and II where $u \equiv -b\tau_2 < -1$.

	γ	β	w	u	$\tilde{\epsilon}$
I	$(-\frac{2}{\sqrt{e}}, 0)$	$(0, \infty)$	$(-\infty, -\frac{3}{2})$	$(-\infty, -1)$	$(-2, 0)$
II	$(-\frac{2}{\sqrt{e}}, -1)$	$(0, \infty)$	$(-1, -\frac{1}{2})$	$(-\infty, -1)$	$(-1, 0)$
III	$(-\frac{2}{\sqrt{e}}, -1)$	$(0, \infty)$	$(-1, -\frac{1}{2})$	$(-1, 0)$	$(-\infty, 0)$
IV	$(-\frac{2}{\sqrt{e}}, 0)$	$(0, \infty)$	$(-\infty, -\frac{3}{2})$	$(-1, 0)$	$(-\infty, 0)$

Table 2.2: Limiting values of different parameters for each one of the regions depicted in Figure 2.2.

Formally the V_F term comprises of three parts, the pure perturbative and non-perturbative parts and a term which is a mixing of both. Before presenting the total V_F, it is useful to examine separately the form of the perturbative and non-perturbative parts. For example, implementing the expansion with respect to η and $\xi/\mathcal{V}$ the perturbative part receives the following simplified form

$$V_F^{(p)} \approx \frac{3}{2}\mathcal{W}_0^2 \frac{\xi + 2\eta \log(\mathcal{V})}{\mathcal{V}^3} + O(\frac{1}{\mathcal{V}^4}) . \tag{2.1.45}$$

[9] For example, the two equations imply $e^{-a\tau_1}(1+2a\tau_1) = -\gamma \Rightarrow 2we^{-a\tau_1} = \gamma$ or $we^{w} = \frac{\gamma}{2\sqrt{e}}$ etc.

From this simplified form of the perturbative part (2.1.45) it is observed that the numerator consists of two terms of different volume dependence. For $\eta < 0$ and $\xi > 0$ in particular $V_F^{(p)}$ acquires a minimum at $\mathcal{V}_0 = e^{\frac{1}{3}+\frac{\xi}{2|\eta|}}$, however the value of the potential at the minimum is negative, $(V_F^{(p)})_{min} = \frac{2}{3}\eta e^{\frac{3\xi}{2\eta}-1} < 0$, i.e., it defines an Anti de Sitter (AdS) vacuum.
The pure non-perturbative part $V_F^{(np)}$ becomes

$$V_F^{(np)} = -\mathcal{W}_0^2 \frac{(u+1)(2w+1)^2}{2uw^2\mathcal{V}^2} \equiv -(\tilde{\varepsilon}\mathcal{W}_0)^2 \frac{u(u+1)}{2\mathcal{V}^2} \,. \tag{2.1.46}$$

Remarkably, this term has a volume dependence $\propto \frac{1}{\mathcal{V}^2}$ which is exactly the dependence of the D-term uplift in ((2.1.103)). For the regions I, II where the approximation is valid, however, because $u(1+u) > 0$ the contribution of this term is negative and deepens the AdS vacuum.[10] The full F-part of the scalar potential comprising all those three parts can be written in a simple form using (2.1.39). These manipulations yield

$$V_F \approx (\tilde{\varepsilon}\mathcal{W}_0)^2 \left(-\frac{u(u+1)}{2\mathcal{V}^2} + \frac{(2u+1)(14u+3)(\xi+2\eta)\log(\mathcal{V}) - 24\eta}{32\mathcal{V}^3} + \right. \tag{2.1.47}$$

$$\left. + \eta\xi \frac{48u - \left(68u^2+60u+9\right)\log\mathcal{V}}{32\mathcal{V}^4} \right) \,. \tag{2.1.48}$$

It is again emphasized that this form is valid for the regions I, II and cannot be used to describe the physics for regions III and IV. In the large volume case where the term $\propto \frac{1}{\mathcal{V}^4}$ can be safely ignored, the minimum of the potential for the volume modulus can be found analytically. Setting the first derivative equal to zero and solving, the volume at the minimum is found to be

$$\mathcal{V}_{min} = -\eta p(u)\, W_0 \left(-\frac{1}{\eta p(u)} e^{q(u) - \frac{\xi}{2\eta}} \right) \,, \tag{2.1.49}$$

where, for the subsequent analysis the following convenient parametrization has been introduced

$$\begin{aligned} p(u) &= \frac{3}{16} \frac{(2u+1)(14u+3)}{u(u+1)} \,, \\ q(u) &= \frac{1}{3} \frac{39+4u(7u+5)}{3+4u(7u+5)} \,. \end{aligned} \tag{2.1.50}$$

Starting with region I, while focusing in the case of large volume limit and small non-perturbative contributions, it can be observed that the requirement of a positive second derivative of the po-

[10] Nonetheless, it will be seen that this term has the same power-law volume dependence with the positive D-term contributions $d/\mathcal{V}^2$ and can be compensated by appropriate values of the parameter d.

tential at the minimum yields

$$\mathcal{V}_{min} > \eta\, p(u) \Rightarrow -\eta\, p(u) W_0 > \eta\, p(u)\,. \tag{2.1.51}$$

From the range of $u \leqslant -1$ (region I, Table 1), it is deduced that $p(u) > 0$ and taking into account the bound $W_0 \geqslant -1$ (for real values of the Lambert function), this implies that $\eta p(u) < 0$ or $\eta < 0$. Furthermore, real W_0 values defined in (2.1.49) imply that its argument should be greater than $-e^{-1}$, which, for $\eta p(u) < 0$ is satisfied for any ξ, η. To determine whether a dS vacuum is attainable, the value of the effective potential at the minimum is required. A straightforward computation yields

$$\begin{aligned} V_{\rm eff}(\mathcal{V}_{min}) &= (\tilde{\epsilon}\mathcal{W}_0)^2\, \frac{\eta(1+2u)(3+14) - 8\mathcal{V}_{min}u(1+u)}{48\,\mathcal{V}_{min}^3} \\ &= -\,(\tilde{\epsilon}\mathcal{W}_0)^2\, \frac{u(1+u)}{6\mathcal{V}_{min}^3}\left(\mathcal{V}_{min} - \frac{2}{3}\eta p(u)\right)\,. \end{aligned} \tag{2.1.52}$$

Taking into account that for the range of $u \in (-\infty, -1)$ the factor $u(1+u) > 0$, it is readily seen that for the parameter space of region I the value of the minimum (2.1.52) is always negative. Hence when only F-term contributions are taken into account, the resulting potential always exhibits an AdS vacuum.

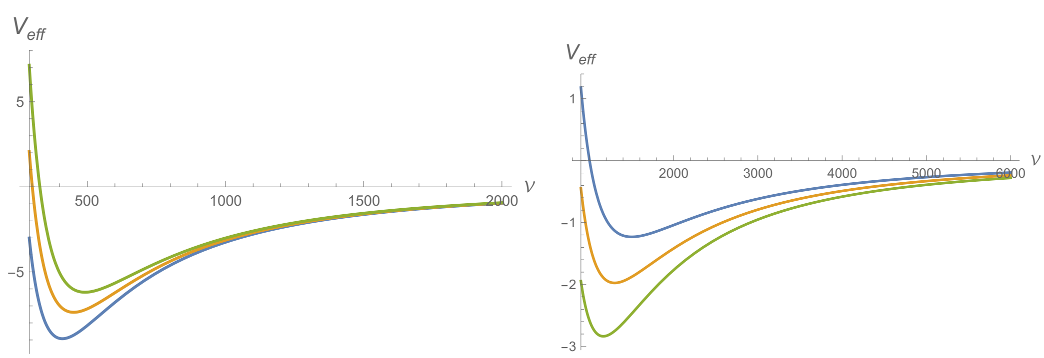

Figure 2.3: Left panel: The F-term potential V_F for $\eta = -0.5, u = -9$ and three values of $\xi = 150, 165, 180$. Lower ξ values imply deeper AdS minima. Right panel: V_F for $\eta = -0.1, \xi = 200$ and three values of $u = -1.2, -1, 25, -1.3$. The larger the $|u|$ values the deeper the AdS minima.

The F-part of the potential is plotted in figure 2.3 for two values of the parameter η and several values of $u = -b\tau_2$. As expected, in all these cases the F-term potential implies always an AdS minimum and an uplift term such as the one coming from a $\overline{D}3$-brane or D-terms induced form possible $U(1)$'s associated with $D7$-branes is necessary.

As a final example, we are going to present a model based on the so called "Swiss-cheese" volume, which is a Calabi-Yau manifold with the following type of form:

$$\mathcal{V} = f_{3/2}(\tau_j) - \sum_{i}^{N_{small}} \lambda \tau_i^{3/2}, \tag{2.1.53}$$

where the f function is homogeneous function of degree 3/2. In these models, there are rigid divisors, whose paramatrized by the blow-up moduli τ_i leaving N_{small} flat direction to the parameter space after stabilization. These scenarios have extensively studied in the past [122; 123; 124], aiming to embed a natural inflation which is dubbed as "Fibre Inflation". Despite the fact that these fibre-like volumes are ideal due to the available flat directions, non-perturbative corrections have been utilized to achieve a stabilized vacuum where additional higher order corrections needed to fully uplift the vacuum. We are going to show that the logarithmic string loop corrections, featured in the previous case studies, could bypass many of the problems appearing, such the strong constraints of the Kähler conditions, from the inclusion of non-perturbative corrections. In order to proceed, we are going to develop a full analysis of the effective potential by imposing the loop effects along each one of the world-volume directions, resulting into a Kähler potential of the following form:

$$\mathcal{K} = -\log(\frac{s-\bar{s}}{i}) - 2\log\left[\mathcal{V} + \frac{\xi}{2}(\frac{s-\bar{s}}{2i})^{3/2} + (\frac{s-\bar{s}}{2i})^{-1/2}\sum_i \eta_i \log(\frac{\tau_i - \bar{\tau}_i}{2})\right] \tag{2.1.54}$$

where τ_i stand for the four-cycle moduli, ξ denotes the α' corrections and the logarithmic corrections $\sim \eta \log(..)$ are induced in every direction of the internal world-volume. As for the exact form of the compactification's volume, we have to start from Calabi-Yau $h^{1,1} = 4$ Kähler moduli.

A chiral global model that features all the above ingredients, is the one described in [123]. The volume form, in terms of the four cycle moduli τ_i, is reduced in:

$$\begin{aligned} \mathcal{V} &= 2t_4 t_6 t_7 + \frac{t_1^3}{3} \xRightarrow{\tau_i = \partial_i \mathcal{V}} \\ \mathcal{V} &= \frac{1}{\sqrt{2}}\sqrt{\tau_4 \tau_6 \tau_7} - \frac{1}{3}\tau_1^{3/2} . \end{aligned} \tag{2.1.55}$$

In the last step, we included the relation of the Kähler cone, where the basis of the Kähler form is written as:

$$J = t_1 D_1 + t_4 D_4 + t_6 D_6 + t_7 D_7 \tag{2.1.56}$$

The Kähler cone conditions are be derived from the Kähler generators as:

$$K_1 = -D_1 + D_4 + D_6 + D_7, \quad K_2 = D_7, \quad K_3 = D_4, \quad K_4 = D_6, \tag{2.1.57}$$

$$r_1 = -t_1 > 0, \quad r_2 = t_1 + t_7 > 0, \quad r_3 = t_3 + t_4 > 0, \quad r_4 = t_1 + t_6 > 0\ . \tag{2.1.58}$$

Moreover, the connections between the two-cycle and four-cycle moduli can be obtained through $\tau_i = \partial_{t_i} \mathcal{V}$:

$$\tau_1 = t_1^2,\ \tau_4 = 2t_6 t_7,\ \tau_6 = 2t_4 t_7,\ \tau_7 = 2t_4 t_6\ . \tag{2.1.59}$$

In addition, one can further reduce the volume form in (2.1.62) using the Kähler cone conditions and the D-term fixing [11] The relevant conditions are summarized below:

$$t_4 \equiv \alpha t_6\ . \tag{2.1.60}$$

$$t_7 > -t_1 > 0 \Rightarrow \begin{cases} t_6 > -t_1 > 0,\ \alpha \geq 1, \\ \alpha t_6 > -t_1 > 0,\ \alpha \leq 1\ , \end{cases} \tag{2.1.61}$$

where after applying these conditions, the volume form is written as:

$$\mathcal{V} = \frac{1}{\sqrt{2\alpha}} \sqrt{\tau_7}\tau_6 - \frac{1}{3}\tau_1^{3/2}\ . \tag{2.1.62}$$

It is important to mention that the size of the volume is controlled by τ_4, τ_6, τ_7 moduli, while the rigid divisor τ_1 parametrizes the diagonal del Pezzo divisor. Regarding the complex structure moduli z_i as well as the axion-dilaton, they are stabilized at high energies by the supersymmetric flatness conditions.

[11] A detailed analysis regarding the geometric construction can be found in sections 3.1-3.5 of [123].

$$D_{z_i}W = 0 = D_{\bar{z}_i}\bar{W},\ D_sW = 0 = D_{\bar{s}}\bar{W}\ . \tag{2.1.63}$$

In the above framework, we are going to present a model which features an alternative to the stabilization procedure of the blow-up modulus scenario. This novel procedure results into one flat direction that appears at the F-term potential level as a consequence of the higher order terms scaling as $\mathcal{O}(1/\mathcal{V}^4)$. Since the scalar potential is parametrized by the three moduli (τ_1, τ_7, τ_6), we would like to trade one of them in order to introduce the volume variable $\mathcal{V}$ in the computations. This reparametrization helps us to perform the large volume expansion. So, in order to include the overall volume in our computations, we solve the equation (2.1.62) with respect to one modulus e.g. τ_6,

$$\tau_6 = \frac{\sqrt{2}\sqrt{\alpha}\left(\tau_1^{3/2} + 3\mathcal{V}\right)}{3\sqrt{\tau_7}}\ . \tag{2.1.64}$$

Using the above definition, we are going to present the necessary computations needed to define the effective F-scalar potential. In the appendix, we provide a detailed derivation of the BBHL potential. Moreover, following the calculations used in [125], the Kähler potential can be written as follows:

$$2Y = 2\mathcal{V} + \hat{\xi} + \hat{\eta}\log\left(\frac{2\alpha\tau_7}{9}\left(\tau_1^{5/2} + 3\mathcal{V}\tau_1\right)^2\right), \tag{2.1.65}$$

where we have used the fact that the axio-dilaton and the free parameters can redefined as:

$$s = c_0 + ie^{-\phi},\ d = e^{-\phi} \Rightarrow \hat{\xi} = \xi\, d^{3/2},\ \hat{\eta} = \eta\, d^{-1/2},\ \ d = \frac{1}{g_s}\ . \tag{2.1.66}$$

The scalar potential can be computed by the $\mathcal{N} = 1$ supergravity formula:

$$e^{-\mathcal{K}}V_k = K^{A\bar{B}}(D_AW)(D_{\bar{B}}\bar{W}) - 3|W|^2,\ \ W = \mathcal{W}_0\ . \tag{2.1.67}$$

The first term of the scalar potential (2.1.67) will be displayed below, where we expand in terms of $\mathcal{O}(\hat{\eta}, \frac{\hat{\xi}}{\mathcal{V}})$ keeping only the first order terms:

$$K^{A\bar{B}}(D_A W)(D_{\bar{B}}\bar{W}) = 3g_S \mathcal{W}_0^2\left(1 + \frac{\hat{\xi} - 16\hat{\eta} + \hat{\eta}w}{4\mathcal{V}} + \frac{\hat{\xi}\hat{\eta}(1-2w)}{2\mathcal{V}^2}\right), \tag{2.1.68}$$

where we define $w = \log\left(\frac{2\alpha\tau_7}{9}(3\mathcal{V}\tau_1 + \tau_1^{5/2})^2\right)$. It is obvious that the second term in (2.1.67) cancels the first term above, and by turning off $\eta \to 0$, it results to:

$$e^{-\mathcal{K}}V_{eff} = \frac{3g_s\mathcal{W}_0^2\hat{\xi}}{4\mathcal{V}} + \mathcal{O}(\frac{\hat{\xi}}{\mathcal{V}^n}) \ . \tag{2.1.69}$$

Based on the above, the scalar potential can be easily derived and it is shown below:

$$V_{eff} = \frac{3g_s\mathcal{W}_0^2(\hat{\xi} - 16\hat{\eta} + \hat{\eta}w)}{4\mathcal{V}^3} - \frac{3g_s\mathcal{W}_0^2\hat{\eta}\hat{\xi}w}{\mathcal{V}^4} + \mathcal{O}(\frac{\hat{\xi}}{\mathcal{V}^n}, \hat{\eta}^n) \ . \tag{2.1.70}$$

The above potential is described in terms of three moduli $V(\mathcal{V}, \tau_1, \tau_7)$, so we need to minimize the potential with respect to all of the above [12]. As discussed in [123; 127], it is a unique feature of spaces described by volumes of the form of (2.1.62) to preserve one flat direction. Their approach is to stabilize first the internal volume and secondly to perform the stabilization of the blow up divisor by non-perturbative effects, while the τ_7 remains flat. Our approach differs from the aforementioned due to the fact that the logarithmic corrections can perform the stabilization while keeping track of the remaining flat direction. The previous studies of this kind of approach requires only keeping terms that scales as $\frac{1}{\mathcal{V}^3}$, but now we will prove that even terms proportional to $\sim \frac{\hat{\eta}\hat{\xi}}{\mathcal{V}^4}$ could be significant. Firstly by inspecting the effective potential (2.1.70), we stabilize w.r.t. the compactified space while considering that $\mathcal{V} \gg \tau_1$:

$$\begin{aligned}
\partial_{\mathcal{V}}V_{eff} &= \frac{9\mathcal{W}_0^2 g_s\left(-\hat{\eta}\log\left(\frac{2\alpha\tau_7}{9}\right) - \hat{\xi} + 2\hat{\eta}\left(\frac{\mathcal{V}}{\tau_1^{3/2}+3\mathcal{V}} + 8\right) - 2\eta\log\left(\tau_1^{5/2} + 3\tau_1\mathcal{V}\right)\right)}{4\mathcal{V}^4} = 0 \Rightarrow \\
\mathcal{V} &\cong \frac{e^{\frac{1}{6}\left(-3\log\left(\frac{2\alpha\tau_7}{9}\right) - \frac{3\hat{\xi}}{\hat{\eta}} + 50\right)} - \tau_1^{5/2}}{3\tau_1} \ .
\end{aligned} \tag{2.1.71}$$

By substituting the above minimum in the scalar potential, the result is:

---

[12] Please check the correct definition of the fluxes in [126].

$$V_{eff}|_{\mathcal{V}_{min}} = -\frac{27\sqrt{2}\hat{\eta}\tau_1^3\mathcal{W}_0^2\left(\alpha\tau_7\right)^{3/2}e^{\frac{3\hat{\xi}}{2\hat{\eta}}}g_s}{\left(\sqrt{2}\sqrt{\alpha\tau_1^5\tau_7}e^{\frac{\hat{\xi}}{2\hat{\eta}}}-3e^{25/3}\right)^3}, \tag{2.1.72}$$

where it can be readily found that both moduli are stabilized at $\tau_{1,7} \to 0$. In order to avoid the above statement, we are going to include in our calculations the next to leading order term

$$V_{eff} = \frac{3g_s\mathcal{W}_0^2(\hat{\xi}-16\hat{\eta}+\hat{\eta}w)}{4\mathcal{V}^3} - \frac{3g_s\mathcal{W}_0^2\hat{\eta}\hat{\xi}(w)}{\mathcal{V}^4} + O\left(\frac{\hat{\xi}^n}{\mathcal{V}^n},\eta^n\right) . \tag{2.1.73}$$

This new correction will not modify the minimum w.r.t. the volume (at least to a degree that would lead to destabilization), since it is suppressed by $\frac{1}{\mathcal{V}^4}$. Nevertheless, it would enhance the contributions to the transverse directions unraveling the importance of quantum corrections to the characterization of the flat direction. So, the effective potential along the volume's minimum is given by:

$$V_{eff}|_{\mathcal{V}_{min}} = \frac{27\tau_1^4\mathcal{W}_0^2g_s\left(\frac{3\sqrt{2}\hat{\eta}e^{\frac{25}{3}-\frac{\hat{\xi}}{2\hat{\eta}}}}{\tau_1\sqrt{\alpha\tau_7}}+12\hat{\xi}(3\hat{\xi}-50\hat{\eta})-2\hat{\eta}\tau_1^{3/2}\right)}{4\left(e^{\frac{1}{6}\left(-3\log\left(\frac{2\alpha\tau_7}{9}\right)-\frac{3\hat{\xi}}{\hat{\eta}}+50\right)}-\tau_1^{5/2}\right)^4}, \tag{2.1.74}$$

where minimizing with respect to τ_7, there exist one minimum:

$$\tau_7 = \frac{9e^{\frac{50}{3}-\frac{\hat{\xi}}{\hat{\eta}}}}{2\alpha\left(12\hat{\xi}\tau_1+\tau_1^{5/2}\right)^2} . \tag{2.1.75}$$

Given the above minimum, we derive an dS minimum as while there is a flat direction in terms of a combination of the τ_1, τ_7 moduli. This is depicted below in the following two plots.

$$V_{eff}|_{\mathcal{V}_{min}}^{\tau_7^{min}} = \frac{3\mathcal{W}_0^2(\hat{\xi}-16\hat{\eta})g_s}{256\hat{\xi}^3} > 0 . \tag{2.1.76}$$

Nevertheless, we cannot stabilize the moduli, since of all the directions are runaway paths. Now, we induce the next to leading order string loop corrections, which fall under two categories: the KK-corrections and the winding loop corrections. These are summarized to the following contributions:

$$K_{g_s}^{KK} = g_s \sum_i \frac{C_i^{KK} t_\perp^i}{\mathcal{V}}, \quad K_{gs}^{w} = \sum_i \frac{C_i^w}{\mathcal{V} t_\cap^i}, \tag{2.1.77}$$

where C_i^{KK} and C_i^w are some functions depending on the complex structure moduli and the open string moduli. The two cycle volume moduli $t_\perp^i$ denote the transverse space between the D_7 branes and orientifold planes O_7. On the other hand, the moduli $t_\cap^i$ correspond to volume curve residing in the intersection of the D_7 branes of the theory. Given this Kähler potential's corrections, the contribution to the effective scalar potential are given by:

$$V_{g_s}^{KK} = k g_s^2 \frac{\mathcal{W}_0^2}{\mathcal{V}^2} \sum_{ij} C_i^{KK} C_j^{KK} K_{ij}^0, \tag{2.1.78}$$

$$V_{gs}^{W} = -2k \frac{W_0^2}{\mathcal{V}^2} K_{gs}^w = -2k \frac{W_0^2}{\mathcal{V}^3} \sum_i \frac{C_i^w}{t_\cap^i}, \quad k = (\frac{g_s}{8\pi}) . \tag{2.1.79}$$

In the above definition, we should also substitute the Kähler metric, which is given by:

$$K_{ij}^0 = \frac{1}{16\mathcal{V}} (2t^i t^j - 4\mathcal{V}\kappa^{ij}) . \tag{2.1.80}$$

Apart from the string loop corrections, there exists higher derivative corrections, where these are a generic feature for all the Calabi Yau manifolds. Their form is given by:

$$V_{F^4} = -k^2 \frac{\lambda \mathcal{W}_0^4}{g_s^{3/2} \mathcal{V}^4} \Pi_i t^i, \tag{2.1.81}$$

where Π_i are the topological numbers depending on the intersection of the divisors and λ is unknown combinatorial factor. We are going to use these subleading corrections to the scalar potential. The effective theory is, then, given by:

$$V_{eff} = \frac{3g_s\mathcal{W}_0^2(\hat{\xi} - 16\hat{\eta} + \hat{\eta}w)}{4\mathcal{V}^3} - \frac{3g_s\mathcal{W}_0^2\hat{\eta}\hat{\xi}(w)}{\mathcal{V}^4} + \frac{c}{\mathcal{V}^4}(t_1 + t_6 + t_7) + V_{up} + O(\frac{c_i}{\mathcal{V}^4}), \qquad (2.1.82)$$

We can exchange the two-cycle moduli in the scalar potential with the four-cycle moduli by using the following identities:

$$t_1 = \sqrt{\tau_1}, \quad t_7 = \frac{1}{\sqrt{2\alpha}}\frac{\tau_6}{\sqrt{\tau_7}}, \quad \tau_6 = \frac{1}{\sqrt{2\alpha}}\sqrt{\tau_7}\,. \qquad (2.1.83)$$

$$V_{F^4} = \frac{c}{\mathcal{V}^4}\left(\frac{\sqrt{\tau_7}}{\sqrt{2}\sqrt{\alpha}} + \sqrt{\tau_1} + \frac{\tau_1^{3/2} + 3\mathcal{V}}{3\tau_7}\right) \qquad (2.1.84)$$

Based on this construction, one can see that the flat direction is lifted, while the vacuum can be uplifted by tiny uplift through an appropriate term V_{up}. In order to study the potential in a more the canonical normalized basis for the fields. To do, we need to write down the leading order terms of the Kähler metric, which are:

$$K_{ij} = \begin{pmatrix} \frac{1}{4\tau_7^2} & 0 & 0 \\ 0 & \frac{1}{2\tau_6^2} & 0 \\ 0 & 0 & \frac{\sqrt{\alpha\tau_7}}{4\sqrt{2}\sqrt{\tau_1}\tau_6\tau_7} \end{pmatrix}, \qquad (2.1.85)$$

where by inverting the defintions of the Kähler moduli to the normalized fields, we derive the new basis as:

$$\tau_7 = e^{\sqrt{2}\varphi 1}, \quad \tau_6 = e^{\varphi 2}, \qquad (2.1.86)$$

$$\tau_1 = \frac{3^{4/3}\varphi 3^{4/3} e^{\frac{1}{3}\left(\sqrt{2}\varphi 1 + 2\varphi 2\right)}}{2^{5/3}\alpha}, \quad \mathcal{V} = \frac{\left(4 - 3\varphi 3^2\right) e^{\frac{\varphi 1}{\sqrt{2}} + \varphi 2}}{4\sqrt{2}\sqrt{\alpha}}\,. \qquad (2.1.87)$$

Given the above form, the kinetic term are now written as:

$$K_{ij}\partial T_i \partial \bar{T}_j = \sum_i \frac{\partial T_i \partial \bar{T}_i}{(T_i+\bar{T}_i)^2} = \sum_i \frac{1}{2}(\partial\varphi_i)^2 + \dots \,. \tag{2.1.88}$$

Finally, we display the scalar potential in the new basis as:

$$\begin{aligned}V_{eff} =& -\frac{1024\alpha^2\hat{\xi}\hat{\eta}\; g_S \mathcal{W}_0^2 e^{-2\sqrt{2}\varphi_1-4\varphi_2}\left(\log\left(\frac{9^4\varphi_3^8}{2^{10}\alpha^2}\right)+8\sqrt{2}\varphi_1+10\varphi_2\right)}{\left(4-3\varphi_3^2\right)^4} + V_{up} - \\ &-\frac{32\sqrt{2}\alpha^{3/2} g_s \mathcal{W}_0^2\; e^{-\frac{3\varphi_1}{\sqrt{2}}-3\varphi_2}\left(\hat{\eta}\left(\log\left(\frac{9^4\varphi_3^8}{2^{10}\alpha^2}\right)+8\sqrt{2}\varphi_1+10\varphi_2-48\right)+3\hat{\xi}\right)}{\left(3\varphi_3^2-4\right)^3} + \\ &+\frac{512\;\; 2^{1/6}\;\alpha^{3/2}\; c\;\; e^{-\frac{5\varphi_1}{\sqrt{2}}-4\varphi_2}\left((9\alpha\;\varphi_3^2\; e^{2\sqrt{2}\varphi_1+\varphi_2})^{1/3}+2^{1/3}\left(e^{\sqrt{2}\varphi_1}+e^{\varphi_2}\right)\right)}{\left(4-3\varphi_3^2\right)^4}\,. \end{aligned} \tag{2.1.89}$$

Due to the complexity of the above potential, we can reduce its form by considering an expansion with respect to a small parameter. One can readily see in the above form, that there is a factor of $4-3\varphi_3^2$, which can be recasted to:

$$\varphi_3^2 = \frac{y+4}{3}\,. \tag{2.1.90}$$

Given, this redefinition the y variable could be small, since the φ_3 describes the small divisor τ_1. So, we can perform a an expansion with respect to this parameter. The leading order terms of this expansion results into:

$$\begin{aligned}V_{eff}^{appr} =& \frac{128\sqrt{2}\;\alpha^{3/2} c\; e^{-\frac{5\varphi_1}{\sqrt{2}}-4\varphi_2}}{3y^4}\Bigg[48\sqrt{2}c\left(e^{\sqrt{2}\varphi_1}+e^{\varphi_2}\right)+4\;2^{5/6}\;(3\alpha)^{1/3}\;c(y+12)\;e^{\frac{1}{3}\left(2\sqrt{2}\varphi_1+\varphi_2\right)} - \\ &-3\mathcal{W}_0^2\; y g_s e^{\sqrt{2}\varphi_1+\varphi_2}\left(2\hat{\eta}\left(\sqrt{2}(-\log(2\alpha)+5\varphi_2-24)+8\varphi_1\right)+3\sqrt{2}\hat{\xi}\right) - \\ &-96\sqrt{\alpha}\;\hat{\xi}\hat{\eta}e^{\frac{\varphi_1}{\sqrt{2}}}\mathcal{W}_0^2 g_s\left(-2\log(2\alpha)+8\sqrt{2}\varphi_1+10\varphi_2+y\right)\Bigg] + V_{up}\,. \end{aligned} \tag{2.1.91}$$

We could further simplify our formula considering the regime where the α parameter is small $\alpha \ll 1$. The simpler formula for the effective potential is then given by:

$$
\begin{aligned}
V_{eff}^{appr} =&\frac{32\alpha^{3/2}e^{-\frac{5\varphi_1}{\sqrt{2}}-4\varphi_2}}{3y^4}\Bigg[4\sqrt{2}c\left(12\left(e^{\sqrt{2}\varphi_1}+e^{\varphi_2}\right)+(y+12)(6\alpha e^{\left(2\sqrt{2}\varphi_1+\varphi_2\right)})^{1/3}\right)-\\
&-\mathcal{W}_0^2 y\, g_s\, e^{\sqrt{2}\varphi_1+\varphi_2}\left(-\sqrt{2}\hat{\eta}\log\left(64\alpha^6\right)+9\sqrt{2}\hat{\xi}+6\hat{\eta}\left(8\varphi_1+\sqrt{2}(5\varphi_2-24)\right)\right)\Bigg]+V_{up}\ .
\end{aligned}
\tag{2.1.92}
$$

From this expression, one can easily derive the minimum with respect to the y variable. This can approximated to be as:

$$
y\cong\frac{64\sqrt{2}c\ \ e^{-\sqrt{2}\varphi_1-\varphi_2}\left((6\alpha e^{\left(2\sqrt{2}\varphi_1+\varphi_2\right)})^{1/3}+e^{\sqrt{2}\varphi_1}+e^{\varphi_2}\right)}{\mathcal{W}_0^2 g_s\left(-\sqrt{2}\hat{\eta}\log\left(64\alpha^6\right)+30\varphi_2-144)+9\sqrt{2}\hat{\xi}+48\hat{\eta}\varphi_1\right)}\ . \tag{2.1.93}
$$

By recalling the redefinition in (2.1.90), the minimum along ϕ_3 direction is proven to be:

$$
\varphi_{3,min}^2=\frac{1}{3}(y+4)\ . \tag{2.1.94}
$$

As for the other two perpendicular directions, we could substitute the minimal value of y in the effective scalar potential of equation (2.1.92), which leads to:

$$
V_{eff}|_y\cong-\frac{\alpha^{3/2}e^{\frac{3\varphi_1}{\sqrt{2}}}\mathcal{W}_0^8 g_s^4\left(\sqrt{2}\hat{\eta}\left(-\log\left(64\alpha^6\right)+30\varphi_2-144\right)+9\sqrt{2}\hat{\xi}+48\hat{\eta}\varphi_1\right)^4}{196608\sqrt{2}c^3\left((6\alpha e^{\left(2\sqrt{2}\varphi_1+\varphi_2\right)})^{1/3}+e^{\sqrt{2}\varphi_1}+e^{\varphi_2}\right)^3} \tag{2.1.95}
$$

By examining the derivative of the above formula with respect to the φ_2, the result is:

$$
\begin{aligned}
\frac{\partial V_{eff}|_y}{\partial\varphi_2}=&-\frac{\alpha^{3/2}e^{\frac{3\varphi_1}{\sqrt{2}}}\mathcal{W}_0^8 g_s^4\left(\sqrt{2}\hat{\eta}\left(-\log\left(64\alpha^6\right)+30\varphi_2-144\right)+9\sqrt{2}\hat{\xi}+48\hat{\eta}\varphi_1\right)^3}{196608c^3\left((6\alpha e^{\left(2\sqrt{2}\varphi_1+\varphi_2\right)})^{1/3}+e^{\sqrt{2}\varphi_1}+e^{\varphi_2}\right)^4}\times\\
&\times e^{\varphi_2}\Bigg[\hat{\eta}\left(264(6\alpha e^{\left(2\sqrt{2}\varphi_1+\varphi_2\right)})^{1/3}+120e^{\sqrt{2}\varphi_1-\varphi_2}+552\right)-\\
&-\left((6\alpha e^{\left(2\sqrt{2}\varphi_1+\varphi_2\right)})^{1/3}+3\right)\left(6\hat{\eta}\left(-\frac{1}{6}\log\left(64\alpha^6\right)+4\sqrt{2}\varphi_1+5\varphi_2\right)+9\hat{\xi}\right)\Bigg]\ .
\end{aligned}
\tag{2.1.96}
$$

The equation on the brackets could provide an approximate solution, which is summarized below and the minimal value is expressed in terms of the Lambert function $W_{0/-1}$.

$$\varphi_{2,min} \cong \frac{1}{30}\left(\log\left(64\alpha^6\right) - \frac{9\hat{\xi}}{\hat{\eta}} - 24\sqrt{2}\varphi_1 + 30\ W_{0/-1}\left(\frac{2\ 2^{4/5} e^{\frac{1}{30}\left(\frac{9\hat{\xi}}{\hat{\eta}}+54\sqrt{2}\varphi_1-184\right)}}{3\alpha^{1/5}}\right) + 184\right) \tag{2.1.97}$$

The same method can be applied for the other field, φ_1, and the approximate solution at the minimum can be expressed as:

$$\varphi_{1,min} \cong \frac{6\hat{\eta}\log(\alpha) - 9\hat{\xi} + 2\hat{\eta}\left(144 + 15\log\left(\frac{13}{5}\right) + \log(8)\right)}{54\sqrt{2}\hat{\eta}}\ . \tag{2.1.98}$$

To prove the validity of our approximate formula of the potential in (2.1.92) and the exact potential in (2.1.89), we are going to sketch the potentials in the vicinity of the global minimum. In the following tables, an numerical example is presented, where the values of the free parameters are displayed along with the values of the moduli/fields at their corresponding minima.

τ_1	τ_7	$\mathcal{V}$
3856	1065	10286
φ_1	φ_2	φ_3
4.92	5.96	1.09

$m^2_{\tau_1}$	$m^2_{\tau_7}$	$m^2_{\mathcal{V}}$
1.43×10^{-13}	1.95×10^{-14}	2.1×10^{-17}
$m^2_{\varphi_1}$	$m^2_{\varphi_2}$	$m^2_{\varphi_3}$
1.39×10^{-10}	8.74×10^{-14}	2.3×10^{-14}

Table 2.3: The numerical solution for the minima with their corresponding masses.

g_s	$\lvert\mathcal{W}_0\rvert$	$\hat{\xi}$	$\lvert\hat{\eta}\rvert$	α	$\lvert\lambda\rvert$	V_{up}
10^{-4}	20	5	0.5	10^{-2}	8×10^{-2}	10^{-13}

Table 2.4: The values used for the model's free parameters.

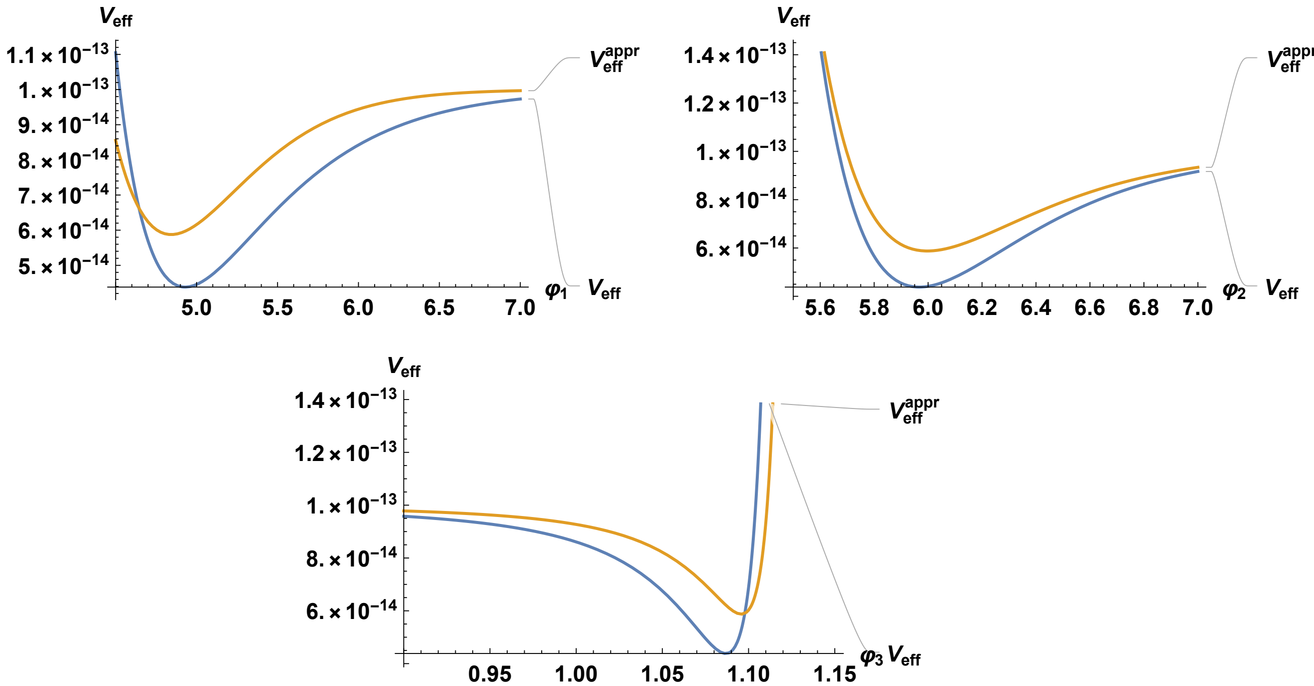

Figure 2.4: The two plots in the upper part display the potentials directions along the φ_1, φ_2 directions, correspondingly. In the lower part of the figure, the small divisor's trajectory is plotted.

2.1.3 Uplifting AdS vacua with D-terms

Both scalar potentials, describing the two different scenarios of equations (2.1.32) and (2.1.48), need to be uplifted by properly imported the effects of D-terms. The case of anti-D_3 branes suffer from many issues regarding the background geometry and the wrapping factors in the conifold. In [113] it was proven that it is sufficient to consider the D-term contributions associated with $U(1)$ factors which arise in the presence of the intersecting $D7$ branes already included in the geometric configuration. Flux generated D-terms have the general form [128; 129]

$$V_D = \frac{g^2_{D7_i}}{2}\left(Q_i\partial_{\rho_i}K + \sum_j q_j|\Phi_j|^2\right)^2, \quad \frac{1}{g^2_{D7_i}} = \mathrm{Im}\rho_i + \cdots \tag{2.1.99}$$

where Q_i, q_j are "charges" and $\{\cdots\}$ stand for flux and dilaton dependent corrections while the Φ_j fields depend on the specific field theory model. For zero Φ_j-vevs the model dependent term vanishes (see discussion in [129]) and it turns out that $V_D \approx Q_i^2/\tau_i^3$. Then, the generic form of the corresponding D-term potential can be approximated by [113]

$$V_{\mathcal{D}} \; = \; \sum_{i=1}^{3} \frac{d_i}{\tau_i}\left(\frac{\partial \mathcal{K}}{\partial \tau_i}\right)^2 \; \approx \; \sum_{i=1}^{3} \frac{d_i}{\tau_i^3} \; \equiv \; \frac{d_1}{\tau_1^3}+\frac{d_3}{\tau_3^3}+\frac{d_2\tau_1^3\tau_3^3}{\mathcal{V}^6}\,, \tag{2.1.100}$$

where, $d_i \approx Q_i^2 > 0$ and in the last expression the modulus τ_2 has been traded with the internal volume modulus $\mathcal{V}$, i.e., $\tau_2 = \mathcal{V}^2/(\tau_1\tau_3)$. Thus, the effective potential being the sum of the (2.1.32) and (2.1.100), $V_{\rm eff} = V_F + V_D$, is given as a function of $\tau_1,\ \tau_3$ and $\mathcal{V}$:

$$V_{\rm eff} \approx -\,(\epsilon\mathcal{W}_0)^2\ \frac{\mathcal{V}-2\xi+4\eta(1-\log(\mathcal{V}))}{4\mathcal{V}^3}+\frac{d_1}{\tau_1^3}+\frac{d_3}{\tau_3^3}+\frac{d_2\tau_1^3\tau_3^3}{\mathcal{V}^6}\ \cdot \tag{2.1.101}$$

Proceeding as in [113], it is found that the $\tau_{1,3}$ moduli are stabilised at

$$\tau_k = \left(\frac{d_k}{d}\mathcal{V}^2\right)^{1/3},\ k=1,3,\ \text{where } d=(d_1d_2d_3)^{\frac{1}{3}} \tag{2.1.102}$$

The potential takes the form

$$V_{\rm eff}|_{\tau_{1,3}^{min}} = -(\epsilon\mathcal{W}_0)^2\frac{\mathcal{V}-2\xi+4\eta(1-\log\mathcal{V})}{4\mathcal{V}^3}+\frac{3d}{\mathcal{V}^2} \tag{2.1.103}$$

At the minimum of the potential the volume modulus takes the value

$$\mathcal{V}_{V'=0} = \frac{6|\eta|}{1-12\mathsf{r}}W_0\left(\frac{1-12\mathsf{r}}{6|\eta|}e^{\frac{4}{3}-\frac{\xi}{2\eta}}\right) \tag{2.1.104}$$

As in the previous case, the following two constraints are imposed: i) the argument of the W_0 function must be larger than $-1/e$ and ii) the potential at the minimum must be positive. Once these restrictions are implemented, the ratio $\mathsf{r} = \frac{d}{(\epsilon\mathcal{W}_0)^2}$ of the F- and D-term coefficients is found to be bounded in the region

$$\frac{1}{12}-\frac{\eta}{3\mathcal{V}_{min}} \leqslant \mathsf{r} \leqslant \frac{1}{12}-\frac{\eta}{2}e^{\frac{\xi}{2\eta}-\frac{7}{3}}, \tag{2.1.105}$$

For large volumes, the above bounds allow only a tiny region in the vicinity of $1/12$. Given the ratio r, the inequalities (2.1.105) imply also an upper bound on ξ:

$$-\frac{\eta}{3\mathcal{V}_{min}} < -\frac{\eta}{2}e^{\frac{\xi}{2\eta}-\frac{7}{3}} \Rightarrow \xi < 2|\eta|\left(\ln\frac{6|\eta|}{12\mathsf{r}-1}-\frac{7}{3}\right) \tag{2.1.106}$$

In figure 2.5 the potential is plotted vs the volume for the set of parameters $\epsilon\mathcal{W}_0 = 1.9, \xi = 10, \eta =$

-1 and three values of the D-term coefficient d. A dS minimum is obtained for a very short range of d. In contrast to the first case, here there is no constant uplift term, all $V_{\rm eff}$ terms are suppressed by powers of $\mathcal{V}$ and the potential asymptotically approaches zero as $\mathcal{V} \to \infty$.

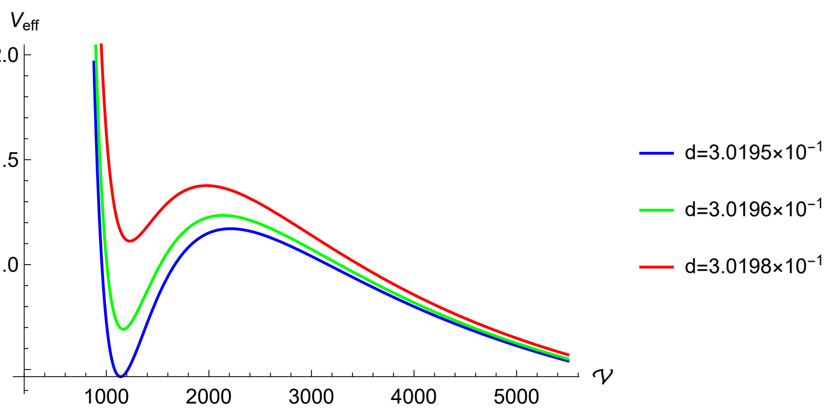

Figure 2.5: Plot of $V_{eff} \times 10^{10}$ potential vs the volume modulus for $\epsilon\mathcal{W}_0 = 1.9, \eta = -1, \xi = 10$ for three values of the D-term coefficient d.

As for the second paradigm, we will follow the same strategy. In the subsequent analysis the case of large τ_1, τ_2 moduli will be considered (i.e. $a\tau_1 \gg 1$ and $b\tau_2 \gg 1$) where the calculations for the stabilization of the directions transverse to the volume are simplified. This will provide a more quantitative comparison of the effect of the "strong" non-perturbative correction to the logarithmic one. Proceeding the way described above, the total potential is written as:

$$V_{\rm eff} \approx (\varepsilon W_0)^2 \frac{7(\xi + 2\eta \log(\mathcal{V})) - 4\mathcal{V}}{8\mathcal{V}^3} + \frac{d_1}{\tau_1^3} + \frac{d_2}{\tau_2^3} + \frac{d_3 \tau_1^3 \tau_2^3}{\mathcal{V}^6} \,. \tag{2.1.107}$$

Minimization of (2.1.107) with respect to the τ_1, τ_2 moduli, leads to the following equations:

$$\tau_1^3 = \frac{d_1^{\frac{2}{3}} \mathcal{V}^2}{(d_2 d_3)^{\frac{1}{3}}} \,, \tag{2.1.108}$$

$$\tau_2^3 = \frac{d_2^{\frac{2}{3}} \mathcal{V}^2}{(d_1 d_3)^{\frac{1}{3}}} \,. \tag{2.1.109}$$

Substituting the above back into (2.1.107), the potential $V_{\rm eff}$ receives the following compact formula:

$$V_{\rm eff} \approx (\varepsilon \mathcal{W}_0)^2 \left(\frac{7}{8} \frac{\xi + 2\eta \log(\mathcal{V})}{\mathcal{V}^3} - \frac{1}{2\mathcal{V}^2} \right) + \frac{3d}{\mathcal{V}^2} \,, \tag{2.1.110}$$

where $d = (d_1 d_2 d_3)^{1/3}$. The volume modulus at the minimum of the potential is

$$\mathcal{V}_{min} = \frac{21\eta}{4(6\mathsf{r}-1)} W_0\Big(\frac{4(6\mathsf{r}-1)}{21\eta} e^{\frac{1}{3}-\frac{\xi}{2\eta}}\Big), \tag{2.1.111}$$

where the new parameter r introduced in the formula of $\mathcal{V}_{min}$ above is the ratio of the F- and D-term coefficients

$$\mathsf{r} = \frac{d}{(\varepsilon \mathcal{W}_0)^2} \ . \tag{2.1.112}$$

For given ξ and η the coefficient r has an upper and a lower bound coming from the following two constraints: i) Real values of the volume are achieved when the argument of the W_0 function must be larger than $-1/e$ and ii) the potential at the minimum must be positive. Implementing these conditions, the following bounds on r are imposed

$$\frac{1}{6} + \frac{7}{12}\frac{|\eta|}{\mathcal{V}} \lesssim \mathsf{r} \lesssim \frac{1}{6} + \frac{7|\eta|}{8} e^{-\frac{\xi}{2|\eta|}-\frac{4}{3}} \ . \tag{2.1.113}$$

For positive and large ξ values, this restricts the values of r in a tiny region close to $\frac{1}{6}$. It should be observed that the exact value $\mathsf{r} = \frac{1}{6}$ eliminates the $\frac{1}{\mathcal{V}^2}$ term form the scalar potential. This would leave only the perturbative F-part $\propto (\xi + 2\eta \log \mathcal{V})/\mathcal{V}^3$ which defines only AdS minima. It is worth noticing that, this value is twice as big compared with that obtained in the case of the effective potential (2.1.48) derived with only one non-perturbative term in the superpotential. It is convenient to define a new parameter

$$\varrho = 10^5(6\mathsf{r}-1) \ , \tag{2.1.114}$$

which can be used to plot the effective potential (2.1.107). Assuming for example the values $\xi = 10, \eta = -0.5$ and using (2.1.113), it can be deduced that a dS minimum exists as long as

$$2.925 \lesssim \varrho \lesssim 3.125 \ .$$

The potential (2.1.110) is plotted in figure 2.6 as a function of the volume for three values of the parameter ϱ. In figure 2.7 a three dimensional plot is shown where the minimum is depicted along $\mathcal{V}$ and τ_1 directions.

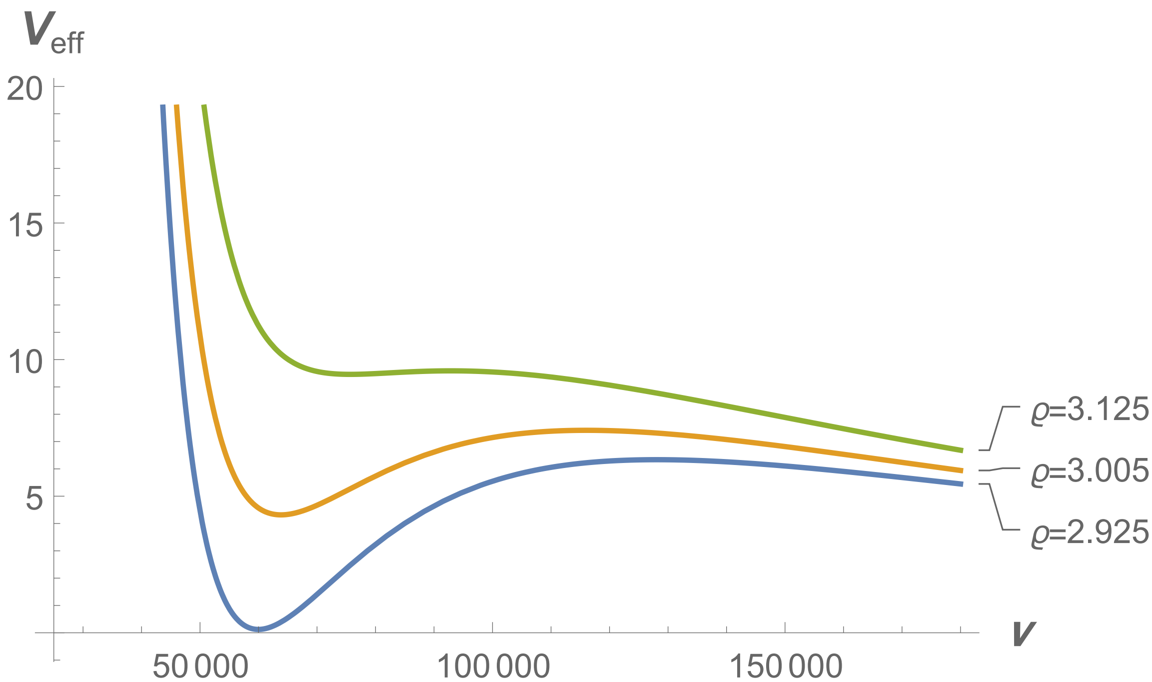

,

Figure 2.6: The potential (2.1.110) for $\eta = -0.5, \xi = 10$ and three values of the parameter $\varrho = 10^5(6r-1)$. For $\varrho = 2.925$ the potential at the minimum vanishes. For larger ϱ values $V_{\text{eff}}(\mathcal{V}_{min}) > 0$ while the minimum disappears for $\varrho \gtrsim 3.125$.

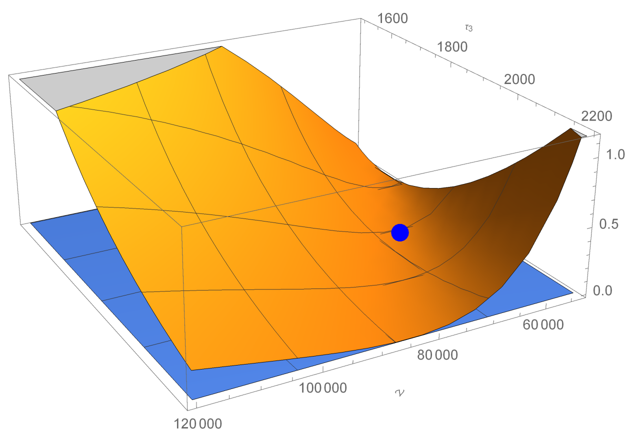

Figure 2.7: The potential (2.1.110) for $\eta = -0.5, \xi = 10, d = 0.6668, \mathcal{W}_0 = -1, \varepsilon \approx 2, \varrho = 3.05, d_2 = d_3 = 1$. The light blue plane is just above $V = 0^+$ and the blue dot is the intersection with V_{eff} which indicates the position of the dS the minimum.

2.2 Dark radiation and dark matter scenarios in stabilized vacua

Developments on the attainability of de-Sitter (dS) vacuum in type IIB string compactifications are populating the literature the recent years. Despite the various swampland conjectures [80; 81; 82; 85; 130; 131; 132; 133; 134], several works are pointing towards a possibility of a dS vacuum either by incorporating non-perturbative corrections in the Kähler potential [86; 135; 136; 137; 138; 139; 140] or by including perturbative quantum dynamics [95; 113; 141; 142; 143]. Among the most plausible explanations on the aforementioned question are focusing in the study of the effective theory, where an Anti de-Sitter (AdS) is evident and various uplifting ingredients are included ($\bar{D}_3$ branes and D-terms) in order to achieve a dS vacuum. The central role in these setups are played by the moduli fields of the theory, which modify not only the relevant scales for the correct embedding of inflation but also the late-time cosmological dynamics of the universe such as the reheating temperature, the effective neutrino species number and a potential connection between dark matter and dark radiation due to their decays. Some recent references regarding the open problem of moduli stabilization, dark radiation and their correlation to dark matter can be found to the followings works [86; 91; 136; 144; 145; 146; 147].

In the present section, we will focus on the importance of the quantum string corrections to the Kähler potential, whose origin can be traced back to the higher derivative terms of the effective string action and the existence of localized Eistein-Hilbert terms [96; 108; 109; 148] in a geometric setup of three intersecting D_7 branes scenario. Their inclusion to the theory provides a novel way to stabilize the Kähler moduli fields of the theory, without considering the non-perturabative corrections whose dynamics could be dangerous regarding the value of the string coupling in different parametric regions of the theory. Moreover, the dS vacuum is achieved by assuming the presence of magnetic fluxes along the cycles of the D_7 branes, which induce some anomalous $U(1)$ symmetries charging this way the Kähler moduli fields. Their result is an induced D-term in the level of the effective potential [90; 149], which despite being moduli dependent, its effect could in principle suffice for the uplifting of the Anti de-Sitter vacuum.

At a second stage, this work focuses on a detailed calculation of the moduli's mass eigenstates and eigenvalues and their correlation with the choice of fluxes $\mathcal{W}_0$ (either exponentially suppressed or order one), which modifies the mass hierarchy and the potential characterization of the longest lived particle field with its corresponding cosmological dynamics. Based on the above the couplings of the normalized fields to the axions, which comprise the dark sector of the theory, are computed unraveling that not only the diagonal decays of the moduli to axions are important but also that off diagonal decays (due to the quantum corrections) contribute at a considerable amount to the dark radiation abundance. On the contrary, the dominant decay to visible sector's degrees of freedom is summarized to the Giudice-Masiero mechanism [150], where it is calculated for the two limiting cases with respect to the fluxes scale, leading to a theoretical estimation of the neutrino number species ΔN_{eff}. Additionally, a discrimination is provided regarding the relevant scale of the reheating temperature ($\mathcal{O}(\text{MeV}) \leq T_{rh} \leq \mathcal{O}(\text{GeV})$ scale for exponentially suppressed fluxes and $T_{rh} \gg \mathcal{O}(\text{Tev})$ for order one fluxes), which explanation could also indicate an early matter dominated phase of the universe for low reheating temperatures as it was pointed by [151]. The effect of the quantum string corrections and the uplift parameters in the aforementioned cosmological observables are highlighted, notifying the differentiation of our work compared to the existing literature.

Finally, we study the production of non-thermal dark matter after the reheating process. The primary candidates in the large volume limit scenarios are the weekly interacting massive particles (WIMPs) and the thermally underproduced (Higgsino-like or Bino-like) particles, which in many previous studies tend to be overproduced [152; 153]. A different scenario proposes the idea of having fuzzy dark matter, where the axions would play the central role in that case [154; 155]. Although, the process we follow is similar to previous studies, the suppression of the reheating temperature provides a fertile ground to study the most common mechanisms of dark matter production (Annihilation scenario and Branching scenario) without the obstacle of overproduction. Focusing more to the so-called WIMP miracle, we are going to provide a scenario where a possible superheavy dark matter could arise from the annihilation scenario, where its mass could lay at 10^{11} GeV. In contrast, the branching scenario could also give the correct dark matter abundance for dark matter particles at the scale of TeV. Given a possible scenario of low scale baryogenesis in [156; 157], this model could in principle furnish an explanation for the dark matter-baryon coincidence, since the modulus could decay to species with B- and CP- violating couplings with the Standard model particles and has the correct scaling for the dilution factor of entropy Y_ϕ, too.

2.2.1 Structure of the Potential

To set the stage, we begin with the $\mathcal{N} = 1$ supergravity Kähler potential $\mathcal{K}$, where the geometric configuration is comprised of three intersecting D_7 branes. The theory contains various scalar fields, but we focus our attention on the complex structure moduli (z_a, $a = 1, 2, 3$), the axio-dilaton (S) and the Kähler moduli T_i, $i = 1, 2, 3$. Supersymmetric conditions $\mathcal{D}_{z_a}\mathcal{W} = \mathcal{D}_S\mathcal{W} = 0$ both fix the complex structure moduli and the axio-dilaton, leaving effectively the Kähler sector completely undetermined. The internal volume of the six dimensional space in the context of IIB string theory is denoted by $\mathcal{V}$, and it is expressed in terms of the two-cycles of the theory as:

$$\mathcal{V} = \frac{1}{6} k_{ijk} v^i v^j v^k, \; v^i = -\mathrm{Im}(T^i), \tag{2.2.1}$$

where the tensor k_{ijk} characterizes the intersection number. A more useful formula for the compactified volume can be extracted in terms of the four-cycles τ_i of the theory, where they are related to the two-cycles as:

$$\tau_i = v^j v^k \to \mathcal{V} = \sqrt{\tau_1 \tau_2 \tau_3}, \tag{2.2.2}$$

where we assume that the non-zero classical triple intersection number is $k_{123} = 1$. Apart from the compactified volume, the Kähler potential contains the quantum string (α'^3) correction ξ, where this correction corresponds to a constant shift of the volume [64]. In addition, we include the effects of quantum string loop corrections along each world-volume direction of the internal space, incorporated in a perturbative form as $\eta \log(\tau_i)$ [95]. Their origin can be traced back to the higher derivative terms of the 10-dimensional supergravity theory, where the leading effects are appearing as an $\mathcal{R}^4$ term, with $\mathcal{R}$ being the Riemann curvature. After dimensional reduction to four dimensions, these effects induce a localized Einstein-Hilbert term, where the computation of the scattering amplitude between these localized graviton vertices and D_7 branes (in the form of closed string modes), leads to a perturbative form of the correction $\eta \log(\tau_i)$ at the Kähler potential level [95].

$$\mathcal{K} = -2 \log(\sqrt{\tau_1 \tau_2 \tau_3} + \xi + \eta_i \log(\tau_i)), \quad \eta = -\frac{1}{2} g_s T_i \xi \; . \tag{2.2.3}$$

For simplicity, we assume the perturbative parameter η to be identical along each directions ($\eta_1 \cong \eta_2 \cong \eta_3$), i.e. the string tension T_i of the corresponding branes is tuned to be the same.

Regarding the superpotential of the theory, we assume the existence of background fluxes $\mathcal{W}_0$ [103] and the non-perturbative effects are turned off.

$$\mathcal{W} = \mathcal{W}_0 \; . \tag{2.2.4}$$

The F-term potential's computation is completely straightforward, taking into account equations (2.2.3) and (2.2.4), and trading one modulus, e.g. $\tau_3 = \mathcal{V}/(\tau_1 \tau_2)$, the whole effective potential is expressed in terms of the volume:

$$V_F = \frac{3\mathcal{W}_0^2(-8\eta + \xi + 2\eta \log(\mathcal{V}))}{2\mathcal{V}^3} - \frac{9 \; \eta \; \xi \mathcal{W}_0^2 \log(\mathcal{V})}{\mathcal{V}^4} + \mathcal{O}(\frac{1}{\mathcal{V}^n}) \; . \tag{2.2.5}$$

It is important to highlight the fact that this very compact and illustrating formula has been ob-

tained, considering that we would like to study the large volume limit where quantum corrections are subleading. This fact enables us to perform an expansion in terms of η and $\frac{\xi}{\mathcal{V}^n}$, while terms proportional to the power of the expansion variables are dropped. In addition, since the leading order terms are of order $\sim \mathcal{O}(\frac{1}{\mathcal{V}^3})$, we do not consider terms of order bigger than $\sim \mathcal{O}(\frac{1}{\mathcal{V}^4})$ in the large volume regime, bearing in mind that these additional terms are proportional to powers of η making them less important.
In order to obtain an AdS vacuum, we have to compute the minimum along the volume $\mathcal{V}$ direction, which is given by:

$$\mathcal{V}_{min} = e^{\frac{13}{3} - \frac{\xi}{2\eta}} \ . \tag{2.2.6}$$

The uplift mechanism for realizing a dS minimum is accomplished by adding the D-terms, related to the three intersecting D7-branes of the geometric configuration. Flux generated D-terms [129; 141; 149; 158] have the following form:

$$V_D = \sum_{i=1}^{3} \frac{g^2_{D_{7_i}}}{2} \Big(\sum_{i \neq j} Q_{ij} \partial_{T_j} \mathcal{K} + \sum_{j \neq i} q_i^j |\Phi_i^j|^2\Big)^2, \tag{2.2.7}$$

where $g_{D_{7_i}}$ stands for the gauge coupling of the D_7 brane, Q_{ij} represents the charges of the Kähler moduli, while q_i^j, Φ_i^j are the charges and the scalar components of the superfields, correspondingly. Considering that the vevs of the matter fields are $\langle \Phi_i^j \rangle = 0$, then the formula is significantly simplified to:

$$V_D \cong \sum_{i=3}^{3} \Big[\frac{1}{\tau_i} \Big(\sum_{i \neq j} Q_{ij} \partial_{T_j} \mathcal{K}\Big)^2\Big] \cong \sum_{i=1}^{3} \frac{d_i}{f_a^3}, \ \ d_i \cong Q_{ij}^2 > 0, \tag{2.2.8}$$

where f_a^3 is cubic polynomial parametrized by a generic four-cycle modulus τ_j. Now, the above formula can be further approximated, as noted in [141; 159; 160], by considering the toroidal-like symmetry of the underlying geometry. Moreover, the three intersecting stacks of D_7 branes (which is the geometric setup of this model) are associated to gauge groups, where in principle the magnetic fluxes can induce some anomalous $U(1)$ symmetries. As studied rigorously in [149; 161; 162] a suggestion made by Burgess et al. and Achucarro et al.[13], D-terms of the above form could, also, be derived from a different origin. From a 4D point of view, this type of D-terms was identified as a Fayet-Iliopoulos term depending on the Kähler moduli in the $\mathcal{N} = 1$ supersymmetric effective action [165]. Taking into account the anomalous $U(1)$, the four-cycle moduli, parametrizing the transverse volume of the magnetic D_7 brane, obtain a charge Q under

[13] A criticism on this approach can be found on [163; 164].

the $U(1)$. Additionally in this approach, there are in general the same charges q_i^j carried by the scalar fields Φ_i^j, which fields can be minimized at zero. As a consequence of the above discussion, we could write down the D-terms of this intersecting D_7 branes model, following the work of [113; 149; 161; 162], as:

$$V_D \cong \sum_{i=1}^{3} \frac{d_i}{\tau_i^3} \,. \tag{2.2.9}$$

To support our approach, we provide in the Appendix A.3 a detailed proof that the above formula gives an equivalent dS vacuum to the vacuum that can be derived from the generic formula (2.2.8) up to a rescaling of the uplifting parameters d_i. As a consequence, we can argue that our approximation does not spoil either the existence of a dS vacuum nor the subsequent analysis. Appending the D-term effects on the F-term potential, the complete effective potential is summarized below:

$$V_{eff} = \frac{3\mathcal{W}_0^2(-8\eta + \xi + 2\eta \log(\mathcal{V}))}{2\mathcal{V}^3} + \frac{d_1}{\tau_1^3} + \frac{d_2}{\tau_2^3} + \frac{d_3}{\tau_3^3} \,. \tag{2.2.10}$$

The τ_3 modulus could be traded with the internal volume modulus $\mathcal{V}$, i.e., $\tau_3 = \mathcal{V}^2/(\tau_1\tau_2)$. Thus, the effective potential is the sum $V_{eff} = V_F + V_D$, while it can expressed as a function of τ_1, τ_2 and $\mathcal{V}$:

$$V_{eff} = \frac{3\mathcal{W}_0^2(-8\eta + \xi + 2\eta \log(\mathcal{V}))}{2\mathcal{V}^3} + \frac{d_1}{\tau_1^3} + \frac{d_2}{\tau_2^3} + \frac{d_3\tau_1^3\tau_2^3}{\mathcal{V}^6} \,. \tag{2.2.11}$$

For the sake of completeness, we are going to describe the minima along the three transverse directions $(\mathcal{V}, \tau_1, \tau_2)$. Minimizing along every direction, we get the following minima and some useful relations constraining the free parameters of the theory. Moreover, the potential along the volume direction is displayed below, where the minimal values for τ_1, τ_2 moduli have been applied.

$$\tau_1 = (\frac{d_1^2}{d_2 d_3})^{1/9}\mathcal{V}^{2/3}, \quad \tau_2 = (\frac{d_2^2}{d_1 d_3})^{1/9}\mathcal{V}^{2/3}, \tag{2.2.12}$$

$$\mathcal{V}_{min} = \frac{3\eta\ \mathcal{W}_0^2\ W_{0/-1}\left(\frac{2de^{\frac{13}{3}-\frac{\xi}{2\eta}}}{3\eta\ \mathcal{W}_0^2}\right)}{2d}, \quad d = (d_1 d_2 d_3)^{1/3} \,, \tag{2.2.13}$$

$$V_{eff}(\mathcal{V}) = \frac{6d\mathcal{V} + 3\mathcal{W}_0^2(\xi - 8\eta) + 6\eta\mathcal{W}_0^2 \log(\mathcal{V})}{2\mathcal{V}^3} \,. \tag{2.2.14}$$

where the W-function denotes the Lambert function. The minimum and the maximum along the volume direction are characterized by the upper W_0 and the lower branch W_{-1}, correspondingly. Now, a dS minimum put a stringent bound on the parameter $\rho = \frac{d}{(\mathcal{W}_0)^2}$, $d = (d_1 d_2 d_3)^{1/3}$, where these bounds are obtained from the Lambert's function definition ($W(x),\ x \geq \frac{1}{e}$) and the positivity of the potential at the minimum.

$$-\frac{\eta}{\mathcal{V}} < \rho < -\frac{3}{2}\eta\ e^{\frac{\xi}{2\eta} - \frac{16}{3}},\ \ \frac{1}{3}\left(26 - 6\log\left(-\frac{3\eta}{2e\rho}\right)\right) < \frac{\xi}{\eta} < 0\ . \tag{2.2.15}$$

A different parametrization for the above coefficients is given below, which would be more useful in the following sections:

$$\frac{\partial^2 V_{eff}}{(\partial\mathcal{V})^2} = -\frac{6d\mathcal{V}_{min} + 9\eta\mathcal{W}_0^2}{\mathcal{V}_{min}^5} > 0 \Rightarrow \frac{\partial^2 V_{eff}}{(\partial\mathcal{V}_{min})^2} = -\frac{-9\eta\mathcal{W}_0^2(\frac{2}{3}q + 1)}{\mathcal{V}_{min}^5} > 0 \Rightarrow q = \frac{d\mathcal{V}_{min}}{\eta\mathcal{W}_0^2} > -\frac{3}{2}, \tag{2.2.16}$$

$$-\frac{\eta}{\mathcal{V}} < \frac{d}{\mathcal{W}_0^2} \Rightarrow q = \frac{d\mathcal{V}_{min}}{\eta\mathcal{W}_0^2} < -1, \tag{2.2.17}$$

where combining the above bounds the q parameter is strictly bounded between:

$$-\frac{3}{2} < q < -1\ . \tag{2.2.18}$$

Clearly, our effective potential could admit a dS vacuum (as it is depicted in Figure 1.) for various combinations of the parameters either in the exponentially suppressed flux limit or for the order one flux case.

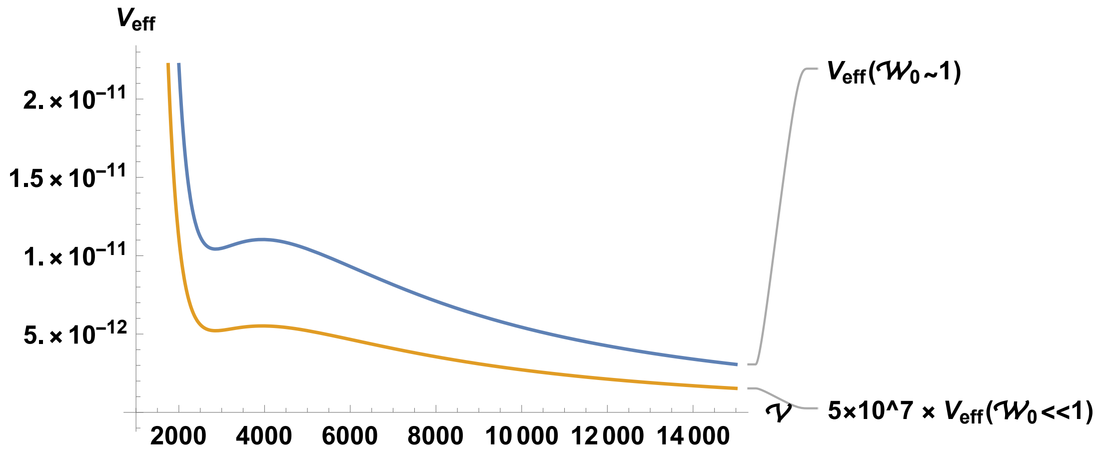

Figure 2.8: Plot of potential (2.2.14) $\xi = 5$, $\mathcal{W}_0 = (1, 10^{-4})$, $d = (4 \times 10^{-4}, 4 \times 10^{-12})$ and $\eta = -0.9$.

2.2.2 Mixing in the kinetic terms and canonical normalized fields

Consistently embedding string inflation within type IIB compactifications is one of the challenging problems in studying early universe cosmology. Various works have attempted to study the universe's inflationary evolution, where different mechanisms are employed [101; 160; 166; 167; 168; 169]. The implications of the inflationary scenario in low energy phenomenology could be viewed indirectly by the correct prediction of the cosmological observables, such as the Big Bang Nucleosynthesis [170; 171], which is correlated with the scale of inflation and the reheating process after it. In this section, we are going to present a detailed analysis on the the canonical normalization of the moduli fields and signify the importance of the logarithmic corrections in the off-diagonal entries of the Kähler metric. Our starting point is the relevant discussion in [160], where they study the inflationary period without expanding to the reheating process and the relevant decay rates of the moduli fields to the visible sector's degrees of freedom in the geometric setup. In this discussion, the quantum corrections are justifying their presence, since the eigenvalue of the volume direction is highly dependent on the quantum parameter η or the general parameter q, which fact modifies its scaling and mixing with the other sectors. In addition, one more advantage of characterizing the mixing between the normalized fields, is that the mass hierarchy could provide many insights on whether inflationary dynamics lay in the category of a single field inflation or a multi-field case. Apart from that, the study of the reheating process and the energy flow to the dark sector is highly influenced by the moduli's decay channels, where the longest lived particle will dominate the energy density in the late cosmological times and clarify the correlation between different important energy scales in the universe's expansion.

Following the discussion above, we need to change the basis from the Kähler moduli τ_i to the normalized canonical fields ϕ_i. First of all, [172], the mixing of the fields is given by the diagonalization of the mass matrix and the transformation of the basis is driven by the canonically corrected kinetic terms. We start by writing down the definition of the Lagrangian in terms of the moduli fields:

$$\mathcal{L} = \mathcal{K}_{ij}\partial_\mu\tau_i\partial^\mu\tau_j - V - \frac{1}{2}V\tau_i\tau_j + \mathcal{O}(\tau^3), \tag{2.2.19}$$

where V is the scalar potential of the moduli fields, while K_{ij} denotes the Kähler metric

$$\mathcal{K}_{ij} = \begin{pmatrix} \frac{1}{4\tau_1^2} & -\frac{\xi+2\eta\log(\mathcal{V})}{8\tau_1\tau_2\mathcal{V}} & -\frac{\tau_2(\xi+2\eta\log(\mathcal{V}))}{8\mathcal{V}^3} \\ -\frac{\xi+2\eta\log(\mathcal{V})}{8\tau_1\tau_2\mathcal{V}} & \frac{1}{4\tau_2^2} & -\frac{\tau_1(\xi+2\eta\log(\mathcal{V}))}{8\mathcal{V}^3} \\ -\frac{\tau_2(\xi+2\eta\log(\mathcal{V}))}{8\mathcal{V}^3} & -\frac{\tau_1(\xi+2\eta\log(\mathcal{V}))}{8\mathcal{V}^3} & \frac{\tau_1^2\tau_2^2}{4\mathcal{V}^4} \end{pmatrix} + \mathcal{O}(\frac{1}{\mathcal{V}^n}, \eta^n)\ . \tag{2.2.20}$$

Is is important to highlight the fact that we have exchanged the τ_3 modulus in term of the overall volume $\mathcal{V}$, which means that the new moduli space is consisted by the $(\tau_1,\tau_2,\mathcal{V})$. Another one thing is that we have kept the leading order terms ($\sim \mathcal{O}(\eta, \xi)$) in the off diagonal entries, which parametrize the quantum corrections to the kinetic terms. Our main interest is to see in what extent these corrections could modify the mixing in the parameter space. The next step would be to compute the mass matrix and the corresponding eigenvalues and eigenvectors. The definition of the mass matrix is given by:

$$M_{ij}^2 = \frac{1}{2}(\mathcal{K})_{ik}^{-1}V_{kj}, \tag{2.2.21}$$

where $V_{kj}, i, j = (\tau_1, \tau_2, \mathcal{V})$ are the second derivatives of the effective potential computed at the global minimum, while the inverse Kähler matrix $\mathcal{K}$ is given by:

$$\mathcal{K}_{ij}^{-1} = \begin{pmatrix} 4\tau_1^2 & \frac{2\tau_1\tau_2(\xi+2\eta\log(\mathcal{V}))}{\mathcal{V}} & \frac{2\mathcal{V}(\xi+2\eta\log(\mathcal{V}))}{\tau_2} \\ \frac{2\tau_1\tau_2(\xi+2\eta\log(\mathcal{V}))}{\mathcal{V}} & 4\tau_2^2 & \frac{2\mathcal{V}(\xi+2\eta\log(\mathcal{V}))}{\tau_1} \\ \frac{2\mathcal{V}(\xi+2\eta\log(\mathcal{V}))}{\tau_2} & \frac{2\mathcal{V}(\xi+2\eta\log(\mathcal{V}))}{\tau_1} & \frac{4\mathcal{V}^4}{\tau_1^2\tau_2^2} \end{pmatrix} + \mathcal{O}(\frac{1}{\mathcal{V}^n}, \eta^n)\ , \tag{2.2.22}$$

$$V_{ij} = \begin{pmatrix} \frac{18}{(d\mathcal{V}^{10})^{1/3}} & 9(\frac{d^2}{\mathcal{V}^{10}})^{1/3} & -18(\frac{d}{\mathcal{V}^{11}})^{1/3} \\ 9(\frac{d^2}{\mathcal{V}^{10}})^{1/3} & 18(\frac{d^5}{\mathcal{V}^{10}})^{1/3} & -\frac{18d^{4/3}}{\mathcal{V}^{11/3}} \\ -18(\frac{d}{\mathcal{V}^{11}})^{1/3} & -\frac{18d^{4/3}}{\mathcal{V}^{11/3}} & \frac{9\eta\mathcal{W}_0^2(2q-1)}{\mathcal{V}^5} \end{pmatrix} + \mathcal{O}(\frac{1}{\mathcal{V}^n}, \eta^n) \ . \tag{2.2.23}$$

Combining all the above ingredients, we can compute the mass matrix in the following basis $(\tau_1, \tau_2, \mathcal{V})$, where we have expanded in terms of the η parameter and kept only leading terms in terms of $\frac{\xi}{\mathcal{V}^n}$. Observing the mass matrix, we could clearly deduce that the quantum corrections are not affecting the scaling of the eigenvalues at a significant level. Nevertheless, the parameter q defined in equation (2.2.18) appears at the 33 entry of the matrix, denoting that one eigenvalue will be correlated to the new effects. This fact may have been neglected in other works, but it is of crucial importance since the q parameter not only satisfies the bounds for a dS vacuum, but also contains the integer fluxes $\mathcal{W}_0$ whose effect is to adjust the scale of the potential at the minimum.

$$M_{ij}^2 \cong \begin{pmatrix} \frac{36d}{\mathcal{V}^2} & \frac{18d^2}{\mathcal{V}^2} & -\frac{36d^{5/3}}{\mathcal{V}^{7/3}} \\ \frac{18}{\mathcal{V}^2} & \frac{36d}{\mathcal{V}^2} & -\frac{36d^{2/3}}{\mathcal{V}^{7/3}} \\ -\frac{36}{(d\mathcal{V}^7)^{1/3}} & -\frac{36d^{2/3}}{\mathcal{V}^{7/3}} & \frac{18\eta\mathcal{W}_0^2(2q-1)}{d^{2/3}\mathcal{V}^{11/3}} \end{pmatrix} + \mathcal{O}(\frac{1}{\mathcal{V}^n}, \eta^n) \ . \tag{2.2.24}$$

In the above matrices, we are obliged to use the minimal values of the all the moduli fields $(\tau_1, \tau_2, \mathcal{V})$ (2.2.13), but to make the formulas more readable we do not substitute the $\mathcal{V}_{min}$. In order to avoid the reader's confusion, in this section and for the rest of the paper $\mathcal{V}$ is denoting its minimum value $\mathcal{V}_{min}$. In order to compute the scaling of the mass eigenvalues, we are going to use the trace and the determinant of the mass matrix M^2:

$$Tr[M^2] = m_1^2 + m_2^2 + m_3^2, \quad \frac{Det[M^2]}{Tr[M^2]^2} = \frac{m_1^2 m_2^2 m_3^2}{(m_1^2 + m_2^2 + m_3^2)^2} \ . \tag{2.2.25}$$

A straightforward computation of the above quantities lead to effectively describe the spectrum's masses as:

$$Tr[M^2] \cong \frac{72d}{\mathcal{V}^2}, \quad \frac{Det[M^2]}{Tr[M^2]^2} \cong -\frac{27\eta\mathcal{W}_0^2\left(\frac{2}{3}q + 1\right)}{8(d^2\mathcal{V}^{10})^{1/3}} \ . \tag{2.2.26}$$

As stated before, the quantum correction η acts as a key player in the masses eigenvalues, where in addition the scale of the fluxes $\mathcal{W}_0$ will also modify the hierarchy in the spectrum. Before attributing these masses to the normalized fields, we would like to derive some useful bounds for the parameters of the theory. So, in an inflationary scenario the inflaton field would be more natural to be identified by the lightest field of the spectrum. The first eigenvalue scales as $\sim \frac{1}{\mathcal{V}^2}$ making it much larger than the second one scaling as $\sim \frac{1}{\mathcal{V}^3}$. Nevertheless, our computation reveals that the uplift parameter and the fluxes have the potential to invert this hierarchy even in large fluxes regime. Having that in mind, Figure 2. shows the exact bound of the product between the uplift parameter and the fluxes with respect to the quantum corrections of the theory, namely the q parameter and the η parameter.

$$\frac{Tr[M^2]}{\frac{Det[M^2]}{Tr[M^2]^2}} \cong -\frac{64 d^{5/3}\mathcal{V}^{4/3}}{3\eta\mathcal{W}_0^2(\frac{2}{3}q+1)} = -\frac{64}{3}\frac{d^{5/3}\mathcal{V}^{4/3}}{\frac{d\mathcal{V}}{q}}\frac{1}{(\frac{2}{3}q+1)} = -\frac{64 d^{1/3}}{3}\frac{q^{4/3}(\eta\mathcal{W}_0^2)^{1/3}}{(\frac{2}{3}q+1)}, \tag{2.2.27}$$

$$\frac{Tr[M^2]}{\frac{Det[M^2]}{Tr[M^2]^2}} < 1 \Rightarrow (d\mathcal{W}_0^2)^{1/3} < -\frac{3}{64}\frac{(\frac{2}{3}q+1)}{q(\eta q)^{1/3}} \Rightarrow d\mathcal{W}_0^2 < -\frac{3^3}{4^9}\frac{(\frac{2}{3}q+1)^3}{\eta q^4} \ll 1\,. \tag{2.2.28}$$

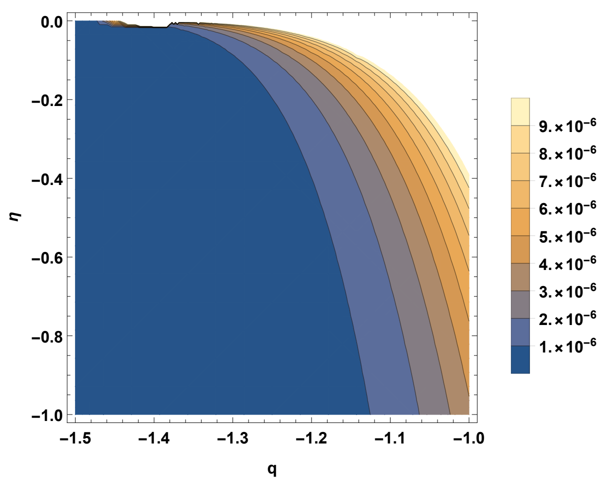

Figure 2.9: Plot of $d\mathcal{W}_0^2$ in terms of η and q.

A crucial difference between the work of [172], it is that we cannot know a priori which normalized field better describes the compactified volume $\mathcal{V}$ or the transverse directions τ_1, τ_2. Additionally, two different regimes will be investigated, the first one will scan the exponentially small fluxes $\mathcal{W}_0 \ll 1$ while the second will search for order one fluxes $\mathcal{W}_0 \sim 1$. These two vastly divergent parametric regions have been studied before [141], while recent studies point towards to dS vacua with small fluxes [91; 118].

In the appendix A.1, we explicitly derive the canonical normalization transformation for the two cases discussed above. The overall scaling of the moduli in terms of the normalized fields (ϕ_i) and the correspondence of the fields to the mass eigenvalues are displayed below:

- α) Having exponentially suppressed fluxes, the mass hierarchy and the field's mixing is defined by:
$$m^2_{\phi_3} \cong \frac{Det[M^2]}{Tr[M^2]^2} \gg m^2_{\phi_1} \cong m^2_{\phi_2} \cong Tr[M^2] \ . \tag{2.2.29}$$
$$\tau_1 \cong P^{\alpha)}_{11}\phi_1, \quad \tau_2 \cong P^{\alpha)}_{22}\phi_2, \quad \mathcal{V} \cong P^{\alpha)}_{33}\phi_3 \ . \tag{2.2.30}$$

- β) Fluxes of order one will result in having ϕ_1 as the heaviest field and the masses are given by:
$$m^2_{\phi_1} \cong Tr[M^2] \gg m^2_{\phi_2} \cong m^2_{\phi_3} \cong \frac{Det[M^2]}{Tr[M^2]^2} \ . \tag{2.2.31}$$
$$\tau_1 \cong P^{\beta)}_{12}\phi_2, \quad \tau_2 \cong P^{\beta)}_{22}\phi_2, \quad \mathcal{V} \cong P^{\beta)}_{33}\phi_3 \ . \tag{2.2.32}$$

It is evident that the above results have a geometric explanation. The moduli, since they are parametrizing the world volume of distinct stack of branes, are given mainly by different normalized fields. This result leads us to deduce that despite the simple form of the compactified volume, there exists a geometric separation between the different sectors of the theory. In addition, the most natural candidate for an inflationary trajectory is the direction of the overall volume $\mathcal{V}$, since it contains a flat direction (as depicted in Figure 1.) and a stable minimum described by equation (2.2.13). The exponentially suppressed $\mathcal{W}_0$ case could be regarded as an non-standard inflationary scenario, since the ϕ_3 is the heaviest field and the dynamics of the moduli's during inflation have to be carefully studied due to destabilization effects. Although, given the three intersecting branes setup, the visible sector's branes could be separated from the hidden sector's branes placed on the perpendicular directions making plausible a string embedding of an inflationary evolution. This regime could easily capsulate the dynamics of a multi-fields inflation, based on the arguments given above, with many similar examples existing in the literature [123; 127]. On the contrary, the case of having order one fluxes renders a scenario where the inflaton behaves as the lightest field in the mass spectrum, making the approach of the effective theory valid. Consequently, this scenario could be characterized as a natural single field inflation case. However, inflation is not our main object of study in this work but we retain our mission for a consistent string embedding in a future work.

Interestingly, if we would like to compare our toy model's structure with the literature, the geometry discussed in [152] and in references therein, shares some interesting features with the above analysis. In their volume form, the visible sector is completely decoupled by the rest moduli and they separate two cases regarding the identification of the inflaton field. In the Kähler inflation case, the inflaton is denoted by the heaviest field and the transverse mode specifies the dark radiation predictions. Compared to our cases, the case α) shares the same features, where due to the newly quantum dynamics the heaviest field is represented by the inflaton, while a transverse field will be the longest lived and eventually will specify the late time universe's energy density (see discussion in section 4.). Now, in the fibre inflation scenario of [152], the inflaton is identified by the lightest particle, just like our case β). In addition to the above, an early matter domination epoch could be included in the Kähler inflation case, which fact is also evident in our case α), since the mass hierarchy is inverted and large non-gaussianities. This paragraph had an aim to place this model in comparison with the known examples with related dynamics in the literature, where the two distinct inflationary paradigms are discriminated by a matter of choice for the inflaton field. Now, this discrimination between the different inflation scenarios could be elucidated through a more natural explanation, in particular the choice of fluxes, even if they are stemming from an alike geometry.

2.2.3 Reheating and dark radiation predictions

After the end of inflation, the inflaton will begin to oscillate around their minima, acquiring a large energy density in the process. Now, this energy density has to be transferred through a specific mechanism to the other fields of the theory, either to the visible sector or to the dark sector. Among this plethora of fields, there is a possibility that the universe's late time cosmological dynamics are going to be addressed not by the inflaton, but by a different field whose decay rate is much smaller. Thus, the final reheating temperature and the effective number of neutrino species will be determined by the decay rate of the aforementioned longest lived particle. Regarding the decay products of the moduli, they fall into two categories. The first are the decays that produce the visible sector's particles, where these particles could be identified as either Higgs boson or other Minimal Supersymmetric Standard model's (MSSM) fields. Among several suggestions to this problem we are going to employ a Giuduce-Masiero mechanism for describing the relevant dynamics of the decays to the visible sector. In addition, there may also be decays to hidden sector states, which is a generic feature shared by string compactifications. The hidden sector contains several candidates for dark radiation, such as the axionic partner of the Kähler moduli fields or light hidden gauge bosons. Based on the analysis of the previous sections, we will identify the longest lived particle in each case study (α and β), by explicitly compute the couplings of the moduli fields to the Higgs field and to the axions. In spite of the criticism receiving these type of stringy constructions regarding the complex dynamics and the uncertainty with respect to the effective theory approximation, interesting proposals point towards the direction, where cosmological solutions could play a bilateral role. Firstly, these solutions provide a stringy origin for the reheating mechanism but also contribute to the identification of various dark matter particles [151; 173; 174; 175], correlating this way the dark sector dynamics to the reheating temperature.

As consequence of above, we are going to start from the Lagrangian's kinetic terms, they can be expanded as:

$$\begin{aligned}\mathcal{L} = {} & \mathcal{K}_{11}\partial_\mu\tau_1\partial^\mu\tau_1 + \mathcal{K}_{12}\partial_\mu\tau_1\partial^\mu\tau_2 + \mathcal{K}_{13}\partial_\mu\tau_1\partial^\mu\mathcal{V} + \mathcal{K}_{21}\partial_\mu\tau_2\partial^\mu\tau_1 + \mathcal{K}_{22}\partial_\mu\tau_2\partial^\mu\tau_2 \\ & + \mathcal{K}_{23}\partial_\mu\tau_2\partial^\mu\mathcal{V} + \mathcal{K}_{31}\partial_\mu\mathcal{V}\partial^\mu\tau_1 + \mathcal{K}_{32}\partial_\mu\mathcal{V}\partial^\mu\tau_2 + \mathcal{K}_{33}\partial_\mu\mathcal{V}\partial^\mu\mathcal{V} + V + \mathcal{O}(\frac{\partial^2 V}{\partial_{\tau_i}\partial_{\tau_j}})\tau_i\tau_j\ .\end{aligned} \tag{2.2.33}$$

Since we would like to highlight the effect of the quantum corrected kinetic terms, we would like to include to the above Lagrangian, terms that contain cubic order interactions and more specifically, the interactions between moduli and their corresponding axionic partners c_i. These trilinear interaction terms have the following structure:

$$\mathcal{L} = (\partial_{\tau_i}\mathcal{K}_{jk})\ \tau_i\partial_\mu c_j\partial^\mu c_k = (\partial_{\tau_i}\mathcal{K}_{jk})\frac{1}{2}(m_i^2 - m_j^2 - m_k^2)\tau_i c_j c_k, \tag{2.2.34}$$

where in the last step we have used the Dirac equation, after integration by parts, to recast the terms in their equivalent form containing their respective masses. As pointed out in [151], the cubic terms obtained by the derivatives of the potential are subleading compared to the ones originated from the kinetic terms. This fact can be addressed to the suppression due to the large volume expansion, where we expect a similar behavior in our geometry. We can take for granted that the masses of the axions are negligible compared to moduli's masses, concluding that only m_i will contribute in the above interaction term. The most crucial point in the above computation is the derivative of the Kähler metric with respect to each modulus of the parameter space, where the corresponding matrices are displayed below.

$$\partial_{\tau_1}\mathcal{K}_{ij} = \begin{pmatrix} -\frac{1}{2d^2\mathcal{V}^2} & \frac{\eta(6-q)}{4d\mathcal{V}^3} & \frac{\eta(6-q)}{4d\mathcal{V}^3} \\ \frac{\eta(6-q)}{4d\mathcal{V}^3} & 0 & -\frac{\eta(q-5)}{12\mathcal{V}^3} \\ \frac{\eta(6-q)}{4d\mathcal{V}^3} & -\frac{\eta(q-5)}{12\mathcal{V}^3} & 0 \end{pmatrix}, \tag{2.2.35}$$

$$\partial_{\tau_2}\mathcal{K}_{ij} = \begin{pmatrix} 0 & \frac{\eta(6-q)}{4d\mathcal{V}^3} & -\frac{\eta(q-5)}{12\mathcal{V}^3} \\ \frac{\eta(6-q)}{4d\mathcal{V}^3} & -\frac{d}{2\mathcal{V}^2} & -\frac{d\eta(q-6)}{4d\mathcal{V}^3} \\ -\frac{\eta(q-5)}{12\mathcal{V}^3} & -\frac{d\eta(q-6)}{4d\mathcal{V}^3} & 0 \end{pmatrix}, \quad \partial_{\mathcal{V}}\mathcal{K}_{ij} = \begin{pmatrix} 0 & \frac{\eta(-q+5)}{6(d\mathcal{V}^{10})^{1/3}} & \frac{\eta(-q+6)}{2(d\mathcal{V}^{10})^{1/3}} \\ \frac{\eta(-q+5)}{6(d\mathcal{V}^{10})^{1/3}} & 0 & -\frac{d^{2/3}\eta(q-6)}{2\mathcal{V}^{10/3}} \\ \frac{\eta(-q+6)}{6(d\mathcal{V}^{10})^{1/3}} & -\frac{d^{2/3}\eta(q-6)}{2\mathcal{V}^{10/3}} & -\frac{d^{2/3}}{\mathcal{V}^{7/3}} \end{pmatrix}. \tag{2.2.36}$$

To all the above matrices, the minimal values of the moduli $\tau_1, \tau_2, \mathcal{V}$ have to be applied. So, every coupling will be expressed only in terms of the free parameters of the theory. Using all the above ingredients, we could compute for example all the relevant coupling constants needed for the various decay rates. In doing so, the formulas in Appendix A.2 will be used. Before proceeding further, it is crucial to rethink which is the longest lived particle on this model, since this will determine the energy's composition of the universe at late-times. The most dominant contribution to the visible sector's energy will come from the decay a the normalized field to Higgses. We focus on the Giudice-Masiero mechanism, where for the MSSM the relevant fields are the Higgses H_u and H_d. Starting from an extended Kähler potential with the Higgses fields included, we will conclude to the formula of the process's decay rate.

$$\mathcal{K} = -3\ln\left[(T_i + \bar{T}_i) + \frac{1}{3}(H_u\bar{H}_u + H_d\bar{H}_d + ZH_u\bar{H}_d)\right], \tag{2.2.37}$$

where expanded to leading order, the final term will be the most dominant one [153; 176; 177]. Thus, the relevant decay rate for the various moduli fields is given by:

$$\Gamma_{\tau_i \to H\bar{H}} \sim \frac{2Z^2}{48\pi}\frac{m_\phi^3}{M_p^2}\,. \tag{2.2.38}$$

Returning to our initial question, which is the determination of the longest lived particle, it is important to recast the moduli fields τ_i to the normalized ones ϕ_i, where this transition will contribute an additional factor (mixing factor) to the above decay rate. This factor can be retrieved from the Appendix A.1. This is the point where the analysis of the previous section comes in handy.

Let us start from the case α) of having exponentially suppressed fluxes, and we should compute the relevant decay rates of every normalized field to Higgses:

$$\Gamma_{\phi_1\to H\bar{H}} = \frac{5184\, Z^2\sqrt{2}d^{19/6}q^2\xi}{\pi w^2\mathcal{V}^2}, \quad \Gamma_{\phi_2\to H\bar{H}} = \frac{432\, Z^2\sqrt{2}d^{5/6}}{\pi s\mathcal{V}^{10/3}}, \quad \Gamma_{\phi_3\to H\bar{H}} = \frac{27\, Z^2(-\eta\mathcal{W}_0^2)^{3/2}(2q+3)^{3/2}}{16\sqrt{2}\pi s\, d^{5/3}\mathcal{V}^{16/3}}, \tag{2.2.39}$$

$$\frac{\Gamma_{\phi_1\to H\bar{H}}}{\Gamma_{\phi_3\to H\bar{H}}} = \frac{6144 d^{29/6}\xi q^2 s\mathcal{V}^{7/3}}{w^2\left(-\eta(2q+3)\mathcal{W}_0^2\right)^{3/2}} \ll 1, \quad \frac{\Gamma_{\phi_1\to H\bar{H}}}{\Gamma_{\phi_2\to H\bar{H}}} = \frac{24\sqrt{2}q^2\xi(d^7\mathcal{V})^{1/3}}{w^2} \ll 1. \tag{2.2.40}$$

The parameters w, s have been properly defined in the Appendix, where they are expressed in terms of the $\mathcal{V}$, d and q. Based on the above fractions between the decay rates, we observe that the smallest one is represented by the Γ_{ϕ_1}, making ϕ_1 the longest lived particle. This conclusion has important consequences in the late-time cosmology's dynamics, since the energy density will be determined by the ϕ_1 instead of ϕ_3 which represents a plausible inflaton. The mixing has added the uplift parameter d and the fluxes $\mathcal{W}_0$ in the computation, suppressing the decay rate sufficiently in order to have a new long lived particle. So sketching up our geometric setup, we have to place the visible sector on the stack of branes represented by the τ_3 world-volume, making this way the τ_1, τ_2 spaces the dark sectors of the geometry. Additionally, as pointed out in [178], any non-perturbative corrections along the cycles supporting the visible sector can not be allowed, since they will intersect with the chiral matter. A solution to this stabilization problem is solved by our proposal of logarithmic loop correction. Rephrasing the above argument, this type of construction could only possible allow axionic degrees of freedom from the transverse space of τ_3. We have to make this particular choice, taking into account the fact that the lightest and longest lived particle could in principle not only solve the dark radiation problem, but also their decays could produce the correct abundance of non-thermal dark matter. Thus, ϕ_1 (i.e. the τ_1 modulus) cannot be identified with the visible sector.

For the case β) of having order one fluxes, a similar discussion could lead to the following results for the decay rates of the normalized fields to Higgses.

$$\Gamma_{\phi_2(\tau_1)\to H\bar{H}} = \frac{54Z^2\sqrt{2}s^2d^{5/6}}{\pi\mathcal{V}^{17/3}},\;\; \Gamma_{\phi_2(\tau_2)\to H\bar{H}} = \frac{81\sqrt{2}d^{2/3}\xi q^2(2q+3)^{3/2}Z^2\left(-\eta\mathcal{W}_0^2\right)^{3/2}}{\pi\mathcal{V}^5 w^2}, \tag{2.2.41}$$

$$\Gamma_{\phi_3\to H\bar{H}} = \frac{729d^{2/3}\xi q^2(2q+3)^{3/2}Z^2\left(-\eta\mathcal{W}_0^2\right)^{3/2}}{4\sqrt{2}\pi\mathcal{V}^5 w^2}\;. \tag{2.2.42}$$

$$\frac{\Gamma_{\phi_2(\tau_1)\to H\bar{H}}}{\Gamma_{\phi_3\to H\bar{H}}} = \frac{16\sqrt[6]{d}s^2w^2}{27\xi q^2\mathcal{V}^{2/3}\left(-\eta(+2q+3)\mathcal{W}_0^2\right)^{3/2}},\;\; \frac{\Gamma_{\phi_2(\tau_2)\to H\bar{H}}}{\Gamma_{\phi_3\to H\bar{H}}} < 1\;. \tag{2.2.43}$$

From the above, we can conclude that the normalized field ϕ_3 corresponds to the longest lived particle in this setup. This case can be considered as more natural, since the longest lived particle is identified with the inflaton and eventually will specify the energy density after inflation. Again, as previously, we have to specify the visible and the hidden sector of the internal geometry. In this case, the visible sector will be identified with the τ_1 stack of branes, while the ϕ_3 field will be important to both the discussions of dark radiation and dark matter.

Returning to our main purpose, which is to calculate the dark radiation predictions of this model, we have to think which are the important decay channels relevant to our purpose. The decay rates of the longest lived particle to axions have to be scrutinized and the first thing to do is to write the interaction terms associated to these processes.

$$\mathcal{L} \supset \left(\partial_{\tau_m}\mathcal{K}_{np}\right)\tau_m\partial_\mu c_n\partial^\mu c_m = \partial_{\tau_m}\mathcal{K}_{np}P^\tau_{mi}P^c_{nj}P^c_{pk}\phi_i\partial_\mu\alpha_j\partial^\mu\alpha_k = \mathcal{K}_{mnp}P^\tau_{mi}P^c_{nj}P^c_{pk}m^2_{\phi_i}\phi_i\alpha_j\alpha_k, \tag{2.2.44}$$

where in the last step we have also transformed the axionic partner c_i of the Kähler modulus to the normalized axion α_i. The P_{ij} matrices represent elements of the mixing matrix, when we apply the basis transformation. The mixing between the axions will be determined by studying the induced scalar potential, when non-perturbative corrections are included in the superpotential $\mathcal{W}$. Geometric constructions, where all type of corrections are turned on, have constructed in the past [142; 143] and the problem of moduli stabilization is not affected. The large volume limit is necessary to ensure the validity of the effective theory and to keep the exponential factor the non perturbative corrections $\mathcal{W} \supset Ae^{-a\tau_i}$ relatively small. Since we focus on the impact of the quantum corrections, we could parametrize this matrix as follows and focus on the qualitative behavior of the decay rates [14].

[14]For an extended discussion in a bottom-up string derived model, follow Appendix B in [151]

$$\begin{pmatrix} c_1 \\ c_2 \\ c_3 \end{pmatrix} = \begin{pmatrix} \lambda_{11} & \lambda_{12} & \lambda_{13} \\ \lambda_{21} & \lambda_{22} & \lambda_{23} \\ \lambda_{31} & \lambda_{32} & \lambda_{33} \end{pmatrix} \begin{pmatrix} \alpha_1 \\ \alpha_2 \\ \alpha_3 \end{pmatrix}. \tag{2.2.45}$$

For our first case study α), the longest lived particle is ϕ_1, which descends from the τ_1 modulus. Comparing with the Lagrangian terms of equation (2.2.44), the m, i indices are determined from our previous analysis, so $m = 1, i = 1$. As for j, k indices, these can only span $(j, k) = (1, 2)$ since the visible sector is represented by the third modulus. The relevant Lagrangian part for this process can be written, after summing all the contributions, as:

$$\phi_1 \to \alpha_1\alpha_1 : \ \mathcal{K}_{1np} P^{\tau}_{11} P^{c}_{n1} P^{c}_{p1} m^2_{\phi_1} \phi_1\alpha_1\alpha_1 = -\frac{144\sqrt{3}\eta d^{5/6}\lambda_{11}\sqrt{\xi}q\left(\frac{\lambda_{11}\mathcal{V}}{d\eta} + \lambda_{21}(q-6)\right)}{\mathcal{V}^5 w}\phi_1\alpha_1\alpha_1 \ . \tag{2.2.46}$$

As for the decay rate, we can use the decay formulas in the Appendix and it is computed to be:

$$\Gamma_{\phi_1\to\alpha_1\alpha_1} = \frac{1296\sqrt{2}\lambda_{11}^2\xi q^2\left(d\eta\lambda_{21}(q-6) + \lambda_{11}\mathcal{V}\right)^2}{\pi d^{5/6}\mathcal{V}^9 w^2} M_p \ . \tag{2.2.47}$$

The second process to study is the $\phi_1 \to \alpha_2\alpha_2$ and the relevant Lagrangian terms are written as:

$$\phi_1 \to \alpha_2\alpha_2 : \ \mathcal{K}_{1np} P^{\tau}_{11} P^{c}_{n2} P^{c}_{p2} m^2_{\phi_1} \phi_2\alpha_2\alpha_1 = -\frac{144\sqrt{3}d^{5/6}\eta\lambda_{12}\sqrt{\xi}q\left(\frac{\lambda_{12}\mathcal{V}}{d\eta} + \lambda_{22}(q-6)\right)}{\mathcal{V}^5 w}\phi_1\alpha_2\alpha_2 \ , \tag{2.2.48}$$

$$\Gamma_{\phi_1\to\alpha_2\alpha_2} = \frac{1296\sqrt{2}\lambda_{12}^2\xi q^2\left(d\eta\lambda_{22}(q-6) + \lambda_{12}\mathcal{V}\right)^2}{\pi d^{5/6}\mathcal{V}^9 w^2} M_p \ . \tag{2.2.49}$$

The final process, which is only present since we have included the off diagonal terms in the Kähler metric, is the following $\phi_1 \to \alpha_1\alpha_2$:

$$\phi_1 \to \alpha_1\alpha_2 : \mathcal{K}_{1np} P^{\tau}_{11} P^{c}_{n1} P^{c}_{p2} m^2_{\phi_1} \phi_1\alpha_1\alpha_2 = -\frac{72\sqrt{3}d^{5/6}\eta\sqrt{\xi}q\left(A(q-6) + \frac{2\lambda_{11}\lambda_{12}\mathcal{V}}{d\eta}\right)}{\mathcal{V}^5 w}\phi_1\alpha_1\alpha_2 \,, \quad (2.2.50)$$

where we have defined $A = \lambda_{12}\lambda_{21} + \lambda_{11}\lambda_{22}$ for simplicity. The corresponding decay rate is summarized to:

$$\Gamma_{\phi_1 \to \alpha_1\alpha_2} = \frac{324\sqrt{2}\xi q^2 \left(Ad\eta(q-6) + 2\lambda_{11}\lambda_{12}\mathcal{V}\right)^2}{\pi d^{5/6}\mathcal{V}^9 w^2} M_p \,. \quad (2.2.51)$$

Now, we have to compare the processes, in order to find the leading contributions to dark radiation, and a good approximation would be to completely forget about the first terms in the parentheses of the numerators. This is justified by the fact that they are suppressed by the uplift parameter and the quantum correction η. So, dividing the two decay rates some simple and self explanatory formulas are derived.

$$\frac{\Gamma_{\phi_1 \to \alpha_1\alpha_1}}{\Gamma_{\phi_1 \to \alpha_2\alpha_2}} = \frac{\lambda_{11}^2 \left(d\eta\lambda_{21}(q-6) + \lambda_{11}\mathcal{V}\right)^2}{\lambda_{12}^2 \left(d\eta\lambda_{22}(q-6) + \lambda_{12}\mathcal{V}\right)^2}, \quad \frac{\Gamma_{\phi_1 \to \alpha_1\alpha_1}}{\Gamma_{\phi_1 \to \alpha_1\alpha_2}} = \frac{4\lambda_{11}^2 \left(d\eta\lambda_{21}(q-6) + \lambda_{11}\mathcal{V}\right)^2}{\left(Ad\eta(q-6) + 2\lambda_{11}\lambda_{12}\mathcal{V}\right)^2} \,. \quad (2.2.52)$$

$$\frac{\Gamma_{\phi_1 \to \alpha_1\alpha_1}}{\Gamma_{\phi_1 \to \alpha_2\alpha_2}} \cong \frac{\lambda_{11}^4}{\lambda_{12}^4}, \quad \frac{\Gamma_{\phi_1 \to \alpha_1\alpha_1}}{\Gamma_{\phi_1 \to \alpha_1\alpha_2}} \cong \frac{\lambda_{11}^2}{\lambda_{12}^2} \,. \quad (2.2.53)$$

One could see that previous works had omitted the mixed decay channel's contribution to dark radiation and only included in their analysis the first process. As for the relevant scale between the diagonal and the off diagonal entries of matrix (2.2.45), it is expected that $\lambda_{11} > \lambda_{12}$ since we assume a normal ordering in the mass hierarchy. So, we have to take into account the contributions from the off diagonal decays of the moduli to axions. This a novel feature due to the quantum corrected kinetic terms, which was underestimated in previous studies.

$$\Gamma_{tot} = \Gamma_{\phi_1 \to \alpha_1\alpha_1} + \Gamma_{\phi_1 \to \alpha_1\alpha_2} \cong \frac{1296\sqrt{2}\lambda_{11}^2\left(\lambda_{11}^2 + \lambda_{12}^2\right)\xi q^2}{\pi d^{5/6}\mathcal{V}^7 w^2} M_p \,. \quad (2.2.54)$$

Based on the above, we are in a point where we need to connect our theoretical computations to the observable quantities such as the effective number of neutrino species and the reheating.

Recall that, the standard definition of the effective number of neutrino species is given by:

$$\Delta N_{eff} = \frac{43}{7}(\frac{10.75}{g_*(T_{rh})})^{1/3}\frac{\Gamma_{tot}}{\Gamma_{\phi_1\to H\bar{H}}} = \frac{43}{7}(\frac{10.75}{g_*(T_{rh})})^{1/3}\frac{\lambda_{11}^2\left(\lambda_{11}^2+\lambda_{12}^2\right)}{4d^4\mathcal{V}^4Z^2} = \frac{43}{7}(\frac{10.75}{g_*(T_{rh})})^{1/3}\frac{\lambda'^2}{4d^4\mathcal{V}^4Z^2}, \tag{2.2.55}$$

where in the last step we have defined for brevity $\lambda'^2 = \lambda_{11}^2\left(\lambda_{11}^2+\lambda_{12}^2\right)$ and $g_*(T_{rh})$ denotes is the number of relativistic degrees of freedom at T_{rh}. The astrophysical and cosmological observations put a constraint on the $\Delta N_{eff} < 0.4$, which fact will be translated to stringent bound on the mixing angles in the axionic sector.

$$\lambda' < 0.5(\frac{g_*(T_{rh})}{10.75})^{1/6}Zd^2\mathcal{V}^2 = 0.5(\frac{g_*(T_{rh})}{10.75})^{1/6}Zq^2\eta^2\mathcal{W}_0^2\ . \tag{2.2.56}$$

Additonally, we are going to define a new quantity for the complete decay rate (both to visible and dark sector):

$$\Gamma' = \Gamma_{\phi_1\to H\bar{H}} + \Gamma_{tot}\ . \tag{2.2.57}$$

Using this quantity, we can compute straightforward the reheating temperature of this model. This is given by:

$$T_{rh} = (\frac{90}{\pi g_*(T_{rh})}\frac{\Gamma_{\phi_1\to H\bar{H}}}{\Gamma'})^{1/4}\sqrt{\Gamma' M_p}\ . \tag{2.2.58}$$

Since the decays of the moduli to axions are heavily suppressed compared to the ones on Higgses, the complete decay rate can be effectively described by the decay rate to the visible sector. The reheating temperature is, then, described by:

$$T_{rh} \cong (\frac{90}{\pi g_*(T_{rh})})^{1/4}\sqrt{\Gamma_{\phi_1\to H\bar{H}}M_p} = -(\frac{90}{\pi g_*(T_{rh})})^{1/4}\frac{72\ 2^{1/4}d^{19/12}\sqrt{\xi}qZ}{\sqrt{\pi}\mathcal{V}^{3/2}w}M_p\ . \tag{2.2.59}$$

Another one important bound for our model is referred as the cosmological moduli problem [179; 180]. The lightest modulus is bounded from below to lay at scales $\mathcal{O}(10)$TeV:

$$m_{\phi_1} = \frac{3\sqrt{2}d^{1/2}}{\mathcal{V}} M_p > 10 \text{ TeV} \Rightarrow \mathcal{W}_0^2 > \frac{10 \text{ TeV}}{3\sqrt{2}\ \eta q M_p} \mathcal{V}^3 . \qquad (2.2.60)$$

Given this very restrictive bound, we would like to comment on that regarding the geometry of the compactified space. Our case study suggests that we are exploring exponentially suppressed integer fluxes. But, the toroidal structure of the volume form seems to not favor a solution for arbitrary small fluxes. Moreover, we expect that our results will not change significantly by preserving higher order terms in the effective potential, since they are subleading due to the suppression because of η^n and $\frac{\xi}{\mathcal{V}^n}$. This fact could also provide a bottop-up proof of why this geometry, studied before in [113], accommodates more easily stabilized solution with order one fluxes. In addition, only moderate values of volume is accepted in this case, since the masses of the moduli would be below the bound presented above. It is imperative to mention that these cosmological implications of stringy constructions could, also, be used as testing ground in order to clarify the properties of the background geometry and the discussion on the smallness of $\mathcal{W}_0$ [91; 181]. Below, we illustrate three numerical examples (Table 1.) for various scales of reheating temperature of our case study α). In addition, the moduli masses at the stable vacuum are presented in Table 2.

	$\mathcal{W}_0$	η	ξ	d	T_{rh} (GeV)	ΔN_{eff}	$(\lambda_{11}, \lambda_{12})$	Z
$\mathcal{V} \cong 2425$	1×10^{-3}	-0.9	5	3.8×10^{-10}	10	0.25	$(8 \times 10^{-4}, 3 \times 10^{-4})$	1
$\mathcal{V} \cong 2425$	1×10^{-4}	-0.9	7	3.8×10^{-12}	8×10^{-3}	0.25	$(8 \times 10^{-5}, 3 \times 10^{-5})$	1
$\mathcal{V} \cong 2900$	1×10^{-2}	-0.9	5	4×10^{-8}	33×10^{3}	0.1	$(8 \times 10^{-3}, 3 \times 10^{-3})$	1

Table 2.5: Different reheating temperatures for various set of parameters. Obviously, exponentially small fluxes tend to reproduce a low reheating scenario.

$m^2_{\phi_i}$ (TeV)	$m^2_{\phi_1}$	$m^2_{\phi_2}$	$m^2_{\phi_3}$
$\mathcal{W}_0 = 1 \times 10^{-3}$	4×10^{8}	8×10^{8}	3×10^{10}
$\mathcal{W}_0 = 1 \times 10^{-4}$	4×10^{7}	8×10^{7}	1×10^{10}
$\mathcal{W}_0 = 1 \times 10^{-2}$	4×10^{9}	7×10^{9}	4×10^{10}

Table 2.6: The moduli masses along the two numerical examples presented above.

Following the above discussion, we are going to discuss the scenario of having fluxes of order

$\mathcal{W}_0 \sim \mathcal{O}(1)$. The longest lived particle in this case (case β)) is the ϕ_3. The relevant Lagrangian part is written as:

$$\mathcal{L} \supset \mathcal{K}_{3np} P^{\tau}_{mi} P^{c}_{nj} P^{c}_{pk} m^2_{\phi_3} \phi_3 \alpha_j \alpha_k \;, \tag{2.2.61}$$

where we inserted $i = 3$ for the ϕ_3 normalized field and $m = 3$, since this field descends from the volume $\mathcal{V}$ modulus. The first coupling constant is computed as:

$$\phi_3 \to \alpha_3\alpha_3 : \; \mathcal{K}_{3np} P^{\tau}_{33} P^{c}_{n3} P^{c}_{p3} m^2_{\phi_3} \phi_3 \alpha_3 \alpha_3 = \frac{9\sqrt{3} d^{5/6} \eta \lambda_{33} \sqrt{\xi} q(2q+3) \mathcal{W}_0^2 \left(\eta \lambda_{23}(q-6) + \lambda_{33}\mathcal{V}\right)}{2\mathcal{V}^{20/3} w} \phi_3 \alpha_3 \alpha_3 \;. \tag{2.2.62}$$

The decay rate for this process is computed to be:

$$\Gamma_{\phi_3 \to \alpha_3\alpha_3} = \frac{81 d^2 \lambda_{33}^2 \xi q^2 \left(-\eta(2q+3)\mathcal{W}_0^2\right)^{3/2} \left(\eta\lambda_{23}(q-6) + \lambda_{33}\mathcal{V}\right)^2}{4\sqrt{2}\pi \mathcal{V}^{35/3} w^2} M_p \;. \tag{2.2.63}$$

The second process we need to inspect is the $\phi_3 \to \alpha_2\alpha_2$. The Lagrangian terms for the above process are summarized to the following expression:

$$\phi_3 \to \alpha_2\alpha_2 : \; \mathcal{K}_{3np} P^{\tau}_{33} P^{c}_{n2} P^{c}_{p2} m^2_{\phi_3} \phi_3 \alpha_2 \alpha_2 = \frac{9\sqrt{3} d^{5/6} \eta \sqrt{\xi} q(2q+3) \mathcal{W}_0^2 \left(\eta \lambda_{23}\lambda_{33}(q-6) + \lambda_{32}^2\mathcal{V}\right)}{2\mathcal{V}^{20/3} w} \phi_3 \alpha_2 \alpha_2 \;. \tag{2.2.64}$$

There is obviously a similarity of the coupling constant with the previous process' coupling constant. This fact leads to a similar form for the decay constant.

$$\Gamma_{\phi_3 \to \alpha_2\alpha_2} = \frac{81 d^2 \xi q^2 \left(-\eta(2q+3)\mathcal{W}_0^2\right)^{3/2} \left(\eta\lambda_{23}\lambda_{33}(q-6) + \lambda_{32}^2\mathcal{V}\right)^2}{4\sqrt{2}\pi \mathcal{V}^{35/3} w^2} M_p \;. \tag{2.2.65}$$

The latter process we have to compute its decay rate refers to the $\phi_3 \to \alpha_2\alpha_3$. Firstly, we have to write down the Lagrangian:

$$\phi_3 \to \alpha_2\alpha_3 : \ \mathcal{K}_{3np}P^{\tau}_{33}P^{c}_{n2}P^{c}_{p3}m^2_{\phi_3}\phi_3\alpha_2\alpha_2 = \frac{9\sqrt{3}d^{5/6}\eta\sqrt{\xi}q(2q+3)\mathcal{W}_0^2\left(\eta\lambda_{23}\left(\lambda_{32}+\lambda_{33}\right)(q-6)+2\lambda_{32}\lambda_{33}\mathcal{V}\right)}{4\mathcal{V}^{20/3}w}\phi_3\alpha_2\alpha_3 \, , \tag{2.2.66}$$

$$\Gamma_{\phi_3\to\alpha_2\alpha_3} = \frac{81d^2\xi q^2\left(-\eta(2q+3)\mathcal{W}_0^2\right)^{3/2}\left(\eta\lambda_{23}\left(\lambda_{32}+\lambda_{33}\right)(q-6)+2\lambda_{32}\lambda_{33}\mathcal{V}\right)^2}{4\sqrt{2}\pi\mathcal{V}^{35/3}w^2}M_p \, . \tag{2.2.67}$$

Now, as in the previous analysis, we have to compare the decay rates in order to find the most dominant contribution to the dark radiation abundance. Following the argument used before regarding the first term in the parentheses of the above equations, we can observe the scaling between the decay rates.

$$\frac{\Gamma_{\phi_3\to\alpha_3\alpha_3}}{\Gamma_{\phi_3\to\alpha_2\alpha_2}} = \frac{\lambda_{33}^2\left(\eta\lambda_{23}(q-6)+\lambda_{33}\mathcal{V}\right)^2}{\left(\eta\lambda_{23}\lambda_{33}(q-6)+\lambda_{32}^2\mathcal{V}\right)^2} \cong \frac{\lambda_{33}^4}{\lambda_{32}^4}, \quad \frac{\Gamma_{\phi_3\to\alpha_3\alpha_3}}{\Gamma_{\phi_3\to\alpha_2\alpha_3}} = \frac{4\lambda_{33}^2\left(\eta\lambda_{23}(q-6)+\lambda_{33}\mathcal{V}\right)^2}{\left(\eta\lambda_{23}\left(\lambda_{32}+\lambda_{33}\right)(q-6)+2\lambda_{32}\lambda_{33}\mathcal{V}\right)^2} \cong \frac{\lambda_{33}^2}{\lambda_{32}^2} \, . \tag{2.2.68}$$

It is evident, again, as to the former case, that the off diagonal entries give rise to new decay rates that were previously underestimated. Based on the above, we have to sum the two contributions $\Gamma_{\phi_3\to\alpha_3\alpha_3}, \Gamma_{\phi_3\to\alpha_2\alpha_3}$, which fact results into:

$$\Gamma_{tot} = \Gamma_{\phi_3\to\alpha_3\alpha_3} + \Gamma_{\phi_3\to\alpha_2\alpha_3} \cong \frac{81d^2\lambda_{33}^2\left(\lambda_{32}^2+\lambda_{33}^2\right)\xi q^2\left(\eta(-(2q+3))\mathcal{W}_0^2\right)^{3/2}}{4\sqrt{2}\pi\mathcal{V}^{29/3}w^2}M_p \, . \tag{2.2.69}$$

In this case, the standard definition of the effective number of neutrino species is given by:

$$\Delta N_{eff} = \frac{43}{7}\left(\frac{10.75}{g_*(T_{rh})}\right)^{1/3}\frac{\Gamma_{\phi_3\to\alpha_3\alpha_3}}{\Gamma_{\phi_3\to H\bar{H}}} = \frac{43}{7}\left(\frac{10.75}{g_*(T_{rh})}\right)^{1/3}\frac{d^{4/3}\lambda''^2}{9\mathcal{V}^{14/3}Z^2}, \tag{2.2.70}$$

where in the last step we have define for brevity $\lambda''^2 = \lambda_{33}^2\left(\lambda_{32}^2+\lambda_{33}^2\right)$. A similar bound as before can be derived by the requirement of $\Delta N_{eff} < 0.4$.

$$\lambda'' < \frac{0.765537\mathcal{V}^{7/3}Z}{d^{2/3}}\left(\frac{10.75}{g_*(T_{rh})}\right)^{-1/6} \, . \tag{2.2.71}$$

Now, the reheating temperature is computed as:

$$T_{rh} \cong (\frac{90}{\pi g_*(T_{rh})})^{1/4} \frac{27\sqrt[3]{d}\sqrt{\xi}q(2q+3)^{3/4} Z\left(-\eta \mathcal{W}_0^2\right)^{3/4}}{2\sqrt[4]{2}\sqrt{\pi}\mathcal{V}^{5/2}w} M_p \,. \tag{2.2.72}$$

Finally, we will show below some numerical examples (Table 3. and Table 4.) for the case of having order one fluxes in this particular toy model. This scenario renders high scale reheating temperatures, while the effective number of neutrinos species is very suppressed even for order one coupling constants. This means that, since the $\Delta N_{eff} \rightarrow 0$ is very close to the Standard model's value.

	$\mathcal{W}_0$	η	ξ	d	T_{rh} (GeV)	Z
$\mathcal{V} \cong 2425$	1	-0.9	5	3.8×10^{-4}	10^{11}	1
$\mathcal{V} \cong 8200$	10	-0.9	7	1.3×10^{-2}	10^{10}	1

Table 2.7: Different reheating temperatures for various set of parameters. Obviously, exponentially small fluxes tend to reproduce a high scale reheating scenario. The effective number of neutrino species ΔN_{eff} is well below the allowed upper bound even for order $\mathcal{O}(0.1)$ coupling λ''.

$m^2_{\phi_i}$ (TeV)	$m^2_{\phi_1}$	$m^2_{\phi_2}$	$m^2_{\phi_3}$
$\mathcal{W}_0 = 1$	5×10^7	1×10^7	2×10^6
$\mathcal{W}_0 = 10$	2×10^8	1×10^6	3×10^5

Table 2.8: The moduli masses along the two numerical examples presented above.

2.2.4 Dark matter scenario in the presence of quantum effects

In various string models, cosmological predictions tend to point towards non-thermal dark matter, produced by decays of heavy scalars. The most common production process would need the decays of the lightest modulus to provide a large amount of entropy, diluting any previous DM abundance, and then its byproducts would yield the necessary relic density. The potential dark matter particles span two categories regarding their thermodynamic origin and more specifically the freeze out temperature $T_f \sim m_{DM}/20$.

- $(T_{rh} > T_f)$: in this case dark matter particles are in a thermodynamical equilibrium and annihilations between themselves favor the thermal origin of dark matter.

- $(T_{rh} < T_f)$: Here, a discrimination with respect to the dark matter annihilations is needed to be stated: the efficiency of the aforementioned annihilations is quantified in the critical abundance Y^c_{DM} of dark matter particles, which quantity is obtained by the Boltzmann equations.

$$Y^c_{DM} \cong \frac{H}{\langle \sigma_{ann} v \rangle_s}|_{T_{rh}} \; . \tag{2.2.73}$$

In the first sub-case, there is a possibility of having the produced abundance exceeds the critical value $Y_{DM} > Y^c_{DM}$. Consequently, there exists some further time for annihilations until the two quantities match, a scenario labeled as "Annihilation scenario". The final relic abundance in this case is computed to be:

$$Y^c_{DM} \sim (\frac{n_{DM}}{s})_{obs} \frac{\langle \sigma_{ann} v \rangle^{th}_f}{\langle \sigma_{ann} v \rangle_f} \frac{T_f}{T_{rh}}, \tag{2.2.74}$$

where n_{DM} represents the number density and $\langle \sigma_{ann} v \rangle^{th}_f \sim 3 \times 10^{-26}$ cm$^3 s^{-1}$ stands for the thermal's case cross section as a requirement to produce the observed value of dark matter abundance [182]

$$(\frac{n_{DM}}{s})_{obs} \cong 5 \times 10^{-10} (\frac{\text{GeV}}{m_{DM}}) \; . \tag{2.2.75}$$

Readily, processes of this type are enhanced by a factor of $\frac{T_f}{T_{rh}}$ as opposed to the thermal production, where possible dark matter particles could be thermally underproduced Higgsino-like or Wino-like particles. In second sub-case, the dark matter abundance is lower compared to the critical value, making the annihilations more sparse. This scenario is labeled as "Branching scenario", where the produced abundance is simply given by:

$$Y_{DM} = Y_\phi \text{Br}_{DM}, \quad Y_\phi = \frac{3T_{rh}}{4m_\phi}, \tag{2.2.76}$$

where the Y_ϕ calculates the abundance of the normalized fields and Br_{DM} quantifies the decays ratio. In this case, Bino-like particles are favored for lower values of Br_{DM}. Following the analysis of the previous section, we are going to use the computed reheating temperature to scan the viability of both scenarios along the presence of the newly introduced quantum effects. According to [174], the branching scenario would better describe the regime of low scale reheating temperatures. This regime spans the region between:

$$\mathcal{O}(MeV) < T_{rh} \leq \mathcal{O}(GeV)\ . \tag{2.2.77}$$

We can easily compute the abundance of the normalized fields, using the reheating temperature of equation (2.2.59):

$$Y_\phi = -\frac{18\sqrt{3}\ 5^{1/4} d^{13/12}\sqrt{\xi} q Z}{\pi^{3/4} g^{1/4}\sqrt{\mathcal{V}} w}\ . \tag{2.2.78}$$

For consistency reasons, we are going to use the values of Table 2., while various plots will be presented to show the bounds on the parameters and the dark matter mass. In the branching scenario, the dark matter abundance has to be equal to the observed value (2.2.75), where the dark matter mass is bounded from below scaling as:

$$T_f > T_{rh} \Rightarrow m_{DM} > -\frac{1440\ 5^{1/4}\sqrt{6} d^{19/12}\sqrt{\xi} q Z}{\pi^{3/4} g^{1/4}\mathcal{V}^{3/2} w} M_p\ , \tag{2.2.79}$$

$$Y_\phi = Y_{DM} \Rightarrow m_{DM} = -\frac{\pi^{3/4} g^{1/4}\sqrt{\mathcal{V}} w}{\sqrt{3}\ 5^{1/4} d^{13/12}\sqrt{\xi} q Z}\ \frac{GeV}{36\times 10^9\ \mathrm{Br}_{DM}}\ . \tag{2.2.80}$$

In the following Figure 3., the required dark matter mass is depicted in order to satisfy the observable dark matter abundance. The values of Table 1. will be used to scan the region of reheating temperatures from a scale of a few MeV up to a few GeV. While in previous works, the branching scenario was promoted only for small dark matter masses, we will show that it can also attribute large values once the branching ratio is lower than $Br_{DM} \leq \mathcal{O}(10^{-3})$ [183; 184]. Recent proposals tend to that direction to obtain superheavy dark matter that could contribute effectively in the relic density. A possible explanation on that can be credited to higher order moduli decay or to non-standard cosmological evolution with a period of early matter domination [173; 185; 186]. As it previously discussed our case study α) resembles the Kähler inflation paradigm, where an early matter domination period could be established. A special attention should be devoted to the third case of Figure 3., where a bizarre coincidence can be addressed. As stated in a past work [156], a Cladogenesis scenario was suggested where the dilution factor due to entropy release by modulus decay Y_ϕ can both solve the dark matter mystery, but also provide a solution for the Baryon-Dark Matter Coincidence. This can be characterized as a late time baryogenesis scenario where the moduli decay could decay naturally in some N species with C- and CP- violation coupling with the visible sector's dofs. To quantify the above statement, the baryon asymmetry of the universe is given by:

$$\eta_B \equiv \frac{\eta_B - \eta_{\bar{B}}}{s} = Y_\phi Br_N \epsilon, \tag{2.2.81}$$

where ϵ is the generated asymmetry during the N particles decay and Br_N denotes the branching ratio of decays to the observable sector particles. Applying the observed value of the asymmetry and our result for the modulus decay, we derive:

$$\eta_B \cong 9 \times 10^{-11} \Rightarrow Br_N \epsilon \cong 1 \times 10^{-2} \ . \tag{2.2.82}$$

Since the generated asymmetry ϵ is created at one loop level, the parameter could easily accommodate a factor of order $\sim \ 10^{-1}$. Thus, a very specific bound for the branching ratio of the N particles can be derived, where in contrast to previous studies, Br_{DM} and Br_N are not of the same order. Additionally, we naturally expect Br_N to lay between $O(10^{-1}, 1)$, since concrete models [157] of this type of baryogenesis have been constructed that service this argument. Bringing attention to the coincidence problem, we can compute the two (dark matter and baryon) densities by:

$$\frac{\Omega_B}{\Omega_{DM}} \cong \frac{\text{GeV}}{m_{DM}} \frac{\epsilon Br_N}{Br_{DM}} \cong 6 \Rightarrow \epsilon Br_N \cong 4.8 \times 10^{-2}, \ Br_{DM} \cong 10^{-8}, \ m_{DM} \sim 800 \text{ TeV} \ . \tag{2.2.83}$$

Remarkably, the problem is solved and an explanation is given in accordance with the scenario described in [156]. Our main difference is that the our dark matter branching ratio is considerably lower than computed in [156], where studies have shown that this is possible once possible higher order corrections are added to the decay rates. These corrections could descend from three or four-body moduli decays to final states with additional dark matter particles, where the branching ratio could lay lower than $Br_{DM} \ll 10^{-4}$.

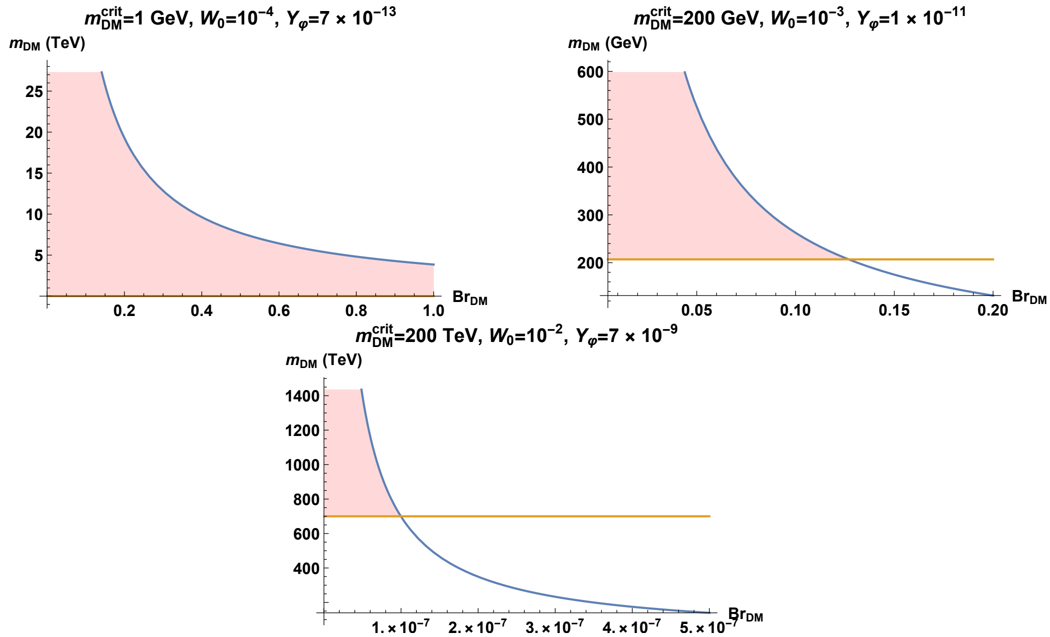

Figure 2.10: Plots for the different cases of Table 1. The shaded region represents the allowed masses for the dark matter particles, where the horizontal line represents the lower bound on m_{DM} set by the requirement $T_f > T_{rh}$.

As for the annihilation scenario, it would fit better to the case of having high scale reheating temperatures $T_{rh} \gg$ GeV. So, our case of order one fluxes could be embedded in this scenario. The reheating temperature, using equation (2.2.72), in this case is given by:

$$T_{rh} = \frac{27\sqrt{3}\ 5^{1/4} d^{1/3} \sqrt{\xi} q (2q+3)^{3/4} Z \left(-\eta \mathcal{W}_0^2\right)^{3/4}}{2 g^{1/4} \pi^{3/4} \mathcal{V}^{5/2} w} M_p \ . \tag{2.2.84}$$

From equation (2.2.74), we can see that the final relic abundance is given in terms of the number density and the freeze-out temperature T_f. A lower bound for the dark matter's mass can be derived by requiring the freeze-out temperature to exceed the T_{rh},

$$T_f > T_{rh} \Rightarrow m_{DM} > \frac{270\sqrt{3}\ 5^{1/4} d^{1/3} \sqrt{\xi} q (2q+3)^{3/4} Z \left(-\eta \mathcal{W}_0^2\right)^{3/4}}{g^{1/4} \pi^{3/4} \mathcal{V}^{5/2} w} M_p \ . \tag{2.2.85}$$

In the following plots (Figure 4.), the bounds on the dark matter mass are depicted based on two of the cases studied in Table 3. The horizontal lines represent two characteristic values for different number densities $\langle \sigma_{ann} v \rangle_f$, while the curve sketches the observed value of DM abundance $Y_{DM}^{obs} \cong (\frac{n_{DM}}{s})_{obs}$. The two examples of the plots are, also, summarized in the equation below, where the relic abundance is computed along with the fluxes and the lower bound on the dark matter mass.

$$Y_{DM}^{c} \sim (\frac{n_{DM}}{s})_{obs} \frac{\langle \sigma_{ann} v \rangle_f^{th}}{\langle \sigma_{ann} v \rangle_f} \frac{T_f}{T_{rh}} \sim \begin{cases} \dfrac{6.8 \times 10^{-47}}{\langle \sigma_{ann} v \rangle_f}, & \mathcal{W}_0 = 1, \quad m_{DM} > 10^{12}\ GeV, \\ \dfrac{1.4 \times 10^{-48}}{\langle \sigma_{ann} v \rangle_f}, & \mathcal{W}_0 = 10, \quad m_{DM} > 10^{11}\ GeV\ . \end{cases} \tag{2.2.86}$$

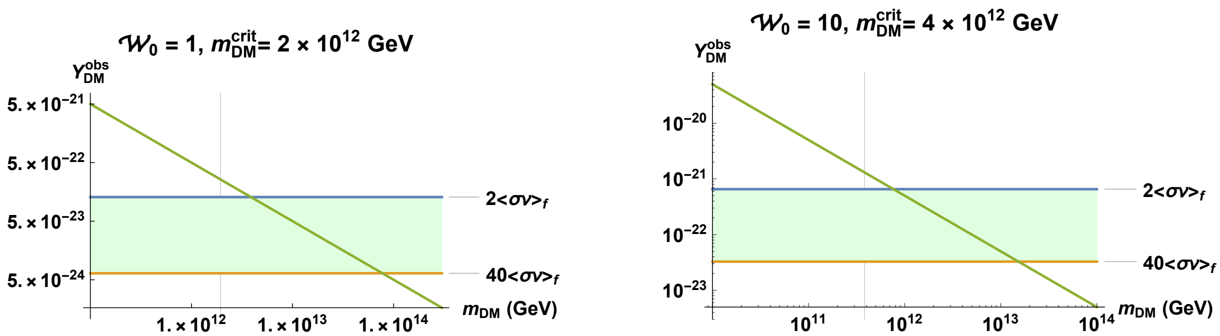

Figure 2.11: Left: The shaded region between the horizontal lines represent the allowed region on the dark matter mass. The horizontal lines depict the dark matter mass on the region between $(2\langle \sigma_{ann} v \rangle_f, 40\langle \sigma_{ann} v \rangle_f)$. The vertical line represents the lower allowed bound for the $T_f > T_{rh}$.

Thus, we see that the annihilation scenario in the case of order one fluxes renders some superheavy dark matter particles with mass $m_{DM} > 10^{11}$ GeV. Some future interesting investigations would be to extend this analysis on more complex Calabi-Yau spaces and observe the overall dynamics in Kähler moduli sector. Additionally, a possible embedding of an inflationary model in accordance with the above analysis would be beneficial in order to clarify some ambiguities in the early universe, like the connection of dark sector's dynamics to the inflationary observable quantities. From a phenomenological point of view, it would be interesting to understand the implications and the experimental signatures of a potential superheavy dark matter candidate, since various existing and future experiments, like Ice Cube [187] and RNO-G [188], are searching for state of the art methods to probe the nature of dark matter. We retain all these questions for a future work.

3 | Phenomenological aspects of local F-theory GUTs

In this chapter, we are going to explore the low energy implications of F-theory GUTs, more specifically by revisiting the flipped $SU(5)$ in the spectral cover approach. Secondly, the newly introduced modular flavor symmetry is going to be embedded in the context of local F-theory. In the present study, an $SO(10)$ divisor is considered augmented by internal fluxes along the $U(1)_\chi$ direction, whose effect is to perform the symmetry breaking. This results exactly to a flipped $SU(5)$ model, after carefully define the hypercharge generator as a combination of the $U(1)_\chi$ and the Abelian factor of $SU(5)$. The phenomenological signatures of this model include the seesaw mechanism as the origin for the neutrino masses, the study of the main decay channels of proton decay and the corresponding bound of the Higgs triplets, the study of the $0\nu\beta\beta$ decay and its lepton flavor violation effects in the determination of mixing between the neutrino states. Furthermore, a consistent gauge coupling unification is performed at very high energies along with the F-theoretic singlet's vevs provided by the flatness conditions. Regarding the modular family symmetry, in the framework of type IIB string theory with D-branes the $SL(2,Z)$ symmetry is playing a prominent role in the determination of the residual symmetries. We now discuss the origins of finite modular symmetries in Type IIB string theory. To this effect, we will study, expanding on [189] Type IIB orientifold compactifications, where one can stabilise the moduli in a vacuum that is invariant to finite modular symmetries. The starting point is Type IIB, which exhibits an explicit modular invariance for the axio-dilaton irrespective of the details of the compact space. Upon choosing a factorisable toroidal orientifold for the compactification, $T^6/\mathbb{Z}_2 = (T_1^2 \times T_2^2 \times T_3^2)/\mathbb{Z}_2$ the theory will also manifest the modular invariance associated with the complex structure moduli of each of the tori, in other words we will have $SL(2,\mathbb{Z})_\tau \otimes (\otimes_{i=1}^3 SL(2,\mathbb{Z})_i)$ before the complex structure moduli are stabilised by Type IIB flux configurations. Once the fluxes acquire nonvanishing VEVs, we will show that the supersymmetry preserving vacuum transforms non-trivially under a congruence subgroup of order N, $\bar{\Gamma}(N)$, of the original modular symmetries, therefore breaking the preserved symmetry to Γ_N.

3.1 Flipped $SU(5)$ and sterile neutrinos in F-theory

3.1.1 Geometric construction

We would like to investigate the flipped $SU(5) \times U(1)$ model in a generic F-theory framework. Within the proposed framework we implement the spectral cover approach and turn on fluxes along $U(1)$'s to determine the geometric properties of the matter curves and the massless spectrum residing on them. At this stage we end up with the flipped $SU(5)$ which we envisage it contains the three generations of the chiral matter fields, and the necessary Higgs representations to break the symmetry.Before we attempt to derive this model from F-theory, we give a brief account of the field theory version. The chiral matter fields of each family constitute a complete $\underline{16}$ spinorial representation of $SO(10)$ which admits the $SU(5) \times U(1)_\chi$ decomposition

$$\underline{16} = 10_{-1} + \bar{5}_3 + 1_{-5} \ . \tag{3.1.1}$$

Denoting with x the 'charge' under $U(1)_\chi$ and y under the $U(1)$ of the familiar Standard Model symmetry group, the hypercharge definition for flipped $SU(5)$ is $Y = \frac{1}{5}\left(x + \frac{1}{6}y\right)$. This implies the following embedding of the Standard Model representations

$$10_{-1} \Rightarrow F_i \ = \ (Q_i, d_i^c, \nu_i^c) \tag{3.1.2}$$

$$\bar{5}_{+3} \Rightarrow \bar{f}_i \ = \ (u_i^c, \ell_i) \tag{3.1.3}$$

$$1_{-5} \Rightarrow \ell_i^c \ = \ e_i^c \ . \tag{3.1.4}$$

As already pointed out, the spontaneous symmetry breaking of the flipped $SU(5)$ symmetry occurs with a pair of Higgs fields accommodated in

$$H \equiv 10_{-1} \ = \ (Q_H, d_H^c, \nu_H^c), \qquad \bar{H} \equiv 10_{+1} \ = \ (\bar{Q}_H, \bar{d}_H^c, \bar{\nu}_H^c) \ . \tag{3.1.5}$$

The MSSM Higgs doublets are found in the fiveplets descending from the $\underline{10}$ of $SO(10)$

$$h \equiv 5_{+2} \ = \ (D_h, h_d), \qquad \bar{h} \equiv \bar{5}_{-2} \ = \ (\bar{D}_h, h_u) \ . \tag{3.1.6}$$

A remarkable fact in the case of the flipped model is that the $U(1)_\chi$ charge assignment distinguishes the Higgs $\bar{5}_{-2}$ fields from matter anti-fiveplets $\bar{5}_3$. In particular, the former contain down-quark type triplets $\bar{D}_h$ while the latter accommodate the u^c quarks.

The fermion masses arise from the following $SU(5)\times U(1)_\chi$ invariant couplings

$$\begin{aligned}\mathcal{W} &\supset \lambda_d\, 10_{-1}\cdot 10_{-1}\cdot 5^h_2 + \lambda_u\, 10_{-1}\cdot \bar{5}_3\cdot \bar{5}^{\bar{h}}_{-2} + \lambda_\ell\, 1_{-5}\cdot \bar{5}_3\cdot 5^h_2 &(3.1.7)\\ &\supset \lambda_d\, Q\, d^c\, h_d + \lambda_u\,(Q\, u^c\, h_u + \ell\nu^c\, h_u) + \lambda_\ell\, e^c\,\ell\, h_d\ . &(3.1.8)\end{aligned}$$

It should be observed that the flipped model at the GUT scale predicts that up-quark and neutrino Dirac mass matrices are linked to each other and in particular, $m_t = m_{\nu_\tau}$. However, in stark contrast to the standard $SU(5)$ model, down quarks and lepton mass matrices are unrelated, since in the flipped model they originate from different Yukawa couplings.

Proceeding with the Higgs sector, as $H, \bar{H}$ acquire large VEVs of the order M_{GUT}, they break $SU(5)\times U(1)_\chi$ down to Standard Model gauge group and at the same time they provide heavy masses to the color triplets. Indeed, the following mass terms are obtained

$$HHh + \bar{H}\bar{H}\bar{h} \;\Rightarrow\; \langle \nu^c_H\rangle d^c_H D + \langle \overline{\nu^c_H}\rangle \bar{d}^c_H \bar{D}\ . \qquad (3.1.9)$$

Moreover, a higher order term providing right-handed neutrinos with Majorana masses is of the form

$$\begin{aligned}\mathcal{W}_{\nu^c} &= \frac{1}{M_S}\overline{10}_{\bar{H}}\overline{10}_{\bar{H}}\, 10_{-1}\, 10_{-1}\\ &= \frac{1}{M_S}\overline{HH}F_iF_j \;\Rightarrow\; \frac{1}{M_S}\langle\overline{\nu^c_H}\rangle^2 \nu^c_i\nu^c_j\ .\end{aligned} \qquad (3.1.10)$$

It should be noted that possible couplings with additional neutral singlets ν_s may extend the seesaw mechanism to type II. As we will see, this is exactly the case of the F-theory version.

In the context of local F-theory constructions we may assume an E_8 point of enhancement where the flipped $SU(5)$ emerges through the following symmetry reduction

$$E_8 \supset SO(10)\times SU(4)_\perp \supset [SU(5)\times U(1)]\times SU(4)_\perp\ , \qquad (3.1.11)$$

where $SU(4)_\perp$ incorporates the symmetries of the spectral cover. Matter fields are accommodated in irreducible representations emerging from the decomposition of the E_8 adjoint under $SO(10)\times SU(4)$

$$248 \longrightarrow (45,1) + (1,15) + (10,6) + (16,4) + (\overline{16},\bar{4})\ , \qquad (3.1.12)$$

followed by the familiar reduction of $SO(10)$ representations given in (3.1.1) and (3.1.6), according to the second stage of breaking $SO(10)\to SU(5)\times U(1)$ as shown in (3.1.11). The following invariant trilinear couplings provide with masses up and down quarks, charged leptons and neutrinos

$$\mathcal{W}_{down} \in (10,4)_{-1} \cdot (10,4)_{-1} \cdot (5,6)_2 \tag{3.1.13}$$

$$\mathcal{W}_{up/\nu} \in (10,4)_{-1} \cdot (\bar{5},4)_3 \cdot (\bar{5},\bar{6})_{-2} \tag{3.1.14}$$

$$\mathcal{W}_{\ell} \in (1,4)_{-5} \cdot (\bar{5},4)_3 \cdot (5,6)_2 \ . \tag{3.1.15}$$

As opposed to the plain field theory model, the corresponding trilinear couplings transform non-trivially under the spectral cover $SU(4)_\perp$ group. However, the matter fields reside on 7-branes whose positions are located at the singularities of the fibration. In the geometric language of F-theory constructions, the matter fields of the effective model are found on the matter curves where the gauge $SU(5)\times U(1)$ symmetry is appropriately enhanced. Moreover, their corresponding trilinear Yukawa couplings are formed at the intersections of three matter curves where the symmetry is further enhanced. In the spectral cover picture the symmetry enhancement of each representation can be described by the appropriate element of the $SU(4)_\perp$ Cartan subalgebra which is parametrized by four weights t_i satisfying $\sum_{i=1}^4 t_i = 0$. The latter are associated with the roots of a fourth degree polynomial related to the $SU(4)_\perp$ spectral cover. The coefficients of this polynomial equation convey information related to the geometric properties of the fibred manifold to the effective theory. Usually, there are non-trivial monodromies [55] identifying roots of the fourth degree polynomial equation associated with $SU(4)_\perp$. In the present case the identification of matter curves occurs through a discrete group which is a subgroup of the maximal discrete (Weyl) group S_4 of $SU(4)_\perp$.

To proceed, first we identify the weights of matter field representations. At the $SO(10)$ level, the $\underline{16}$ transforms in $4 \in SU(4)_\perp$ and $\underline{10}$ in $6 \in SU(4)_\perp$ so we make the following identifications In principle, there are four matter curves to accommodate $\underline{16} + \overline{\underline{16}}$ representations and six for the $\underline{10}$'s of $SO(10)$. We will focus on the phenomenologically viable case of the minimal Z_2 monodromy. This choice implies rank-one mass matrices where only the third family of quarks are present at tree-level ensuring a heavy top-quark mass in accordance with the experiments. Thus, implementing the Z_2 monodromy by imposing the identification of the two weights $t_1 \leftrightarrow t_2$, the matter curves of (3.1.1) reduce to

Information regarding the geometric properties of the matter curves and the representations accommodated on them can be extracted from the polynomial equation for the $SU(4)$ spectral cover. This equation is

$$\sum_{k=0}^{4} b_k s^{4-k} = b_0 s^4 + b_1 s^3 + b_2 s^2 + b_1 s^3 + b_4 = 0 \ . \tag{3.1.16}$$

The coefficients b_k are sections of $[b_k] = \eta - kc_1$ while we have defined $\eta = 5c_1 - t$ with c_1 $(-t)$ being the 1^{st} Chern class of the tangent (normal) bundle to the GUT 'surface'. Under the assumed Z_2 monodromy the spectral cover equation is factorized as follows

$$\begin{aligned} C_4 &= (a_1 + a_2 s + a_3 s^2)(a_4 + a_5 s)(a_6 + a_7 s) \\ &= a_1 a_4 a_6 + (a_1 a_5 a_6 + a_2 a_4 a_6 + a_1 a_4 a_7) s \\ &+ (a_1 a_5 a_7 + a_2 a_5 a_6 + a_3 a_4 a_6) s^2 + (a_3 a_5 a_6 + a_2 a_5 a_7) s^3 + a_3 a_5 a_7 s^4 \ . \end{aligned} \tag{3.1.17}$$

Comparing this to (3.1.16) we extract equations of the form $b_k = b_k(a_i)$

$$\begin{aligned} b_4 &= a_1 a_4 a_6 \\ b_3 &= a_1 a_5 a_6 + a_2 a_4 a_6 + a_1 a_4 a_7 \\ b_2 &= a_1 a_5 a_7 + a_2 a_5 a_6 + a_3 a_4 a_6 \\ b_1 &= a_3 a_5 a_6 + a_3 a_4 a_7 + a_2 a_5 a_7 \\ b_0 &= a_3 a_5 a_7, \end{aligned} \tag{3.1.18}$$

and use them to derive the relations for the homologies $[a_i]$ of the coefficients a_i. There are five equations relating b_k's with products of a_i coefficients and all five of them can be cast in the form

$$\eta - k\, c_1 = [a_l] + [a_m] + [a_n], \quad \text{where} \quad k + l + m + n = 15 \ , \tag{3.1.19}$$

with $k = 0, 1, 2, 3, 4$ and l, m, n take the values $1, 2, \ldots, 7$. For example, the term $a_3 a_4 a_6 s^2$ in (3.1.17) gives $[a_3] + [a_4] + [a_6] + 2[s] = (\eta - 2c_1) - 2c_1 = c_1 - t$ and analogously for the other terms. The system (3.1.19) consists of five linear equations involving products of the coefficients a_i with yet unspecified homologies $[a_i]$ which must be determined in terms of the known $[b_k]$. Since there are five linear equations with seven unknowns we can express $[a_i]$ in terms of two arbitrary parameters defined as follows:

$$\chi_5 = [a_5], \chi_7 = [a_7], \ \chi = \chi_5 + \chi_7 \ .$$

Then, we find that

$$[\alpha_i] = \eta - (3 - i)c_1 - \chi, \ i = 1, 2, 3 \ ; \ [a_5] = [a_4] + c_1 = \chi - \chi_7 \ ; \ [a_7] = [a_6] + c_1 = \chi_7 \ .$$

Note that because of the vanishing of the coefficient $b_1 = 0$, we also need to solve the constraint $b_1(a_i) = 0$. It can be readily seen that a possible solution is achieved by defining a new section k

Matter	t_i charges	Section	Homology	$U(1)_\chi$
$\underline{16}$	t_1	a_1	$\eta - 2c_1 - \chi$	$M - P$
$\underline{16}$	t_3	a_4	$-c_1 + \chi_5$	P_5
$\underline{16}$	t_4	a_6	$-c_1 + \chi_7$	P_7
$\underline{10}$	$t_1 + t_3$	$a_1 - \kappa a_4 a_6$	$\eta - 2c_1 - \chi$	$M - P$
$\underline{10}$	$t_1 + t_4$	$a_1 - \kappa a_4 a_6$	$\eta - 2c_1 - \chi$	$M - P$
$\underline{10}$	$2t_1$	$a_5 a_6 + a_4 a_7$	$-c_1 + \chi$	P
$\underline{10}$	$t_3 + t_4$	$a_5 a_6 + a_4 a_7$	$-c_1 + \chi$	P

Table 3.1: Properties of $SO(10)$ representations in the $\mathcal{Z}_2$ monodromy.

with $[\kappa] = \eta - 2\chi$ such that

$$a_3 = \kappa a_5 a_7, \quad a_2 = -\kappa(a_5 a_6 + a_4 a_7) \ . \tag{3.1.20}$$

Using the above topological data we can now specify the flux restrictions on the matter curves and determine the multiplicities of the zero mode spectrum and other properties of the effective field theory model.

From the first of equations (3.1.18), the condition $b_4 = 0$ becomes $a_1 a_4 a_6 = 0$, which defines three $\underline{16}$'s localized at

$$a_1 = 0, \ a_4 = 0, \ a_6 = 0 \ .$$

Similarly, the equation $b_3^2(a_i) = 0$ determines the topological properties and the multiplicity of $\underline{10}$'s. Substituting (3.1.20) into b_3, we obtain

$$(a_5 a_6 + a_4 a_7)\,(a_1 - \kappa a_4 a_6) = 0 \ .$$

Knowing the homologies of the individual a_i's we can compute those of the various matter curves. The results are shown in the fifth column of Table 3.1 where for convenience homologies are parametrized with respect to the free parameters $\chi_5, \chi_7, \chi = \chi_5 + \chi_7$.

As already noted, the $SO(10) \to SU(5) \times U(1)_\chi$ breaking is achieved by turning on a $U(1)_\chi$ flux. At the same time this flux will have implications on the gauge couplings unification [1] and the

[1]For such effects see for example [190; 191; 192].

zero-mode multiplicities of the spectrum on the various matter curves. To quantify these effects we introduce the symbol $\mathcal{F}_1$ for the $U(1)_\chi$ flux parameter and consider the flux restrictions on the matter curves

$$P = \mathcal{F}_1 \cdot (\chi - c_1);\ P_n = \mathcal{F}_1 \cdot (\chi_n - c_1);\ n = 5, 7;\ M = \mathcal{F}_1 \cdot (\eta - 3c_1);\ C = -\mathcal{F}_1 \cdot c_1\ . \tag{3.1.21}$$

In this way we obtain the results shown in the last column of Table 3.1. We should mention that if we wish to protect the $U(1)_\chi$ boson from receiving a Green-Schwarz (GS) mass we need to impose

$$\mathcal{F}_1 \cdot \eta = 0\ \&\ \mathcal{F}_1 \cdot c_1 = 0\ ,$$

which automatically imply $M = C = 0$. In this case, the sum $P = P_5 + P_7$ stands for the total flux permeating matter curves while one can observe form Table 3.1 that the flux vanishes independently on the Σ_{16} and Σ_{10} matter curves (Table 3.2).
Assuming that M_{10}^a is the number of $\underline{10}_{t_1+t_3} \in SO(10)$, after the $SO(10)$ breaking we obtain the multiplicities for flipped representations:

$$\underline{16}_1 = \begin{cases} 10_{t_1},\ M_1 \\ \bar{5}_{t_1},\ M_1 + P \\ 1_{t_1},\ M_1 - P \end{cases} ,\quad \underline{16}_2 = \begin{cases} 10_{t_3},\ M_3 \\ \bar{5}_{t_3},\ M_3 - P_5 \\ 1_{t_3},\ M_3 + P_5 \end{cases} ,\quad \underline{16}_3 = \begin{cases} 10_{t_4},\ M_4 \\ \bar{5}_{t_4},\ M_4 - P_7 \\ 1_{t_4},\ M_4 + P_7 \end{cases} \tag{3.1.22}$$

$$10_1 = \begin{cases} 5^{(1)}_{-t_2-t_4},\ M_{10}^2 \\ \bar{5}^{(1)}_{t_1+t_3},\ M_{10}^1 + P \end{cases} ,\quad 10_2 = \begin{cases} 5^{(2)}_{-2t_1},\ M_{10}^1 \\ \bar{5}^{(2)}_{t_3+t_4},\ M_{10}^1 - P \end{cases} \tag{3.1.23}$$

M_1	M_3	M_4	P	P_5	P_7	M_{10}^1	M_{10}^2
3	1	-1	0	1	-1	1	0

Table 3.2: Model 1

$$\begin{aligned} &10_{t_1} : 3 \times (Q_i, d_i^c, \nu_i^c),\quad 10_{t_3} : 1 \times (H),\quad 10_{t_4} : -1 \times (\bar{H}) \\ &\bar{5}_{t_1} : 3 \times (u_i^c, L_i),\quad 1_{t_3} : 2 \times (E_i^c),\quad 1_{t_4} : -2 \times (\bar{E}_i^c),\ 1_{t_1} : 3 \times e_i^c \\ &\bar{5}_{t_4+t_3} : 1 \times (\bar{h}),\quad 5_{-2t_1} : 1 \times (h)\ , \end{aligned} \tag{3.1.24}$$

where M_{10_i}, M_{5_j} stand for the numbers of $10 \in SU(5)$ and $5 \in SU(5)$ representations (a negative value corresponds to the conjugate representation). $M_{S_{ij}}$ denote the multiplicities of the singlet fields. In fact, as for any other representation, this means that

$$M_{ij} = \#1_{t_i - t_j} - \#1_{t_j - t_i}, \tag{3.1.25}$$

thus, if $M_{ij} > 0$ then there is an excess of M_{ij} singlets $1_{t_i - t_j} = \theta_{ij}$ and vice versa.

3.1.2 Low energy superpotential

We will construct a model with all three families residing on the same matter curve. Later on, we will explain how in this case the masses to lighter families can be generated by non-commutative fluxes [193] or non perturbative effects [48; 194].

Taking into account the transformation properties of the various $SU(5) \times U(1)_\chi$ representations presented in the previous section, we can readily write down the superpotential of the model. Regarding the field content transforming non-trivially under $SU(5) \times U(1)_\chi$, we make the following identifications

$$10_{t_1} \longrightarrow F_i,\ \bar{5}_{t_1} \longrightarrow \bar{f}_i,\ 1_{t_1} \longrightarrow e^c_j,\ 1_{t_3} \longrightarrow E^c_m,\ 1_{-t_4} \longrightarrow \bar{E}^c_n, \tag{3.1.26}$$

$$10_{t_3} \longrightarrow H,\ \overline{10}_{-t_4} \longrightarrow \overline{H},\ 5_{-2t_1} \longrightarrow h,\ \bar{5}_{t_3+t_4} \longrightarrow \bar{h}\ . \tag{3.1.27}$$

Here the indices i, j run over the number of families, i.e., $i, j = 1, 2, 3$. All the representations emerging from the first matter curve labeled with t_1, share the same symbols as those of the field theory version of flipped $SU(5)$ of the previous section. The two extra pairs with the quantum numbers of the right-handed electron and its complex conjugate are denoted with $E^c, \bar{E}^c$.

Regarding the singlets $\theta_{pq},\ p, q = 1, 2, 3, 4$, taking into account the Z_2 monodromy $t_1 t_2$ we introduce the following naming:

$$\theta_{12} \equiv \theta_{21} = s,\ \theta_{13} = \chi,\ \theta_{31} = \bar{\chi},\ \theta_{14} \longrightarrow \psi,\ \theta_{41} = \bar{\psi},\ \theta_{34} \longrightarrow \zeta,\ \theta_{43} \longrightarrow \bar{\zeta}\ . \tag{3.1.28}$$

The new symbols assigned to the $SU(5)$ massless spectrum of the flipped model are collected in Table 3.3. A standard matter parity has also been assumed for all fields.

Matter Fields	Symbol	Parity	Matter Fields	Parity	
10_{-1}	F_i	$-$	χ	$+$	$M-P$
$\bar{5}_3$	$\bar{f}_i$	$-$	$\bar{\chi}$	$+$	P_5
1_{-5}	e^c_i	$-$	ψ	$+$	P_7
1_0	s	$-$	$\bar{\psi}$	$+$	$M-P$
1_5	$\bar{E}^c_n$	$-$	ζ	$+$	P
1_{-5}	E^c_m	$-$	$\bar{\zeta}$	$+$	P
5_2	h	$+$	H	$+$	P
$\bar{5}_{-2}$	$\bar{h}$	$+$	H	$+$	P

Table 3.3: The $SU(5)\times U(1)_\chi$ representations with their R-parity assignment. Their multiplicities are counted by the integers $M, P, P_{5,7}$ in the last column.

Note that due to t_1t_2 identification after the monodromy action, both types of singlets, θ_{12} and θ_{21}, are identified with the same one denoted with s_j, with a multiplicity $j=1,2,\ldots,n_s$ determined by (3.1.25). For $M_{ij}=0$ there is an equal number of θ_{12} and θ_{21} fields and large mass terms of the form $M_{s_{ij}}s_is_j$ for all s_i are normally expected. However, for $M_{ij}\neq 0$ some singlets are not expected to receive tree-level masses. Such 'sterile' singlets s_j, (denoted collectively with s in the following) will play a significant role in relation to neutrino sector. Clearly, in addition to this, several other identifications will take place among the various flipped representations and the Yukawa couplings. As an example, implementing the Z_2 monodromy and the above definitions, the following gauge invariant terms are rewritten as

$$10_{t_1}\bar{5}_{t_2}\bar{5}_{t_3+t_4} \xrightarrow{Z_2} 10_{t_1}\bar{5}_{t_1}\bar{5}_{t_3+t_4} \longrightarrow F_i\bar{f}_j\bar{h} \tag{3.1.29}$$

$$10_{-t_4}10_{t_1}\theta_{21}\theta_{42} \xrightarrow{Z_2} 10_{-t_4}10_{t_1}\theta_{21}\theta_{41} \longrightarrow HF_is\bar{\psi}\ . \tag{3.1.30}$$

With this notation the superpotential terms are written in the familiar field theory notation as follows:

$$\mathcal{W} = \lambda^u_{ij}F_i\bar{f}_j\bar{h} + \lambda^d_{ij}F_iF_jh + \lambda^e_{ij}e^c_i\bar{f}_jh + \kappa_i\overline{H}F_is\,\bar{\psi} \tag{3.1.31}$$

$$+\,\alpha_{mj}\bar{E}^c_me^c_j\,\bar{\psi} + \beta_{mn}\bar{E}^c_mE^c_n\,\bar{\zeta} + \gamma_{nj}E^c_n\bar{f}_jh\chi\ . \tag{3.1.32}$$

The first three terms provide Dirac masses to the charged fermions and the neutrinos. It can be observed that the up-quark Yukawa coupling ($\propto F\bar{f}\bar{h}$) appears at tree-level, as well as the bottom and charged lepton Yukawa couplings. Because in this construction $U(1)_Y$ fluxes are not turned on, there is no splitting of the $SU(5)$ representations and thus, their corresponding content of the three generations resides on the same matter curve. Using the geometric structure of the theory it is possible to generate the fermion mass hierarchies and the Kobayashi-Maskawa mixing. Here we give a brief account of the mechanism, while the details are described in a considerable amount of work devoted to this issue [47; 49; 195; 196; 197; 198].

We first recall that chiral matter fields reside on matter-curves at the intersections of the GUT surface with other 7-branes, while the corresponding wavefunctions, dubbed here Ψ_i, can be determined by solving the appropriate equations [196] where it is found that they have a gaussian profile along the directions transverse to the matter-curve. The tree-level superpotential terms of matter fields are formed at triple intersections and each Yukawa coupling coefficient is determined by integrating over the overlapping wavefuctions

$$\lambda_{ij} \propto \int_M \Psi_i \Psi_j \Phi_H dz_1 \wedge d\bar{z}_1 \wedge dz_2 \wedge d\bar{z}_2 \; ,$$

where Φ_H is the wavefucntion of the Higgs field. Detailed computations of the Yukawa couplings with matter curves supporting the three generations, have shown that hierarchical Yukawa matrices -reminiscent of the Froggatt-Nielsen mechanism- are naturally obtained [47; 49; 195; 197; 198] with eigenmasses and mixing in agreement with the experimental values.

Returning to the superpotential terms (3.1.32), when the Higgs fields $\bar{H}$ and the singlet $\bar{\psi}$ acquire non-vanishing VEVs, the last term of the first line in particular, generates a mass term coupling the right-handed neutrino with the singlet field s [2] :

$$\kappa_i \langle \overline{H} \rangle \langle \bar{\psi} \rangle F_i s \; = \; M_{\nu_i^c s} \nu^c s \; ,$$

where $M_{\nu_i^c s} = \kappa_i \langle \overline{H} \rangle \langle \bar{\psi} \rangle$. Bearing in mind that the top Yukawa coupling also implies a 3×3 Dirac mass for the neutrino $m_{\nu_D} \; = \; \lambda_{ij}^u \langle \bar{h} \rangle$, and taking into account a mass term $M_s ss$ allowed by the

[2] In order to simplify the notation, occasionally the powers of $1/M_{str}^n$ (where M_{str} is of the order of the string scale) in the non-renormalizable terms will be omitted. Hence we will write $\bar{\psi}$ instead of $\bar{\psi}/M_{str}$ and so on.

χ	$\bar{\chi}$	ψ	$\bar{\psi}$	ζ	$\bar{\zeta}$
5.6×10^{10}	7.7×10^{15}	2.2×10^{7}	89.3×10^{3}	7.8×10^{15}	4.4×10^{15}

Table 3.4: Masses in GeV scale. $M_{str} = M_{GUT} = 1.4 \times 10^{16}$ GeV.

symmetries of the model, the following neutrino mass matrix emerges

$$\mathcal{M}_\nu = \begin{pmatrix} 0 & m_{\nu_D} & 0 \\ m_{\nu_D}^T & 0 & M_{\nu^c s}^T \\ 0 & M_{\nu^c s} & M_s \end{pmatrix}, \tag{3.1.33}$$

whereas additional non-renormalizable terms are also possible. The low energy implications on various lepton flavor and lepton number violating processes will be analysed in section 6. Furthermore, the following terms are also consistent with the symmetries of the model:

$$\mathcal{W} \supset \lambda_\mu \chi \left(\psi + \overline{H} H \chi\right) \bar{h}\, h + \lambda_{\bar{H}} \overline{H}\overline{H}\bar{h}\bar{\zeta} + \lambda_H HHh(\chi^2 + \bar{\zeta}^2\psi^2)\,. \tag{3.1.34}$$

When the various singlets acquire non-zero VEVs the following fields receive masses. The term proportional to λ_μ contains a non-renormalizable term proportional to $\chi\psi$ and a higher order one generated by the VEVs of Higges $\overline{H}H$. The terms proportional to $\lambda_{\bar{H}}, \lambda_H$ must provide heavy masses to the extra color triplet pairs

$$\lambda_{\bar{H}} \langle \overline{H} \rangle \frac{\langle \bar{\zeta} \rangle}{M_{str}} D^c_{\bar{H}} D_h + \lambda_H \langle H \rangle \left(\frac{\langle \chi^2 \rangle}{M^2_{str}} + \frac{\langle \bar{\zeta}^2 \psi^2 \rangle}{M^4_{str}} \right) D^c_{\bar{H}} D_h \,.$$

Since the magnitude of $\langle \chi \rangle$ is constrained from the size of the μ term, large mass for the second triplet pair requires a large VEV for $\langle \psi \bar{\zeta} \rangle$. The solution of the flatness conditions in the appendix show that this is possible [3]. According to the solution for flatness conditions problem obtained in the appendix, the useful singlets $\bar{\zeta}, \bar{\psi}, \chi$ acquire the desirable VEVs shown at Table 3.4, generating this way an acceptable μ-term for the Standard Model Higgs fields.

Continuing with the color triplet fields, we now collect all mass terms derived from non-renormalizable contributions to the superpotential. They generate a 2×2 mass matrix which is shown in Table 3.5.

[3] One might think that it would be possible to eliminate the term $\chi\bar{h}h$ while keeping the $\bar{H}\bar{H}\bar{h}$ and $HHh\bar{\zeta}\chi$ terms, by choosing appropriate Z_2 parity assignments for χ and the other fields. It can be easily shown, however, that there is no such Z_2 assignment and possibly generalized Z_N or more involved symmetries are required. Such discrete symmetries are available either from the spectral cover [199], or from the torsion part of the Mordell-Weil group.

$M^2_{D_h}$	D^c_H	$\overline{D^c_H}$
D_h	$\langle H\rangle(\frac{\chi^2}{M^2_{str}}+\frac{\psi^2\bar{\zeta}^2}{M^4_{str}})$	$\langle H\bar{H}\rangle(\frac{\chi^2}{M^3_{str}})$
$\overline{D_h}$	$\langle H\bar{H}\rangle(\frac{\chi^2}{M^3_{str}})$	$\langle\overline{H}\rangle\frac{\overline{\zeta}}{M_{str}}$

Table 3.5: The mass matrix for the down-type colour triplets.

The Higgs color triplets mediate baryon decay processes through dimension-four, and dimension-five operators, thus their mass scale is of crucial importance. Their eigenmasses are

$$m_{D^c_H} = \langle H\rangle(\frac{\chi^2}{M^2_{str}}+\frac{\psi^2\bar{\zeta}^2}{M^4_{str}})\cos^2(\theta) - \langle H\bar{H}\rangle(\frac{\chi^2}{M^3_{str}})\sin(2\theta) + \langle\overline{H}\rangle\frac{\overline{\zeta}}{M_{str}}\sin^2(\theta)$$
$$m_{\overline{D^c_H}} = \langle\overline{H}\rangle\frac{\overline{\zeta}}{M_{str}}\cos^2(\theta) + \langle H\bar{H}\rangle(\frac{\chi^2}{M^3_{str}})\sin(2\theta) + \langle H\rangle(\frac{\chi^2}{M^2_{str}}+\frac{\psi^2\bar{\zeta}^2}{M^4_{str}})\sin^2(\theta)\ ,$$

where the mixing angle θ is determined by

$$\tan(2\theta) = \frac{2\langle\bar{H}\rangle\langle\chi^2\rangle M_{str}}{\langle\chi^2\rangle M^2_{str}+\langle\psi^2\bar{\zeta}^2\rangle}\ . \tag{3.1.35}$$

For singlets VEVs of the order $10^{-1}M_{GUT}$, the triplets acquire heavy masses in the range 10^{14}-10^{15} GeV, ($\theta\sim\frac{\pi}{6}$), protecting this way the proton from fast decays. For completeness, we summarize the possible proton decay processes in the next section.

3.1.3 Proton decay and neutrino sector

Having determined the masses of the color triplet fields $D,\bar{D}$, we are now able to examine possible bounds on the parameter space from proton decay processes. After the spontaneous breaking of the flipped $SU(5)$ gauge group, the resulting MSSM Yukawa Lagrangian contains B and L violating operators giving rise to proton decay channels[200] such as $p\to(\pi^0,K^0)e^+$. Focusing our attention on the dangerous dimension five operators, in particular, the main contribution comes from the two relevant couplings $F_iF_jh,\ F_i\bar{f}_j\bar{h}$ in the superpotential (3.1.32). Also, it is important to mention that color triplets can contribute through chirality flipping (LLLL and RRRR) operators and chirality non-flipping (LLRR) ones. Following [201; 202; 203], these operators could be expressed in the mass eigenstate basis:

$$
\begin{aligned}
&10_{t_1} : (Q, VPd^c, U_{\nu^c}\nu^c), \quad Q = (u, VPd)\\
&\bar{5}_{t_1} : (u^c, U_L L), \quad L = (U_{PMNS}\nu, e)\\
&1_{t_1} : (U_e e^c) \ .
\end{aligned}
\tag{3.1.36}
$$

Therefore, the color triplets couplings to ordinary MSSM matter fields are expressed as

$$
\begin{aligned}
&\lambda_{ij}^u : Q(V^*\lambda^{(d^c)}V^\dagger)QD_H^c\\
&\lambda_{ij}^e : u^c(U_L^\dagger\lambda^{(e^c)})e^c D_H^c\\
&\lambda_{ij}^u : L(U_L\lambda^{(Q,\nu)})Q\overline{D_H^c}\\
&\lambda_{ij}^u : u^c(\lambda^{(Q,\nu)}V)d^c\overline{D_H^c},
\end{aligned}
\tag{3.1.37}
$$

where V is the Cabbibo-Kobayashi-Maskawa (CKM) matrix with the corresponding phases and U_L is the leptonic part of the $PMNS$-matrix $U_{PMNS} = U_L^* U_\nu^\dagger$, plus the CP-phases $P = \mathrm{diag}(e^{i\phi_i})$. The dominant effects on proton decay originate from LLRR channels, where after integrating out the Higgs triplets (recall that in this diagram chirality flipped dressing with a higgsino is required), are discussed below. These operators, also, should respect the $SU(4)_\perp$ charge conservation, so for each operator the appropriate singlet fields must be introduced. Since the masses of these singlets are substantially lower that the string scale, further suppression of the anticipated baryon violating operators is expected. The relevant operators take the form

$$
\begin{aligned}
\delta_1\frac{10_{t_1}10_{t_1}10_{t_1}\bar{5}_{t_1}}{M_{str}}\left(\frac{\theta_{31}\theta_{41}}{M_{str}^2}+\frac{\theta_{31}^2\theta_{43}}{M_{str}^3}\right) &\to \delta_1\frac{\langle\bar{\chi}^2\bar{\zeta}\rangle+\langle\bar{\chi}\bar{\zeta}\rangle M_{str}}{M_{str}^4}(Q_iQ_jQ_kL_m)\\
\delta_2\frac{10_{t1}\bar{5}_{t_1}\bar{5}_{t_1}1_{t_1}}{M_{str}}\left(\frac{\theta_{31}\theta_{41}}{M_{str}^2}+\frac{\theta_{31}^2\theta_{43}}{M_{str}^3}\right) &\to \delta_2\frac{\langle\bar{\chi}^2\bar{\zeta}\rangle+\langle\bar{\chi}\bar{\zeta}\rangle M_{str}}{M_{str}^4}(d_i^c u_j^c u_k^c e_m^c),
\end{aligned}
\tag{3.1.38}
$$

where $\delta_{1,2}$ are

$$
\delta_1 \sim \frac{\langle h\rangle}{m_{D_H^c}m_{\overline{D_H^c}}}\left[(V^*\lambda^{(d^c)}V^\dagger)(\lambda^{(Q,\nu)}U_L^*)\right], \quad \delta_2 \sim \frac{\langle h\rangle}{m_{D_H^c}m_{\overline{D_H^c}}}\left[(U_L^*\lambda^{(e^c)})(\lambda^{(Q,\nu)}V)\right] . \tag{3.1.39}
$$

Given the scale difference between the bidoublet $\langle h\rangle$ and the triplet $M_{D_H}^c$, these operators are highly suppressed. The novelty of F-theory model building constructions compared to GUT-model building [202; 203], is that the t_i-charge conservation implies additional suppression. Regarding the chirality flipping diagrams, as it is pointed out in [202], they are severely constrained in the flipped $SU(5)$ model, as opposed to their behavior in the standard $SU(5)$ [204].

We investigate now the implications of the various dimension-6 operators. In this case, baryon violating decays are mediated by both $SU(5)$ vector gauge fields and color Higgs triplets. The corresponding diagrams differ from dimension five operators, since chirality flipping is not needed in this case, so the extra suppression factor $\frac{\langle h\rangle}{M_D}$ is absent. From the low energy superpotential (3.1.32), the relevant to proton decay couplings are:

$$\lambda^u_{ij}F_i\bar{f}_j\bar{h} + \lambda^d_{ij}F_iF_jh\,\bar{\psi} + \lambda^e_{ij}e^c_i\bar{f}_jh\,\bar{\psi}\,, \tag{3.1.40}$$

whereas, the effective operators corresponding to dimension-6 operators are:

$$10\ \bar{5}\ 10^\dagger\ \bar{5}^\dagger,\quad 10\ 10\ \bar{5}^\dagger\ 1^\dagger\ .$$

The gauge interactions inducing the dimension six operators can be summarized as:

$$\mathcal{L} \sim g_5\left(\epsilon_{ij}u^cX^iU_L^*L^j + \epsilon_{abc}Q^{\dagger a}X^bVP^*d^c + \epsilon_{\alpha\beta}\nu^{\dagger c}X^\alpha Q^\beta + h.c.\right), \tag{3.1.41}$$

and

$$\mathcal{L}_{(6)} \sim C^{ijkm}_{(6)\alpha}\left(u_i^{\dagger c}d_j^{\dagger c}(u_ke_m + d_k\nu_m)\right) + C^{ijkm}_{(6)\beta}\left(u_i(VP^*d_j) + (V^*Pd_i)u_j\right)u_k^{\dagger c}e_m^{\dagger c}\ . \tag{3.1.42}$$

The coefficients $C^{ijkm}_{(6)\alpha,\beta}$ are given by [202; 203]

$$\begin{aligned}
C^{ijkm}_{(6)\alpha} &= \left(\frac{(U_L)_{km}V^*_{ij}}{M_G^2} + \frac{(V^\dagger\lambda^{(Q,\nu)})_{ij}(U_L\lambda^{(Q,\nu)}_{km})}{m^2_{D^c_H}}\right)\\
C^{ijkm}_{(6)\beta} &= \left(\frac{(V^*P\lambda^{(d^c)}V)_{km}(U_L^\dagger\lambda^{(e^c)})_{ij}}{m^2_{D^c_H}}\right),
\end{aligned} \tag{3.1.43}$$

where M_G is the mass of the gauge boson and the Yukawa couplings λ are the diagonal matrices. It is important to emphasize that the flipped $SU(5)$ gauge bosons do not couple to the right-handed leptons, in contrast to the standard $SU(5)$. The final state is different in these two cases and their experimental implication makes the flipped version much more phenomenologically attainable (see also [201]). As an illustrative example, we present the charged lepton decay channels $p \rightarrow$

$(K^0, \pi^0) l^+_{(e,\mu)}$. First of all the mixing factors, for the two Wilson coefficients stated above, are:

$$\begin{aligned} p \to \pi^0 l_i^+ : &\quad (U_L)_{i1} V^*_{ud} (e^{\phi_u}, e^{\phi_d}) \\ p \to K^0 l_i^+ : &\quad (U_L)_{i1} V^*_{us} (e^{\phi_u}, e^{\phi_s}), \end{aligned} \tag{3.1.44}$$

where the index i denotes the generation of the lepton involved in the proton decay. The decay rates can be computed as:

$$\begin{aligned} \Gamma_{p\to\pi^0 e^+} &= |(U_L)_{11} V^*_{ud} (e^{\phi_u}, e^{\phi_d})|^2 \mathcal{K}(m_\pi, m_p) \mathcal{M}^2(\pi^0, e^+) \left[A_\alpha^2 \left(\frac{1}{M_G^2} + \frac{f^2(u)}{m^2_{\overline{D^c_H}}}\right)^2 + A_\beta^2 \left(\frac{g^2(d,e^+)}{m^2_{D^c_H}}\right)^2 \right], \\ \Gamma_{p\to K^0 e^+} &= |(U_L)_{11} V^*_{us} (e^{\phi_u}, e^{\phi_s})|^2 \mathcal{K}(m_{K^0}, m_p) \mathcal{M}^2(K^0, e^+) \left[A_\alpha^2 \left(\frac{1}{M_G^2} + \frac{f^2(u)}{m^2_{\overline{D^c_H}}}\right)^2 + A_\beta^2 \left(\frac{g^2(s,e^+)}{m^2_{D^c_H}}\right)^2 \right], \end{aligned} \tag{3.1.45}$$

where A_α, A_β are the renormalization factors obtained from the RGE equations (in one-loop level) for the Wilson coefficients contributing to the proton decay processes [201; 202; 203]. Since there are some additional states in the low energy spectrum (namely the vector-like singlets E^c), we do not expect a significant deviation for the gauge coupling unification regarding the supersymmetry (susy) breaking scale around TeV, as obtained by similar analysis [205]. The rest of the parameters used in the decay rates are summarized below:

$$\begin{aligned} \mathcal{K}(m_\pi, m_p) &= \frac{m_p}{32\pi}\left(1 - \frac{m^2_{\pi^0}}{m_p^2}\right)^2, \quad \mathcal{M}(\pi^0, (e^+, \mu^+)) = \langle \pi^0 | (ud)_R u_L | p \rangle_{l^+} = (-0.131, -0.118)\ \text{GeV}^2, \\ \mathcal{K}(m_{K^0}, m_p) &= \frac{m_p}{32\pi}\left(1 - \frac{m^2_{K^0}}{m_p^2}\right)^2, \quad \mathcal{M}(K^0, (e^+, \mu^+)) = \langle \pi^0 | (us)_R u_L | p \rangle_{l^+} = (0.103, 0.099)\ \text{GeV}^2, \\ f^2(u) &= \frac{m_u^2}{\langle h_u \rangle^2}, \quad g^2(d, e^+) = \frac{m_u m_{e^+}}{\langle h_d \rangle^2}, \quad g^2(s, e^+) = \frac{m_s m_{e^+}}{\langle h_d \rangle^2}, \quad \tan(\beta) = \frac{\langle h_u \rangle}{\langle h_d \rangle}\,. \end{aligned} \tag{3.1.46}$$

In figure 3.1 we plot the proton lifetime of the above decay channels, as a function of the triplet mass m_{D_H} for assuming various values of $\tan\beta$, where the horizontal lines represent the current Super-K [206] and Hyper-K [207] bounds. Regarding the formulas for the proton decay through the muon's channel, they can be easily derived if we trade the $e^+ \to \mu^+$.

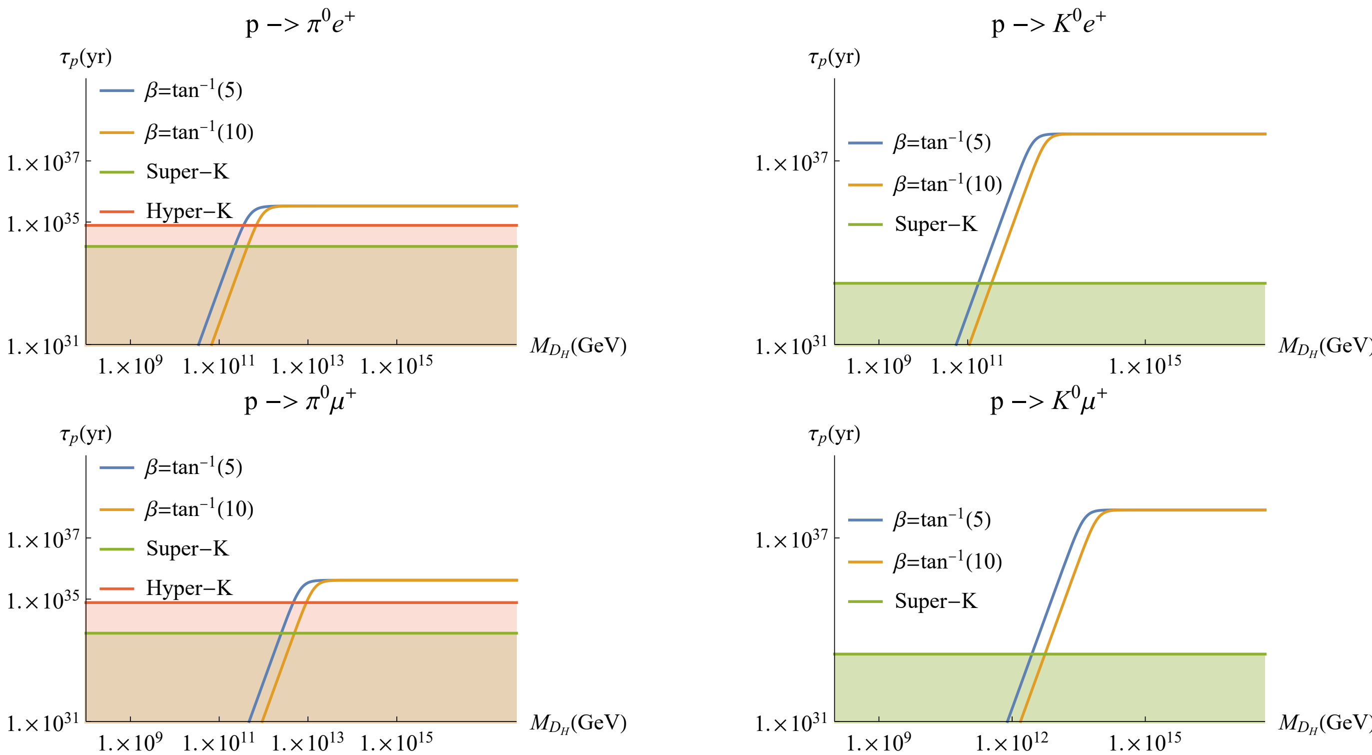

Figure 3.1: The lifetime of the proton along the two decay channels ($p \longrightarrow \pi^0(e^+, \mu^+)$, $p \longrightarrow K^0(e^+\mu^+)$) for different values of $\tan(\beta)$. It is deduced that the triplets mass is bounded at $m_{\overline{D^c_H}} = m_{D^c_H} \geq 10^{11}$ GeV, $M_G = 10^{16}$ GeV. The asymptotic value of the lifetime is controlled by the masses of the Higgs triplets.

In this section we are going to examine in some detail the mass matrix (3.1.33) involving the neutrinos and the neutral singlet fields s. Recall that the latter are identified with the singlets θ_{12}, θ_{21} and that their number is determined by global dynamics of the model. In the present semi-local construction we will treat them as a free parameter. The following Yukawa couplings

$$m_{\nu_D} = \lambda^u_{ij}\langle \bar{h} \rangle, \quad M_{\nu^c_i s} = \frac{\kappa_i \langle \overline{H} \rangle \langle \bar{\psi} \rangle}{M_{str}}, \tag{3.1.47}$$

define the Dirac neutrino mass submatrix and the mixing between the right-handed neutrinos and the singlet fields. Additional non-renormalizable terms may also generate masses for the right-handed neutrinos ν^c_i due to a coupling of the form :

$$\begin{aligned} \mathcal{W} &\sim \frac{\lambda_{ij}}{M^3_{str}} \overline{H}\overline{H} F_i F_j \left(\langle \bar{\psi}^2 \rangle + \frac{\langle \bar{\zeta} \rangle^2 \langle \bar{\chi} \rangle^2}{M^2_{str}} \right) \Rightarrow \\ M_{\nu^c_i} &= \frac{\lambda_{ij} \langle \bar{\nu}^c_H \rangle^2}{M^3_{str}} \left(\langle \bar{\psi}^2 \rangle + \frac{\langle \bar{\zeta} \rangle^2 \langle \bar{\chi} \rangle^2}{M^2_{str}} \right). \end{aligned} \tag{3.1.48}$$

Hence, the final structure of the neutrino mass sector is

$$\mathcal{M}_\nu = \begin{pmatrix} 0 & m_{\nu_D} & 0 \\ m^T_{\nu_D} & M_{\nu^c_i} & M^T_{\nu^c s} \\ 0 & M_{\nu^c s} & M_s \end{pmatrix} . \tag{3.1.49}$$

This matrix involves vastly different scales. We assume (also justified by the singlet VEVs) the hierarchy $m_{\nu_D} \ll M_s \ll M_{\nu^c_i s}, M_{\nu^c_i}$ and implement a double inverse seesaw mechanism to determine the eigenvalues of the light spectrum. Below we sketch the procedure for obtaining the normal-order mass hierarchy in the light neutrinos sector. We define:

$$M_{\nu_D} = \begin{pmatrix} m_{\nu_D} \\ 0 \end{pmatrix}, \quad M_{R'} = \begin{pmatrix} M_{\nu^c_i} & M^T_{\nu^c s} \\ M_{\nu^c s} & M_s \end{pmatrix} , \tag{3.1.50}$$

and

$$M_\nu = \begin{pmatrix} 0 & M^T_D \\ M_D & M_{R'} \end{pmatrix} . \tag{3.1.51}$$

Then, implementing the double inverse seesaw formula (see for example [208]) we obtain

$$\begin{aligned} m_{\nu_i} = &- m_{\nu_D} (M_{\nu^c_i} - M_{\nu^c s} M_s^{-1} M^T_{\nu^c s})^{-1} m^T_{\nu_D} \\ m_{\nu_D} &\ll (M_{\nu^c_i} - M_{\nu^c s} M_s^{-1} M^T_{\nu^c s}) \ . \end{aligned} \tag{3.1.52}$$

Depending on the scale of the neutral singlets s, there are two basic limits of the previous equation, which yield different parametric regions for the right-handed neutrinos and the singlets. In the subsequent sections we would like to implement a leptogenesis scenario, hence it is of crucial importance to pursue an intermediate mass scale ($\sim$ TeV) in the heavy neutrinos sector and to characterize the properties of the extra singlets. Having this in mind, we proceed with the analysis of the limiting cases.

α) We assume the hierarchies $M_{\nu^c_i} \ll M_{\nu^c s}$ and $M_s \ll M_{\nu^c s}$.
In this case, the $\{22\}$-entry in the neutrino mass matrix is less significant and the model reduces to the standard double seesaw:

$$m_{\nu_i} = m_{\nu_D}(M^T_{\nu^c s})^{-1} M_s M^{-1}_{\nu^c s} m^T_{\nu_D} \; . \tag{3.1.53}$$

This scenario accommodates effectively the light neutrino masses, where for example requiring light neutrinos at sub-eV scale $m_{\nu_i} \lesssim 0.1 \; eV$ and sterile masses around $M_s \sim 5 \; keV$ ($m_{\nu_D} \sim 100 \; GeV$), the seesaw scale for the right-handed neutrinos is set at $M_{\nu^c s} \sim TeV$. A much more interesting and testable prediction from such a case would be the calculation of unitarity violation η in the leptonic mixing matrix [209]:

$$V = (1+\eta)U_0, \tag{3.1.54}$$

where the V matrix diagonalizes the light neutrinos and U_0 represents the unitary matrix (identified with U_{PMNS} in the lepton sector), while the η matrix can in principle be hermitian. Deviations from the unitary form of the PMNS mixing matrix are displayed into the rare leptonic decays ($l_a \longrightarrow l_b \gamma$). These decays put stringent bounds on the discrepancies in the mixing matrix, whose origin can be traced back to the seesaw mechanism. In order the explain how deviations can be expressed, it is important to recall the GIM mechanism [210] . Flavor changing neutral currents are induced at loop level in the Standard Model, where their decay rate is parametrized in terms of the mixing matrix in 1-loop as [211]:

$$\begin{gathered}\frac{\Gamma(l_a \longrightarrow l_b \gamma)}{\Gamma(l_a \longrightarrow \nu_a l_b \bar{\nu}_b)} \sim \frac{|\sum_k V_{ak} V^\dagger_{kb} F(\frac{m_\nu^2}{m_W^2})|^2}{(VV^\dagger)_{aa}(VV^\dagger)_{bb}}, \\ F(x) = \frac{10 - 43x + 78x^2 - 49x^3 + 4x^4 + 18x^3 \log(x)}{3(x-1)^4}, \end{gathered} \tag{3.1.55}$$

where for unitary mixing matrix U the GIM mechanism implies a vanishing contribution for $a \neq b$ [212]. In the case of non-unitary mixing matrix, a typical process $\mu \longrightarrow e\gamma$ results in the experimental bound $(U_{e\mu} U^\dagger_{\mu e}) < 10^{-4}$,which represents the typical condition needed to be met by seesaw scenarios. Regarding the computation of the unitary violating effects η, they can be computed by the neutrino matrix (3.1.51), using the matrix (3.1.54), as:

$$\eta \cong -\frac{1}{2} M^\dagger_D (M^*_R)^{-1} (M_R)^{-1} M_D \; . \tag{3.1.56}$$

Regarding the unitarity violation in the seesaw mechanism analysed here, an estimate of the η can be computed after the scales of the seesaw matrix are set. Nevertheless, in both of the two limits of the seesaw mechanism analyzed here, the η parameter is of order:

$$\eta \sim O(\frac{m_{\nu_D}^2}{M_{\nu^c s}^2}) \sim 10^{-6}, \tag{3.1.57}$$

i.e., two orders below the present bound.

β) $M_s \ll M_{\nu^c s} \ll M_{\nu^c}$. In this limit, the two heavy states are

$$\begin{aligned} \hat{m}_s &= M_s - M_{\nu^c s}^T M_{\nu^c}^{-1} M_{\nu^c s}, \\ \hat{m}_{\nu^c} &= M_{\nu^c} \ . \end{aligned} \tag{3.1.58}$$

Regarding the light neutrino states, depending on the heavy mass hierarchies, we distinguish two cases. For $M_{\nu^c} \ll M_{\nu^c s} M_s^{-1} M_{\nu^c s}^T$,

$$m_\nu = m_{\nu_D} (M_{\nu^c s}^T)^{-1} M_s M_{\nu^c s}^{-1} m_{\nu_D}^T, \tag{3.1.59}$$

and for $M_{\nu^c} \gg M_{\nu^c s} M_s^{-1} M_{\nu^c s}^T$,

$$m_\nu = -m_{\nu_D} M_{\nu^c}^{-1} m_{\nu_D}^T \ . \tag{3.1.60}$$

In the first case, the paradigm (α) is reproduced and in the second one the typical seesaw is obtained. Here, the new intermediate scale $\tilde{m}_s$ could be useful for a dark matter particle, since the mixing angle between the active and the sterile neutrino is highly suppressed. This angle could be obtained after integrating out the heavy right-handed neutrino scale M_{ν^c}, leading to:

$$\tan(2\theta_{\nu s}) \cong \frac{2m_{\nu_D}}{M_{\nu^c s}}, \quad (M_{\nu_i^c}, M_s \ll M_{\nu^c s}) \ \& \ (M_{\nu^c} \ll M_{\nu^c s} M_s^{-1} M_{\nu^c s}^T), \tag{3.1.61}$$

$$\tan(2\theta_{\nu s}) \cong \frac{m_{\nu_D} M_{\nu^c s}}{2 M_s M_{\nu^c}}, \quad M_{\nu^c} \gg M_{\nu^c s} M_s^{-1} M_{\nu^c s}^T \ . \tag{3.1.62}$$

The mixing angle of the active-sterile neutrinos are of crucial importance, since this angle characterizes the sterile neutrinos' properties regarding its nature as a dark matter particle. Astrophysical data have already opened two "windows" for sterile dark matter particles, the first one at keV scale with the mixing angle $\theta_{\nu s} \sim (10^{-6}, 10^{-4})$ and the second one at MeV scale with $\theta_{\nu s} \sim (10^{-9}, 10^{-6})$.

Next we examine the leptogenesis scenario in the context of the flipped $SU(5)$ model presented in this work. Our analysis shows that a possible implementation of the leptogenesis scenario can be realized in the second case (i.e., case β). As is well known, right-handed neutrinos can decay to a lepton and a Higgs field, producing this way lepton asymmetry. The relevant Yukawa couplings are

$$\mathcal{W} = \lambda^u_{ij} F_i \bar{f}_j \bar{h} + \kappa'_i \overline{H} F_i s\,\bar{\psi}, \quad \kappa'_i = \kappa_i \frac{\langle\bar{\psi}\rangle}{M_{str}} \,. \tag{3.1.63}$$

Figure 2 shows the relevant vertex of the right-handed neutrino and the standard one-loop graph contributing to the lepton asymmetry. There are also two wavefucntion self-energy one-loop correction graphs depicted in figure 3 which also contribute.

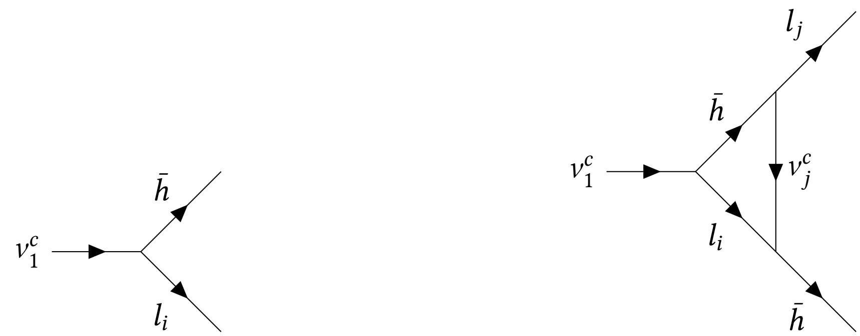

Figure 3.2: Standard contributions to the generated lepton asymmetry.

Figure 3.3: Loop diagrams contributions to the generated lepton asymmetry.

The decay rate is given by

$$\Gamma(\nu_i^c) = \frac{1}{4\pi}\left(\lambda^\nu_{ij}(\lambda^\nu_{ij})^\dagger + \kappa'(\kappa')^\dagger\right)_{ii} M_{\nu_i^c} \,, \tag{3.1.64}$$

where λ and κ' are the relevant Yukawa couplings in the equation (3.1.32) for the neutrino sector. The lepton asymmetry factor is summarized to the following contributions:

$$\epsilon_1 = -\sum_i \frac{\Gamma_1(\nu_1^c \to \bar{l}_i \bar{h}) - \Gamma_2(\nu_1^c \to l_i h)}{\Gamma_{12}(\nu_1^c)}, \tag{3.1.65}$$

where $\Gamma_{12} = \Gamma_1(\nu_1^c \to \bar{l}_i\bar{h}) + \Gamma_2(\nu_1^c \to l_i h)$ indicates the overall decay rates. The lepton asymmetry in such a scenario can be written as [213]:

$$\epsilon_1 = \frac{1}{8\pi}\sum_{j\neq 1}\left((f_1(x_j) + f_2(x_j))G_{j1} + f_2(x_j)G'_{j1}\right), \tag{3.1.66}$$

$$f_1(x_j) = \sqrt{x}(1-(1+x)\ln(\frac{1+x}{x})),\ \ f_2(x) = \frac{\sqrt{x_j}}{1-x_j},\ \ x_j = \frac{M^2_{\nu^c_j}}{M^2_{\nu^c_1}}, \tag{3.1.67}$$

where the f-factors are the vertex contributions of the Feynman diagrams. Now, the G-factors contain the Yukawa couplings as:

$$G = \frac{Im\left[(\lambda^\nu_{ij}(\lambda^\nu_{ij})^\dagger)^2\right]}{(\lambda^\nu(\lambda^\nu)^\dagger + \kappa'(\kappa')^\dagger)_{11}},\ \ G' = \frac{Im\left[(\lambda^\nu_{ij}(\lambda^\nu_{ij})^\dagger)(\kappa'(\kappa')^\dagger)\right]}{(\lambda^\nu(\lambda^\nu)^\dagger + \kappa'(\kappa')^\dagger)_{11}}\ . \tag{3.1.68}$$

With regard to the impact of the loop corrections of the second graph in figure 3, the lepton asymmetry factor can be divided into two cases with respect to the right-handed neutrino mass hierarchy $x_j = \frac{M^2_{\nu^c_j}}{M^2_{\nu^c_1}}$. For the case of large hierarchy, $x_j \gg 1$, the contribution from the loops is negligible resulting in [214]:

$$\begin{aligned}\epsilon_1 &\cong -\frac{3M_{\nu^c_1}}{16\pi\langle v\rangle^2}\frac{Im\left[(\lambda^\nu_{ij})^* m_\nu(\lambda^\nu_{ij})^\dagger\right]}{(\lambda^\nu(\lambda^\nu)^\dagger + \kappa'(\kappa')^\dagger)_{11}} \Rightarrow \\ |\epsilon_1| &\lesssim \frac{3M_{\nu^c_1}}{16\pi\langle m_{\nu_D}\rangle^2}(m_{\nu_3} - m_{\nu_1})\ .\end{aligned} \tag{3.1.69}$$

From the above, it is obvious that in order to obtain the observed lepton asymmetry $\epsilon_1 \sim [10^{-6}, 10^{-5}]$, the scale for the right-handed neutrinos should lay close to:

$$M_{\nu^c_1} \gtrsim \frac{16\epsilon_1\pi\langle m_{\nu_D}\rangle^2}{3(m_{\nu_3} - m_{\nu_1})} \gtrsim 10^9\ GeV\ . \tag{3.1.70}$$

The case $x_j \cong 1$ describes the enhancement due to the loop diagrams (resonant procedure), where the asymmetry factor is:

$$\epsilon_1 \cong -\frac{1}{16\pi}\left\{\frac{M_{\nu^c_2}}{\langle m_{\nu_D}\rangle^2}\frac{\mathrm{Im}[(\lambda^\nu_{ij})^* m_\nu(\lambda^\nu_{ij})^\dagger]}{(\lambda^\nu(\lambda^\nu)^\dagger + \kappa'(\kappa')^\dagger)_{11}} + \frac{\sum_{j\neq 1}\mathrm{Im}[(\lambda^\nu_{ij}(\lambda^\nu_{ij})^\dagger)(\kappa'(\kappa')^\dagger)]}{(\lambda^\nu(\lambda^\nu)^\dagger + \kappa'(\kappa')^\dagger)_{11}}\right\}\frac{M_{\nu^c_2}}{M_{\nu^c_2} - M_{\nu^c_1}}\ . \tag{3.1.71}$$

It is worth emphasizing that if the first term dominates, fine tuning is required due to the dependence of the mass splitting in the right-handed neutrino sector. Despite the fact that thermal low scale leptogenesis in most cases requires a tiny mass gap in the heavy states, the second term (first diagram in figure 3), could accommodate a less constrained mass gap through the suppression due to the existence of Yukawa couplings λ, κ' [215; 216; 217]. However, due to the heavy Higgs $\bar{H}$ mass included in the loop, this contribution is expected to be suppressed. Simplifying the contributions of the two terms in the above equation, the results are summarized to:

$$i) \qquad |\epsilon_1| \sim \frac{M_{\nu_2^c}}{16\pi\langle m_{\nu_D}\rangle^2}\sqrt{\Delta m^2_{\nu_{31}}}\frac{M_{\nu_2^c}}{M_{\nu_2^c}-M_{\nu_1^c}} \tag{3.1.72}$$

$$ii) \qquad |\epsilon_1| \sim \frac{M_{\nu_2^c}}{16\pi\langle m_{\nu_D}\rangle^2}\sqrt{\Delta m^2_{\nu_{31}}}\frac{M_{\nu_2^c}}{M_{\nu_2^c}-M_{\nu_1^c}} \times |\lambda^{\nu}_{ij}|^2|\kappa'|^2 \,. \tag{3.1.73}$$

These couplings are referring not to the first generation, since the lightest of the sterile neutrino's coupling is bounded by the thermodynamic condition $\Gamma(\nu_1^c) < H(T = M_{\nu_1^c})$, where H stands for the Hubble expansion. The novelty of the F-theory implementation of the leptogenesis scenario is that fine tuning is not a problem, since the singlets can acquire appropriate VEVs regulating this way the scale of the produced asymmetry, without the requirement of $\Delta m_{\nu^c_{21}} \to 0$. The coupling κ' is suppressed by the string scale, an effect which is absent in the standard field theory GUT framework.

3.1.4 $0\beta\beta\nu$ decay and the W-boson mass anomaly

We have already observed in the analysis of the neutrino mass matrix the involvement of new neutral states s which act as sterile neutrinos. Furthermore, the Majorana nature of neutrino states implies violation of lepton number by two units $\Delta L = 2$. The presence of these ingredients could potentially provide low energy signals which are worth investigating. Amongst those implications, neutrinoless double beta decay (for a review see [218]) seems a suitable experimental process, where the presence of additional sterile neutrinos could enhance the decay's amplitude and shed some light on the mixing between the active and sterile sectors. Clearly, within the context of the inverse seesaw mechanism of the present model, the described scenarios of leptogenesis, unitarity violation and double beta decay are entangled and the goal of this section is to extract some bounds for the mass splitting of the right-handed neutrinos and their Majorana phases.

As can be inferred even a simple extension of the SM with a Majorana mass term could predict the occurrence of the $\beta\beta$-decay process through a Lagrangian term of the form

$$\mathcal{L} \supset \sum_{i=1}^{3} g_F^2 U_{e_i}^2 \gamma_\mu P_R \frac{\not{p} + m_i}{p^2 - m_i^2} \gamma_\nu P_L, \tag{3.1.74}$$

where the m_i represent the masses of the neutrinos and p is the momentum of the virtual particle in the decaying process [4].

The neutrinoless double beta decay, $0\nu\beta\beta$, in the presence of the light neutrinos is described by the effective mass:

$$m_{ee} = |\sum_{i=1}^{3} U_{ei}^2 m_i| \tag{3.1.75}$$

In this model, the summation in the above formula is modified in order to accommodate the extended neutrino sector [220]:

$$m_{ee} = \sum_{i=1}^{3+n} U_{e_j}^2 p^2 \frac{m_i}{p^2 - m_i^2}, \tag{3.1.76}$$

where $U_{e_j}^2$ stands for the mixing of the electron neutrino with the other states and the decay width is proportional to $\Gamma_{0\nu 2\beta} \sim m_{ee}$. Recent experimental constraints put a stringent bound on the allowed region [219; 221; 222], which is:

$$|m_{ee}| \in [10^{-3}, 10^{-1}] \text{ eV} . \tag{3.1.77}$$

It is obvious that for high scale masses of the right-handed neutrinos ($m_{\nu^c} \gg$ TeV) and intermediate scale sterile singlets ($m_s \sim$ keV), sizable effects on the $0\nu\beta\beta$ decay could be attributed to the mass of heavy neutrinos and the mixing of the various sectors. From (3.1.76), there exist two important limits concerning the mass of the extra neutrinos [220; 223], where the propagator is modified as:

[4] As a matter of fact, this propagator is related to the Nuclear Matrix Element (NME), which is being used to capture the nucleus dynamics - see for example eq. (3) in [219].

$$i)\ m_i \ll p^2 : \frac{1}{p^2 - m_i^2} = \frac{1}{p^2} + \frac{m_i^2}{p^4} + O(\frac{m_i^4}{p^6}) , \tag{3.1.78}$$

$$m_{ee} = \sum_{i=1}^{3+n} U_{e_i}^2 m_i , \tag{3.1.79}$$

$$ii)\ m_i \gg p^2 : \frac{1}{p^2 - m_i^2} = -\frac{1}{m_i^2} + O(\frac{m_i^4}{p^6}) , \tag{3.1.80}$$

$$m_{ee} = -\sum_{i=1}^{3+n} U_{e_i}^2 m_i \frac{p^2}{m_i^2} . \tag{3.1.81}$$

$$U(\nu_e, \nu_1^c, \nu_2^c, s) = \begin{pmatrix} 1 & 0 & 0 & 0 \\ 0 & c_{12} & s_{12} & 0 \\ 0 & -s_{12} & c_{12} & 0 \\ 0 & 0 & 0 & 1 \end{pmatrix} \begin{pmatrix} c_{\mathrm{e}2} & 0 & e^{-i\delta} s_{\mathrm{e}2} & 0 \\ 0 & 1 & 0 & 0 \\ -e^{i\delta} s_{\mathrm{e}2} & 0 & c_{\mathrm{e}2} & 0 \\ 0 & 0 & 0 & 1 \end{pmatrix} \begin{pmatrix} c_{\mathrm{e}1} & s_{\mathrm{e}1} & 0 & 0 \\ -s_{\mathrm{e}1} & c_{\mathrm{e}1} & 0 & 0 \\ 0 & 0 & 1 & 0 \\ 0 & 0 & 0 & 1 \end{pmatrix}$$
$$\begin{pmatrix} c_{\mathrm{es}} & 0 & 0 & s_{\mathrm{es}} \\ 0 & 1 & 0 & 0 \\ 0 & 0 & 1 & 0 \\ -s_{\mathrm{es}} & 0 & 0 & c_{\mathrm{es}} \end{pmatrix} \begin{pmatrix} 1 & 0 & 0 & 0 \\ 0 & c_{\mathrm{s}1} & 0 & s_{\mathrm{s}1} \\ 0 & 0 & 1 & 0 \\ 0 & -s_{\mathrm{s}1} & 0 & c_{\mathrm{s}1} \end{pmatrix} \begin{pmatrix} 1 & 0 & 0 & 0 \\ 0 & 1 & 0 & 0 \\ 0 & 0 & c_{\mathrm{s}2} & s_{\mathrm{s}2} \\ 0 & 0 & -s_{\mathrm{s}2} & c_{\mathrm{s}2} \end{pmatrix} \cdot \Phi, \tag{3.1.82}$$

We are going to analyze the neutrinoless double beta decay in both of these limits. The case *ii*, in particular, represents the seesaw mechanism presented above, but the "light" neutrinos (case *i*) could also be interesting for experiments searching low energy sterile neutrinos. In order to get an insight for the neutrinos sector and reach some representative conclusion, we adopt a tangible strategy and work in a simplified effective scenario. Thus, for the light neutrinos, it would be reasonable to consider a single neutrino (e.g. the electron neutrino), whilst for the heavier sector we will assume a case of three neutrinos (two right-handed ones and one sterile). Similar approach has been considered in previous literature (for a few representative papers, see for example relatable examples with 3+1 or 3+2 neutrinos in [220; 224; 225; 226; 227]). In [225], a similar model was considered, however the present analysis considers three different scales (eV-keV-TeV) and as stated above it would be ideal to derive a bound for the mass splitting of the heavy neutrinos, since this fraction is used in leptogenesis. In addition, we are going to sketch the production mechanism of the sterile neutrinos, if they were to be identified as a dark matter particle, through their coupling with the right-handed neutrinos. Consequently, the mixing matrix would be 4×4, which can be parameterized as shown in equation (3.1.82). The last matrix in (3.1.82) represents the Majorana phases $\Phi = \text{diag}(1, e^{i\varphi_1}, e^{i\varphi_2}, e^{i\varphi_s})$, where $\phi \in (0, \pi)$ and δ is the Dirac phase (this will not play a crucial role, since we treat light neutrinos as a single state) and $s_{ij}, c_{ij}, \ (i, j = e, 1, 2, s), \ \theta \in (0, \frac{\pi}{2})$ are the mixing angles between the neutrinos. Now, denoting with $\hat{M}(\hat{m}_\nu, \hat{m}_{\nu_i^c}, \hat{m}_s)$ the diagonalized neutrino mass matrix the following equation holds:

$$U\hat{M}(\hat{m}_\nu, \hat{m}_{\nu_i^c}, \hat{m}_s)U^T = \mathcal{M}_\nu \ . \tag{3.1.83}$$

where,

$$\mathcal{M}_\nu = \begin{pmatrix} 0 & m_{\nu_D} & 0 & 0 \\ m_{\nu_D} & M_{11} & M_{12} & M_{1s} \\ 0 & M_{21} & M_{22} & M_{2s} \\ 0 & M_{1s} & M_{2s} & M_s \end{pmatrix} . \tag{3.1.84}$$

where M_{ij} denote the elements of the 2×2 right-handed neutrino matrix $M_{\nu_i^c}$ in this example. Comparing particular elements of the mass matrix $\mathcal{M}_\nu$ with the mass eigenbasis matrix $\hat{M}(\hat{m}_\nu, \hat{m}_{\nu_i^c}, \hat{m}_s)$ we can extract some useful bounds. First of all, a few assumptions need to be taken into account in order to simplify the calculations. Hence, we will assume that the mixing angles between the active neutrinos ν_e and the sterile ones $\nu_{1,2}^c$, ν_s are small, plus that the masses of the heavy states are much heavier compared to the light and the sterile states:

$$\begin{gathered} \theta_{e1}, \theta_{e2}, \theta_{es} \ll 1 \Rightarrow cos(\theta) \cong 1, \ sin(\theta) \cong \theta, \\ \frac{\hat{m}_\nu}{\hat{m}_{1,2}}, \frac{\hat{m}_s}{\hat{m}_{1,2}} \ll 1 \ . \end{gathered} \tag{3.1.85}$$

Under these assumptions, the sines (s_{e1}, s_{e2}, s_{es}) represent small angles, but we are not going to change their symbols in the calculations below. Observing the structure of the neutrino mass matrix $\mathcal{M}_\nu$ given in (3.1.84), we compare the two zero entries {11},{13} and the {33} element $M_s \to \mu$ with the corresponding ones of $\hat{M}(\hat{m}_\nu, \hat{m}_{\nu_i^c}, \hat{m}_s)$. These yield the following equations

$$\mathcal{M}_{\nu}^{11} = (U\hat{M}(\hat{m}_{\nu}, \hat{m}_{\nu_i^c}, \hat{m}_s)U^T)_{11} = 0, \tag{3.1.86}$$
$$\mathcal{M}_{\nu}^{13} = (U\hat{M}(\hat{m}_{\nu}, \hat{m}_{\nu_i^c}, \hat{m}_s)U^T)_{13} = 0, \tag{3.1.87}$$
$$\mathcal{M}_{\nu}^{33} = (U\hat{M}(\hat{m}_{\nu}, \hat{m}_{\nu_i^c}, \hat{m}_s)U^T)_{33} = \mu \ . \tag{3.1.88}$$

For (3.1.86) we obtain:

$$\mathcal{M}_{\nu}^{11} = \frac{\hat{m}_{\nu}}{\hat{m}_1} e^{-i(\delta+2\phi_2)} - 2e^{-i\delta} c_{s1} s_{es} \left[(e^{i2\Delta\phi_{21}} + c_{s2}^2 z - \frac{\hat{m}_2}{\hat{m}_1}) s_{e1} s_{s1} + e^{-i\delta} z c_{s2} s_{e2} s_{s2} \right] = 0, \tag{3.1.89}$$

where we have introduced the definitions

$$z = \frac{\hat{m}_2}{\hat{m}_1} - \frac{\hat{m}_s}{\hat{m}_1} e^{i2\Delta\phi_{21}} \cong \frac{\hat{m}_2}{\hat{m}_1}; \ \text{ and } \ \Delta\phi_{21} = \phi_2 - \phi_1 \ .$$

Then,

$$\frac{s_{e1}}{s_{e2}} = -e^{-i\delta} \frac{\hat{m}_2 c_{s2} s_{s2}}{s_{s1}(\hat{m}_1 e^{i2\Delta\phi_{21}} - \hat{m}_2 s_{s2}^2)} \ . \tag{3.1.90}$$

Since we have assumed only a single light neutrino, the Dirac phase from this point on is taken $\delta = 0$. In this limit, for small active-sterile angles, we expect the fraction between them to be positive, which can be translated using the denominator of (3.1.90) to:

$$s_{s2}^2 > \frac{\hat{m}_1}{\hat{m}_2} \cos(2\Delta\phi_{21}) \ . \tag{3.1.91}$$

It is readily seen, that, the mixing between the left and right-handed neutrinos are fully determined by the “dark" sector i.e. the right-handed neutrinos and the sterile singlet. Proceeding to the {33} element, a similar analysis leads to the following bounds:

$$\begin{aligned} \mathcal{M}_{\nu}^{33} &= e^{i2\phi_1} \hat{m}_1 s_{s1}^2 + c_{s1}^2 \left[e^{i2\Delta\phi_{s1}} c_{s2}^2 m_s + e^{i2\phi_2} \hat{m}_2 s_{s2}^2 \right] = \mu, \\ \frac{\mu}{\hat{m}_1} e^{-i2\phi_1} &= s_{s1}^2 + c_{s1}^2 \left[e^{i2\Delta\phi_{s1}} c_{s2}^2 \frac{\hat{m}_s}{\hat{m}_1} + e^{i2\phi_2} \frac{\hat{m}_2}{\hat{m}_1} s_{s2}^2 \right] \ . \end{aligned} \tag{3.1.92}$$

Now, implementing the Cauchy-Schwarz theorem for the {33} element we obtain:

$$\frac{\mu}{\hat{m}_1} \leq s_{s1}^2 + c_{s1}^2 \Big(\frac{\hat{m}\hat{m}_s^2}{\hat{m}_1^2} c_{s2}^4 + \frac{\hat{m}_2^2}{\hat{m}_1^2} s_{s2}^4 + \frac{\hat{m}_s \hat{m}_2}{\hat{m}_1^2} \sin(2\theta_{s2}) \cos(2\Delta\phi_{s2}) \Big)^{1/2} \Rightarrow$$

$$c_{s1}^2 \leq \frac{\hat{m}_1 - \mu}{\hat{m}_1 - \hat{m}_2 s_{s2}^2}, \; s_{s2}^2 < \frac{\hat{m}_1}{\hat{m}_2}, \tag{3.1.93}$$

where the last inequality has been derived under the assumptions that $\hat{m}_1 > \mu$ and $c_{s1}^2 > 0$. Remarkably, using (3.1.91), a very narrow bound can be derived:

$$\frac{\hat{m}_1}{\hat{m}_2} \cos(2\Delta\phi_{21}) < s_{s2}^2 < \frac{\hat{m}_1}{\hat{m}_2} \, . \tag{3.1.94}$$

The inequality (3.1.93) which describes the mixing of the sterile sector, can be written equivalently as:

$$c_{s1}^2 \leq \frac{\frac{\hat{m}_1}{\hat{m}_2} - \frac{\mu}{\hat{m}_2}}{\frac{\hat{m}_1}{\hat{m}_2} - s_{s2}^2} \, . \tag{3.1.95}$$

Proceeding as previously the equality (3.1.90) yields:

$$\frac{\hat{m}_1}{\hat{m}_2} \geq s_{s2} \Big(1 - \frac{s_{e2} c_{s2}}{s_{s1} s_{e1}}\Big) \, . \tag{3.1.96}$$

Regarding the Majorana phases from the (3.1.92), the imaginary part of the equation implies:

$$\frac{\sin(2\phi_1)}{\sin(2\Delta\phi_{21})} = -\frac{\hat{m}_2}{\mu} c_{s1}^2 s_{s2}^2, \tag{3.1.97}$$

where this equation is valid only for specific regions for $\phi \in (0, \pi)$. In figure 4, we plot the left hand side of equation (3.1.97). In the lower right square the two heavy neutrinos have the same (negative) CP charge and represent Majorana fermions. In the upper left square, the heave neutrinos have opposite CP charge and they can form a pseudo-Dirac pair. Considering the case, where the mass scale $\mu \to 0$, we expect that lepton number violation is absent and $\Delta L = 2$ processes are suppressed.

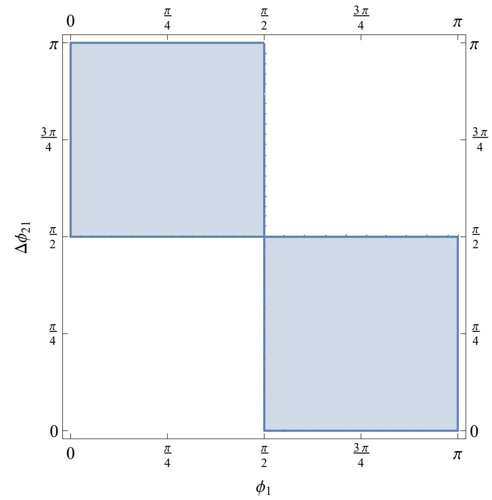

Figure 3.4: The left hand side of the equation (3.1.97) where we see that that the right-handed neutrinos can have opposite CP charge (upper left square) or the same (lower right square), which would yield interesting phenomenological implications. See main text.

The third and last constraint to be imposed is associated with the {13} element. This can be used to constrain the mixing s_{es} between the active neutrino and the singlet s. Thus, $\mathcal{M}_\nu^{13} = 0$ yields

$$\frac{s_{es}}{s_{e2}} = \frac{s_{e1}}{s_{e2}} s_{s1} c_{s1} \frac{-\Delta\hat{m}_{21} + \hat{m}_1 e^{i4\Delta\phi_{21}} - \hat{m}_2 e^{i2\Delta\phi_{21}}}{\hat{m}_1 - c_{s1}^2(\hat{m}_1 - \hat{m}_2 s_{s2}^2 e^{i2\Delta\phi_{21}})} + O(\frac{\hat{m}_{\nu,s}}{\hat{m}_{1,2}}), \tag{3.1.98}$$

where $\Delta\hat{m}_{21} = \hat{m}_2 - \hat{m}_1$, while for a controllable calculation we have neglected terms suppressed by the heavy neutrinos. After the parametrization of the different mixing angles and the phases, we are in a position to estimate their impact on the neutrinoless double beta decay. Following the discussion around equations (3.1.78,3.1.80), two distinct regimes can be defined:

$$\begin{aligned}
i) \qquad & m_{ee} = \hat{m}_{\nu_L} + U_{e1}^2\hat{m}_1 + U_{e2}^2\hat{m}_2 + U_{es}^2\hat{m}_s, \;\; \hat{m}_i \ll p^2 \\
& m_{ee} = U_{e2}^2\Big(\frac{\hat{m}_{\nu_L}}{U_{e2}^2} + \frac{U_{e1}^2}{U_{e2}^2}\hat{m}_1 + \hat{m}_2 + \frac{U_{se}^2}{U_{e2}^2}\hat{m}_s\Big), \\
ii) \qquad & m_{ee} = \hat{m}_{\nu_L} - U_{e1}^2\frac{p^2}{\hat{m}_1} - U_{e2}^2\frac{p^2}{\hat{m}_2} + U_{se}^2\hat{m}_s, \;\; \hat{m}_i \gg p^2 \\
& m_{ee} = U_{e2}^2\Big(\frac{\hat{m}_{\nu_L}}{U_{e2}^2} - \frac{U_{e1}^2}{U_{e2}^2}\frac{p^2}{\hat{m}_1} - \frac{p^2}{\hat{m}_2} + \frac{U_{es}^2}{U_{e2}^2}\hat{m}_s\Big),
\end{aligned} \tag{3.1.99}$$

where in both regimes the amplitude is defined up to an overall factor, but the terms in the parentheses are in principle responsible for the process. The mixing matrices U_{ei}^2 for small angles can be represented by the sines ($U_{ei}^2 \to s_{ei}$) computed before, so from the previous analysis we know every fraction (see equations (3.1.90,3.1.98) appearing in the formulas. We have neglected the mixing of the left handed neutrinos, since we have used only the electron neutrino. Consequently, the whole process is parametrized up to an overall factor U_{e2}^2. It is worth noticing that $\frac{U_{es}^2}{U_{e2}^2} = \gamma \frac{U_{e1}^2}{U_{e2}^2}$,

$$\gamma = s_{s1} c_{s1} \frac{-\Delta \hat{m}_{21} + \hat{m}_1 e^{i4\Delta\phi_{21}} - \hat{m}_2 e^{i2\Delta\phi_{21}}}{\hat{m}_1 - c_{s1}^2 (\hat{m}_1 - \hat{m}_2 s_{s2}^2 e^{i2\Delta\phi_{21}})}, \tag{3.1.100}$$

simplifying both of the parentheses in equation (3.1.99) as:

$$\begin{aligned} i)\ m_{ee} &= U_{e2}^2 \Big(\frac{\hat{m}_{\nu_L}}{U_{e2}^2} + \hat{m}_2 + \frac{U_{e1}^2}{U_{e2}^2} (\hat{m}_1 + \gamma \hat{m}_s) \Big) > 0 \\ ii)\ m_{ee} &= U_{e2}^2 \Big(\frac{\hat{m}_{\nu_L}}{U_{e2}^2} - \frac{p^2}{\hat{m}_2} + \frac{U_{e1}^2}{U_{e2}^2} (-\frac{p^2}{\hat{m}_1} + \gamma \hat{m}_s) \Big) > 0 \end{aligned} \tag{3.1.101}$$

The requirement of having positive mass for the m_{ee} leads the quantities in the parentheses to be bounded as:

$$\begin{aligned} i)& \frac{\hat{m}_{\nu_L}}{U_{e2}^2} + \hat{m}_2 > -\frac{U_{e1}^2}{U_{e2}^2} (\hat{m}_1 + \gamma \hat{m}_s) \Rightarrow \gamma < -\frac{\hat{m}_1}{\hat{m}_s} \\ ii)& \frac{\hat{m}_{\nu_L}}{U_{e2}^2} - \frac{p^2}{\hat{m}_2} > \frac{U_{e1}^2}{U_{e2}^2} (\frac{p^2}{\hat{m}_1} - \gamma \hat{m}_s) \Rightarrow \gamma > \frac{p^2}{\hat{m}_1 \hat{m}_s}\ . \end{aligned} \tag{3.1.102}$$

Since we expect a positive fraction (3.1.98) for the mixing angles, we must also have $\gamma > 0$. Hence the first case above is incompatible, since the assumptions stated in (3.1.85) imply $\gamma < 0$. In the second case a bound for the γ variable is extracted, which is going to be used to define the allowed parametric region for the neutrinoless double beta decay. In order to get an insight for the leptogenesis scenario regarding the nature of right-handed neutrinos participating in it, we need to check the asymptotic region of the fraction $\frac{\hat{m}_1}{\hat{m}_2} \to (0, 1)$. In the vanishing mass limit, the $\frac{s_{e1}}{s_{e2}} \gamma$ variable reduces to:

$$\frac{s_{e1}}{s_{e2}} \gamma = -2 \frac{\cos^2(\Delta\phi_{21})}{\cos(2\Delta\phi_{21})} \frac{c_{s2}}{c_{s1} s_{s2}^3} \Rightarrow \Delta\phi_{21} \in (\frac{\pi}{4}, \frac{\pi}{2}) \cup (\frac{\pi}{2}, \frac{3\pi}{4})\ . \tag{3.1.103}$$

In this limit, neutrinoless double beta decay scans the Majorana nature of the right-handed neutrinos and if baryon asymmetry is explained through leptogenesis, it is expected to happen due to the lightest heavy neutrino as in equation (3.1.70). Inversely stated, if two sterile neutrinos are observed, the mass fraction and their relative CP-charge difference can be used in order to extract the scale of neutrinoless double beta decay and the scale of possible sterile singlet through the analysis above. In the degenerate mass limit $\frac{\hat{m}_1}{\hat{m}_2} \to 1$, some useful conclusions can be extracted with respect to the mixing of the sterile neutrinos with the two heavy states. In this case the $\frac{s_{e1}}{s_{e2}}\gamma$ variable is written as

$$\frac{s_{e1}}{s_{e2}}\gamma = \frac{c_{s1}c_{s2}\left(\cos\left(2\Delta\phi_{21}\right) - \cos\left(4\Delta\phi_{21}\right)\right)s_{s2}}{\left(\cos\left(2\Delta\phi_{21}\right) - s_{s2}^2\right)\left(c_{s1}^2\left(\cos\left(2\Delta\phi_{21}\right)s_{s2}^2 - 1\right) + 1\right)} \,. \tag{3.1.104}$$

As it can be observed in the numerator above, there is a sign flip in the region of $\Delta\phi_{21} \in (\frac{\pi}{3}, \frac{2\pi}{3})$, where in this region the sterile singlet couples stronger with the second sterile neutrino $\theta_{s1} > \theta_{s2}$. Hence, in this limit if the two sterile neutrinos are observed with $\Delta\phi_{21} \in (0, \frac{\pi}{2})$, the neutrinoless double beta decay is expected to be suppressed due to the Pseudo-Dirac pair, while in the $\Delta\phi_{21} \in (\frac{\pi}{2}, \pi)$ they represent two Majorana fermions with degenerate mass.

We are going to present the masses of the neutrinos for the singlet VEVs, whose values are shown in Table (3.4). For these particular VEVs, the neutrinos are computed through the case β) (3.1.60) of section 6., the leptogenesis through the case ii) (3.1.73) and the neutrinoless double beta decay is expected at the degenerate mass limit (Table 3.6).

$\hat{m}_{\nu_i}$ (eV)	$\hat{m}_{\nu^c}$ (GeV)	$\hat{m}_s$ (keV)	ϵ_1	η	$\theta_{\nu s}$
0.1	4.3×10^{14}	0.55	2.3×10^{-6}	2.1×10^{-3}	4.7×10^{-4}

Table 3.6: Masses computed for the following scales: $m_{\nu_D} = 174$ GeV, $M_{\nu^c} = 4.3{\times}10^{14}$ GeV, $M_s = 19.1$ keV, $M_{\nu^c s} = 89.3 \times 10^3$ GeV, $\Delta m_{31}^2 = 2.2 \times 10^{-3}$ eV^2, and the first and second generation of heavy neutrinos at $\left(1.8 \times 10^{10}, 3 \times 10^{10}\right)$ GeV. Regarding the neutrinoless double beta decay, the model probes the blue region of $\frac{\hat{m}_1}{\hat{m}_2} \to 0.6$.

Also, in the two plots of figure 3.5 a couple of solutions of the equation (3.1.99) are depicted for various values of U_{e2}^2 and the effective electron neutrino mass m_{ee}.

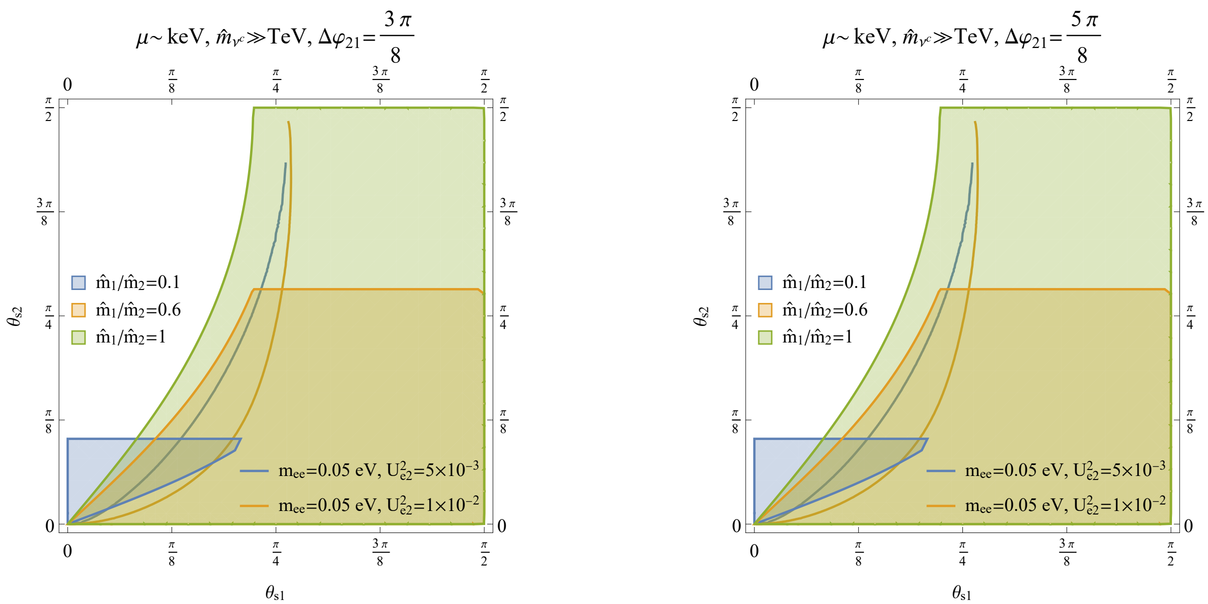

Figure 3.5: The shaded region depicts the allowed parameter space defined by the inequalities (3.1.94),(3.1.95),(3.1.102) and the curves represent the solutions for the neutrinoless double beta decay from the equation (3.1.99).

The extra vector-like states appearing in the zero-mode spectrum of the F-theory flipped $SU(5)$ are a possible source of the $g_\mu - 2$ enhancement [228; 229]. The relevant couplings are

$$\mathcal{W} = \lambda' \bar{h} h \frac{\langle \chi \psi^2 \rangle}{M_S^3} \bar{\psi} + \lambda^e_{ij} e^c_i \bar{f}_j h + \alpha_{mj} \bar{E}^c_m e^c_j \bar{\psi} + \beta_{mn} \bar{E}^c_m E^c_n \bar{\zeta} + \gamma_{nj} E^c_n \bar{f}_j h \chi \,. \tag{3.1.105}$$

which give rise to the one-loop graph shown in figure 6.

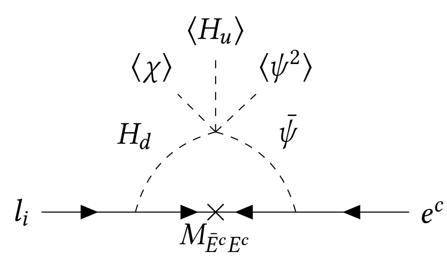

Figure 3.6: Feynman diagram for the contribution of the vector-like pair in the $g_\mu - 2$ process

Its contribution to $g_\mu - 2$ is highly dependent on the mass of the additional vector-like lepton-type charged singlets $E^c, \bar{E}^c$, since the latter participate in the loop. In the model under consideration their mass is given in terms of the VEV of the singlet $\bar{\zeta}$, i.e., $M_{\bar{E}^c E} = \langle \bar{\zeta}^2 \rangle$. It is also worth mentioning that, the very same VEV appears in the proton decay process, where the masses of the Higgs triplets are assigned a high scale mass due to this singlet. Consequently, low scale supersymmetry could not be a viable choice, in the case we would like to have a substantial contribution to $\Delta\alpha_\mu \sim \frac{m_\mu\langle h\rangle}{\langle\bar{\zeta}^2\rangle}$. Split susy fits better in such a scenario, where the mass of vector-like singlets can be lowered down to TeV scale and sufficiently explain the $g_\mu - 2$ discrepancy. Although, due to the mixing of the vector like leptons with the leptonic sector of the model, a mass matrix is constructed as it is shown in Table 3.7.

M^2_{Ee}	E^c	e^c_j
L_i	$\frac{\langle h\rangle\chi}{M_{str}}$	$\langle h\rangle$
$\overline{E}^c$	$\bar{\zeta}$	$\bar{\psi}$

Table 3.7: Mixing between the vector like leptons and the electrons.

In this case, the resulting mass of the states, which contribute in the above process could in principle be around TeV scale.

$$\begin{aligned} m_1 &= \frac{\langle h\rangle\chi}{M_{str}}\cos^2(\theta) - \frac{\langle h\rangle + \bar{\zeta}}{2}\sin(2\theta) + \bar{\psi}\sin^2(\theta) \\ m_2 &= \bar{\psi}\cos^2(\theta) + \frac{\langle h\rangle + \bar{\zeta}}{2}\sin(2\theta) + \frac{\langle h\rangle\chi}{M_{str}}\sin^2(\theta)\ . \end{aligned} \tag{3.1.106}$$

For the singlet VEVs mentioned at the previous sections, there are in principle light states after the mixing between the electrons and the vector-like singlets. Consequently, the heaviest of these singlets will lay at TeV scale, contributing to the $g_\mu - 2$ sufficiently to explain the discrepancy. Using the vevs of the model described before, the contribution to the $g - 2$ anomaly can be summarized to the following calculation as:

$$\Delta\alpha_\mu \sim \frac{m_\mu\langle h\rangle}{m_2^2} \sim \frac{105\times10^{-3}\ 174\ \mathrm{GeV}^2}{(89.3\times10^3)^2\mathrm{GeV}^2} \sim 23\times10^{-10} \tag{3.1.107}$$

Recently, the CDF II collaboration [230] using data collected in proton-antiproton collisions at the Fermilab Tevatron collider, has measured the W-boson mass to be $m_W = 80,433.5 \pm 9.4\,\mathrm{MeV}/c^2$. This value is in glaring discrepancy with the SM prediction, and the LEP-Tevatron combination which is $M_W = 80,385 \pm 15\,\mathrm{MeV}/c^2$. Since then several SM and MSSM extensions with the inclusion of new particles have been proposed to explain theoretically the experimental prediction of the W-mass. Taking the CDF result at face value, in the following we will show how the new ingredients in the present flipped $SU(5)$ construction may predict this W-mass enhancement. We first recall that the neutrino mass matrix formed by the three left- and right-handed neutrinos, as well as the sterile ones, is diagonalized by a unitary transformation. However, the mixing matrix diagonalizing the effective 3×3 light neutrino mass matrix obtained after the implementation of the inverse seesaw mechanism, need not be unitary. Consequently, this can in principle lead to a non-unitary leptonic mixing matrix which in section 6 has been parametrized as $V_\ell = (1+\eta)U_{PMNS}$. We will see that such effects can in principle modify the mass of the W-boson. In the context of the Standard Model, the mass of the W-boson can be inferred by comparing the muon decay prediction with the Fermi model [231]

$$M_W^2\left(1-\frac{M_W^2}{M_Z^2}\right)=\frac{\pi\alpha_{em}}{\sqrt{2}G_F}(1+\Delta r)\,, \tag{3.1.108}$$

where α_{em} and G_F are the fine structure and Fermi constants respectively, and Δr stands for all possible radiative corrections [232; 233]. Once Δr is known, the SM prediction of the W-boson mass is obtained by solving the formula (3.1.108). However, in the present case the non-unitarity in the PMNS matrix affects drastically the muon decays and consequently the measurement of the muon lifetime. The precise knowledge of these effects are essential since they determine the Fermi constant G_F which is involved in the determination of the W and Z boson masses. Thus, one might expect possible deviations from the G_F value when measured (G_μ) in muon decay. The non-unitary corrections are connecting them according to [234; 235]:

$$G_F = G_\mu(1+\eta_{ee}+\eta_{\mu\mu}), \tag{3.1.109}$$

where $\eta_{ee}, \eta_{\mu\mu}$ are the $\{11\}, \{22\}$ elements of the unitarity violation matrix η. Implementing the above formula for the Fermi constant, and solving (3.1.108), the mass of the W-boson is given by

$$M_W^2=\frac{1}{2}\left(M_Z^2+\sqrt{1-\frac{4\pi\alpha_{em}(1-\eta_{\mu\mu}-\eta_{ee})}{\sqrt{2}G_\mu M_Z^2}(1+\Delta r)}\right)\,, \tag{3.1.110}$$

Clearly, a possible increment of the W-mass may arise either due to non-unitarity inducing positive $\eta_{ee,\mu\mu}$ contributions, or from possible suppression of the radiative corrections Δr. Notice that Δr can also receive additional corrections due to the pair $E^c + \bar{E}^c$ appearing in the flipped $SU(5)$ spectrum. Their couplings in the superpotential induce a Wilson coefficient $(C_{h\ell})_{ij} = -\lambda_i\lambda_j^*/(4m_E^2)$ which gives a sufficient contribution to the W-mass for $M_E \sim 5$ GeV [236; 237]. Using the bounds for the mixing angles and the $\eta_{\alpha\beta}$ elements from Table IV of [234], we can plot the mass of the W-boson in terms of the non-unitary effects, where it is clearly seen that for small deviations from the unitary form of the leptonic mixing matrix can explain the experimental result.

From the diagonalization of the neutrino matrix (3.1.49), we expect two forms for the unitarity violation, corresponding to the two cases mentioned there. These two cases are

$$\alpha)\ \ \eta \cong O(\frac{1}{2}\frac{m_{\nu_D}^2}{M_{\nu^c s}^2}), \qquad \beta)\ \ \eta \cong O(\frac{1}{2}\frac{m_{\nu_D}^2(M_{\nu^c s}^2 + M_s^2)}{(M_{\nu^c s}^2 - M_{\nu^c}M_s)^2})\ . \tag{3.1.111}$$

Since we are interested in the second case, it is obvious that the scale M_s, which is responsible for the lepton number violation will play a crucial role. The specific form (texture) of the fermion mass matrices, of course, can in principle produce different -model dependent- scenarios of the unitarity violation. Despite this, we can derive the scale of the η matrix and extract some preliminary insights for the experimental signal. In figure 7, we plot the mass of the W-boson for different values of the lepton number violating scale M_s. As it is pointed out in [235], the insertion of right-handed neutrinos in the model produces a positive definite η matrix which is a necessary condition to explain the CDF-measurement of the W-boson mass. In fact a small lepton number violation can accommodate the W-mass discrepancy. Notably, at the same time, the sterile states can explain the Cabibbo angle anomaly [238] through the mixing term $\kappa_i \overline{H} F_i s\, \bar{\psi}$, although, the Cabibbo angle anomaly is not completely related to neutrinos, but to the inert singlet states involved in the seesaw mechanism.

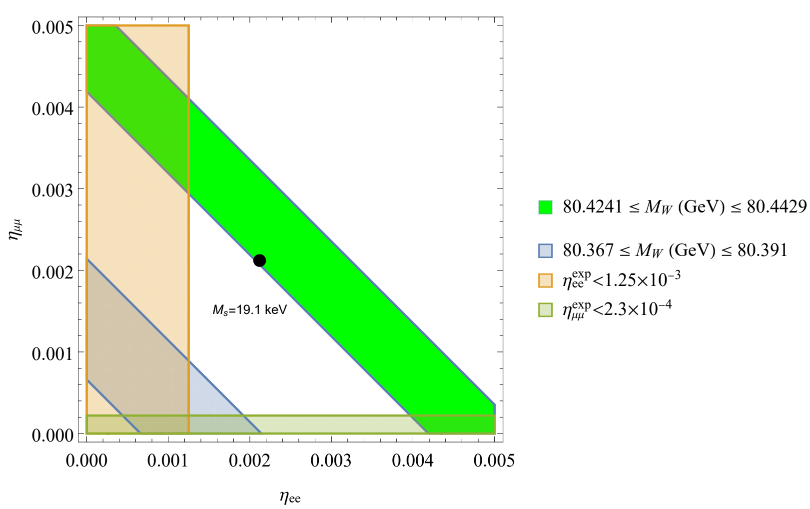

Figure 3.7: Plot of case β) η (3.1.111) (black dots under the assumption $\eta_{ee} \sim \eta_{\mu\mu}$), using $m_{\nu_D} = 174$ GeV, $M_{\nu^c} = 4.3 \times 10^{14}$ GeV, $M_s = 19.1$ keV, $M_{\nu^c s} = 89.3 \times 10^3$ GeV. Blue shaded region is the previous W-boson mass and green is the current measurement.

It is readily seen from the above that unitarity violation plays a crucial role in the mass of the

W-boson. The main characteristic of the inverse seesaw mechanism [5] is the small violation in the lepton number by the scale M_s. Large deviations from the PMNS-matrix can occur in the case where the sterile neutrinos lay at an intermediate scale (keV − MeV), since there is significant mixing between those states with the active neutrinos. In conclusion, one could conjecture that the neutrino masses, or more specifically the violation in the lepton number, play a significant role in the LFV physics, where sterile states allow this type of processes to evade the GIM suppression of SM. In conclusion, under the above mentioned circumstances, the rich structure of the F-theory flipped $SU(5)$ may suggest a viable interpretation of the W-mass increment [6].

As for the oblique parameters, which parameterize the effects of new physics in the electroweak observables, they have a direct implication on the recently observed mass shift of the W boson. Following the work of [241] with respect to the mass of W boson and [242] for the recently obtained fit on the oblique parameters, we could test our model and the unitary violation as a proposed solution.

$$\frac{M_W^{new}}{M_W} = -\frac{a\left(-\frac{U\left(c_W^2-s_W^2\right)}{2s_W^2} - 2c_W^2 T + S\right)}{4\left(c_W^2 - s_W^2\right)} - \frac{\Delta G s_W^2}{2\left(c_W^2 - s_W^2\right)} + 1, \tag{3.1.112}$$

where $s_W^2 = 1 - \frac{M_W^2}{M_Z^2}$ and the ΔG is the modification of the Fermi constant $G_F = G_\mu(1 + \Delta G)$. So, in our scenario, ΔG can be identified with the unitarity violation terms $\Delta G = \eta_{ee} + \eta_{\mu\mu}$. In the two figures below, we plot equation (3.1.112) for various values of the S, T parameters with a fixed U. So, after inserting $\Delta G = 2 \times 2.1 \times 10^{-3}$ and the masses of the W, Z bosons, the solutions are depicted below (Fig. 3.8).

$$\begin{aligned} &S \in (-0.04, 0.16),\ T \in (-0.01, 0.23),\ U \in (0.04, 0.22) \\ &S \in (0.06, 0.22),\ T \in (0.2, 0.32), U = 0 \end{aligned} \tag{3.1.113}$$

[5] We note that another solution with Type III seesaw with the presence of an $SU(2)$ Higgs triplet has been also suggested [239].

[6] In the context of F-theory, a different explanation with D3 branes has been suggested in [240].

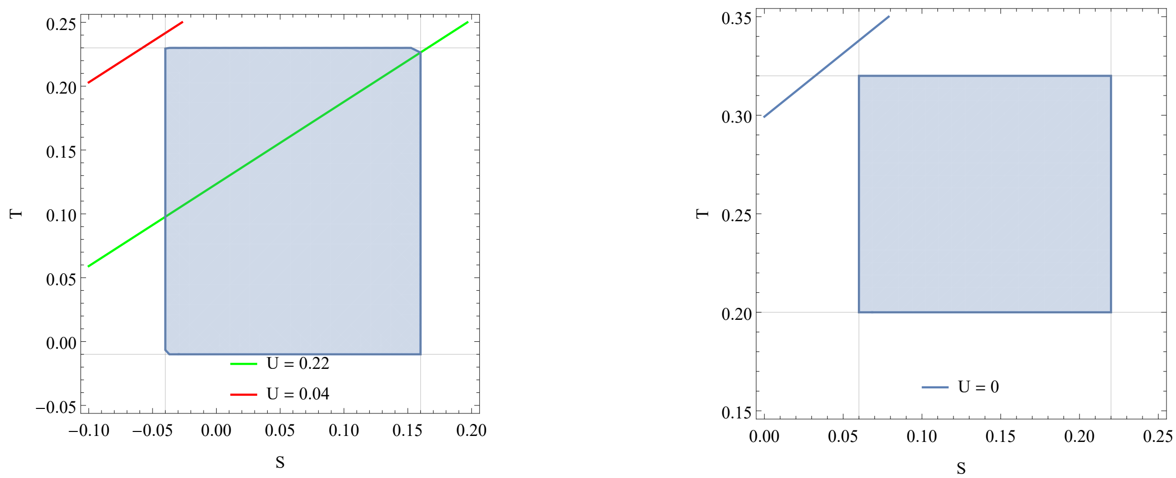

Figure 3.8: Left: Solution for S,T parameters with fixed parameter U, where the blue shaded region covers the bounds, as obtained by fit taking into account the new mass of W boson. Right: No solutions found when U is vanishing.

3.1.5 Gauge coupling unification

For the RGE's analysis of our model, we consider a low energy spectrum of the MSSM model accompanied by the presence of the vector-like singlets E^c. Starting with the beta function concerning the MSSM and the flipped $SU(5)$ particle content (for beta functions of flipped see for example [243; 244]), we summarize the formulas below:

$$
\begin{aligned}
b_1 &= \frac{3}{5}\left(\frac{3n}{10} + \frac{1}{2}n_H\right) + n_v \\
b_2 &= -6 + 2n + \frac{1}{2}n_H + n_v \\
b_3 &= -9 + 2n + n_v, \\
b_5 &= \frac{3n_{10}}{2} + \frac{n_5}{2} + 2n - 15 \\
b_{1_\chi} &= \frac{n_{10}}{4} + \frac{n_5}{2} + 2n
\end{aligned}
\tag{3.1.114}
$$

where n is the number of generations and n_v is the number of vector-like families. We can easily deduce that for $n = 3, n_v = 0$ we get the usual beta functions of the MSSM:

$$
\{b_1, b_2, b_3\} = \{\frac{33}{5}, 1, -3\} \tag{3.1.115}
$$

After inserting a vector-like pair in the low energy spectrum, we can plot the running of the coupling constants at 1-loop level and we can, eventually, spot the unification point. After the insertion of the parameter $a = \frac{g^2}{4\pi}$, we get

$$a_i^{-1}(Q) = a_i^{-1}(Q_0) - \frac{b_i}{2\pi}\log(\frac{Q}{Q_0}), \tag{3.1.116}$$

where the effect of a vector-like singlet family in the model in the beta functions is $\Delta b_i^{MSSM} = \{1, 1, 1\}$. There are two energy regions: from $0 < \mu < M_Z$, we run the beta functions of the SM, from $M_Z < \mu < M_{E^c}$ we run the MSSM plus the vector like particles and finally we run the flipped $SU(5)$ till a unification point. Plotting the running parameters of the model, we can see in the following plot that the unification scale is about $M_{GUT} \sim 10^{17}$ GeV.

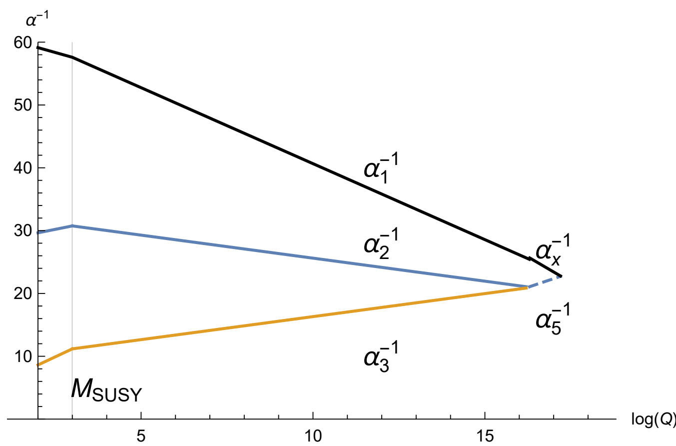

The unification scale is at $M_U \cong 10^{17}$GeV, where the couplings constants are

$$\alpha_1^{-1}(M_Z) = 59.38,\ \ \alpha_2^{-1}(M_Z) = 29.74,\ \ \alpha_3^{-1}(M_Z) = 8.44,\ \ \alpha_U^{-1} = 22.5 \tag{3.1.117}$$

As for the Yukawa couplings, we only consider the third generation (where the for the top, bottom quarks and the τ lepton are denoted as h_t, h_b, h_τ respectively) and the mixing effects of the abelian $U(1)$ symmetries ,during the evolution down to the low energy values, are being neglected. For the computation, the Mathematica code SARAH-4.15.0 [245] was used and the following plot depicts with thick lines the running of the spectrum with the vector-like family, where the dashed line contains the same information without the additional particles. During the computation, we have taken into account that the largest correction due to loops of sparticles is affecting the bottom Yukawa coupling as:

$$\delta h_b \cong \frac{g_3^2}{12\pi^2}\frac{\mu m_g \tan\beta}{m_b^2} + \frac{h_t^2}{32\pi^2}\frac{\mu A_t \tan\beta}{m_t^2}, \tag{3.1.118}$$

where $m_b = \frac{m_{b_1}+m_{b_2}}{2}$, $m_t = \frac{m_{t_1}+m_{t_2}}{2}$ are the average masses of the top and bottom squark. Consequently, we could safely extract the conclusion that even at high energies, Yukawa couplings stay under control at a perturbative regime (Fig. 3.9).

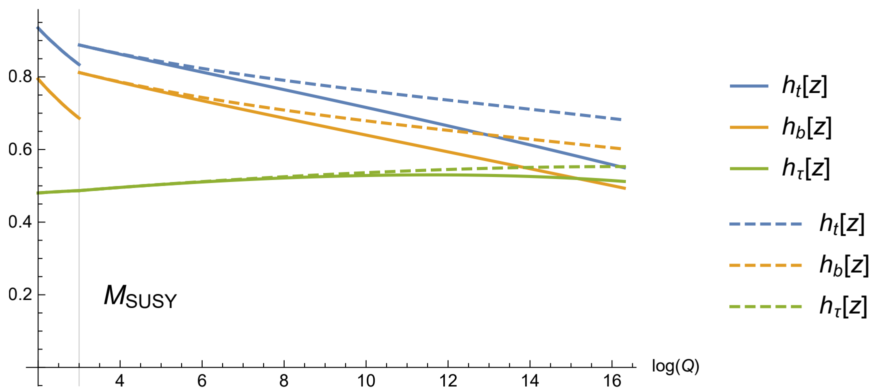

Figure 3.9: Yukawa evolution for the following parameters SUSY parameters $m_g = 2$ TeV, $\mu = 0.5$ TeV, $\tan\beta = 58$, $\mathrm{m_t} = 3$ TeV, $\mathrm{h_t}(0) = 0.94$, $\mathrm{h_b}(0) = 0.8$, $\mathrm{h}_\tau(0) = 0.48$. The dashed lines are the Yukawa without the vector like families where they deviate for $\tan\beta > 50$ as expected. The thick lines present the Yukawa couplings evolution with the insertion of a vector like family.

3.2 Modular Family Symmetry from the Bottom-up

3.2.1 Geometric origin of discrete finite modular symmetries

We now discuss how the finite modular symmetry can arise in F-Theory constructions. We first revisit Type IIB (the perturbative limit of F-Theory) vacua with discrete finite modular symmetry and explicitly obtain an S_4 invariant vacuum. We then turn to F-Theory, which inherits the S-duality from Type IIB, to identify the axio-dilaton modular symmetry, which endows the matter Yukawa couplings with modular symmetry transformation properties. Finally, we present our conjecture that F-Theory matter curves can carry a geometric modular symmetry, which will manifest itself in the Yukawa couplings, endowing F-Theory fluxed GUTs with a discrete modular family symmetry.

We now discuss the origins of finite modular symmetries in Type IIB string theory. To this effect, we will study, expanding on [189] Type IIB orientifold compactifications, where one can stabilise the moduli in a vacuum that is invariant to finite modular symmetries. The starting point is Type IIB, which exhibits an explicit modular invariance for the axio-dilaton irrespective of the details of the compact space. Upon choosing a factorisable toroidal orientifold for the compactification, $T^6/\mathbb{Z}_2 = (T_1^2 \times T_2^2 \times T_3^2)/\mathbb{Z}_2$ the theory will also manifest the modular invariance associated with the complex structure moduli of each of the tori, in other words we will have $SL(2,\mathbb{Z})_\tau \otimes (\otimes_{i=1}^3 SL(2,\mathbb{Z})_i)$ before the complex structure moduli are stabilised by Type IIB flux configurations. Once the fluxes acquire nonvanishing VEVs, we will show that the supersymmetry preserving vacuum transforms non-trivially under a congruence subgroup of order N, $\bar{\Gamma}(N)$, of the original modular symmetries, therefore breaking the preserved symmetry to Γ_N. As mentioned, we start with the Type IIB string theory, which is characterised by the strong-weak coupling duality (S-duality for short) which relates the theory with string coupling g_s to that with g_s^{-1}. S-duality is a non-perturbative symmetry based on the $SL(2,\mathbb{Z})$ modular group and is realised by the axio-dilaton modulus τ whose imaginary component is identified with the inverse string coupling

$$\tau = C_0 + ie^{-\phi} \equiv C_0 + i\frac{1}{g_s} \equiv C_0 + is\,, \tag{3.2.1}$$

where ϕ is the dilaton, and for convenience the definition $s = g_s^{-1}$ has been introduced. The four-dimensional (4d) effective action of the string moduli is described by the Kähler potential and the superpotential, both dependent on the complex structure moduli. The Kähler potential is parametrised in terms of the moduli and the axio-dilaton

$$K = -\ln(-i(\tau - \bar{\tau})) - 2\ln(\mathcal{V}) - 2\ln\left(e^{-\frac{3}{2}\phi}\int J \wedge J \wedge J\right)\,, \tag{3.2.2}$$

where ϕ is the dilaton, τ is the axio-dilaton defined in (3.2.1), $\mathcal{V}$ is the volume of the compactified space, and J its Kähler form $dJ = 0$ which depends on the complex coordinates z^i and $g_{i\bar{j}}$ the Kähler metric, and in its most general form is given by

$$J = ig_{i\bar{j}}dz^i \wedge d\bar{z}^j\,.$$

The superpotential for the moduli fields is given by the standard Gukov-Vafa-Witten formula

$$W = \int G_3 \wedge \Omega, \tag{3.2.3}$$

where the three form flux G_3 and the holomorphic three form Ω are given by:

$$G_3 = F_3 - \tau H_3 \tag{3.2.4}$$
$$\Omega = dz_1 \wedge dz_2 \wedge dz_3 \; . \tag{3.2.5}$$

Finally, for the toroidal case we define $z_i = x_i + \tau_i y_i$ so that,

$$dz_i = dx_i + \tau^i dy^i \; ,$$

where z_i corresponds to the three complex coordinates of the compactified space, and τ^i are the complex structure moduli of the orientifold. In general, the complex structure moduli form a matrix, τ^{ij}, parameterising the 3-cycles of the compactification, but here we take it to be a diagonal matrix, as we will be considering factorisable toroidal orientifolds.

Let now the basis for 3-forms be (α_i, β^j)

$$\begin{aligned} \alpha_0 &= dx^1 \wedge dx^2 \wedge dx^3, \quad \alpha_i = \frac{1}{2}\epsilon_{ilm}\, dx^l \wedge dx^m \wedge dy^i \\ \beta^0 &= dy^1 \wedge dy^2 \wedge dy^3, \quad \beta^i = -\frac{1}{2}\epsilon_{ilm} dy^l \wedge dy^m \wedge dx^i \; , \end{aligned} \tag{3.2.6}$$

where we notice that there is no sum in $i = 1, 2, 3$, and we have

$$\int \alpha_i \wedge \beta^j = \delta_i^j \; , \tag{3.2.7}$$

where the integral is over the compact space. The 3-form field strengths are expanded in terms of the basis as

$$\begin{aligned} F_3 &= m^0 \alpha_0 + m^i \alpha_i + n_i \beta^i + n_0 \beta^0 \\ H_3 &= p^0 \alpha_0 + p^i \alpha_i + q_i \beta^i + q_0 \beta^0 \; , \end{aligned} \tag{3.2.8}$$

where m, n, p, and q are quantised flux components, and are therefore integer valued. In fact, in the absence of exotic O3-planes, these are all even integers. The 3-form fluxes induce a D3-brane charge which has to fulfill a tadpole cancellation condition

$$N_{D3} + \frac{1}{2} N_{\text{flux}} = \frac{1}{4} N_{O3} \; , \tag{3.2.9}$$

where N_{D3} is the number of D3-branes, N_{O3} the number of O3-planes to be set by the details of the compactified space, and

$$N_{\text{flux}} = \int H_3 \wedge F_3 \ , \tag{3.2.10}$$

which can be explicitly evaluated to obtain

$$p^0 n_0 - q_0 m^0 + \sum_i (p^i n_i - q_i m^i) = 2\left(\frac{1}{4}N_{O3} - N_{D3}\right) \ . \tag{3.2.11}$$

The most general form of the superpotential for the moduli fields in the basis presented above is then

$$\begin{aligned} W &= (m^0 - \tau p^0)(\Pi_j \tau_j) - (m^i - \tau p^i)(\Pi_{j\neq i}\tau_j) - (n_i - \tau q_i)\tau^i - (n_0 - \tau q_0) \\ &= \tau_1\tau_3\tau_2(m^0 - p^0\tau) - \tau_3\tau_2(m^1 - p^1\tau) - \tau_1\tau_3(m^2 - p^2\tau) - \tau_1\tau_2(m^3 - p^3\tau) - \\ &- \tau_1(n_1 - \tau q_1) - \tau_2(n_2 - \tau q_2) - \tau_3(n_3 - \tau q_3) - (n_0 - \tau q_0) \ . \end{aligned} \tag{3.2.12}$$

The non-vanishing flux components will fix the moduli along flat directions, where the potential is minimised, $D_\tau W = D_{\tau_k} W = 0$, without breaking supersymmetry. Along these flat directions, the invariance of the fluxes under the modular symmetries of the axio-dilaton, τ, and the complex structure moduli, τ_i, will lead to vacua which are invariant under a finite modular subgroup. To see this, we focus on factorisable toroidal orientifold compactification $T^6/\mathbb{Z}_2 = (T_1^2 \times T_2^2 \times T_3^2)/\mathbb{Z}_2$.

The Type IIB action and the superpotential, (3.2.3), are invariant under the axio-dilaton modular symmetry, $SL(2,\mathbb{Z})_\tau$, according to which the axio-dilaton and the 3-forms F_3, H_3 transform as [246]

$$\tau' = R(\tau) = \frac{a\tau + b}{c\tau + d} \tag{3.2.13}$$

$$\begin{pmatrix} F_3' \\ H_3' \end{pmatrix} = \begin{pmatrix} a & b \\ c & d \end{pmatrix} \begin{pmatrix} F_3 \\ H_3 \end{pmatrix}, \quad R \in SL(2,\mathbb{Z})_\tau \ . \tag{3.2.14}$$

Furthermore, since the compactified space is a factorised torus, we can identity three complex moduli τ_i, where each has its own modular symmetry for vanishing fluxes. Each torus T_i, is defined as the quotient of the complex plane $\mathbb{C}/\Lambda_i$, where Λ_i is a lattice spanned by the vectors $\mathbf{e}_i = (e_{y_i}, e_{x_i})^T = (\tau_i, 1)^T$. One can further define $\xi_i = (y_i, x_i)^T$ where the coordinates $x_i \in [0,1)$, $y \in [0,1]$

and z_i are introduced according to [247]

$$z_i = \xi_i^T \mathbf{e}_i \equiv (y_i, x_i) \begin{pmatrix} e_{y_i} \\ e_{x_i} \end{pmatrix} \tag{3.2.15}$$

and for $(e_{y_i}, e_{x_i})^T = (\tau_i, 1)^T$ in particular,

$$z_i = (y_i, x_i) \begin{pmatrix} \tau_i \\ 1 \end{pmatrix} \equiv x_i + \tau_i y_i z \ . \tag{3.2.16}$$

Under modular symmetry $SL(2, \mathbf{Z})$

$$R_i = \begin{pmatrix} a_i & b_i \\ c_i & d_i \end{pmatrix}, \ R_i \in SL(2, \mathbf{Z}) \tag{3.2.17}$$

the vectors $\mathbf{e}_i$ transform according to

$$\mathbf{e}_i' = R_i \mathbf{e}_i \ . \tag{3.2.18}$$

Both vectors, $\mathbf{e}'$ and $\mathbf{e}_i$, span the same lattice, and, since $R_i R_i^{-1} = I$,

$$z = (y_i, x_i) R_i R_i^{-1} \begin{pmatrix} e_{y_i} \\ e_{x_i} \end{pmatrix} = e_{x_i}'(x_i' + \tau_i' y_i'),$$

where the modulus τ_i describes the shape of the torus transforms as

$$\tau_i = \frac{e_{y_i}}{e_{x_i}} \mapsto \tau_i' = \frac{e_{y_i}'}{e_{x_i}'} = \frac{a_i \tau_i + b_i}{c_i \tau_i + d_i} \ . \tag{3.2.19}$$

Thus, we recover the modular symmetry transformation presented in the previous section. This transformation also affects the real coordinates

$$z_i = (y_i, x_i) \mathbf{e}_i \mapsto z_i' = (y_i', x_i') \mathbf{e}_i' = (y_i', x_i') R_i \mathbf{e}_i \ , \tag{3.2.20}$$

therefore, modular invariance implies that (y_i, x_i) transform under $SL(2,\mathbb{Z})_i$ as

$$\begin{pmatrix} y_i' \\ x_i' \end{pmatrix} = (R_i^{-1})^T \begin{pmatrix} y_i \\ x_i \end{pmatrix} . \tag{3.2.21}$$

For the remaining of the analysis, it is useful to consider the transformation properties of the 1-forms. Thus, for the torus T_i^2, according to the above reasoning, we have [247]

$$\omega = \omega_l d\xi_i^l,\ d\xi_i^k = \begin{pmatrix} dy_i^k \\ dx_i^k \end{pmatrix},\ \omega_k' = R_{kl}\omega_l . \tag{3.2.22}$$

As can be readily checked, an immediate consequence of the above setup is that the holomorphic 3-form Ω, defined in (3.2.5), transforms as

$$\Omega \mapsto \frac{\Omega}{\Pi_{i=1}^3 (c_i\tau_i + d_i)} . \tag{3.2.23}$$

Furthermore, for a factorisable orientifold, in the large volume limit, the last term of the Kähler potential, (3.2.2), takes the explicit form

$$-2\ln\left(e^{-\frac{3}{2}\phi}\int J\wedge J\wedge J\right) = -\ln\left(i(\tau_1-\bar\tau_1)(\tau_2-\bar\tau_2)(\tau_3-\bar\tau_3)\right) , \tag{3.2.24}$$

and under $\otimes_{i=1}^3 SL(2,\mathbb{Z})_i$ transforms as

$$\begin{aligned} -\ln\left(i(\tau_1-\bar\tau_1)(\tau_2-\bar\tau_2)(\tau_3-\bar\tau_3)\right) \mapsto &-\ln\left(i(\tau_1-\bar\tau_1)(\tau_2-\bar\tau_2)(\tau_3-\bar\tau_3)\right) \\ &+\ln\left(\Pi_{i=1}^3 |c_i\tau_i + d_i|^2\right) , \end{aligned} \tag{3.2.25}$$

where we notice that the extra term cancels exactly the factor from (3.2.23) in the supergravity action, which implies that G_3 needs to be invariant under the tori modular symmetries. Therefore, under the axio-dilaton and the three tori modular symmetries, both 3-forms H_3, F_3, and the real coordinates pairs (x_i, y_i) on which the 3-form basis is defined transform non-trivially, while G_3 itself remains invariant under the tori modular symmetries. This will imprint non-trivial constraints on the flux data. Furthermore, along flat directions of the superpotential, the flux data allowed by modular invariance will fix the moduli. To see this, we first introduce the following configuration for the fluxes

$$p_3 = -f m^0,\ q_1 = f m^2,\ q_2 = f m^1,\ q_0 = f n_3, \tag{3.2.26}$$

where f is an integer. For this set of fluxes, the superpotential is given by

$$W = (f\tau - \tau_3)\left(\tau_1\left(m^2 - m^0\tau_2\right) + m^1\tau_2 + n_3\right)\ . \tag{3.2.27}$$

Using the definition (3.2.22), the 3-forms can now be written as [247]

$$F_3 = A_{ij} d\xi_1^i \wedge d\xi_2^j \wedge dx_3\ , \tag{3.2.28}$$

$$H_3 = B_{ij} d\xi_1^i \wedge d\xi_2^j \wedge dy_3\ , \tag{3.2.29}$$

where $B_{ij} = -f A_{ij}$ with

$$A = \begin{pmatrix} -n_3 & m^1 \\ m^2 & m^0 \end{pmatrix}\ . \tag{3.2.30}$$

Under the transformation of the modular symmetries associated with the tori $i = 1, 2$, i.e. $SL(2,\mathbb{Z})_1 \times SL(2,\mathbb{Z})_2$, the 3-forms F_3, H_3 transform as

$$F_3 \mapsto (R_1^{-1} A (R_2^{-1})^T)_{ij} d\xi_1^i \wedge d\xi_2^j \wedge dx_3 \tag{3.2.31}$$

$$H_3 \mapsto (R_1^{-1} A (R_2^{-1})^T)_{ij} d\xi_1^i \wedge d\xi_2^j \wedge dx_3\ , \tag{3.2.32}$$

and in order for G_3 to remain invariant the following relation must hold true

$$R_1^{-1} A (R_2^{-1})^T = A\ . \tag{3.2.33}$$

This imposes non-trivial constraints on the values of the flux data. We now consider the superpotential in (3.2.27) and its flat supersymmetric directions, $\partial_\tau W = \partial_{\tau_i} W = W = 0$, which yield

$$\tau_3 = f\tau \tag{3.2.34}$$

$$\tau_1 = \frac{-n_3 - m^1\tau_2}{m^2 - m^0\tau_2}\ . \tag{3.2.35}$$

From (3.2.34), we see that for $f = 1$ the axio-dilaton τ and the complex structure τ_3 are identified, $\tau = \tau_3$. This implies that the diagonal $SL(2,\mathbb{Z}) \subset SL(2,\mathbb{Z})_\tau \times SL(2,\mathbb{Z})_{\tau_3}$ remains unbroken by the vacuum

$$\tau_3' = R_3(\tau_3) = R(\tau) = \tau' \, , \tag{3.2.36}$$

and therefore we have $R = R_3$, effectively connecting the axio-dilaton modular symmetry with that of the torus T_3^2. We now focus on the symmetries associated with the tori with labels $i = 1, 2$. Following the above discussion, we first solve (3.2.33) with respect to R_2

$$R_2 = A^T (R_1^{-1})^T (A^{-1})^T \, . \tag{3.2.37}$$

Next from (3.2.30) we have

$$A^T = \begin{pmatrix} -n_3 & m^2 \\ m^1 & m^0 \end{pmatrix}, \quad (A^{-1})^T = \frac{1}{m^1 m^2 + m^0 n_3} \begin{pmatrix} -m^0 & m^2 \\ m^1 & n_3 \end{pmatrix}, \tag{3.2.38}$$

from which we finally get[7]

$$R_2 = \begin{pmatrix} \dfrac{m^1 m^2 a_1 + m^0 m^2 b_1 + m^1 n_3 c_1 + m^0 n_3 d_1}{m^1 m^2 + m^0 n_3} & \dfrac{-(m^2)^2 b_1 + (n_3)^2 c_1 + m^2 n_3 (a_1 - d_1)}{m^1 m^2 + m^0 n_3} \\ \dfrac{(m^0)^2 b_1 - (m^1)^2 c_1 + m^0 m^1 (a_1 - d_1)}{m^1 m^2 + m^0 n_3} & \dfrac{m^0 n_3 b_1 - m^0 m^2 b_1 - m^1 n_3 c_1 + m^1 m^2 d_1}{m^1 m^2 + m^0 n_3} \end{pmatrix} . \tag{3.2.39}$$

The above result generalises that of [189], which can be reproduced in the limit $(n_3, m^0) \longrightarrow 0$. Furthermore, one can show that the vacuum direction set by (3.2.35) is invariant under $\tau_1 \mapsto \tau_1' = R_1(\tau_1)$ and $\tau_2 \mapsto \tau_2' = R_2(\tau_2)$ with R_2 given by eq:R2. Being an element of $SL(2,\mathbb{Z})_2$, the entries of R_2 are integers, and the determinant equals unity. This is not a trivial requirement, as the entries are now parametrically defined by the entries of an R_1 element and flux data. However, we can find which congruence subgroup, $\Gamma(N)$, of $SL(2,\mathbb{Z})_2$ the matrix R_2 belongs to. To do this, we first consider the case where the following relations hold

$$m^1 = -2m^0, \; m^0 = n_3, \; n_3 = x m^2 \, . \tag{3.2.40}$$

[7] Here we make use of $\det(R_1) = 1$ to simplify the denominator in eq:ATranspose arising from $(R_1)^{-1}$.

With these, R_2 can be expressed as

$$R_2 = \begin{pmatrix} \frac{x(-b_1+2c_1+d_1x)-2a_1}{x^2-2} & \frac{b_1-x(-a_1+c_1x+d_1)}{x^2-2} \\ \frac{4c_1-x(2a_1+b_1x-2d_1)}{x^2-2} & \frac{x(a_1x+b_1-2c_1)-2d_1}{x^2-2} \end{pmatrix} . \tag{3.2.41}$$

We can now find the explicit congruence subgroup of level N to which R_2 corresponds to, once the fluxes are fixed. To do so, we first inspect the off-diagonal terms in (3.2.41). The requirement that $R_2 \in SL(2,\mathbb{Z})_2$ readily suggests that q_1 is proportional to x^2-2 while s_1 is proportional to $(x^2-2)/4$. Therefore, we can identify $\Gamma\left(4/(x^2-2)^2\right)$ as the principal congruence subgroup of $SL(2,\mathbb{Z})_1$ of level $N = 4/(x^2-2)^2$. Since N needs to be an integer, it can take only two possible values

$$N = \begin{cases} 1 & , \ x = -2, 0, 2 \\ 4 & , \ x = -1, 1 \end{cases} . \tag{3.2.42}$$

We observe that the values $x = -2, 0, 2$ lead to $N = 1$, i.e., a trivial finite modular group, hence we focus on the second solution, $x^2 = 1$ with $N = 4$. In this case, (3.2.41) takes the form

$$R_2 = \begin{pmatrix} \frac{x(-b_1+2c_1+d_1x)-2a_1}{x^2-2} & b_1 - x\left(a_1 + c_1x + d_1\right) \\ c_1 - \frac{1}{4}x\left(2a_1 + b_1x - 2d_1\right) & \frac{x(a_1x+b_1-2c_1)-2d_1}{x^2-2} \end{pmatrix} . \tag{3.2.43}$$

Additionally, if $R_1 \in \Gamma\left(4/(x^2-2)^2\right)$, we have

$$b_1 = c_1 = 0 \mod 4/(x^2-2)^2 \tag{3.2.44}$$

$$a_1 = d_1 = 1 \mod 4/(x^2-2)^2 \,, \tag{3.2.45}$$

which leads to

$$R_2 \mod 4/(x^2-2)^2 = \begin{pmatrix} 1 & 0 \\ 0 & 1 \end{pmatrix} \mod 4/(x^2-2)^2 \,, \tag{3.2.46}$$

regardless of the sign of x. Therefore, we have encountered the principal congruence subgroup of level $N = 4/(x^2-2)^2 = 4$ of the homogeneous modular groups associated with the moduli with labels $i = 1, 2$, which will lead to a finite modular group $\Gamma_4 \simeq \bar{\Gamma}/\bar{\Gamma}(4) \simeq S_4$. An explicit choice of fluxes that produces a vacuum that breaks the full modular group to Γ_4 is

$$\{m^1 = -4,\ m^2 = 2,\ m^0 = 2,\ n_3 = 2\}\ , \tag{3.2.47}$$

which produces the total flux, c.f. (3.2.11), $N_{\text{flux}} = 8$. To check if this is a valid Type IIB solution, we first notice that the factorisable toroidal orientifold $T^6/\mathbb{Z}_2 = (T_1^2 \times T_2^2 \times T_3^2)/\mathbb{Z}_2$ has 64 fixed points, each associated with an O3-plane. To preserve $\mathcal{N} = 1$ SUSY in 4d, there cannot be anti-D3-branes, for which $N_{D3} \geq 0$. Therefore, $N_{\text{flux}} = 8$ is consistent with the tadpole cancellation condition eq:tadpole

$$N_{\text{flux}} = 2\left(\frac{1}{4}N_{O3} - N_{D3}\right) = 2(16 - N_{D3}) \leq 32\ . \tag{3.2.48}$$

In summary, in this section, we have derived the supersymmetric conditions on the fluxes of the moduli superpotential which predict an S_4 finite modular group from Type IIB orientifold compactification. However, this result pertains only to the Type IIB supergravity action and does not include matter fields and their interactions. To address this, we now move towards F-Theory constructions.

3.2.2 The axio-dilaton in Type IIB and F-Theory

The axio-dilaton is related to the string coupling g_s as $\tau = C_0 + i/g_s$. In Type IIB (and its geometric counterpart, F-Theory which inherits S-duality from Type IIB) the Yukawa coupling is expected to depend on the string coupling g_s as

$$\lambda(g_s, z_i) = g_s^{\alpha}\lambda(z_i)\ , \tag{3.2.49}$$

but it is also expected to depend on the complex structure moduli through $z_i = x_i + \tau_i y_i$, and possible flux parameters. These moduli fields will each transform under their respective $SL(2,\mathbb{Z})$ symmetries. In this subsection we shall be concerned with the axio-dilaton which is common to both Type IIB and F-Theory.

The Yukawa coupling λ will then be transformed under the $SL(2,\mathbb{Z})_\tau$, modular group associated with the axio-dilaton. From (3.2.1)

$$\tau - \bar{\tau} = 2is \longrightarrow \text{Im}\tau \equiv s = \frac{\tau - \bar{\tau}}{2i} = \frac{1}{g_s}\ , \tag{3.2.50}$$

and therefore

$$\frac{1}{g_s} \equiv \text{Im}\tau \;\longrightarrow\; \text{Im}\tau' = \frac{ad-bc}{|c\tau+d|^2}\,\text{Im}\tau \;=\; \frac{1}{|c\tau+d|^2}\,\text{Im}\tau \;\equiv\; \frac{1}{|c\tau+d|^2}\frac{1}{g_s}\,, \tag{3.2.51}$$

where the fact that $ad-bc=1$ has been utilised. Hence, for an arbitrary power of g_s, we have

$$\gamma g_s^{-\alpha} = \frac{g_s^{-\alpha}}{|c\tau+d|^{2\alpha}}\,. \tag{3.2.52}$$

Focusing on $\alpha=1$, for the T generator we have $a=b=1, c=0, d=1$, and hence

$$\tau \longrightarrow \tau+1: \qquad\qquad C_0 \longrightarrow C_0+1,\;\; s\longrightarrow s\,. \tag{3.2.53}$$

On the other hand, for the S generator we take $a=0, b=1, c=-1, d=0$, and so the denominator in (3.2.52) becomes

$$|c\tau+d|^2 = \tau\bar{\tau} = C_0^2+s^2\,, \tag{3.2.54}$$

and therefore the transformation acquires a specific structure given only in terms of the axion C_0 and the inverse string coupling $g_s^{-1}=s$

$$\tau \longrightarrow -\frac{1}{\tau}: \qquad\qquad C_0 \longrightarrow -\frac{C_0}{C_0^2+s^2},\;\; s\longrightarrow \frac{s}{C_0^2+s^2}\,. \tag{3.2.55}$$

This case is known as strong-weak duality or S-duality since it transforms the string coupling g_s to its inverse g_s^{-1}. Recall now that the axio-dilaton part of the tree-level Kähler potential is

$$K = -\log(-i(\tau-\bar{\tau})) + \cdots = -\log\left(\frac{\tau-\bar{\tau}}{2i}\right) - \log(2) + \cdots = -\log(s) + \cdots\,, \tag{3.2.56}$$

so that the $SL(2,\mathbb{Z})_\tau$ transformation implies that $-\log(s) \longrightarrow -\log\frac{s}{|c\tau+d|^2}$ and thus the exponential e^K transforms as

$$e^K \longrightarrow |c\tau+d|^2 e^K\,. \tag{3.2.57}$$

On the other hand, the gravitino mass is

$$m_{3/2}^2 = e^K|W|^2\,, \tag{3.2.58}$$

and since it must stay invariant we must have

$$W \rightarrow \frac{W}{c\tau+d} \;\Rightarrow\; |W|^2 \rightarrow \frac{|W|^2}{|c\tau+d|^2}\,. \tag{3.2.59}$$

It is now apparent that if S-duality is to be maintained by the perturbative superpotential Yukawa couplings [248], then the fields must have transformation properties with respect to it. A generic trilinear term with a tree-level Yukawa coupling of MSSM fields has the form

$$W \supset \lambda_{ij}(g_s) f_i f_j h \,. \tag{3.2.60}$$

In the simplest context, the Yukawa coupling could simply be taken $\lambda_{ij}(g_s) \longrightarrow \lambda_{ij}(z_k) g_s^{-1/2}$ where the parameters $\lambda_{ij}(z_k)$ may depend on other moduli fields. Then, the $\tau \longrightarrow -1/\tau$ transformation discussed above entails

$$\lambda \propto g_s^{-1/2} \xrightarrow{\tau \to -\frac{1}{\tau}} \frac{g_s^{-1/2}}{|C_0^2 + g_s^{-2}|^{1/2}} \,, \tag{3.2.61}$$

which matches exactly the transformation property of the tree-level superpotential W w.r.t. axio-dilaton τ. In a more general context, as we will see, the dependence of the Yukawa couplings on moduli fields is more involved and non-zero modular weights for the matter fields f_i, f_j, h should also be considered. Furthermore, the Yukawa couplings, which are 3×3 matrices in the flavour space, could transform non-trivially under the congruence group left over from the supersymmetric conditions imposed on fluxes of the moduli superpotential part. The specific choice of fluxes of the previous section indicates that the underlying flavour symmetry governing the Yukawa lagangian is $\Gamma_4 \simeq \Gamma/\bar{\Gamma}(4) \simeq S_4$ with Yukawa matrices being certain modular forms which belong to specific representations of the S_4 group. Additional restrictions are expected to be derived from the geometric structure of the compactification manifold to further suggest a specific implementation of the above scenario. In the following, we continue with F-Theory, where some of these hints become more transparent.

3.2.3 Yukawa Couplings and Fermion Mass Matrices in F-Theory

We now turn our attention to the Yukawa couplings in F-Theory. Our starting point is an effective F-Theory GUT model, which is derived from an ADE-type singularity with the world-volume of a 7-brane that wraps the space $R^{3,1} \times S$ with S being a Kähler manifold of two complex dimensions z_1, z_2. At low energies, F-Theory is described by an eight-dimensional YM theory on $R^{3,1} \times \mathcal{S}$ which must be topologically twisted to preserve $N = 1$ supersymmetry.

The compactification space is a fibred eight-dimensional space (CY fourfold CY_4) where the fibre over the base $B_3 = CY_3$ associated with the six-dimensional compact space is described by a two-dimensional torus whose modulus is the axio-dilaton $\tau = C_0 + ie^{-\phi} = C_0 + i/g_s$. Therefore, the $SL(2,\mathbb{Z})_\tau$ S-duality describes the variation of the modulus τ of the 2-torus over the compactification manifold. The geometric configuration consists of 7-branes filling the Minkowski 4D-space while wrapping a 4D ‘surface’ S – associated with some GUT symmetry – which is a complex Kähler manifold so that supersymmetry is preserved. The four-dimensional effective F-Theory model arises upon compactification of the eight-dimensional theory on S. The possible GUT groups, in particular, are associated with specific types of geometric singularities where the modulus τ acquires certain values. The massless fields of the low energy spectrum reside on Riemann surfaces, called matter curves, formed by 7-branes intersecting the GUT surface, while Yukawa couplings are formed at specific points where triple intersections of matter curves occur. [8]

Within this framework, the corresponding gauge theory is that of the eight-dimensional $N = 1$ supersymmetric YM theory with minimal field content. The bosonic spectrum, in particular, includes the gauge field A and a holomorphic two-form scalar Φ. Both fields are found in the adjoint representation and descend from the decomposition of the 10-dimensional gauge field $\mathcal{A}$. Since 7-branes are wrapped on a curved $R^{(3,1)} \times S$ space, unbroken $\mathcal{N} = 1$ supersymmetry requires Φ to be a holomorphic (2,0)-form as a result of the topological twisting [249]. [9]The superpotential W_{8d} of the eight-dimensional fields and an associated D-term take the form

$$W_{8d} = m_*^4 \int_S \mathrm{Tr}(F \wedge \Phi), \quad D = \int_S \omega \wedge F + \frac{1}{2}[\Phi, \bar{\Phi}] \, , \tag{3.2.62}$$

where $F = dA - iA \wedge A$ and $\omega = ig/2(dz_1 \wedge \bar{d}z_1 + dz_2 \wedge \bar{d}z_2)$ is the Kähler form on S.

The eight-dimensional fields can be organised as one $\mathcal{N} = 1$ vector multiplet, $\mathbf{V}$, and two $\mathcal{N} = 1$ chiral supermultiplets, $\mathbf{A}_{\bar{m}}$ and $\mathbf{\Phi}_{mn}$,

$$\mathbf{V} = (A_\mu, \eta^\alpha, \mathcal{D}) \tag{3.2.63}$$

$$\mathbf{A}_{\bar{m}} = (A_{\bar{m}}, \psi^\alpha_{\bar{m}}, \mathcal{G}_{\bar{m}})) \tag{3.2.64}$$

$$\mathbf{\Phi}_{mn} = (\varphi_{mn}, \chi^\alpha_{mn}, \mathcal{H}_{mn}) \, , \tag{3.2.65}$$

where $\mathcal{G}_{\bar{m}}, \mathcal{H}_{\bar{m}\bar{n}}$ are F-term components, and $\mathcal{D}$ represents the D-term, whilst, $\eta^{\dot{\alpha}}, \psi^\alpha_{\bar{m}}, \chi^{\dot{\alpha}}_{mn}$ are the fermionic components, which, in the twisted YM theory are associated with a zero, one- and two-form respectively [251],

$$\eta^{\dot{\alpha}}, \ \psi^\alpha = \psi^\alpha_{\bar{m}} d\bar{z}^{\bar{m}}, \ \chi^{\dot{\alpha}} = \bar{\chi}^{\dot{\alpha}}_{\bar{m}\bar{n}} d\bar{z}^{\bar{m}} \wedge d\bar{z}^n \, .$$

[8]Equivalently, the torus over B_3 can be described by the Weierstraśs equation $y^2 = x^3 + f(z)x^2 + g(z)$, where z is a coordinate of the complex projective space CP^1 (Riemann sphere). Then $\tau = \tau(z) = C_0(z) + ie^{-\phi(z)}$ and singularities occur at $\Delta(z_i) = 0$. The torus is associated with the invariant $j(\tau(z))$, which, together with the vanishing of Δ determines $\tau \sim \frac{1}{2\pi i}\log(z - z_i)$. Hence, for given z, τ is fixed. Also, going around the singularity, there is a shift to the real part of the modulus $C_0 \to C_0 + 1$ that corresponds to $\tau \to \tau + 1$ of $SL(2, \mathbb{Z})_\tau$.

[9]Within such an F-Theory framework it is well known that there are many complex structure moduli, associated with the positions of the 7-branes. The positions of the 7-branes are determined by tuning the complex structure moduli and can produce additional structure in the elliptic fibration [250].

The indices m, n take the values 1,2, the complex scalars $A_{\bar{m}}$, φ_{mn} have dimensions of mass M and $\mathcal{G}, \mathcal{H}, \mathcal{D}$ of squared mass M^2.

To preserve the supersymmetric vacuum, all variations of the eight-dimensional fields must vanish. In the context of the four-dimensional theory, this corresponds to imposing the F- and D-flantess of the superpotential. Minimising the superpotential (3.2.62) and imposing D-flatness, one arrives at the following equations

$$\bar{\partial}_A \Phi = 0 \tag{3.2.66}$$

$$F^{(2,0)} = 0 \tag{3.2.67}$$

$$\omega \wedge F + \frac{1}{2}[\Phi^\dagger, \Phi] = 0 \ . \tag{3.2.68}$$

The above equations have long been derived in reference [249] and are the basic ingredients for studying the properties of fields in generic 7-brane configurations. Here, we are interested in solutions for massless fields residing on 7-brane configurations. The equations can be solved by expanding the fields A, Φ assuming linear fluctuations around the background:

$$A_{\bar{m}} \longrightarrow \langle A_{\bar{m}} \rangle + a_{\bar{m}}, \quad \Phi \longrightarrow \langle \Phi \rangle + \varphi \ , \tag{3.2.69}$$

with the definitions

$$a = a_{\bar{z}_1} d\bar{z}_1 + a_{\bar{z}_2} d\bar{z}_2, \quad \varphi = \varphi_{\bar{z}_1 \bar{z}_2} d\bar{z}_1 \wedge d\bar{z}_2 \ . \tag{3.2.70}$$

Then, keeping only linear terms regarding the fluctuations φ, a, in the holomorphic gauge the EoM take the form

$$\bar{\partial}_{\langle A \rangle} a = 0 \tag{3.2.71}$$

$$\bar{\partial}_{\langle A \rangle} \varphi - i[a, \langle \bar{\Phi} \rangle] = 0 \tag{3.2.72}$$

$$\omega \wedge \partial_{\langle A \rangle} a - \frac{1}{2}[\langle \bar{\Phi} \rangle, \varphi] = 0 \ . \tag{3.2.73}$$

Substituting the expansions of the fields into (3.2.62) it is found that the holomorphic trilinear Yukawa coupling is written in terms of ϕ and a as follows

$$W_{\text{Yuk}} = -i m_*^4 \int_S \text{Tr}(\varphi \wedge a \wedge a) \ , \tag{3.2.74}$$

where m_* is the scale associated with the supergravity limit of F-Theory.

The fluctuations φ and a can be determined by solving the equations (3.2.71-3.2.73) for a variety of

diagonal or non-diagonal backgrounds [48; 193], the latter being known as T-branes [193]. They are associated with the zero-modes residing on the matter curves and when three of the latter define triple intersection a Yukawa coupling is formed. Depending on the details of the model, it is often the case that multiple zero-modes are accommodated on the same matter curve.
It can be shown that the general form of the solution for zero modes localised on a specific matter curve, say z_2 , takes the generic form

$$\varphi = R_a \chi_a = R_a f(z_2) g(z_1, \bar{z}_1, q) e^{-\sqrt{M_{z_1}^4 + m^4} z_1 \bar{z}_1} e^{\pm 2M_{z_2}^2 z_2 \bar{z}_2} , \tag{3.2.75}$$

where M_{z_i} appear when fluxes are also introduced [10]. It can be observed that locally the solution is described by a Gaussian profile, with its peak along the matter curve and waning out along the transverse direction z_1. The function $f(z_2)$ is a holomorphic function of z_2 left undetermined from the equations of motion and R_a encodes the group structure [48] associated with the background. Analogous solutions can be written for the other intersecting matter curves in the vicinity of the triple intersection. The integration (3.2.74) [11] is performed over the three overlapping wavefunctions where all of them are peaked at the triple intersection and since they are strongly localised, the integral can be restricted to a small region near the intersection point. At every triple intersection the gauge symmetry is enhanced and generically zero-mode states are assembled into representations of the higher symmetry. At the same time, multiple states accommodated on a certain matter curve may be organised into representations of the underlying symmetry of the complex structure of the matter curve.
Furthermore, assuming for example toroidal compactifications, the function f may depend explicitly on the complex structure moduli of the curve, and thus it is conceivable that they may transform as modular forms, as we argue in the next section. We discuss now the overall dependence of the Yukawa coupings on the mass scales of the theory, and their relation to the axio-dilaton modulus [253]. In string frame, the overall scale m_* in (3.2.74), is given by $m_*^8 = m_s^8 g_s^{-2}$ [253], hence, the resulting dependence of the Yukawa coupling on g_s is (see details in section 4 of [253])

$$\lambda \propto \frac{m_*^4}{m_s^4} = \frac{1}{g_s} . \tag{3.2.76}$$

The string coupling is related to the GUT scale. Indeed, let $\mathcal{V}_S \sim R_S^4 \sim 1/m_{GUT}^4$ be the volume

[10]For example, in a $U(3)$ model the flux assumes the form $\langle F \rangle = -(2i/3)M^2(\bar{z}_1 \wedge dz_1 - \bar{z}_2 \wedge dz_2)\mathrm{diag}(1, -2, 1)$. In a generic context, however, when non-Abelian T-branes are considered, a non-primitive flux is required $\omega \wedge F \neq 0$ to satisfy the D-term [48]. For a comprehensive presentation, see review [252].

[11]In section 3 eq (3.28) of [193]- using the notion of twisted one-forms, the connection $\psi = a + \hat{\kappa} \wedge \varphi$, $\hat{\kappa} = g^{1\bar{i}} g^{2\bar{j}} \bar{\Omega}_{\overline{ijz}} d\bar{z}$ is implemented - and the Yukawa coupling receives a symmetric form. See the appendix for the relevant computation.

of the GUT surface and $\mathcal{V}_B \sim R^6$ that of the base B_3 of the fibration. Compactification to four dimensions implies $M_{Pl}^2 \approx m_*^8 \mathcal{V}_B$ while from the kinetic term of the field strength it follows $\alpha_{GUT}^{-1} \approx m_*^4 \mathcal{V}_S$. Combining these relations we obtain a rough estimate

$$\frac{1}{\alpha_{GUT}} \sim {m_*}^4 \mathcal{V}_S = \frac{m_*^4}{m_s^4} \frac{m_s^4}{m_{GUT}^4} = \frac{m_s^4}{m_{GUT}^4} \frac{1}{g_s} \,, \tag{3.2.77}$$

Taking into account the various normalisation effects, the dependence on g_s is more involved. One finds [47; 48]

$$\lambda = C\, a_{GUT}^{3/4} \,, \tag{3.2.78}$$

where C may depend on other moduli fields via the wavefunctions of the form (3.2.75) involved in the triple intersections. This implies that S-duality symmetry is preserved only if the undetermined parts of the wavefunctions associated with the Yukawa coupling under consideration exhibit the appropriate dependence on g_s.

3.2.4 Yukawa matrices in a $SU(5) \times S_4$ model

Hitherto, we described a basic F-Theory approach to Yukawa couplings and presented a generic solution for the EoM. From the above analysis we inferred that the Yukawa coupling inherits group properties encoded in the matter wavefunctions. The latter depend on the complex structure moduli through holomorphic functions of the complex coordinates z_i left unspecified by the EoM. Nevertheless, from the preceding sections and more particularly from Section 3.1, we know that the fluxed superpotential of the moduli fields is subject to modular restrictions. Therefore, if the Yukawa sector for the ordinary matter of the superpotential is required to retain the same modular symmetry or a subgroup thereof, its origin is expected to come from the yet unspecified part of that solution. We are then given the opportunity to consider the wavefunctions transformed as modular forms. For example,

$$f(\tau_i) \to (c\tau_i + d)^{-k_i} f(\tau_i) \,, \tag{3.2.79}$$

where τ_i is a complex structure modulus associated with the complex coordinate z_i. Additionally, the holomorphic Yukawa coupling, being formed at the intersection of three matter curves, would be naturally transformed in a non-trivial representation of the congruence subgroup of the modular group. To illustrate the main idea of the bottom-up approach to F-Theory fluxed GUTs with modular symmetry, we give a simple example of an $SU(5)$ GUT embedded in E_6 which has been derived in an F-Theory framework [254]. The novel feature of this example is the inclusion of an S_4 finite modular family symmetry. As has already been pointed out, in this context matter fields reside on curves which are formed at the intersections of 7-branes with the GUT surface S, itself wrapped with 7-branes. We consider a divisor with an E_6 geometric singularity which, according to the F-Theory prescription, corresponds to an E_6 gauge symmetry of the effective theory. In the present setup, there are three matter curves accommodating three $27_{t_i'}$ representations of E_6. These are distinguished from each other by the weights t_i' of the $SU(3)$ Cartan sublagebra ($t_1' + t_2' + t_3' = 0$). We impose a $\mathcal{Z}_2$ monodromy $t_1' \leftrightarrow t_2'$, and hence only two distinct matter curves remain, e.g. $\Sigma_{27_{t_{1,3}'}}$, and use $U(1)$ fluxes to reduce the gauge symmetry down to $SU(5)$. Alternatively, one may derive this model starting from the maximum admissible (well behaved) singularity that corresponds to a E_8 gauge symmetry subsequently decomposed to

$$E_8 \supset SU(5) \times SU(5)_\perp \supset SU(5) \times U(1)^4_{t_i}, \quad \sum_{i=1}^{5} t_i = 0\,, \tag{3.2.80}$$

where now t_i correspond to the Cartan subalgebra of $SU(5)_\perp$. The E_6 and $SU(5)\times SU(5)_\perp$ properties of the matter and Higgs multiplets are given in Table 3.8. Due to the aforementioned restrictions on t_i' and the monodromy imposed, the only allowed trilinear E_6 term in the superpotential is $W \supset 27_{t_1'} 27_{t_1'} 27_{t_3'}$. We then assign the fermion supermultiplets to $27_{t_1'}$ and the Higgs fields to $27_{t_3'}$.

We break the $SU(5)$ gauge symmetry by turning on a flux along $U(1)_Y \in SU(5)$, which also splits the 10 and $\bar{5}$ representations of $SU(5)$. However, anomaly cancellation conditions impose constraints on the multiplicities of the latter which are as follows:

$$M_{10_M} = M_{5_1} = -M_{5_2} = -M_{5_3},\ M_{10_2} = -M_{5_4} = -M_{5_5} = M_{5_{H_u}}. \tag{3.2.81}$$

Furthermore, to eliminate extraneous and exotic matter derived from the decomposition of the 78-dimensional representation, we impose the conditions

$$M_{10_3} = M_{10_4} = M_{5_6} = N_8 = N_9 = 0, \tag{3.2.82}$$

These imply that [254]

$$\tilde{N} \equiv N_7\,. \tag{3.2.83}$$

The SM zero mode states derived from the complete $27_{t_i'}$ representations after various successive symmetry-breaking stages with the $U(1)$ fluxes shown in the last column of Table 3.9. Their multiplicities are expressed in terms of the flux integers which have remained undetermined by

E_6	$SO(10)$	$SU(5)$	Weight
$27_{t_1'}$	16	$\overline{5}_3$	t_1+t_5
$27_{t_1'}$	16	10_M	t_1
$27_{t_1'}$	16	θ_{15}	t_1-t_5
$27_{t_1'}$	10	5_1	$-t_1-t_3$
$27_{t_1'}$	10	$\overline{5}_2$	t_1+t_4
$27_{t_1'}$	1	θ_{14}	t_1-t_4
$27_{t_3'}$	16	$\overline{5}_5$	t_3+t_5
$27_{t_3'}$	16	10_2	t_3
$27_{t_3'}$	16	θ_{35}	t_3-t_5
$27_{t_3'}$	10	5_{H_u}	$-2t_1$
$27_{t_3'}$	10	$\overline{5}_4$	t_3+t_4
$27_{t_3'}$	1	θ_{34}	t_3-t_4

Table 3.8: $SO(10)$ and $SU(5)$ decompositions of $27 \in E_6$. The $SU(5)$ indices in $5_i, 10_j$ representations designate their origin of the corresponding matter curve (Σ_{5_i} and Σ_{10_j}), and 10_M accommodates ordinary matter fields.

the consistency conditions mentioned above.

In the present work, an explicit model is constructed by choosing the fluxes given in tab:fluxes. This choice leads to the spectrum given in tab:f-theory-spectrum where both the down quarks and leptons originate from $27_{t_1'}$. As we have argued in the previous section, the states supported on a matter curve will inherit modular symmetry properties related to the complex structure moduli parametrising that curve. Therefore, states supported on a given curve are expected to have the same modular weights and to furnish full representations of the discrete modular group that survives the compactification. Imposing these modular symmetry properties in the above representations, a version of the model presented above with non-trivial discrete modular group S_4 can be written as

$$\begin{aligned}\mathcal{W} = {}& \alpha\ (u^c_{1,2}Q_{1,2}Y^{(4)}_1)_1 H_u + \beta\ (u^c_{1,2}Q_{1,2}Y^{(4)}_2)_1 H_u + \gamma\ (u^c_3 Q_3 Y^{(4)}_1)_1 H_u + \delta\ (u^c_{1,2}Q_3 Y^{(4)}_2)_1 H_u \\ &+ \Big(\alpha'\ (d^c_{1,2}Q_{1,2}Y^{(6)}_1)_1 H_d + \beta'\ (d^c_{1,2}Q_{1,2}Y^{(6)}_2)_1 H_d + \gamma'_1\ (d^c_3 Q_{1,2}Y^{(8)}_{2,1})_1 H_d \\ &+ \gamma'\ (d^c_3 Q_{1,2}Y^{(8)}_{2,2})_1 H_d + +\delta'\ (d^c_{1,2}Q_3 Y^{(6)}_2)_1 H_d + \epsilon'\ (d^c_3 Q_3 Y^{(8)}_1)_1 H_d\Big)\frac{\theta_{31}}{M}, \end{aligned} \tag{3.2.84}$$

E_6	$SO(10)$	$SU(5)$	Weight vector	N_Y	$M_{U(1)}$	SM particle content
$27_{t_1'}$	16	$\overline{5}_3$	$t_1 + t_5$	$\tilde{N}$	$-M_{5_3}$	$-M_{5_3}d^c + (-M_{5_3} + \tilde{N})L$
$27_{t_1'}$	16	10_M	t_1	$-\tilde{N}$	$-M_{5_3}$	$-M_{5_3}Q + (-M_{5_3} + \tilde{N})u^c + (-M_{5_3} - \tilde{N})e^c$
$27_{t_1'}$	16	θ_{15}	$t_1 - t_5$	0	$-M_{5_3}$	$-M_{5_3}\nu^c$
$27_{t_1'}$	10	5_1	$-t_1 - t_3$	$-\tilde{N}$	$-M_{5_3}$	$-M_{5_3}D + (-M_{5_3} - \tilde{N})H_u$
$27_{t_1'}$	10	$\overline{5}_2$	$t_1 + t_4$	$\tilde{N}$	$-M_{5_3}$	$-M_{5_3}\overline{D} + (-M_{5_3} + \tilde{N})H_d$
$27_{t_1'}$	1	θ_{14}	$t_1 - t_4$	0	$-M_{5_3}$	$-M_{5_3}S$
$27_{t_3'}$	16	$\overline{5}_5$	$t_3 + t_5$	$-\tilde{N}$	$M_{5_{H_u}}$	$M_{5_{H_u}}d^c + (M_{5_{H_u}} - \tilde{N})L$
$27_{t_3'}$	16	10_2	t_3	$\tilde{N}$	$M_{5_{H_u}}$	$M_{5_{H_u}}Q + (M_{5_{H_u}} - \tilde{N})u^c + (M_{5_{H_u}} + \tilde{N})e^c$
$27_{t_3'}$	16	θ_{35}	$t_3 - t_5$	0	$M_{5_{H_u}}$	$M_{5_{H_u}}\nu^c$
$27_{t_3'}$	10	5_{H_u}	$-2t_1$	$\tilde{N}$	$M_{5_{H_u}}$	$M_{5_{H_u}}D + (M_{5_{H_u}} + \tilde{N})H_u$
$27_{t_3'}$	10	$\overline{5}_4$	$t_3 + t_4$	$-\tilde{N}$	$M_{5_{H_u}}$	$M_{5_{H_u}}\overline{D} + (M_{5_{H_u}} - \tilde{N})H_d$
$27_{t_3'}$	1	θ_{34}	$t_3 - t_4$	0	$M_{5_{H_u}}$	$M_{5_{H_u}}S$

Table 3.9: Complete 27s of E_6 and their $SO(10)$ and $SU(5)$ decompositions. The indices of the $SU(5)$ non-trivial states $10, 5$ refer to the labelling of the corresponding matter curve (we use the notation of [56]). We impose the extra conditions on the integers N_Y and $M_{U(1)}$ from the requirement of having complete 27s of E_6 and no 78 matter. The $SU(5)$ matter states decompose into SM states as $\overline{5} \to d^c, L$ and $10 \to Q, u^c, e^c$ with right-handed neutrinos $1 \to \nu^c$, while the $SU(5)$ Higgs states decompose as $5 \to D, H_u$ and $\overline{5} \to \overline{D}, H_d$, where $D, \overline{D}$ are exotic colour triplets and antitriplets. We identify RH neutrinos as $\nu^c = \theta_{15,35}$ and extra singlets from the 27 as $S = \theta_{14,34}$.

where M is the F-Theory characteristic compacfication scale and we will set, for simplicity, $\theta_{31}/M \simeq 1$ as we expect the VEVs of the singlets to be close to the scale M and this quantity can be reabsorbed into the definition of the primed coefficients.

According to the superpotential (3.2.84), the up-type quarks Yukawa matrix is given by

$$\lambda_u = \begin{pmatrix} \alpha\left(Y_1^2 + Y_2^2\right) - \beta\left(Y_2^2 - Y_1^2\right) & 2\beta Y_1 Y_2 & \delta\left(Y_2^2 - Y_1^2\right) \\ 2\beta Y_1 Y_2 & \alpha\left(Y_1^2 + Y_2^2\right) + \beta\left(Y_2^2 - Y_1^2\right) & 2\delta Y_1 Y_2 \\ 0 & 0 & \gamma\left(Y_1^2 + Y_2^2\right) \end{pmatrix}, \tag{3.2.85}$$

and for the down-type quarks, the relevant Yukawa matrix is written as

$$\lambda_d = \begin{pmatrix} \alpha' Y_1\left(3Y_2^2 - Y_1^2\right) - \beta' Y_1\left(Y_1^2 + Y_2^2\right) & \beta' Y_2\left(Y_1^2 + Y_2^2\right) & \delta' Y_1\left(Y_1^2 + Y_2^2\right) \\ \beta' Y_2\left(Y_1^2 + Y_2^2\right) & \alpha' Y_1\left(3Y_2^2 - Y_1^2\right) + \beta' Y_1\left(Y_1^2 + Y_2^2\right) & \delta' Y_2\left(Y_1^2 + Y_2^2\right) \\ \gamma'\left(Y_1^2 - 3Y_2^2\right)Y_1^2 + \gamma_1'\left(Y_2^2 - Y_1^2\right)\left(Y_1^2 + Y_2^2\right) & \gamma' Y_1 Y_2\left(Y_1^2 - 3Y_2^2\right) + 2\gamma_1' Y_1 Y_2\left(Y_1^2 + Y_2^2\right) & \epsilon'\left(Y_1^2 + Y_2^2\right)^2 \end{pmatrix}. \tag{3.2.86}$$

M_{10_M}	M_{5_3}	M_{5_1}	M_{5_2}	M_{10_2}	M_{5_5}	M_{5_4}	M_{H_u}	$M_{\theta_{15}}$	$\tilde{N}$
4	−4	3	−3	−1	1	0	0	2	1

Table 3.10: The choice of Fluxes used in this model.

E_6	$SO(10)$	$SU(5)$	Weight vector	N_Y	$M_{U(1)}$	SM particle content	Low energy spectrum
$27_{t_1'}$	16	$\overline{5}_3$	$t_1 + t_5$	1	4	$4d^c + 5L$	$3d^c + 3L$
$27_{t_1'}$	16	10_M	t_1	−1	4	$4Q + 5u^c + 3e^c$	$3Q + 3u^c + 3e^c$
$27_{t_1'}$	16	θ_{15}	$t_1 - t_5$	0	3	$3\nu^c$	-
$27_{t_1'}$	10	5_1	$-t_1 - t_3$	−1	3	$3D + 2H_u$	-
$27_{t_1'}$	10	$\overline{5}_2$	$t_1 + t_4$	1	3	$3\overline{D} + 4H_d$	H_d
$27_{t_3'}$	16	$\overline{5}_5$	$t_3 + t_5$	−1	−1	$\overline{d^c} + 2\overline{L}$	-
$27_{t_3'}$	16	10_2	t_3	1	−1	$\overline{Q} + 2\bar{u}^c$	-
$27_{t_3'}$	16	θ_{35}	$t_3 - t_5$	0	0	−	-
$27_{t_3'}$	10	5_{H_u}	$-2t_1$	1	0	H_u	H_u
$27_{t_3'}$	10	$\overline{5}_4$	$t_3 + t_4$	−1	0	$\overline{H_d}$	-
$27_{t_3'}$	1	θ_{34}	$t_3 - t_4$	0	1	θ_{34}	-
-	1	θ_{31}	$t_3 - t_1$	0	4	θ_{31}	-
-	1	θ_{53}	$t_5 - t_3$	0	1	θ_{53}	-
-	1	θ_{14}	$t_1 - t_4$	0	3	θ_{14}	-
-	1	θ_{45}	$t_4 - t_5$	0	2	θ_{45}	-

Table 3.11: Complete 27s of E_6 and their $SO(10)$ and $SU(5)$ decompositions. We use the notation of ref [56] for the indices of the $SU(5)$ states and impose the extra conditions on the integers N_Y and $M_{U(1)}$ from the requirement of having complete 27s of E_6 and no 78 matter. The $SU(5)$ matter states decompose into SM states as $\overline{5} \longrightarrow d^c, L$ and $10 \longrightarrow Q, u^c, e^c$ with right-handed neutrinos $1 \longrightarrow \nu^c$, while the $SU(5)$ Higgs states decompose as $5 \longrightarrow D, H_u$ and $\overline{5} \longrightarrow \overline{D}, H_d$, where $D, \overline{D}$ are exotic colour triplets and antitriplets. We identify RH neutrinos as $\nu^c = \theta_{15}$. Extra singlets are needed to given mass to neutrinos and exotics and to ensure F- and D- flatness.

The charged leptons have the same Yukawa matrix structure as the down-type quarks. However, inspecting the spectrum of F-Theory zero modes in tab:f-theory-spectrum, we see that the three families of L, Q, e^c, and d^c descend from different linear combinations of UV states from F-Theory zero modes. Therefore, the superpotential coefficients for the down-type quarks and the charged leptons are not the same, leading to a realisation of a Georgi-Jarlskog mechanism [255]. We then

MSSM fields	Matter Curves	Charge	S_4	k
$Q_{1,2}, u^c_{1,2}, e^c_{1,2}$	10_M	t_1	2	2
Q_3, u^c_3, e^c_3	10_M	t_1	1	2
$d^c_{1,2}, L_{1,2}$	$\bar{5}_3$	$t_1 + t_5$	2	4
d^c_3, L_3	$\bar{5}_3$	$t_1 + t_5$	1	6
H_u	5_{H_u}	$-2t_1$	1	0
H_d	5_2	$t_1 + t_4$	1	0
ν^c	θ_{15}	$t_1 - t_5$	3	0

Table 3.12: Perpendicular charges, modular weights, and S_4 discrete modular group representations associated with the matter curves hosting the model from tab:f-theory-spectrum.

write down the charged leptons Yukawa matrix as

$$\lambda_L = \begin{pmatrix} \alpha'' Y_1\left(3Y_2^2 - Y_1^2\right) - \beta'' Y_1\left(Y_1^2 + Y_2^2\right) & \beta'' Y_2\left(Y_1^2+Y_2^2\right) & \delta'' Y_1\left(Y_1^2+Y_2^2\right) \\ \beta'' Y_2\left(Y_1^2+Y_2^2\right) & \alpha'' Y_1\left(3Y_2^2 - Y_1^2\right) + \beta'' Y_1\left(Y_1^2+Y_2^2\right) & \delta'' Y_2\left(Y_1^2+Y_2^2\right) \\ \gamma''\left(Y_1^2 - 3Y_2^2\right)Y_1^2 + \gamma_1''\left(Y_2^2 - Y_1^2\right)\left(Y_1^2+Y_2^2\right) & \gamma'' Y_1 Y_2\left(Y_1^2 - 3Y_2^2\right) + 2\gamma_1'' Y_1 Y_2\left(Y_1^2+Y_2^2\right) & \epsilon''\left(Y_1^2+Y_2^2\right)^2 \end{pmatrix}, \tag{3.2.87}$$

where the modular form components have the same dependence on τ_d as those appearing in the down-type quark Yukawa matrix.

In the following discussion, we are going to sketch a scenario in which conjugate right-handed neutrinos are identified with the singlets θ_{15}, which are included in the particle spectrum of the F-Theory model. Since these fields are considered as degrees of freedom that lie in the transverse space of the matter curves [256], this fact leads us to consider the case that they do not carry any modular weight. However, a simple model is presented here in which the singlets transform as a triplet under the S_4 modular symmetry. In addition to the singlets mentioned before, more degrees of freedom are needed to give a Majorana mass to θ_{15}, leading to the implementation of a (type-I) seesaw scenario for the light neutrino masses. An important condition is that the additional singlets of the model have to cancel the perpendicular charges of coupling. The superpotential, following the transformation properties of Table (3.12), is written as:

$$\mathcal{W}_\nu = \zeta\ (\nu^c L_{1,2} Y_3^{(4)})_1 H_u + \eta\ (\nu^c L_3 Y_3^{(6)})_1 H_u + \lambda\ (\nu^c \nu^c)_1\ \frac{\theta_{53}^2 \theta_{31}^2}{M^3}, \tag{3.2.88}$$

where in the last coupling stands for the Majorana mass term of the conjugate right-handed neutrinos. Given the first two couplings the Yukawa matrix responsible for the neutrino Dirac mass can be written as:

$$\lambda_\nu = \begin{pmatrix} -2\zeta Y_2 Y_3 & 0 & \eta Y_1(Y_4^2 - Y_5^2) \\ -\frac{1}{2}\zeta(\sqrt{3}Y_1Y_4 + Y_2Y_5) & \frac{\sqrt{3}}{2}\zeta(\sqrt{3}Y_1Y_5 + Y_2Y_4) & -\eta Y_3(Y_1Y_4 + \sqrt{3}Y_2Y_5) \\ -\frac{1}{2}\zeta(\sqrt{3}Y_1Y_5 + Y_2Y_4) & \frac{\sqrt{3}}{2}\zeta(\sqrt{3}Y_1Y_4 + Y_2Y_5) & \eta Y_3(Y_1Y_5 + \sqrt{3}Y_2Y_4) \end{pmatrix}, \tag{3.2.89}$$

where the modular form components depend on the same modulus of the up-type quark, τ_u, and the conjugate right-handed neutrino Majorana mass matrix can be easily read out as

$$M_R = \begin{pmatrix} 1 & 0 & 0 \\ 0 & 0 & 1 \\ 0 & 1 & 0 \end{pmatrix} \lambda \frac{\theta_{53}^2 \theta_{31}^2}{M^3}, \tag{3.2.90}$$

where we will take $\lambda\theta_{53}^2\theta_{31}^2/M^3 = \tilde{\lambda} M_{GUT}$.

Given the above matrices, we could implement a type-I seesaw mechanism in our model to explain the neutrino masses. The light neutrino mass matrix is given by:

$$M_\nu = -M_D^T M_R^{-1} M_D , \tag{3.2.91}$$

where $M_D = v\lambda_\nu$, with $v = 173$ GeV being the Standard Model Higgs vacuum expectation value.

3.2.5 Numerical study

We now perform a brief numerical study to find whether the model presented above and explicitly stated by the superpotential in superpot1 can provide a good fit to quark masses and mixing. To do so, we will compare the model predictions against the values of the quark masses and mixing data at the GUT scale, which, for $\tan\beta = 5$, can be found in tab:quarkdata. The neutrino data are taken from the latest `NuFit 5.3`, [257] and is shown in tab:leptondata alongside the charged lepton Yukawa eigenvalues.

We use the effective Yukawa coupling matrices for the quarks, eq:Lambdau,eq:Lambdad, as well as for the neutrinos, eq:lambdan,eq:majorana, to compute the predictions and compare them to the data in tab:quarkdata,tab:leptondata. Although the coefficients of the superpotential are in principle calculable in F-Theory (see, for example, [47; 48; 195] for Yukawa couplings and [52] for R-Parity violating terms), in this work we will consider these coefficients as free parameters and

Quark and CKM Data			
y_d	$(4.81 \pm 1.06) \times 10^{-6}$	θ_{12}	$13.027° \pm 0.0814°$
y_s	$(9.52 \pm 1.03) \times 10^{-5}$	θ_{23}	$2.054° \pm 0.384°$
y_b	$(6.95 \pm 0.175) \times 10^{-3}$	θ_{13}	$0.1802° \pm 0.0281°$
y_u	$(2.92 \pm 1.81) \times 10^{-6}$	δ_{CP}	$69.21° \pm 6.19°$
y_c	$(1.43 \pm 0.100) \times 10^{-3}$		
y_t	0.534 ± 0.0341		

Table 3.13: Quark and CKM data [258; 259; 260].

Lepton and PMNS Data			
y_e	$(1.97 \pm 0.024) \times 10^{-6}$	$\sin^2\theta_{12}^L$	0.307 ± 0.012
y_μ	$(4.16 \pm 0.05) \times 10^{-4}$	$\sin^2\theta_{23}^L$	0.572 ± 0.023
y_τ	$(7.07 \pm 0.073) \times 10^{-3}$	$\sin^2\theta_{13}^L$	$(2.203 \pm 0.58) \times 10^{-2}$
Δm_{12}^2	$(7.41 \pm 0.21) \times 10^{-5}$ eV^2	δ_{CP}^L	$197° \pm 41°$
Δm_{13}^2	$(2.511 \pm 0.027) \times 10^{-3}$ eV^2		

Table 3.14: Lepton and PMNS data. Neutrino masses are given in normal ordering [257; 258; 259; 260]. When the uncertainty interval is asymmetric, the larger values was taken in the analysis for the Gaussian likelihood profile.

leave the study of their computation for future work. Additionally, we also have the dependency on the complex structure moduli fields parametrising the geometry of the matter curves, from which the matter fields inherit their discrete modular symmetry properties. Since up- and down-type quark Yukawas emerge at different intersection points in the internal geometry between different curves, the geometry describing each Yukawa coupling is in general different from each other and parametrised by its own modulus, i.e. the components of the modular forms appearing in the up- and down-type Yukawas can depend on different moduli fields, τ_u and τ_d, respectively. However, the charged leptons (neutrino) Yukawa matrix arises from the same intersection as the down-type (up-type) quark Yukawas and should therefore depend on the same modulus. Therefore, our (effective) parametric freedom encompasses:

- Four complex coefficients (α, β, δ, γ) and a complex modulus (τ_u) for the up-type Yukawa matrix,
- three complex coefficients (ζ, η, $\tilde{\lambda}$) for the neutrino sector (as well as a dependency on τ_u),
- six coefficients (α', β', γ', γ_1', ϵ') and one complex modulus (τ_d) for the down-type Yukawa matrix,

- six coefficients (α'', β'', γ'', γ_1'', ϵ'') for the charged lepton Yukawa matrix (as well as a dependency on τ_d).

This sums up to a total of 19 complex parameters, or 38 real parameters. Although this seems to over-parameterise our problem, as we only have 19 observables in tab:quarkdata,tab:leptondata, we must reiterate that the complex coefficients are in principle calculable in F-Theory and that the analysis present here simplifies this step.

To find whether we can jointly fit all observables, we employ an artificial intelligence search algorithm called Covariant Matrix Approximation Evolutionary Strategy (CMAES) [263], which was first proposed in [261] to simplify the task of finding valid points in highly constrained multidimensional BSM parameter spaces.[12] CMAES can be seen as a population-based optimisation algorithm that can find minima of any arbitrary function, irrespective of its continuity and differentiability. Therefore, we will use CMAES to minimise the minus log-likelihood of the data, D, given a point of the parameter space, θ,[13]

$$-llh(D|\theta) = \sum_i \frac{(\bar{\mu}_i - \mu_i(\theta))^2}{2\sigma_i^2}\ , \tag{3.2.92}$$

where i runs over the observables, $\mu_i(\theta)$ is the prediction for the observable i given a parameter space point θ, the data, D, are comprised of the set of tuples $\{(\bar{\mu}_i, \sigma_i)\}$, where $\bar{\mu}_i$, σ_i are, respectively, the central and 1-σ uncertainty values of the observables and are listed in (3.13) (3.14), and we have assumed a Gaussian profile likelihood for the data. We implemented CMAES using the `python` package `cmaes` [263], and we performed 1000 independent runs, each running until converged to a minimum of (3.2.92), and kept all points whose observable predictions were within 3-σ.[14]. The parameters of our model were bounded, so that the superpotential coefficients remain perturbative and the moduli take values in their fundamental domain with an upper bound on the imaginary part

$$\left\{\tau_i \in \mathbb{C},\ s.t.\ |\Re(\tau_i)| \leq 0.5 \wedge \sqrt{1-\Re(\tau_i)^2} \leq \Im(\tau_i) \leq 10\right\}\ , i = u,\ d\ \ . \tag{3.2.93}$$

Multiple successful runs converged, generating 18×10^6 points that fit all observables within 3-σ. The best point across all runs, that minimises the eq:llh at a value 1.15×10^{-15} (i.e., effectively

[12]See also [262] for a recent application to the Z_3 3HDM, where CMAES was shown to have up to nine orders of magnitude improvement in sampling efficiency over random sampling.

[13]Or, equivalently, to minimise the sum of the χ^2.

[14]This methodology is justified by the fact that our goal is not to draw a complete portrait of the parameter space, but rather to find examples of viable points.

with vanishing χ^2 or likelihood of 1), is given by the set of parameters (to up to one decimal digit)

$$\begin{aligned}
(\alpha,\beta,\delta,\gamma) =&(-1.8\times10^{-3}+1.8\times10^{-5}i, 4.5\times10^{-5}-1.4\times10^{-4}i,\\
&3.2\times10^{-4}+1.8\times10^{-3}i, 1.8\times10^{-1}+4.0\times10^{-2}i)\\
\left(\lambda',\beta',\gamma',\gamma_1',\epsilon'\right) =&(2.1\times10^{-5}-8.8\times10^{-8}i, -3.3\times10^{-5}+3.2\times10^{-8}i,\\
&-4.4\times10^{-5}+7.2\times10^{-5}i, -2.3\times10^{-4}-2.3\times10^{-4}i,\\
&-7.7\times10^{-5}+1.4\times10^{-4}i, 1.3\times10^{-4}-4.6\times10^{-3}i)\\
(\zeta,\eta,\tilde{\lambda}) =&(-6.1\times10^{-2}+9.1\times10^{-1}i, -1.5\times10^{-1}+7.2\times10^{-3}i,\\
&1.8\times10^{-1}+5.3\times10^{-2}i)\\
\left(\lambda'',\beta'',\gamma'',\gamma_1'',\epsilon''\right) =&(7.5\times10^{-5}+1.4\times10^{-7}i, 2.7\times10^{-4}-7.3\times10^{-7}i,\\
&-1.0\times10^{-3}+1.9\times10^{-3}i, 1.2\times10^{-4}+2.6\times10^{-8}i,\\
&-2.9\times10^{-3}+4.1\times10^{-5}i, 4.2\times10^{-4}-1.7\times10^{-3}i)\\
\tau_u =&-4.1\times10^{-1}+9.1\times10^{-1}i\\
\tau_d =&-5.0\times10^{-1}+1.2i\,,
\end{aligned} \tag{3.2.94}$$

where we organised the parameters by mass sector. We notice that the point above requires some hierarchy between superpotential coefficients which should be around the same order, e.g. $|\gamma|\sim\mathcal{O}(1)$ whereas $|\alpha|\sim\mathcal{O}(10^{-3})$. This hierarchy between coefficients of operators arising from the intersection of the same matter curves at the same intersection point is at odds with our F-Theory expectations, which requires further study involving their explicit computation. In (3.10) we show the values of the moduli field that were obtained by CMAES, where we see that lower values of the imaginary part of the moduli are preferred, and most points have $\Im(\tau_i)\lesssim 2$. We omit scatter plots for the remaining parameters as these are, in principle, computable in F-Theory, and the details of their numerical realisation are left to future study. We also note that one should not attempt to make statistical interpretations of the results of CMAES, as it is not an algorithm designed to populate a posterior (as Monte Carlo Markov Chains do in Bayesian inference) as it produces points through the path of quickest descent of the loss function (and therefore the points should also not be used for frequentist interpretations as one usually does with random sampling). However, all points are within 3-σ of all observables and therefore have a very high likelihood, or, conversely, a very small χ^2.

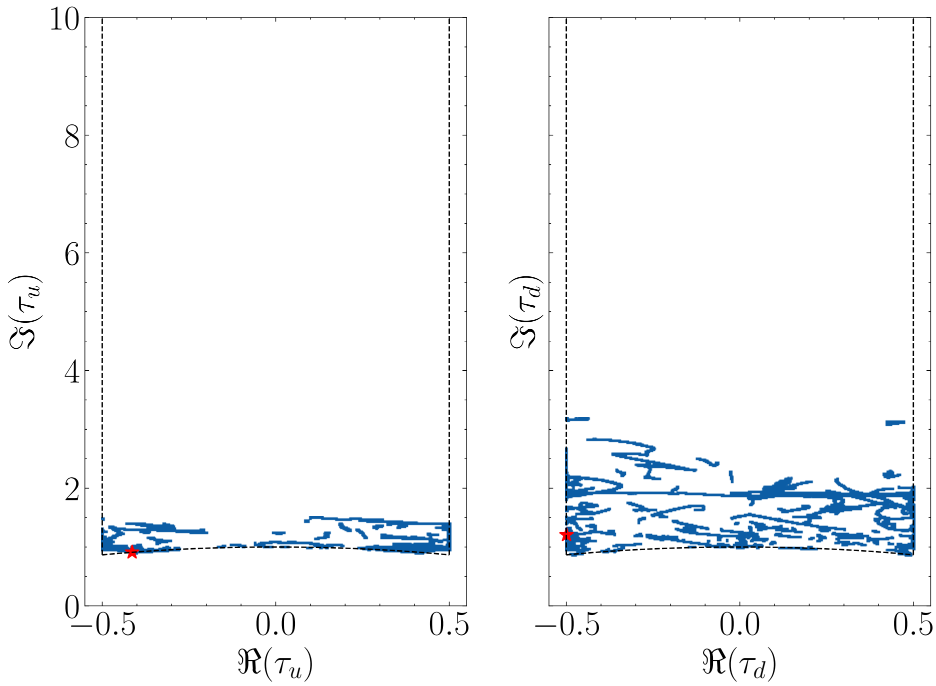

Figure 3.10: τ_u and τ_d values for the CMAES scan. All the points hold predictions within 3-σ. The red star point represents the best fit point, (3.2.94). Dashed line represents the boundary of the fundamental domain.

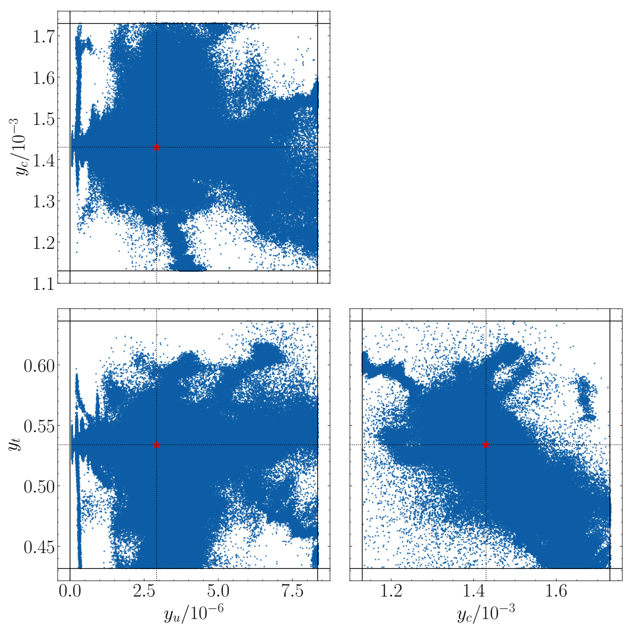

Figure 3.11: Up-type quark Yukawa eigenvalues obtained for the CMAES scan. All the points hold predictions within 3-σ. The red star point represents the best fit point, (3.2.94). The dashed (full) lines represent the central value (3-σ bounds) from (3.13).

We first look at the results pertaining to the quark data. In (3.11) we can observe the resulting values for the up-type quark Yukawa eigenvalues of points obtained, and in (3.12) we present the equivalent plots for the down-type quarks. We see that many points can be arbitrarly close to the central value, but also span the region within the 3-σ limits, showing that the model produces a good fit to the data. The same can be observed in (3.13) for the CKM mixing angle and CP violating phase.

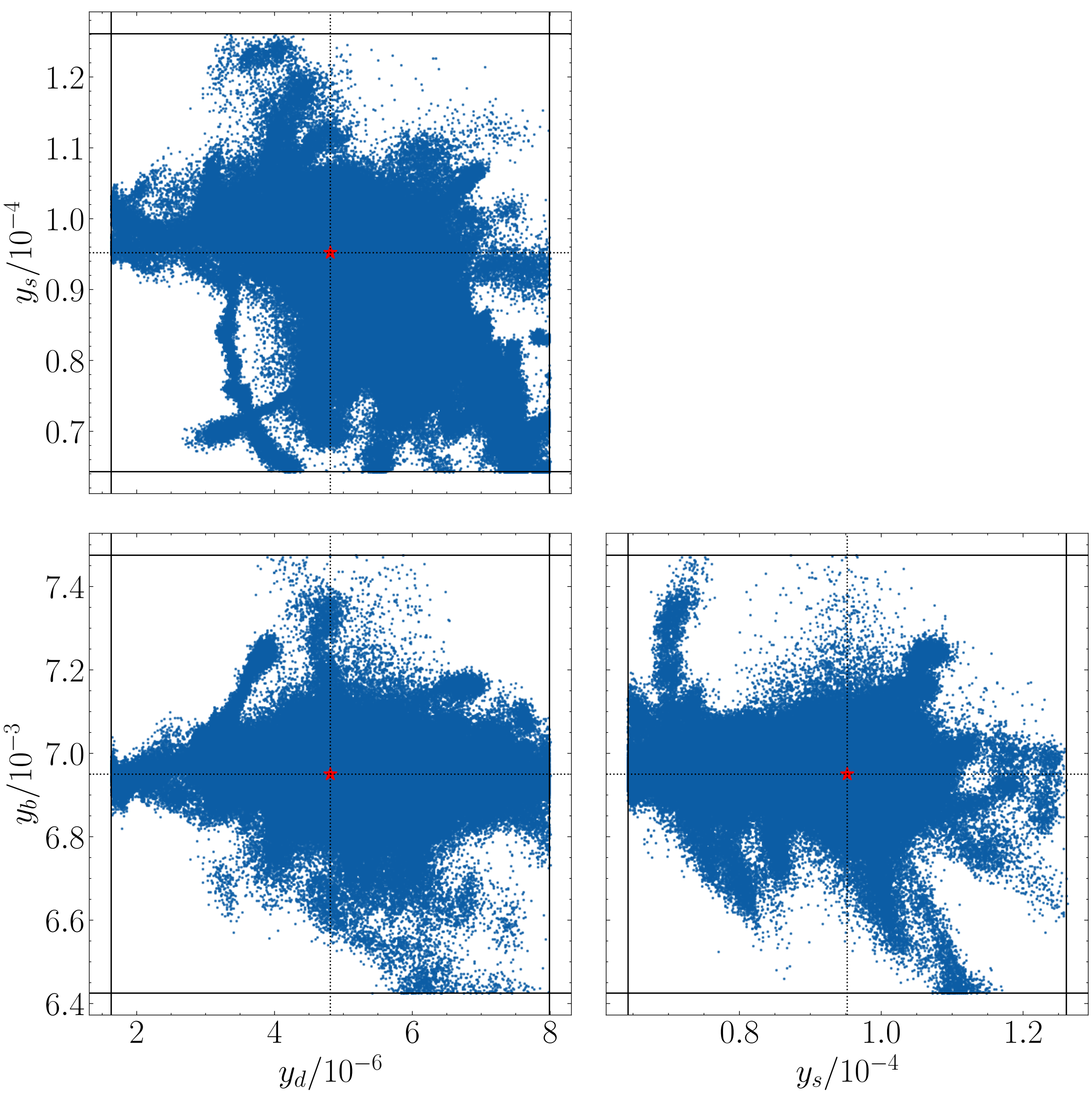

Figure 3.12: Down-type quark Yukawa eigenvalues obtained for the CMAES scan. All the points hold predictions within 3-σ. The red star point represents the best fit point, (3.2.94). The dashed (full) lines represent the central value (3-σ bounds) from (3.13).

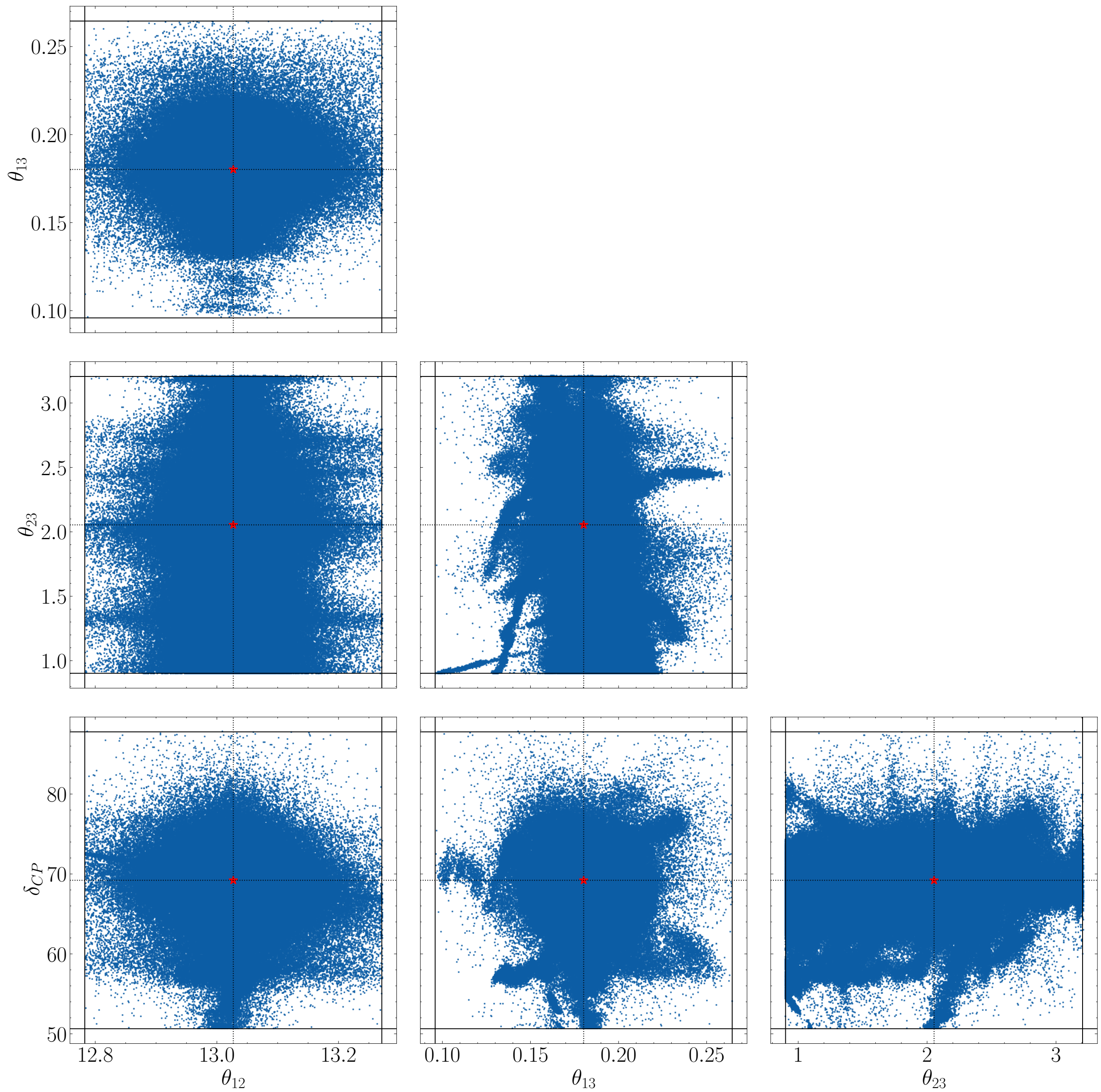

Figure 3.13: CKM angles and CP phase obtained for the CMAES scan. All the points hold predictions within 3-σ. The red star point represents the best fit point, (3.2.94). The dashed (full) lines represent the central value (3-σ bounds) from (3.13).

In (3.14) we can arrive at similar conclusions regarding the charged lepton Yukawa eigenvalues, neutrinos squared mass differences, PMNS mixing angles, and CP violating phase.

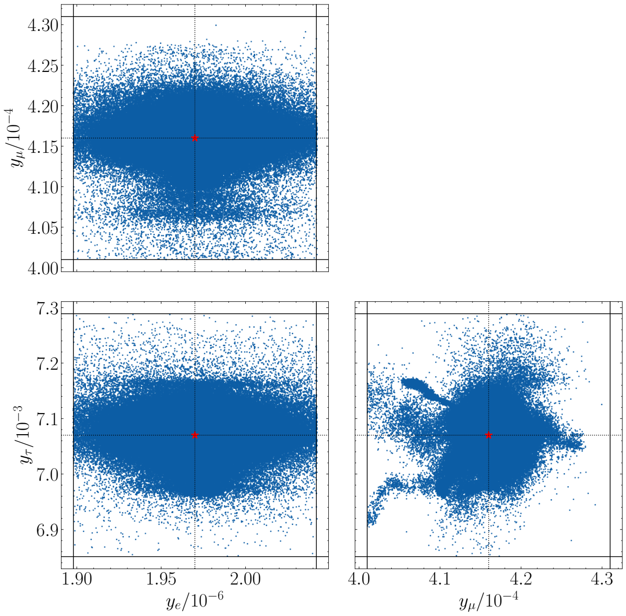

Figure 3.14: Charged leptons Yukawa eigenvalues obtained for the CMAES scan. All the points hold predictions within 3-σ. The red star point represents the best fit point, (3.2.94). The dashed (full) lines represent the central value (3-σ bounds) from (3.14).

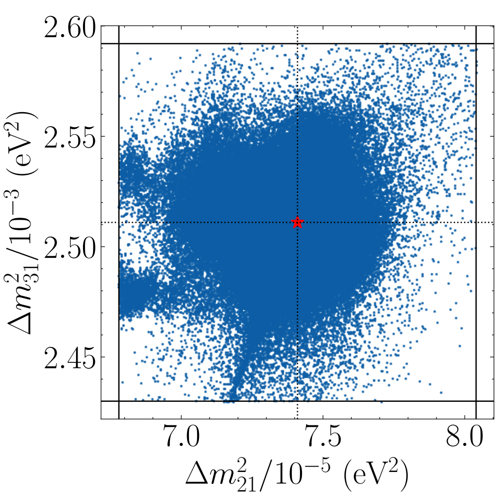

Figure 3.15: Neutrino squared mass differences obtained for the CMAES scan. All the points hold predictions within 3-σ. The red star point represents the best fit point, (3.2.94). The dashed (full) lines represent the central value (3-σ bounds) from (3.14).

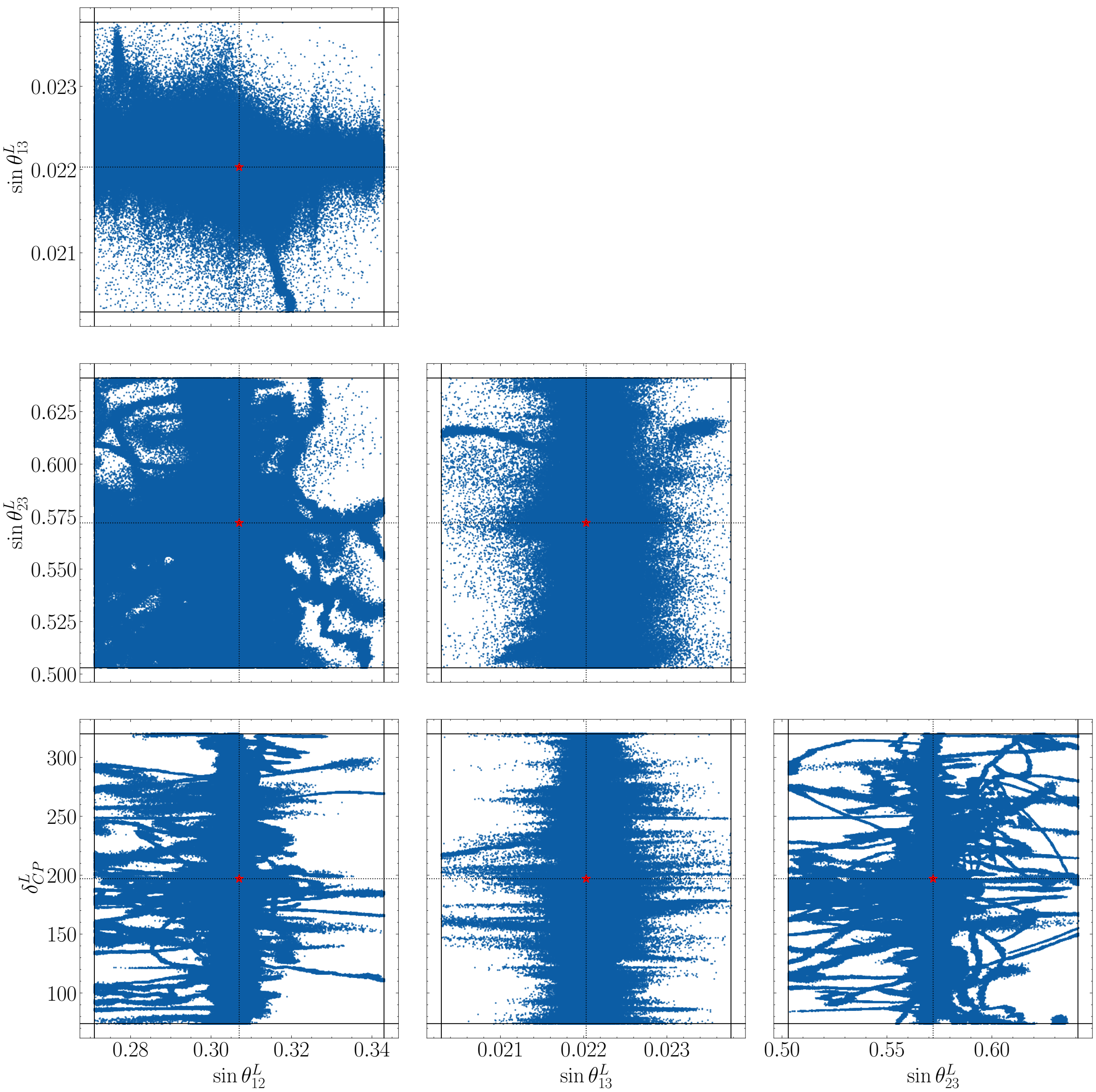

Figure 3.16: PMNS angles and CP phase obtained for the CMAES scan. All the points hold predictions within 3-σ. The red star point represents the best fit point, (3.2.94). The dashed (full) lines represent the central value (3-σ bounds) from (3.14).

The above results show that our model can fit the data very well, with the best point having a likelihood close to unity or, conversely, a vanishingly small χ^2. However, the problem is over-parametrised by the number of superpotential coefficients, which, although in principle calculable in F-Theory, are considered free parameters in this analysis. To assess whether we can reduce the parametric freedom, we considered alternative scenarios with reduced parametric freedom with respect to the moduli. In our first alternative scenario, we fixed the moduli to take the same values (i.e. $\tau_u = \tau_d$ but otherwise allowed the moduli to take values in the fundamental domain (3.2.93)) even though our F-Theory construction naturally provides distinct moduli for each Yukawa type. The scans converged successfully as before, from which we can conclude that our model does not require two independent moduli to fit the data. For the second case, we fixed the moduli to special values $\tau_u,\ \tau_d \in \{i,\ i\infty, \omega = \exp(2\pi i/3)\}$ (but not necessarily equal). In this scenario, CMAES failed to find points that fit the data. To further study this scenario, we restricted the problem to only fit the quark data, and even then the best-case scenario was for the configuration $\tau_u = i\infty$, $\tau_d = i$, for which we were able to fit all the observables within 3-σ except for the θ_{12} angle of the CKM matrix. The fact that the best-case scenario relies on $\tau_u = i\infty$ suggests that it is indeed not possible to find good points that fit all the data with the moduli stabilised at special values, as we have seen in (3.10) that the scans showed a preference for small values of $\Im(\tau_i)$. Therefore, we conclude that, despite being over-parameterised, the model works with fewer parameters although we lack F-Theoretical motivations to restrict their number.

4 | Conclusion

In this thesis, we presented some recent progress on modern topics of string phenomenology. From the more formal point of view, the problem of moduli stabilization in type IIB compactifications was scrutinized based on the recently introduced perturbative loop corrections, where different aspects of the stability and uplifting conditions were studied along with the possible connection between those quantum corrections with the dark sector of the stringy geometries. At the phenomenological frontier, two local F-theory GUTs were constructed providing some explanations on the various low-energy phenomena, like neutrino masses and the origin of flavor symmetry.

Chapter 2 features the perturbative moduli stabilization procedure followed to ensure the attainability of dS vacua in four dimensional effective string theories. The new ingredient in this approach has to do with the inclusion of string loop correction to the Kähler potential, where their origin can be traced by to graviton scattering in the bulk. In the current geometric framework of intersecting D_7 branes, the transverse space could accommodate the aforementioned string effects as corrections of logarithmic scaling parametrizing the localization width of the wavefuctions in an orbifold limit. Upon the insertion of those types of corrections to the Kähler potential, their combined effects with the non-perturbative effects in the superpotential lead to various AdS vacua for the scalar potential. In the large volume limit, i.e. in the regime where the moduli take large values, the asymptotic behavior of the scalar potential along the volume direction is largely modified by the loop effects. In addition, the supersymmetric flatness conditions could fix the value of the moduli, appearing in the superpotential, at large values by properly choosing the values of the integer fluxes $\mathcal{W}_0 \sim \mathcal{O}(1)$, since the solution is given in terms of the Lambert function. Additionally, the stability conditions of the moduli ratios and the compactified volume $\mathcal{V}$ admit the allowed parameter space for the free parameters of the theory, pointing towards the relative sign of the logarithmic correction to the Kähler potential. The uplifting mechanism utilized are the magnetically induced D-terms, which could uplfting the previous vacua up to Minkowski or dS space. Through this mechanism, despite acquiring the desired result, the parameter space is very stringent, since the Lambert function implies the correlation between the uplift parameter d, the a' correction ξ and the perturbative one η. In a more complex scenario compared to the symmetric form of the compactified volume, the fibred or "Swiss-cheese" like CY spaces are also given a similar treatment, where the logarithmic corrections could provide a glimpse to the internal geometry by determining the branes setup and the orientifold involution. Finally, a model of dark radiation and dark matter is presented where the non-diagonal entries of the Kähler metric, endowed by the logarithmic effects, modify the decays of the moduli to axions. The new contributions could not be underestimated, since axion can be overproduced and saturate the bounds provide by the BBN and the effective neutrino number of species. Moreover, two limiting cases (high and low scale) regarding the reheating temperatures are studied, where WIMP dark matter candidates are found after moduli decays to degrees of freedom of the dark sector.

In chapter 3, the phenomenology of local F-theory GUTs is presented. In the first subsection, a flipped $F\text{-}SU(5)$ is studied focusing in the implications to the neutrino sector and the W-boson mass anomaly. The complete model building is providing, where the spectral cover approach is used attributing to the matter curves and to the corresponding matter representations their homological indeces. The multiplicity of the representations are given according to the symmetry breaking pattern and the anomaly cancellation is performed through the Green–Schwarz mechanism. The low energy superpotential terms allow an inverse seesaw mechanism, where the new scale M_s is introduced due to the presence of singlet states. The novelty of F-theory constructions is that the weights of the perpendicular symmetry modify the couplings in the superpotential, since singlet states have to be augmented and their vevs will characterize the scale of the Yukawa terms. Proton decay is safely stable as long as the masses of the dangerous Higgs triplets are acquiring masses at M_{GUT} scale, while neutrinoless double beta decay is used as probe for measuring the lepton number violating effects in the presence of the sterile states. The model;s spectrum contains an additional electron-like pair of neutral singlets, whose vevs can be connected to an explanation for the $g_\mu - 2$ anomaly since these vector-like singlets mix with the leptonic sector. In the last part of this thesis, we argue that the different patterns of quarks and leptons could be understood through imposing a flavor symmetry. An F-theory derived $SU(5)$ model is presented where internal fluxes break the modular group down to S_4 due to stabilized complex structure moduli. This discrete modular family group along with the assigned different modular weights for the matter fields lead to Yukawa matrices, whose textures are parametrized by modular forms' components. Despite lacking the string framework that would provide additional constraints to the free parameters of the model, this approach on model building provides insights on the potential embedding of the families into the representations, especially on how they are seperated in the superpotential level due to their modular weight. To support our arguments and justify the existence of correct prediction for the CKM and the PMNS matrix, a numerical χ^2 analysis is performed scanning the parameter space for available solutions, which also indicate the values of the complex structure moduli which should lay on the plane shaped by the residual congruence modular group.

5 | Appendix

5.1 Mixing matrix for dark radiation section

Given the case studies discussed in section 3., we are going to characterize the mixing between the moduli and the normalized fields ϕ_i, based on the mass matrix in equation (2.2.24). In the following form and tracking the procedure given in [151; 172], the mixing matrix P_{ij} for the two cases can be written as:

$$\begin{pmatrix} \tau_1 \\ \tau_2 \\ \mathcal{V} \end{pmatrix} = \begin{pmatrix} \\ \vec{u}_1 \\ \\ \end{pmatrix} \phi_1 + \begin{pmatrix} \\ \vec{u}_2 \\ \\ \end{pmatrix} \phi_2 + \begin{pmatrix} \\ \vec{u}_3 \\ \\ \end{pmatrix} \phi_3, \quad P_{ij} = \begin{pmatrix} \vec{u}_1 \\ \vec{u}_2 \\ \vec{u}_3 \end{pmatrix}^T . \tag{5.1.1}$$

For the derivation of the corresponding eigenvectors can be derived by following the recipe:

$$M^2_{ij} \vec{u}_i = m_i^2 \vec{u}_i, \quad \vec{u}_i^T \cdot \mathcal{K} \cdot \vec{u}_j = \delta_{ij}, \tag{5.1.2}$$

where the two components of the each eigenvector will be defined by the first relation, while the normalization condition will fix the latter component. Consequently, for each case discussed in section 3., the mixing of the moduli can be approximated to:

$$P_{ij}^{\alpha)} \sim \begin{pmatrix} \frac{16\sqrt{3}d^{5/6}\sqrt{\xi}q}{w} & \frac{512\sqrt{3}d^{7/6}\sqrt{\xi}q^2}{w^2} & \frac{512\sqrt{3}d^{13/6}\sqrt{\xi}q^2}{w^2} \\ -\frac{2\sqrt{2}\sqrt[3]{d}\sqrt[6]{\mathcal{V}}}{\sqrt{s}} & -\frac{2\sqrt{2}}{\sqrt[3]{d}\sqrt{s}\sqrt[6]{\mathcal{V}}} & \sqrt{2}\sqrt{\frac{\mathcal{V}}{s}} \\ \sqrt{2}\sqrt{\frac{\mathcal{V}}{s}} & -\frac{2\sqrt{2}\sqrt[3]{d}\sqrt[6]{\mathcal{V}}}{\sqrt{s}} & -\frac{2\sqrt{2}}{\sqrt[3]{d}\sqrt{s}\sqrt[6]{\mathcal{V}}} \end{pmatrix}, \quad P_{ij}^{\beta)} \sim \begin{pmatrix} -s\left(\frac{d}{\mathcal{V}}\right)^{4/3} & -\frac{s}{\sqrt[3]{d\mathcal{V}^4}} & \frac{s}{2\mathcal{V}} \\ \frac{512\sqrt{3}d^{13/6}\sqrt{\xi}q^2}{w^2} & \frac{16\sqrt{3}d^{5/6}\sqrt{\xi}q}{w} & \frac{512\sqrt{3}q^2\sqrt{d^3\xi}}{w^2} \\ \frac{512\sqrt{3}d^{13/6}\sqrt{\xi}q^2}{w^2} & \frac{512\sqrt{3}q^2\sqrt{d^3\xi}}{w^2} & \frac{48\sqrt{3}d^{5/6}\sqrt{\xi}q}{w} \end{pmatrix}, \tag{5.1.3}$$

where the variables s, w are defined as:

$$s = \sqrt{(d\mathcal{V})^{2/3} + 8}, \quad w = 48q\sqrt[3]{d^2\mathcal{V}} + 2q + 3 \, . \tag{5.1.4}$$

The corresponding eigenvalues for both cases are given below:

$$m_{\phi_i}^{2\,\alpha)} \cong \Big(\frac{Tr[M^2]}{4}, Tr[M^2], \frac{Det[M^2]}{Tr[M^2]^2}\Big), \quad m_{\phi_i}^{2\,\beta)} \cong \Big(Tr[M^2], \frac{Det[M^2]}{Tr[M^2]^2}, \frac{Det[M^2]}{4Tr[M^2]^2}\Big) \, . \tag{5.1.5}$$

Now, the crucial next step is to define which normalized field mainly describes each one of the geometric moduli. Starting from the first case α), one can easily observe the dependence of the textures on the uplift parameter d. This observation is important since, in this case, the uplift parameter is exponentially small due to the smallness of the integer fluxes. Thus, the denominator of the fractions containing the parameter d turns to be extremely small and the mixing between the fields is rendered trivial.

$$\begin{aligned} \tau_1 &\cong O\Big(\frac{d^{5/6}}{3+2q}\Big)\phi_1 + O\Big(\frac{d^{7/6}}{(3+2q)^2}\Big)\phi_2 + O\Big(\frac{d^{13/6}}{(3+2q)^2}\Big)\phi_3 \cong P_{11}^{\alpha)}\phi_1, \\ \tau_2 &\cong O(d^{1/3}\mathcal{V}^{1/6})\phi_1 + O(d^{-1/3}\mathcal{V}^{-1/6})\phi_2 + O(\mathcal{V}^{1/2})\phi_3 \cong P_{22}^{\alpha)}\phi_2, \\ \mathcal{V} &\cong O(\mathcal{V}^{1/2})\phi_1 + O(d^{1/3}\mathcal{V}^{1/6})\phi_2 + O(d^{-1/3}\mathcal{V}^{-1/6})\phi_3 \cong P_{33}^{\alpha)}\phi_3 \, . \end{aligned} \tag{5.1.6}$$

From the above, it is remarkable that in the regime of exponentially small fluxes $|\mathcal{W}_0| \ll 1$, there exists a geometric separation between the world volumes. The overall volume is given by ϕ_3, while the transverse directions are approximately independent of this field. Additionally, one could also observe the correlation of the uplift parameter and the value of $\mathcal{V}$ at the minimum. Even in the case of $\mathcal{V} \gg 1$, the uplift parameter d will compensate the suppression of the mixing, providing this nice geometric result.

The second case β) of mixing following the same reasoning results in a qualitatively same mixing:

$$\tau_1 \cong \mathcal{O}(2\sqrt{2}\, d^{4/3}\mathcal{V}^{-4/3})\phi_1 + \mathcal{O}(2\sqrt{2}\, d^{-1/3}\mathcal{V}^{-4/3})\phi_2 + \mathcal{O}(\sqrt{2}\mathcal{V}^{-1})\phi_3 \cong P^{\beta)}_{22}\phi_2,$$
$$\tau_2 \cong \mathcal{O}(\frac{2}{3\sqrt{3}}\, d^{5/6}\mathcal{V}^{-2/3})\phi_1 + \mathcal{O}(d^{1/6}\mathcal{V}^{-1/3})\phi_2 + \mathcal{O}(\frac{2}{3\sqrt{3}}\, d^{1/6}\mathcal{V}^{-2/3})\phi_3 \cong P^{\beta)}_{22}\phi_2,$$
$$\mathcal{V} \cong \mathcal{O}(\frac{2}{3\sqrt{3}}\, d^{5/6}\mathcal{V}^{-2/3})\phi_1 + \mathcal{O}(\frac{2}{3\sqrt{3}}\, d^{1/6}\mathcal{V}^{-2/3})\phi_2 + \mathcal{O}(d^{1/6}\mathcal{V}^{-1/3})\phi_3 \cong P^{\beta)}_{33}\phi_3\,. \tag{5.1.7}$$

Again, in this case the overall volume $\mathcal{V}$ is given by a single normalized field ϕ_3. It is remarkable that geometric separation is a generic feature shared by this compactified space, where this fact is unraveled only after the process of finding the correct eigenvectors of the system. This feature was not given much attention on previous works [101], where the inflation scenario was studied as a multi-field system. This could be avoided after picking the appropriate scale for the fluxes $\mathcal{W}_0$. A final remark is that the computations given in this appendix will also be used in section 4., where the coupling of the normalized fields to the axions and Higgses will be calculated.

5.2 Decay rate formulas

For the derivation of the decay rates given in the main body of this paper, we used the standard formula:

$$\Gamma = \frac{1}{S}\int \frac{|M|^2}{2E} dLIPS, \tag{5.2.1}$$

where the d_{LIPS} is the element of the Lorentz invariant phase space and S is the symmetry factor. The decaying particle's energy is parametrized by E. There are two possible decay channels, which can be written as:

$$\mathcal{L} \supset g\phi_i\psi^2 + g\phi_i\psi\chi\,. \tag{5.2.2}$$

In the above equation, we have assumed that the mass of ϕ_i is much heavier than ψ, χ. The symmetry factor and the matrix element for the first case is given $S = 2$ and $|M|^2 = 4g^2$, while for the latter one is summarized to $S = 1, |M|^2 = g^2$. The corresponding coupling g in each process will be read by the Lagrangian terms, so the two decay rates are evaluated to be:

$$\Gamma_{\phi_i\to\psi\psi} = \frac{g^2}{8\pi m_{\phi_i}}, \quad \Gamma_{\phi_i\to\psi\chi} = \frac{g^2}{16\pi m_{\phi_i}} \ . \tag{5.2.3}$$

5.3 General form of D-terms

In this appendix, we provide a detailed stabilization using the generic D-terms formula, following the work of [141; 159; 160], and we focus on finding the relevance of the derived vacuum with our approximation in equation (2.2.9). Starting from the generic formula of the D-terms (2.2.7), it can be expanded to:

$$V_D \cong \sum_{i=3}^{3} \Big[\frac{1}{\tau_i}\Big(\sum_{i\neq j} Q_{ij}\partial_{T_j}\mathcal{K}\Big)^2\Big] = \frac{d_1}{\tau_1}\left(\frac{Q_{12}}{\tau_2}+\frac{Q_{13}}{\tau_3}\right)^2 + \frac{d_2}{\tau_2}\left(\frac{Q_{21}}{\tau_1}+\frac{Q_{23}}{\tau_3}\right)^2 + \frac{d_3}{\tau_3}\left(\frac{Q_{31}}{\tau_1}+\frac{Q_{32}}{\tau_2}\right)^2 . \tag{5.3.1}$$

The global embedding of this toy model has been analyzed in [159]. In this work, we need to stabilize two moduli by the D-terms, which fact is of particular importance for embedding consistent inflationary paradigms in such string scenarios [141; 159; 160]. In order to do so, we are going to assume that the charges Q_{ij} obey to the following relations:

$$Q_{12} = Q_{23} = Q_{31}, \quad Q_{21} = Q_{13} = Q_{32}, \quad Q_{12} \neq Q_{21} \ . \tag{5.3.2}$$

In addition to that, we could in general assume that $Q_{12} = 1, Q_{21} = 0$, since this could significantly simplify the form of the moduli's eigenvalues and eigenvectors, helping us to study the qualitative behavior of dark radiation in a stabilized dS vacuum. Also, since we would like to compare this new vacuum with the vacuum presented in the main body of the paper, we are going to redefine the τ_1, τ_2 moduli as τ_1', τ_2'.

$$V_D = \frac{d_1}{\tau_2'^2\tau_1'} + \frac{d_2\tau_2'\tau_1'^2}{\mathcal{V}^4} + \frac{d_3\tau_2'}{\tau_1'\mathcal{V}^2} \ . \tag{5.3.3}$$

Minimizing with respect to τ_1', τ_2' and $\mathcal{V}$, we have the following minima:

$$\tau_1' =(\frac{d_3}{d_2})^{1/3}\mathcal{V}^{2/3}, \quad \tau_2' = (\frac{d_1}{d_3})^{1/3}\mathcal{V}^{2/3},$$
$$\mathcal{V}_{min} = \frac{3\eta\mathcal{W}_0^2 W_{0/-1}\left(\frac{2de^{\frac{13}{3}-\frac{\xi}{2\eta}}}{3\eta\mathcal{W}_0^2}\right)}{2d} \ . \tag{5.3.4}$$

After applying the minimal values of τ_1', τ_2' at the D-terms, we get the expected formula:

$$V_D = \frac{3d}{\mathcal{V}^2}, \quad d = (d_1 d_2 d_3)^{1/3} \ . \tag{5.3.5}$$

Readily, one can see that we haved arrived to the exact same minimal value for the volume modulus $\mathcal{V}_{min}$. Taking into account the derived minima in equation (2.2.13) and the minima derived from the generic form (5.3.4), it readily found that they are related up to a scaling in the uplifting parameter d.

$$\tau_1 = \tau_1' \frac{(d_1 d_2)^{2/9}}{d_3^{4/9}}, \quad \tau_2 = \tau_2' \frac{(d_2 d_3)^{2/9}}{d_1^{4/9}},$$
$$\tau_1 = d^{2/3}\tau_1', \quad \tau_2 = \frac{\tau_2'}{d^{4/3}} \ . \tag{5.3.6}$$

In the last step we have used $d_1 = d^3/(d_2 d_3),\ d_2 = 1,\ d_3 = 1$. Consequently, we can deduce that this equivalence of the vacua does not spoil the analysis with respect to the observable quantities in this model, since the scaling (and the minimal value) with respect to the compactified volume $\mathcal{V}$ is the same.

5.4 Supersymmetric conditions for the flipped $SU(5)$

Consistency with supersymmetry and anomaly cancellation requires that the singlet VEVs are subject to F- and D-flatness conditions. The following hierarchy of scales is assumed $\langle H\rangle \sim \langle H\rangle \sim M_{GUT} \cong M_{str}$. The singlet VEVs are also assumed to be smaller than the string scale M_{str}. Using the identification (3.1.28) and Z_2 monodromy, the Yukawa lagrangian for the singlet fields is $W_{\mathcal{S}} = \lambda_1 \bar{\chi}\bar{\zeta}\psi + \lambda_2 \bar{\psi}\zeta\chi + M_s s^2 + M_\chi \bar{\chi}\chi + M_\psi \bar{\psi}\psi + M_\zeta \bar{\zeta}\zeta\ .Themassscales$M$_\zeta, M_\chi$ etc are assumed to be arbitrary and will be fixed through the flatness conditions. The F-flatness equations are

$$
\begin{aligned}
\frac{\partial W_{\mathcal{S}}}{\partial \chi} &= 0 \Rightarrow \lambda_2 \bar{\psi}\zeta + M_\chi \bar{\chi} = 0 \\
\frac{\partial W_{\mathcal{S}}}{\partial \psi} &= 0 \Rightarrow \lambda_1 \bar{\chi}\bar{\zeta} + M_\psi \bar{\psi} = 0 \\
\frac{\partial W_{\mathcal{S}}}{\partial \zeta} &= 0 \Rightarrow \lambda_2 \bar{\psi}\chi + M_\zeta \bar{\zeta} = 0 \\
\frac{\partial W_{\mathcal{S}}}{\partial \bar{\chi}} &= 0 \Rightarrow \lambda_1 \bar{\zeta}\psi + M_\chi \chi = 0 \\
\frac{\partial W_{\mathcal{S}}}{\partial \bar{\psi}} &= 0 \Rightarrow \lambda_2 \chi\zeta + M_\psi \psi = 0 \\
\frac{\partial W_{\mathcal{S}}}{\partial \bar{\zeta}} &= 0 \Rightarrow \lambda_1 \bar{\chi}\psi + M_\zeta \zeta = 0 \ .
\end{aligned}
\tag{5.4.1}
$$

The D-term flatness constraint needs, also, to be imposed which has the following form:

$$
\begin{gathered}
\sum_{i \neq j} q_i (\theta_{ij}^2 - \theta_{ji}^2) = -c M_{str}^2 \Rightarrow \\
q_\chi(\chi^2 - \bar{\chi}^2) + q_\psi(\psi^2 - \bar{\psi}^2) + q_\zeta(\zeta^2 - \bar{\zeta}^2) = -c M_{str}^2 \ .
\end{gathered}
\tag{5.4.2}
$$

In order to derive a solution to the flatness condition, we need to impose the following conditions

$$
M_\chi = -\lambda_1 M_\psi, \ q_i = 1 \ . \tag{5.4.3}
$$

Then, we obtain

$$
\begin{gathered}
\chi = \frac{M_\zeta \rho}{\lambda_1 \lambda_2 \sigma}, \quad \bar{\chi} = \frac{M_\psi \sigma}{\rho} \\
\psi = -\frac{M_\zeta}{\lambda_1}, \quad \bar{\psi} = \frac{M_\psi \lambda_1}{\lambda_2} \\
\zeta = \frac{M_\psi \sigma}{\rho}, \quad \bar{\zeta} = -\frac{M_\psi \rho}{\sigma} \\
\rho = \left((M_\zeta^2 + c M_{str}^2 \lambda_1^2)\lambda_2^2 - \lambda_1^4 M_\psi^2\right)^{1/2}, \quad \sigma = \left(\lambda_1^2 M_\psi^2 - M_\zeta^2\right)^{1/2} \ .
\end{gathered}
\tag{5.4.4}
$$

Demanding the μ-term (χ singlet) and $\bar{\psi}$ to lay at the TeV scale, we are going to derive some bounds on the parameters above.

$$\frac{\bar{\chi}}{\zeta} = 1,\ \frac{\chi}{\psi\bar{\zeta}} = \frac{1}{M_\psi},\ \bar{\psi} = \frac{M_\psi \lambda_1}{\lambda_2},\ M_\psi \gg 1\ . \tag{5.4.5}$$

So, the corresponding bounds for the parameters are:

$$\frac{\lambda_2}{\lambda_1} \ll \frac{M_\psi}{\bar{\psi} \sim TeV},\ M_\zeta^2 < M_\psi^2 \lambda_1^2,\ c > \frac{M_\psi^2 \lambda_1^4 - M_\zeta^2 \lambda_2^2}{\lambda_1^2 M_{str}^2}\ . \tag{5.4.6}$$

5.5 Additional Models for the flipped $F - SU(5)$

In this paper we have explored a flipped $SU(5)$ model based on a specific choice of fluxes and choosing a particular matter curve to accommodate the Higgs fields. However, there are other choices which may lead to somewhat modified phenomenological implications. Here we present two possible modifications.

We may change the Higgs doublets of the model, discussed in the main text by choosing the fluxes $M_{10}^1 \to M_{10}^2 = 1$, so the new Higgs fields are

$$h_{-t_1-t_4},\quad \bar{h}_{t_1+t_3}, \tag{5.5.1}$$

$$\begin{aligned} W_{matter} =& \lambda_{ij}^u F_i \bar{f}_j \bar{h} \bar{\psi} + \lambda_{ij}^d F_i F_j h \bar{\psi} + \lambda_{ij}^e e_i^c \bar{f}_j h \bar{\psi} + k_i \bar{H} F_i s \bar{\psi} \\ &+ a_{mj} \bar{E}_m^c e_j^c \bar{\psi} + \beta_{mn} \bar{E}_m^c E_n^c \bar{\zeta} + \gamma_{nj} E_n^c \bar{f}_j h \bar{\zeta}, \end{aligned} \tag{5.5.2}$$

$$W_{higgs} = \lambda_\mu \bar{\zeta}(1 + \lambda_\mu' \bar{H} H \bar{\zeta}) \bar{h} h + \lambda_{\bar{H}} \bar{H} \bar{H} \bar{h} \bar{\psi} \bar{\zeta} + \lambda_H H H h (\chi \bar{\zeta} + \bar{\zeta}^2 \psi)\ . \tag{5.5.3}$$

An alternative model with non-zero flux P is the following:

M_1	M_3	M_4	P	P_5	P_7	M_{10}^1	M_{10}^2
3	−1	1	−1	−2	1	1	−1

This leads to the matter field assignment:

$$\begin{aligned}
&10_{t_1}(F_i) : 3\times(Q, d_i^c, \nu_i^c), \quad \bar{5}_{t_1}(\bar{f}) : 2\times(u_i^c, L_i), \quad \bar{5}_{t_3}(\bar{f}') : 1\times(u_3^c, L_3) \\
&1_{t_1} : 4\times(e_i^c), \quad 1_{t_4} : 2\times(E^c), \quad 1_{-t_3} : -3\times(\bar{E}^c), \quad 5_{-2t_1} : 1\times h, \quad \bar{5}_{t_1+t_4} : 1\times\bar{h},
\end{aligned} \tag{5.5.4}$$

The superpotential for the matter fields is

$$\begin{aligned}
W_{matter} =& \lambda_{ij}^u F_i \bar{f}_j \bar{h}\chi + \lambda_{ij}^{\prime u} F_i \bar{f}_j' \bar{h} + \lambda_{ij}^d F_i F_j h + \lambda_{ij}^e e_i^c \bar{f}_j h + \lambda_{ij}^{\prime e} e_i^c \bar{f}_j' h\chi + \\
& + k_i \bar{H} F_i s \bar{\chi} + a_{mj} \bar{E}_m^c e_j^c \bar{\chi} + \beta_{mn} \bar{E}_m^c E_n^c \zeta + \gamma_{nj} E_n^c \bar{f}_j h\psi \\
& + \gamma_{nj}' E_n^c \bar{f}_j' h\chi\psi,
\end{aligned} \tag{5.5.5}$$

and for the Higgs

$$W_{higgs} = \lambda_\mu \psi(1 + \lambda_\mu' \bar{H} H \zeta)\bar{h}h + \lambda_H H H h(\psi^2 + \chi^2\zeta^2) + \lambda_{\bar{H}} \bar{H}\bar{H}\bar{h}\bar{\chi}\zeta \ . \tag{5.5.6}$$

Bibliography

[1] V. Basiouris, "A string loop origin for dark radiation and superheavy dark matter in type IIB compactifications," [arXiv:2411.18737 [hep-ph]].

[2] V. Basiouris, M. Crispim Romão, S. F. King and G. K. Leontaris, "Modular family symmetry in fluxed GUTs," Phys. Rev. D **111** (2025) no.1, 015012 doi:10.1103/PhysRevD.111.015012 [arXiv:2407.06618 [hep-ph]].

[3] V. Basiouris and G. K. Leontaris, "Sterile neutrinos, $0\nu\beta\beta$ decay and the W-boson mass anomaly in a flipped SU(5) from F-theory," Eur. Phys. J. C **82** (2022) no.11, 1041 doi:10.1140/epjc/s10052-022-11005-5 [arXiv:2205.00758 [hep-ph]].

[4] V. Basiouris and G. K. Leontaris, "Remarks on the Effects of Quantum Corrections on Moduli Stabilization and de Sitter Vacua in Type IIB String Theory," Fortsch. Phys. **70** (2022) no.2-3, 2100181 doi:10.1002/prop.202100181 [arXiv:2109.08421 [hep-th]].

[5] V. Basiouris and G. K. Leontaris, "Note on de Sitter vacua from perturbative and non-perturbative dynamics in type IIB/F-theory compactifications," Phys. Lett. B **810** (2020), 135809 doi:10.1016/j.physletb.2020.135809 [arXiv:2007.15423 [hep-th]].

[6] V. Basiouris and D. Chakraborty, "Three-Field String Inflation with Perturbative Corrections: Dynamics and Implications," [arXiv:2502.06958 [hep-th]].

[7] S. L. Glashow, "Partial Symmetries of Weak Interactions," Nucl. Phys. **22** (1961), 579-588 doi:10.1016/0029-5582(61)90469-2

[8] S. Weinberg, "A Model of Leptons," Phys. Rev. Lett. **19** (1967), 1264-1266 doi:10.1103/PhysRevLett.19.1264

[9] A. Salam, "Weak and Electromagnetic Interactions," Conf. Proc. C **680519** (1968), 367-377 doi:10.1142/9789812795915_0034

[10] D. J. Gross and F. Wilczek, "Asymptotically Free Gauge Theories - I," Phys. Rev. D **8** (1973), 3633-3652 doi:10.1103/PhysRevD.8.3633

[11] D. J. Gross and F. Wilczek, "ASYMPTOTICALLY FREE GAUGE THEORIES. 2.," Phys. Rev. D **9** (1974), 980-993 doi:10.1103/PhysRevD.9.980

[12] G. Aad *et al.* [ATLAS], "Observation of a new particle in the search for the Standard Model Higgs boson with the ATLAS detector at the LHC," Phys. Lett. B **716** (2012), 1-29 doi:10.1016/j.physletb.2012.08.020 [arXiv:1207.7214 [hep-ex]].

[13] S. Chatrchyan *et al.* [CMS], "Observation of a New Boson at a Mass of 125 GeV with the CMS Experiment at the LHC," Phys. Lett. B **716** (2012), 30-61 doi:10.1016/j.physletb.2012.08.021 [arXiv:1207.7235 [hep-ex]].

[14] Y. Nambu, "Quasiparticles and Gauge Invariance in the Theory of Superconductivity," Phys. Rev. **117** (1960), 648-663 doi:10.1103/PhysRev.117.648

[15] J. Goldstone, "Field Theories with Superconductor Solutions," Nuovo Cim. **19** (1961), 154-164 doi:10.1007/BF02812722

[16] N. Cabibbo, "Unitary Symmetry and Leptonic Decays," Phys. Rev. Lett. **10** (1963), 531-533 doi:10.1103/PhysRevLett.10.531

[17] M. Kobayashi and T. Maskawa, "CP Violation in the Renormalizable Theory of Weak Interaction," Prog. Theor. Phys. **49** (1973), 652-657 doi:10.1143/PTP.49.652

[18] Y. Fukuda *et al.* [Super-Kamiokande], "Evidence for oscillation of atmospheric neutrinos," Phys. Rev. Lett. **81** (1998), 1562-1567 doi:10.1103/PhysRevLett.81.1562 [arXiv:hep-ex/9807003 [hep-ex]].

[19] N. Aghanim *et al.* [Planck], "Planck 2018 results. VI. Cosmological parameters," Astron. Astrophys. **641** (2020), A6 [erratum: Astron. Astrophys. **652** (2021), C4] doi:10.1051/0004-6361/201833910 [arXiv:1807.06209 [astro-ph.CO]].

[20] S. Weinberg, "The Cosmological Constant Problem," Rev. Mod. Phys. **61** (1989), 1-23 doi:10.1103/RevModPhys.61.1

[21] A. D. Sakharov, "Violation of CP Invariance, C asymmetry, and baryon asymmetry of the universe," Pisma Zh. Eksp. Teor. Fiz. **5** (1967), 32-35 doi:10.1070/PU1991v034n05ABEH002497

[22] M. Yoshimura, “Unified Gauge Theories and the Baryon Number of the Universe,” Phys. Rev. Lett. **41** (1978), 281-284 [erratum: Phys. Rev. Lett. **42** (1979), 746] doi:10.1103/PhysRevLett.41.281

[23] V. A. Kuzmin, V. A. Rubakov and M. E. Shaposhnikov, “On the Anomalous Electroweak Baryon Number Nonconservation in the Early Universe,” Phys. Lett. B **155** (1985), 36 doi:10.1016/0370-2693(85)91028-7

[24] L. Randall and R. Sundrum, “A Large mass hierarchy from a small extra dimension,” Phys. Rev. Lett. **83** (1999), 3370-3373 doi:10.1103/PhysRevLett.83.3370 [arXiv:hep-ph/9905221 [hep-ph]].

[25] L. Randall and R. Sundrum, “An Alternative to compactification,” Phys. Rev. Lett. **83** (1999), 4690-4693 doi:10.1103/PhysRevLett.83.4690 [arXiv:hep-th/9906064 [hep-th]].

[26] S. B. Giddings, S. Kachru and J. Polchinski, “Hierarchies from fluxes in string compactifications,” Phys. Rev. D **66** (2002), 106006 doi:10.1103/PhysRevD.66.106006 [arXiv:hep-th/0105097 [hep-th]].

[27] M. B. Green, J. H. Schwarz and E. Witten, “SUPERSTRING THEORY. VOL. 1: INTRODUCTION,” 1988, ISBN 978-0-521-35752-4

[28] M. B. Green, J. H. Schwarz and E. Witten, “SUPERSTRING THEORY. VOL. 2: LOOP AMPLITUDES, ANOMALIES AND PHENOMENOLOGY,” 1988, ISBN 978-0-521-35753-1

[29] K. Becker, M. Becker and J. H. Schwarz, “String theory and M-theory: A modern introduction,” Cambridge University Press, 2006, ISBN 978-0-511-25486-4, 978-0-521-86069-7, 978-0-511-81608-6 doi:10.1017/CBO9780511816086

[30] B. R. Greene and M. R. Plesser, “Duality in Calabi-Yau Moduli Space,” Nucl. Phys. B **338** (1990), 15-37 doi:10.1016/0550-3213(90)90622-K

[31] P. Candelas and X. de la Ossa, “Moduli Space of Calabi-Yau Manifolds,” Nucl. Phys. B **355** (1991), 455-481 doi:10.1016/0550-3213(91)90122-E

[32] C. Vafa, “Evidence for F theory,” Nucl. Phys. B **469** (1996), 403-418 doi:10.1016/0550-3213(96)00172-1 [arXiv:hep-th/9602022 [hep-th]].

[33] A. Sen, “F theory and orientifolds,” Nucl. Phys. B **475** (1996), 562-578 doi:10.1016/0550-3213(96)00347-1 [arXiv:hep-th/9605150 [hep-th]].

[34] On compact Analytic surfaces K. Kodaira Annals Math. 77 (1963) 563

[35] M. Bershadsky, K. A. Intriligator, S. Kachru, D. R. Morrison, V. Sadov and C. Vafa, "Geometric singularities and enhanced gauge symmetries," Nucl. Phys. B **481** (1996), 215-252 doi:10.1016/S0550-3213(96)90131-5 [arXiv:hep-th/9605200 [hep-th]].

[36] D. R. Morrison and W. Taylor, "Matter and singularities," JHEP **01** (2012), 022 doi:10.1007/JHEP01(2012)022 [arXiv:1106.3563 [hep-th]].

[37] R. Blumenhagen, T. W. Grimm, B. Jurke and T. Weigand, "Global F-theory GUTs," Nucl. Phys. B **829** (2010), 325-369 doi:10.1016/j.nuclphysb.2009.12.013 [arXiv:0908.1784 [hep-th]].

[38] M. Esole and S. T. Yau, "Small resolutions of SU(5)-models in F-theory," Adv. Theor. Math. Phys. **17** (2013) no.6, 1195-1253 doi:10.4310/ATMP.2013.v17.n6.a1 [arXiv:1107.0733 [hep-th]].

[39] Algorithm for Determining the Type of a Singular Fiber in an Elliptic Pencil J. Tate

[40] J. J. Heckman and C. Vafa, "Flavor Hierarchy From F-theory," Nucl. Phys. B **837** (2010), 137-151 doi:10.1016/j.nuclphysb.2010.05.009 [arXiv:0811.2417 [hep-th]].

[41] A. Font and L. E. Ibanez, "Yukawa Structure from U(1) Fluxes in F-theory Grand Unification," JHEP **02** (2009), 016 doi:10.1088/1126-6708/2009/02/016 [arXiv:0811.2157 [hep-th]].

[42] S. Cecotti, M. C. N. Cheng, J. J. Heckman and C. Vafa, "Yukawa Couplings in F-theory and Non-Commutative Geometry," [arXiv:0910.0477 [hep-th]].

[43] H. Hayashi, T. Kawano, R. Tatar and T. Watari, "Codimension-3 Singularities and Yukawa Couplings in F-theory," Nucl. Phys. B **823** (2009), 47-115 doi:10.1016/j.nuclphysb.2009.07.021 [arXiv:0901.4941 [hep-th]].

[44] H. Hayashi, T. Kawano, Y. Tsuchiya and T. Watari, "Flavor Structure in F-theory Compactifications," JHEP **08** (2010), 036 doi:10.1007/JHEP08(2010)036 [arXiv:0910.2762 [hep-th]].

[45] A. Font and L. E. Ibanez, "Matter wave functions and Yukawa couplings in F-theory Grand Unification," JHEP **09** (2009), 036 doi:10.1088/1126-6708/2009/09/036 [arXiv:0907.4895 [hep-th]].

[46] S. Cecotti, C. Cordova, J. J. Heckman and C. Vafa, "T-Branes and Monodromy," JHEP **07** (2011), 030 doi:10.1007/JHEP07(2011)030 [arXiv:1010.5780 [hep-th]].

[47] G. K. Leontaris and G. G. Ross, "Yukawa couplings and fermion mass structure in F-theory GUTs," JHEP **02** (2011), 108 doi:10.1007/JHEP02(2011)108 [arXiv:1009.6000 [hep-th]].

[48] L. Aparicio, A. Font, L. E. Ibanez and F. Marchesano, "Flux and Instanton Effects in Local F-theory Models and Hierarchical Fermion Masses," JHEP **08** (2011), 152 doi:10.1007/JHEP08(2011)152 [arXiv:1104.2609 [hep-th]].

[49] P. G. Camara, E. Dudas and E. Palti, "Massive wavefunctions, proton decay and FCNCs in local F-theory GUTs," JHEP **12** (2011), 112 doi:10.1007/JHEP12(2011)112 [arXiv:1110.2206 [hep-th]].

[50] A. Karozas, S. F. King, G. K. Leontaris and A. Meadowcroft, "Discrete Family Symmetry from F-Theory GUTs," JHEP **09** (2014), 107 doi:10.1007/JHEP09(2014)107 [arXiv:1406.6290 [hep-ph]].

[51] A. Karozas, S. F. King, G. K. Leontaris and A. K. Meadowcroft, "Phenomenological implications of a minimal F-theory GUT with discrete symmetry," JHEP **10** (2015), 041 doi:10.1007/JHEP10(2015)041 [arXiv:1505.00937 [hep-ph]].

[52] M. Crispim Romão, A. Karozas, S. F. King, G. K. Leontaris and A. K. Meadowcroft, "MSSM from F-theory SU(5) with Klein Monodromy," Phys. Rev. D **93** (2016) no.12, 126007 doi:10.1103/PhysRevD.93.126007 [arXiv:1512.09148 [hep-ph]].

[53] M. Crispim Romão, A. Karozas, S. F. King, G. K. Leontaris and A. K. Meadowcroft, "R-Parity violation in F-Theory," JHEP **11** (2016), 081 doi:10.1007/JHEP11(2016)081 [arXiv:1608.04746 [hep-ph]].

[54] R. Donagi and M. Wijnholt, "Higgs Bundles and UV Completion in F-Theory," Commun. Math. Phys. **326** (2014), 287-327 doi:10.1007/s00220-013-1878-8 [arXiv:0904.1218 [hep-th]].

[55] J. J. Heckman, A. Tavanfar and C. Vafa, "The Point of E(8) in F-theory GUTs," JHEP **08** (2010), 040 doi:10.1007/JHEP08(2010)040 [arXiv:0906.0581 [hep-th]].

[56] E. Dudas and E. Palti, "On hypercharge flux and exotics in F-theory GUTs," JHEP **09** (2010), 013 doi:10.1007/JHEP09(2010)013 [arXiv:1007.1297 [hep-ph]].

[57] J. Marsano and S. Schafer-Nameki, "Yukawas, G-flux, and Spectral Covers from Resolved Calabi-Yau's," JHEP **11** (2011), 098 doi:10.1007/JHEP11(2011)098 [arXiv:1108.1794 [hep-th]].

[58] J. M. Maldacena and C. Nunez, "Supergravity description of field theories on curved manifolds and a no go theorem," Int. J. Mod. Phys. A **16** (2001), 822-855 doi:10.1142/S0217751X01003937 [arXiv:hep-th/0007018 [hep-th]].

[59] B. de Wit, D. J. Smit and N. D. Hari Dass, "Residual Supersymmetry of Compactified D=10 Supergravity," Nucl. Phys. B **283** (1987), 165 doi:10.1016/0550-3213(87)90267-7

[60] S. B. Giddings, S. Kachru and J. Polchinski, "Hierarchies from fluxes in string compactifications," Phys. Rev. D **66** (2002), 106006 doi:10.1103/PhysRevD.66.106006 [arXiv:hep-th/0105097 [hep-th]].

[61] S. Kachru, R. Kallosh, A. D. Linde and S. P. Trivedi, "De Sitter vacua in string theory," Phys. Rev. D **68** (2003), 046005 doi:10.1103/PhysRevD.68.046005 [arXiv:hep-th/0301240 [hep-th]].

[62] V. Balasubramanian, P. Berglund, J. P. Conlon and F. Quevedo, "Systematics of moduli stabilisation in Calabi-Yau flux compactifications," JHEP **03** (2005), 007 doi:10.1088/1126-6708/2005/03/007 [arXiv:hep-th/0502058 [hep-th]].

[63] S. R. Coleman and F. De Luccia, "Gravitational Effects on and of Vacuum Decay," Phys. Rev. D **21** (1980), 3305 doi:10.1103/PhysRevD.21.3305

[64] K. Becker, M. Becker, M. Haack and J. Louis, "Supersymmetry breaking and alpha-prime corrections to flux induced potentials," JHEP **06** (2002), 060 doi:10.1088/1126-6708/2002/06/060 [arXiv:hep-th/0204254 [hep-th]].

[65] S. Weinberg, "Baryon and Lepton Nonconserving Processes," Phys. Rev. Lett. **43** (1979), 1566-1570 doi:10.1103/PhysRevLett.43.1566

[66] R. N. Mohapatra and G. Senjanovic, "Neutrino Mass and Spontaneous Parity Nonconservation," Phys. Rev. Lett. **44** (1980), 912 doi:10.1103/PhysRevLett.44.912

[67] R. N. Mohapatra and G. Senjanovic, "Neutrino Masses and Mixings in Gauge Models with Spontaneous Parity Violation," Phys. Rev. D **23** (1981), 165 doi:10.1103/PhysRevD.23.165

[68] R. Foot, H. Lew, X. G. He and G. C. Joshi, "Seesaw Neutrino Masses Induced by a Triplet of Leptons," Z. Phys. C **44** (1989), 441 doi:10.1007/BF01415558

[69] G. J. Ding and S. F. King, "Neutrino mass and mixing with modular symmetry," Rept. Prog. Phys. **87** (2024) no.8, 084201 doi:10.1088/1361-6633/ad52a3 [arXiv:2311.09282 [hep-ph]].

[70] S. F. King, A. Merle and A. J. Stuart, "The Power of Neutrino Mass Sum Rules for Neutrinoless Double Beta Decay Experiments," JHEP **12** (2013), 005 doi:10.1007/JHEP12(2013)005 [arXiv:1307.2901 [hep-ph]].

[71] S. F. King and C. Luhn, "Neutrino Mass and Mixing with Discrete Symmetry," Rept. Prog. Phys. **76** (2013), 056201 doi:10.1088/0034-4885/76/5/056201 [arXiv:1301.1340 [hep-ph]].

[72] S. F. King, "Unified Models of Neutrinos, Flavour and CP Violation," Prog. Part. Nucl. Phys. **94** (2017), 217-256 doi:10.1016/j.ppnp.2017.01.003 [arXiv:1701.04413 [hep-ph]].

[73] F. Feruglio, "Are neutrino masses modular forms?," doi:10.1142/9789813238053_0012 [arXiv:1706.08749 [hep-ph]].

[74] S. Ferrara, D. Lust, A. D. Shapere and S. Theisen, "Modular Invariance in Supersymmetric Field Theories," Phys. Lett. B **225** (1989), 363 doi:10.1016/0370-2693(89)90583-2

[75] S. Ferrara, D. Lust and S. Theisen, "Target Space Modular Invariance and Low-Energy Couplings in Orbifold Compactifications," Phys. Lett. B **233** (1989), 147-152 doi:10.1016/0370-2693(89)90631-X

[76] M. C. Chen, S. Ramos-Sánchez and M. Ratz, "A note on the predictions of models with modular flavor symmetries," Phys. Lett. B **801** (2020), 135153 doi:10.1016/j.physletb.2019.135153 [arXiv:1909.06910 [hep-ph]].

[77] H. P. Nilles, S. Ramos-Sánchez and P. K. S. Vaudrevange, "Eclectic Flavor Groups," JHEP **02** (2020), 045 doi:10.1007/JHEP02(2020)045 [arXiv:2001.01736 [hep-ph]].

[78] H. P. Nilles, S. Ramos-Sanchez and P. K. S. Vaudrevange, "Lessons from eclectic flavor symmetries," Nucl. Phys. B **957** (2020), 115098 doi:10.1016/j.nuclphysb.2020.115098 [arXiv:2004.05200 [hep-ph]].

[79] H. Ohki, S. Uemura and R. Watanabe, "Modular flavor symmetry on a magnetized torus," Phys. Rev. D **102** (2020) no.8, 085008 doi:10.1103/PhysRevD.102.085008 [arXiv:2003.04174 [hep-th]].

[80] C. Vafa, "The String landscape and the swampland," [arXiv:hep-th/0509212 [hep-th]].

[81] G. Obied, H. Ooguri, L. Spodyneiko and C. Vafa, "De Sitter Space and the Swampland," [arXiv:1806.08362 [hep-th]].

[82] P. Agrawal, G. Obied, P. J. Steinhardt and C. Vafa, "On the Cosmological Implications of the String Swampland," Phys. Lett. B **784** (2018), 271-276 doi:10.1016/j.physletb.2018.07.040 [arXiv:1806.09718 [hep-th]].

[83] E. Palti, "The Swampland: Introduction and Review," Fortsch. Phys. **67** (2019) no.6, 1900037 doi:10.1002/prop.201900037 [arXiv:1903.06239 [hep-th]].

[84] U. H. Danielsson and T. Van Riet, "What if string theory has no de Sitter vacua?," Int. J. Mod. Phys. D **27** (2018) no.12, 1830007 doi:10.1142/S0218271818300070 [arXiv:1804.01120 [hep-th]].

[85] S. Kachru, R. Kallosh, A. D. Linde and S. P. Trivedi, "De Sitter vacua in string theory," Phys. Rev. D **68** (2003), 046005 doi:10.1103/PhysRevD.68.046005 [arXiv:hep-th/0301240 [hep-th]].

[86] J. P. Conlon, F. Quevedo and K. Suruliz, "Large-volume flux compactifications: Moduli spectrum and D3/D7 soft supersymmetry breaking," JHEP **08** (2005), 007 doi:10.1088/1126-6708/2005/08/007 [arXiv:hep-th/0505076 [hep-th]].

[87] J. Polchinski, "Brane/antibrane dynamics and KKLT stability," [arXiv:1509.05710 [hep-th]].

[88] S. AbdusSalam, S. Abel, M. Cicoli, F. Quevedo and P. Shukla, "A systematic approach to Kähler moduli stabilisation," JHEP **08** (2020) no.08, 047 doi:10.1007/JHEP08(2020)047 [arXiv:2005.11329 [hep-th]].

[89] H. Abe, T. Higaki and T. Kobayashi, "KKLT type models with moduli-mixing superpotential," Phys. Rev. D **73** (2006), 046005 doi:10.1103/PhysRevD.73.046005 [arXiv:hep-th/0511160 [hep-th]].

[90] S. L. Parameswaran and A. Westphal, "de Sitter string vacua from perturbative Kahler corrections and consistent D-terms," JHEP **10** (2006), 079 doi:10.1088/1126-6708/2006/10/079 [arXiv:hep-th/0602253 [hep-th]].

[91] M. Demirtas, M. Kim, L. Mcallister and J. Moritz, "Vacua with Small Flux Superpotential," Phys. Rev. Lett. **124** (2020) no.21, 211603 doi:10.1103/PhysRevLett.124.211603 [arXiv:1912.10047 [hep-th]].

[92] F. Carta, J. Moritz and A. Westphal, "Gaugino condensation and small uplifts in KKLT," JHEP **08** (2019), 141 doi:10.1007/JHEP08(2019)141 [arXiv:1902.01412 [hep-th]].

[93] C. P. Burgess, M. Cicoli, D. Ciupke, S. Krippendorf and F. Quevedo, "UV Shadows in EFTs: Accidental Symmetries, Robustness and No-Scale Supergravity," Fortsch. Phys. **68** (2020) no.10, 2000076 doi:10.1002/prop.202000076 [arXiv:2006.06694 [hep-th]].

[94] R. Blumenhagen, B. Kors, D. Lust and S. Stieberger, "Four-dimensional String Compactifications with D-Branes, Orientifolds and Fluxes," Phys. Rept. **445** (2007), 1-193 doi:10.1016/j.physrep.2007.04.003 [arXiv:hep-th/0610327 [hep-th]].

[95] I. Antoniadis, Y. Chen and G. K. Leontaris, "Logarithmic loop corrections, moduli stabilisation and de Sitter vacua in string theory," JHEP **01** (2020), 149 doi:10.1007/JHEP01(2020)149 [arXiv:1909.10525 [hep-th]].

[96] I. Antoniadis and C. Bachas, "Branes and the gauge hierarchy," Phys. Lett. B **450** (1999), 83-91 doi:10.1016/S0370-2693(99)00102-1 [arXiv:hep-th/9812093 [hep-th]].

[97] W. D. Goldberger and M. B. Wise, "Renormalization group flows for brane couplings," Phys. Rev. D **65** (2002), 025011 doi:10.1103/PhysRevD.65.025011 [arXiv:hep-th/0104170 [hep-th]].

[98] L. E. Ibanez, R. Rabadan and A. M. Uranga, "Sigma model anomalies in compact D = 4, N=1 type IIB orientifolds and Fayet-Iliopoulos terms," Nucl. Phys. B **576** (2000), 285-312 doi:10.1016/S0550-3213(00)00059-6 [arXiv:hep-th/9905098 [hep-th]].

[99] M. Bianchi, A. Collinucci and L. Martucci, "Magnetized E3-brane instantons in F-theory," JHEP **12** (2011), 045 doi:10.1007/JHEP12(2011)045 [arXiv:1107.3732 [hep-th]].

[100] M. J. Duff, R. Minasian and E. Witten, "Evidence for heterotic / heterotic duality," Nucl. Phys. B **465** (1996), 413-438 doi:10.1016/0550-3213(96)00059-4 [arXiv:hep-th/9601036 [hep-th]].

[101] I. Antoniadis, Y. Chen and G. K. Leontaris, "Inflation from the internal volume in type IIB/F-theory compactification," Int. J. Mod. Phys. A **34** (2019) no.08, 1950042 doi:10.1142/S0217751X19500428 [arXiv:1810.05060 [hep-th]].

[102] I. Antoniadis, O. Lacombe and G. K. Leontaris, "Hybrid inflation and waterfall field in string theory from D7-branes," JHEP **01** (2022), 011 doi:10.1007/JHEP01(2022)011 [arXiv:2109.03243 [hep-th]].

[103] S. Gukov, C. Vafa and E. Witten, "CFT's from Calabi-Yau four folds," Nucl. Phys. B **584** (2000), 69-108 [erratum: Nucl. Phys. B **608** (2001), 477-478] doi:10.1016/S0550-3213(00)00373-4 [arXiv:hep-th/9906070 [hep-th]].

[104] E. Witten, "Nonperturbative superpotentials in string theory," Nucl. Phys. B **474** (1996), 343-360 doi:10.1016/0550-3213(96)00283-0 [arXiv:hep-th/9604030 [hep-th]].

[105] E. Kiritsis and B. Pioline, "On R**4 threshold corrections in IIb string theory and (p, q) string instantons," Nucl. Phys. B **508** (1997), 509-534 doi:10.1016/S0550-3213(97)00645-7 [arXiv:hep-th/9707018 [hep-th]].

[106] M. B. Green and P. Vanhove, "D instantons, strings and M theory," Phys. Lett. B **408** (1997), 122-134 doi:10.1016/S0370-2693(97)00785-5 [arXiv:hep-th/9704145 [hep-th]].

[107] J. G. Russo and A. A. Tseytlin, "One loop four graviton amplitude in eleven-dimensional supergravity," Nucl. Phys. B **508** (1997), 245-259 doi:10.1016/S0550-3213(97)00631-7 [arXiv:hep-th/9707134 [hep-th]].

[108] I. Antoniadis, S. Ferrara, R. Minasian and K. S. Narain, "R**4 couplings in M and type II theories on Calabi-Yau spaces," Nucl. Phys. B **507** (1997), 571-588 doi:10.1016/S0550-3213(97)00572-5 [arXiv:hep-th/9707013 [hep-th]].

[109] I. Antoniadis, R. Minasian and P. Vanhove, "Noncompact Calabi-Yau manifolds and localized gravity," Nucl. Phys. B **648** (2003), 69-93 doi:10.1016/S0550-3213(02)00974-4 [arXiv:hep-th/0209030 [hep-th]].

[110] I. Antoniadis, R. Minasian, S. Theisen and P. Vanhove, "String loop corrections to the universal hypermultiplet," Class. Quant. Grav. **20** (2003), 5079-5102 doi:10.1088/0264-9381/20/23/009 [arXiv:hep-th/0307268 [hep-th]].

[111] M. Berg, M. Haack and B. Kors, "String loop corrections to Kahler potentials in orientifolds," JHEP **11** (2005), 030 doi:10.1088/1126-6708/2005/11/030 [arXiv:hep-th/0508043 [hep-th]].

[112] M. Haack and J. U. Kang, "Field redefinitions and Kähler potential in string theory at 1-loop," JHEP **08** (2018), 019 doi:10.1007/JHEP08(2018)019 [arXiv:1805.00817 [hep-th]].

[113] I. Antoniadis, Y. Chen and G. K. Leontaris, "Perturbative moduli stabilisation in type IIB/F-theory framework," Eur. Phys. J. C **78** (2018) no.9, 766 doi:10.1140/epjc/s10052-018-6248-4 [arXiv:1803.08941 [hep-th]].

[114] D. Baumann, A. Dymarsky, S. Kachru, I. R. Klebanov and L. McAllister, "D3-brane Potentials from Fluxes in AdS/CFT," JHEP **06** (2010), 072 doi:10.1007/JHEP06(2010)072 [arXiv:1001.5028 [hep-th]].

[115] J. J. Blanco-Pillado, C. P. Burgess, J. M. Cline, C. Escoda, M. Gomez-Reino, R. Kallosh, A. D. Linde and F. Quevedo, "Racetrack inflation," JHEP **11** (2004), 063 doi:10.1088/1126-6708/2004/11/063 [arXiv:hep-th/0406230 [hep-th]].

[116] A. D. Linde, "Inflationary Cosmology," Lect. Notes Phys. **738** (2008), 1-54 doi:10.1007/978-3-540-74353-8_1 [arXiv:0705.0164 [hep-th]].

[117] R. Álvarez-García, R. Blumenhagen, M. Brinkmann and L. Schlechter, "Small Flux Superpotentials for Type IIB Flux Vacua Close to a Conifold," Fortsch. Phys. **68** (2020), 2000088 doi:10.1002/prop.202000088 [arXiv:2009.03325 [hep-th]].

[118] I. Broeckel, M. Cicoli, A. Maharana, K. Singh and K. Sinha, "On the Search for Low W0," Fortsch. Phys. **70** (2022) no.6, 2200002 doi:10.1002/prop.202200002 [arXiv:2108.04266 [hep-th]].

[119] Y. Honma and H. Otsuka, "Small flux superpotential in F-theory compactifications," Phys. Rev. D **103** (2021) no.12, 126022 doi:10.1103/PhysRevD.103.126022 [arXiv:2103.03003 [hep-th]].

[120] F. Denef and M. R. Douglas, "Distributions of flux vacua," JHEP **05** (2004), 072 doi:10.1088/1126-6708/2004/05/072 [arXiv:hep-th/0404116 [hep-th]].

[121] K. Choi, A. Falkowski, H. P. Nilles, M. Olechowski and S. Pokorski, "Stability of flux compactifications and the pattern of supersymmetry breaking," JHEP **11** (2004), 076 doi:10.1088/1126-6708/2004/11/076 [arXiv:hep-th/0411066 [hep-th]].

[122] M. Cicoli, F. Muia and P. Shukla, "Global Embedding of Fibre Inflation Models," JHEP **11** (2016), 182 doi:10.1007/JHEP11(2016)182 [arXiv:1611.04612 [hep-th]].

[123] M. Cicoli, D. Ciupke, V. A. Diaz, V. Guidetti, F. Muia and P. Shukla, "Chiral Global Embedding of Fibre Inflation Models," JHEP **11** (2017), 207 doi:10.1007/JHEP11(2017)207 [arXiv:1709.01518 [hep-th]].

[124] M. Cicoli, S. Krippendorf, C. Mayrhofer, F. Quevedo and R. Valandro, "D-Branes at del Pezzo Singularities: Global Embedding and Moduli Stabilisation," JHEP **09** (2012), 019 doi:10.1007/JHEP09(2012)019 [arXiv:1206.5237 [hep-th]].

[125] G. K. Leontaris and P. Shukla, "Stabilising all Kähler moduli in perturbative LVS," JHEP **07** (2022), 047 doi:10.1007/JHEP07(2022)047 [arXiv:2203.03362 [hep-th]].

[126] J. P. Conlon, "Moduli Stabilisation and Applications in IIB String Theory," Fortsch. Phys. **55** (2007), 287-422 doi:10.1002/prop.200610334 [arXiv:hep-th/0611039 [hep-th]].

[127] M. Cicoli, C. P. Burgess and F. Quevedo, "Fibre Inflation: Observable Gravity Waves from IIB String Compactifications," JCAP **03** (2009), 013 doi:10.1088/1475-7516/2009/03/013 [arXiv:0808.0691 [hep-th]].

[128] C. P. Burgess, R. Kallosh and F. Quevedo, "De Sitter string vacua from supersymmetric D terms," JHEP **10** (2003), 056 doi:10.1088/1126-6708/2003/10/056 [arXiv:hep-th/0309187 [hep-th]].

[129] M. Haack, D. Krefl, D. Lust, A. Van Proeyen and M. Zagermann, "Gaugino Condensates and D-terms from D7-branes," JHEP **01** (2007), 078 doi:10.1088/1126-6708/2007/01/078 [arXiv:hep-th/0609211 [hep-th]].

[130] H. Ooguri and C. Vafa, "On the Geometry of the String Landscape and the Swampland," Nucl. Phys. B **766** (2007), 21-33 doi:10.1016/j.nuclphysb.2006.10.033 [arXiv:hep-th/0605264 [hep-th]].

[131] H. Ooguri and C. Vafa, "Non-supersymmetric AdS and the Swampland," Adv. Theor. Math. Phys. **21** (2017), 1787-1801 doi:10.4310/ATMP.2017.v21.n7.a8 [arXiv:1610.01533 [hep-th]].

[132] H. Ooguri, E. Palti, G. Shiu and C. Vafa, "Distance and de Sitter Conjectures on the Swampland," Phys. Lett. B **788** (2019), 180-184 doi:10.1016/j.physletb.2018.11.018 [arXiv:1810.05506 [hep-th]].

[133] F. Denef, A. Hebecker and T. Wrase, "de Sitter swampland conjecture and the Higgs potential," Phys. Rev. D **98** (2018) no.8, 086004 doi:10.1103/PhysRevD.98.086004 [arXiv:1807.06581 [hep-th]].

[134] G. A. Mitchell and R. Brandenberger, "Note on shape moduli stabilization, string gas cosmology and the swampland criteria," Eur. Phys. J. C **81** (2021) no.1, 39 doi:10.1140/epjc/s10052-021-08843-0 [arXiv:2008.13251 [hep-th]].

[135] J. P. Conlon and F. Quevedo, "On the explicit construction and statistics of Calabi-Yau flux vacua," JHEP **10** (2004), 039 doi:10.1088/1126-6708/2004/10/039 [arXiv:hep-th/0409215 [hep-th]].

[136] V. Balasubramanian, P. Berglund, J. P. Conlon and F. Quevedo, "Systematics of moduli stabilisation in Calabi-Yau flux compactifications," JHEP **03** (2005), 007 doi:10.1088/1126-6708/2005/03/007 [arXiv:hep-th/0502058 [hep-th]].

[137] M. Cicoli, J. P. Conlon and F. Quevedo, "Systematics of String Loop Corrections in Type IIB Calabi-Yau Flux Compactifications," JHEP **01** (2008), 052 doi:10.1088/1126-6708/2008/01/052 [arXiv:0708.1873 [hep-th]].

[138] R. J. Danos, A. R. Frey and R. H. Brandenberger, "Stabilizing moduli with thermal matter and nonperturbative effects," Phys. Rev. D **77** (2008), 126009 doi:10.1103/PhysRevD.77.126009 [arXiv:0802.1557 [hep-th]].

[139] R. Brandenberger, Y. K. E. Cheung and S. Watson, "Moduli stabilization with string gases and fluxes," JHEP **05** (2006), 025 doi:10.1088/1126-6708/2006/05/025 [arXiv:hep-th/0501032 [hep-th]].

[140] I. Broeckel, M. Cicoli, A. Maharana, K. Singh and K. Sinha, "Moduli Stabilisation and the Statistics of SUSY Breaking in the Landscape," JHEP **10** (2020), 015 doi:10.1007/JHEP09(2021)019 [arXiv:2007.04327 [hep-th]].

[141] G. K. Leontaris and P. Shukla, "Stabilising all Kähler moduli in perturbative LVS," JHEP **07** (2022), 047 doi:10.1007/JHEP07(2022)047 [arXiv:2203.03362 [hep-th]].

[142] V. Basiouris and G. K. Leontaris, "Note on de Sitter vacua from perturbative and non-perturbative dynamics in type IIB/F-theory compactifications," Phys. Lett. B **810** (2020), 135809 doi:10.1016/j.physletb.2020.135809 [arXiv:2007.15423 [hep-th]].

[143] V. Basiouris and G. K. Leontaris, "Remarks on the Effects of Quantum Corrections on Moduli Stabilization and de Sitter Vacua in Type IIB String Theory," Fortsch. Phys. **70** (2022) no.2-3, 2100181 doi:10.1002/prop.202100181 [arXiv:2109.08421 [hep-th]].

[144] L. McAllister and F. Quevedo, "Moduli Stabilization in String Theory," [arXiv:2310.20559 [hep-th]].

[145] M. Cicoli, J. P. Conlon, A. Maharana, S. Parameswaran, F. Quevedo and I. Zavala, "String cosmology: From the early universe to today," Phys. Rept. **1059** (2024), 1-155 doi:10.1016/j.physrep.2024.01.002 [arXiv:2303.04819 [hep-th]].

[146] A. Hebecker, "Naturalness, String Landscape and Multiverse: A Modern Introduction with Exercises," Lect. Notes Phys. **979** (2021), 1-313 2021, ISBN 978-3-030-65150-3, 978-3-030-65151-0 doi:10.1007/978-3-030-65151-0 [arXiv:2008.10625 [hep-th]].

[147] C. Damian and O. Loaiza-Brito, "More stable de Sitter vacua from S-dual nongeometric fluxes," Phys. Rev. D **88** (2013) no.4, 046008 doi:10.1103/PhysRevD.88.046008 [arXiv:1304.0792 [hep-th]].

[148] I. Antoniadis, C. Bachas, C. Fabre, H. Partouche and T. R. Taylor, "Aspects of type I - type II - heterotic triality in four-dimensions," Nucl. Phys. B **489** (1997), 160-178 doi:10.1016/S0550-3213(96)00514-7 [arXiv:hep-th/9608012 [hep-th]].

[149] C. P. Burgess, R. Kallosh and F. Quevedo, "De Sitter string vacua from supersymmetric D terms," JHEP **10** (2003), 056 doi:10.1088/1126-6708/2003/10/056 [arXiv:hep-th/0309187 [hep-th]].

[150] G. F. Giudice and A. Masiero, "A Natural Solution to the mu Problem in Supergravity Theories," Phys. Lett. B **206** (1988), 480-484 doi:10.1016/0370-2693(88)91613-9

[151] M. Cicoli, A. Hebecker, J. Jaeckel and M. Wittner, "Axions in string theory — slaying the Hydra of dark radiation," JHEP **09** (2022), 198 doi:10.1007/JHEP09(2022)198 [arXiv:2203.08833 [hep-th]].

[152] M. Cicoli, K. Sinha and R. Wiley Deal, "The dark universe after reheating in string inflation," JHEP **12** (2022), 068 doi:10.1007/JHEP12(2022)068 [arXiv:2208.01017 [hep-th]].

[153] M. Cicoli, J. P. Conlon and F. Quevedo, "Dark radiation in LARGE volume models," Phys. Rev. D **87** (2013) no.4, 043520 doi:10.1103/PhysRevD.87.043520 [arXiv:1208.3562 [hep-ph]].

[154] M. Cicoli, V. Guidetti, N. Righi and A. Westphal, "Fuzzy Dark Matter candidates from string theory," JHEP **05** (2022), 107 doi:10.1007/JHEP05(2022)107 [arXiv:2110.02964 [hep-th]].

[155] E. Dimastrogiovanni, M. Fasiello, J. M. Leedom, M. Putti and A. Westphal, "Gravitational axiverse spectroscopy: seeing the forest for the axions," JHEP **08** (2024), 072 doi:10.1007/JHEP08(2024)072 [arXiv:2312.13431 [hep-th]].

[156] R. Allahverdi, B. Dutta and K. Sinha, "Cladogenesis: Baryon-Dark Matter Coincidence from Branchings in Moduli Decay," Phys. Rev. D **83** (2011), 083502 doi:10.1103/PhysRevD.83.083502 [arXiv:1011.1286 [hep-ph]].

[157] R. Allahverdi, B. Dutta and K. Sinha, "Baryogenesis and Late-Decaying Moduli," Phys. Rev. D **82** (2010), 035004 doi:10.1103/PhysRevD.82.035004 [arXiv:1005.2804 [hep-ph]].

[158] M. Cicoli, M. Goodsell, J. Jaeckel and A. Ringwald, "Testing String Vacua in the Lab: From a Hidden CMB to Dark Forces in Flux Compactifications," JHEP **07** (2011), 114 doi:10.1007/JHEP07(2011)114 [arXiv:1103.3705 [hep-th]].

[159] S. Bera, D. Chakraborty, G. K. Leontaris and P. Shukla, “Inflating in perturbative LVS: global embedding and robustness,” JCAP **09** (2024), 004 doi:10.1088/1475-7516/2024/09/004 [arXiv:2405.06738 [hep-th]].

[160] W. Ahmed, A. Karozas, G. K. Leontaris and I. Tavellaris, “Hybrid inflation, reheating and dark radiation in a IIB perturbative moduli stabilization scenario,” JHEP **07** (2024), 282 doi:10.1007/JHEP07(2024)282 [arXiv:2301.00329 [hep-ph]].

[161] A. Achucarro, B. de Carlos, J. A. Casas and L. Doplicher, “De Sitter vacua from uplifting D-terms in effective supergravities from realistic strings,” JHEP **06** (2006), 014 doi:10.1088/1126-6708/2006/06/014 [arXiv:hep-th/0601190 [hep-th]].

[162] M. Haack, D. Krefl, D. Lust, A. Van Proeyen and M. Zagermann, “Gaugino Condensates and D-terms from D7-branes,” JHEP **01** (2007), 078 doi:10.1088/1126-6708/2007/01/078 [arXiv:hep-th/0609211 [hep-th]].

[163] K. Choi, A. Falkowski, H. P. Nilles and M. Olechowski, “Soft supersymmetry breaking in KKLT flux compactification,” Nucl. Phys. B **718** (2005), 113-133 doi:10.1016/j.nuclphysb.2005.04.032 [arXiv:hep-th/0503216 [hep-th]].

[164] S. P. de Alwis, “Effective potentials for light moduli,” Phys. Lett. B **626** (2005), 223-229 doi:10.1016/j.physletb.2005.08.096 [arXiv:hep-th/0506266 [hep-th]].

[165] M. Dine, N. Seiberg and E. Witten, “Fayet-Iliopoulos Terms in String Theory,” Nucl. Phys. B **289** (1987), 589-598 doi:10.1016/0550-3213(87)90395-6

[166] R. Brandenberger, D. A. Easson and A. Mazumdar, “Inflation and brane gases,” Phys. Rev. D **69** (2004), 083502 doi:10.1103/PhysRevD.69.083502 [arXiv:hep-th/0307043 [hep-th]].

[167] A. Let, A. Sarkar, C. Sarkar and B. Ghosh, “Single-field slow-roll effective potential from Kähler moduli stabilizations in type-IIB/F-theory,” EPL **139** (2022) no.5, 59002 doi:10.1209/0295-5075/ac8952 [arXiv:2208.06606 [hep-th]].

[168] M. Brinkmann, M. Cicoli and P. Zito, “Starobinsky inflation from string theory?,” JHEP **09** (2023), 038 doi:10.1007/JHEP09(2023)038 [arXiv:2305.05703 [hep-th]].

[169] J. Holland, I. Zavala and G. Tasinato, “On chromonatural inflation in string theory,” JCAP **12** (2020), 026 doi:10.1088/1475-7516/2020/12/026 [arXiv:2009.00653 [hep-th]].

[170] B. Fields and S. Sarkar, “Big-Bang nucleosynthesis (2006 Particle Data Group mini-review),” [arXiv:astro-ph/0601514 [astro-ph]].

[171] R. H. Cyburt, "Primordial nucleosynthesis for the new cosmology: Determining uncertainties and examining concordance," Phys. Rev. D **70** (2004), 023505 doi:10.1103/PhysRevD.70.023505 [arXiv:astro-ph/0401091 [astro-ph]].

[172] M. Cicoli and A. Mazumdar, "Reheating for Closed String Inflation," JCAP **09** (2010), 025 doi:10.1088/1475-7516/2010/09/025 [arXiv:1005.5076 [hep-th]].

[173] R. Allahverdi, I. Broeckel, M. Cicoli and J. K. Osiński, "Superheavy dark matter from string theory," JHEP **02** (2021), 026 doi:10.1007/JHEP02(2021)026 [arXiv:2010.03573 [hep-ph]].

[174] R. Allahverdi, M. Cicoli, B. Dutta and K. Sinha, "Correlation between Dark Matter and Dark Radiation in String Compactifications," JCAP **10** (2014), 002 doi:10.1088/1475-7516/2014/10/002 [arXiv:1401.4364 [hep-ph]].

[175] S. Angus, "Dark Radiation in Anisotropic LARGE Volume Compactifications," JHEP **10** (2014), 184 doi:10.1007/JHEP10(2014)184 [arXiv:1403.6473 [hep-ph]].

[176] T. Higaki and F. Takahashi, "Dark Radiation and Dark Matter in Large Volume Compactifications," JHEP **11** (2012), 125 doi:10.1007/JHEP11(2012)125 [arXiv:1208.3563 [hep-ph]].

[177] L. Aparicio, D. G. Cerdeno and L. E. Ibanez, "Modulus-dominated SUSY-breaking soft terms in F-theory and their test at LHC," JHEP **07** (2008), 099 doi:10.1088/1126-6708/2008/07/099 [arXiv:0805.2943 [hep-ph]].

[178] R. Blumenhagen, S. Moster and E. Plauschinn, "Moduli Stabilisation versus Chirality for MSSM like Type IIB Orientifolds," JHEP **01** (2008), 058 doi:10.1088/1126-6708/2008/01/058 [arXiv:0711.3389 [hep-th]].

[179] G. D. Coughlan, W. Fischler, E. W. Kolb, S. Raby and G. G. Ross, "Cosmological Problems for the Polonyi Potential," Phys. Lett. B **131** (1983), 59-64 doi:10.1016/0370-2693(83)91091-2

[180] T. Banks, D. B. Kaplan and A. E. Nelson, "Cosmological implications of dynamical supersymmetry breaking," Phys. Rev. D **49** (1994), 779-787 doi:10.1103/PhysRevD.49.779 [arXiv:hep-ph/9308292 [hep-ph]].

[181] M. Demirtas, M. Kim, L. McAllister, J. Moritz and A. Rios-Tascon, "Small cosmological constants in string theory," JHEP **12** (2021), 136 doi:10.1007/JHEP12(2021)136 [arXiv:2107.09064 [hep-th]].

[182] A. Albert *et al.* [Fermi-LAT and DES], “Searching for Dark Matter Annihilation in Recently Discovered Milky Way Satellites with Fermi-LAT,” Astrophys. J. **834** (2017) no.2, 110 doi:10.3847/1538-4357/834/2/110 [arXiv:1611.03184 [astro-ph.HE]].

[183] R. Wiley Deal, K. Sankharva, K. Sinha and S. Watson, “Multi-component Dark Matter and small scale structure formation,” JHEP **02** (2024), 085 doi:10.1007/JHEP02(2024)085 [arXiv:2308.16242 [hep-ph]].

[184] A. Banik and M. Drees, “Non-thermal WIMP production from higher order moduli decay,” JCAP **12** (2023), 032 doi:10.1088/1475-7516/2023/12/032 [arXiv:2308.15380 [hep-ph]].

[185] R. Allahverdi, C. Arina, M. Chianese, M. Cicoli, F. Maltoni, D. Massaro and J. K. Osiński, “Phenomenology of superheavy decaying dark matter from string theory,” JHEP **02** (2024), 192 doi:10.1007/JHEP02(2024)192 [arXiv:2312.00136 [hep-ph]].

[186] R. Allahverdi, N. P. D. Loc and J. K. Osiński, “Dark matter from mediator decay in early matter domination,” Phys. Rev. D **110** (2024) no.2, 023511 doi:10.1103/PhysRevD.110.023511 [arXiv:2402.18557 [hep-ph]].

[187] M. G. Aartsen *et al.* [IceCube-Gen2], “IceCube-Gen2: the window to the extreme Universe,” J. Phys. G **48** (2021) no.6, 060501 doi:10.1088/1361-6471/abbd48 [arXiv:2008.04323 [astro-ph.HE]].

[188] J. A. Aguilar *et al.* [RNO-G], “Design and Sensitivity of the Radio Neutrino Observatory in Greenland (RNO-G),” JINST **16** (2021) no.03, P03025 [erratum: JINST **18** (2023) no.03, E03001] doi:10.1088/1748-0221/16/03/P03025 [arXiv:2010.12279 [astro-ph.IM]].

[189] T. Kobayashi and H. Otsuka, “Classification of discrete modular symmetries in Type IIB flux vacua,” Phys. Rev. D **101** (2020) no.10, 106017 doi:10.1103/PhysRevD.101.106017 [arXiv:2001.07972 [hep-th]].

[190] R. Blumenhagen, “Gauge Coupling Unification in F-Theory Grand Unified Theories,” Phys. Rev. Lett. **102** (2009), 071601 doi:10.1103/PhysRevLett.102.071601 [arXiv:0812.0248 [hep-th]].

[191] G. K. Leontaris and N. D. Tracas, “Gauge coupling flux thresholds, exotic matter and the unification scale in F-SU(5) GUT,” Eur. Phys. J. C **67** (2010), 489-498 doi:10.1140/epjc/s10052-010-1298-2 [arXiv:0912.1557 [hep-ph]].

[192] G. K. Leontaris and Q. Shafi, “Phenomenology with F-theory SU(5),” Phys. Rev. D **96** (2017) no.6, 066023 doi:10.1103/PhysRevD.96.066023 [arXiv:1706.08372 [hep-ph]].

[193] S. Cecotti, M. C. N. Cheng, J. J. Heckman and C. Vafa, “Yukawa Couplings in F-theory and Non-Commutative Geometry,” [arXiv:0910.0477 [hep-th]].

[194] F. Marchesano, D. Regalado and G. Zoccarato, “Yukawa hierarchies at the point of E_8 in F-theory,” JHEP **04** (2015), 179 doi:10.1007/JHEP04(2015)179 [arXiv:1503.02683 [hep-th]].

[195] J. J. Heckman and C. Vafa, “Flavor Hierarchy From F-theory,” Nucl. Phys. B **837** (2010), 137-151 doi:10.1016/j.nuclphysb.2010.05.009 [arXiv:0811.2417 [hep-th]].

[196] J. J. Heckman and C. Vafa, “CP Violation and F-theory GUTs,” Phys. Lett. B **694** (2011), 482-484 doi:10.1016/j.physletb.2010.10.034 [arXiv:0904.3101 [hep-th]].

[197] F. Marchesano and S. Schwieger, “T-branes and α'-corrections,” JHEP **11** (2016), 123 doi:10.1007/JHEP11(2016)123 [arXiv:1609.02799 [hep-th]].

[198] M. Cvetic, L. Lin, M. Liu, H. Y. Zhang and G. Zoccarato, “Yukawa Hierarchies in Global F-theory Models,” JHEP **01** (2020), 037 doi:10.1007/JHEP01(2020)037 [arXiv:1906.10119 [hep-th]].

[199] I. Antoniadis and G. K. Leontaris, “Neutrino mass textures from F-theory,” Eur. Phys. J. C **73** (2013), 2670 doi:10.1140/epjc/s10052-013-2670-9 [arXiv:1308.1581 [hep-th]].

[200] L. E. Ibanez and G. G. Ross, “Discrete gauge symmetries and the origin of baryon and lepton number conservation in supersymmetric versions of the standard model,” Nucl. Phys. B **368** (1992), 3-37 doi:10.1016/0550-3213(92)90195-H

[201] J. Ellis, M. A. G. Garcia, N. Nagata, D. V. Nanopoulos and K. A. Olive, “Proton Decay: Flipped vs Unflipped SU(5),” JHEP **05** (2020), 021 doi:10.1007/JHEP05(2020)021 [arXiv:2003.03285 [hep-ph]].

[202] K. Hamaguchi, S. Hor and N. Nagata, “R-Symmetric Flipped SU(5),” JHEP **11** (2020), 140 doi:10.1007/JHEP11(2020)140 [arXiv:2008.08940 [hep-ph]].

[203] M. Mehmood, M. U. Rehman and Q. Shafi, “Observable proton decay in flipped SU(5),” JHEP **02** (2021), 181 doi:10.1007/JHEP02(2021)181 [arXiv:2010.01665 [hep-ph]].

[204] N. Sakai and T. Yanagida, “Proton Decay in a Class of Supersymmetric Grand Unified Models,” Nucl. Phys. B **197** (1982), 533 doi:10.1016/0550-3213(82)90457-6

[205] J. Jiang, T. Li and D. V. Nanopoulos, “Testable Flipped SU(5) x U(1)(X) Models,” Nucl. Phys. B **772** (2007), 49-66 doi:10.1016/j.nuclphysb.2007.02.025 [arXiv:hep-ph/0610054 [hep-ph]].

[206] K. Abe *et al.* [Super-Kamiokande], "Search for proton decay via $p \to e^+\pi^0$ and $p \to \mu^+\pi^0$ in 0.31 megaton·years exposure of the Super-Kamiokande water Cherenkov detector," Phys. Rev. D **95** (2017) no.1, 012004 doi:10.1103/PhysRevD.95.012004 [arXiv:1610.03597 [hep-ex]].

[207] K. Abe *et al.* [Hyper-Kamiokande], "Hyper-Kamiokande Design Report," [arXiv:1805.04163 [physics.ins-det]].

[208] Y. L. Zhou, "Neutrino masses and flavor mixing in a generalized inverse seesaw model with a universal two-zero texture," Phys. Rev. D **86** (2012), 093011 doi:10.1103/PhysRevD.86.093011 [arXiv:1205.2303 [hep-ph]].

[209] H. Hettmansperger, M. Lindner and W. Rodejohann, "Phenomenological Consequences of sub-leading Terms in See-Saw Formulas," JHEP **04** (2011), 123 doi:10.1007/JHEP04(2011)123 [arXiv:1102.3432 [hep-ph]].

[210] S. L. Glashow, J. Iliopoulos and L. Maiani, "Weak Interactions with Lepton-Hadron Symmetry," Phys. Rev. D **2** (1970), 1285-1292 doi:10.1103/PhysRevD.2.1285

[211] S. T. Petcov, "The Processes $\mu \to e + \gamma, \mu \to e + \overline{e}, \nu' \to \nu + \gamma$ in the Weinberg-Salam Model with Neutrino Mixing," Sov. J. Nucl. Phys. **25** (1977), 340 [erratum: Sov. J. Nucl. Phys. **25** (1977), 698; erratum: Yad. Fiz. **25** (1977), 1336] JINR-E2-10176.

[212] S. Antusch, C. Biggio, E. Fernandez-Martinez, M. B. Gavela and J. Lopez-Pavon, "Unitarity of the Leptonic Mixing Matrix," JHEP **10** (2006), 084 doi:10.1088/1126-6708/2006/10/084 [arXiv:hep-ph/0607020 [hep-ph]].

[213] L. Covi, E. Roulet and F. Vissani, "CP violating decays in leptogenesis scenarios," Phys. Lett. B **384** (1996), 169-174 doi:10.1016/0370-2693(96)00817-9 [arXiv:hep-ph/9605319 [hep-ph]].

[214] S. Davidson and A. Ibarra, "A Lower bound on the right-handed neutrino mass from leptogenesis," Phys. Lett. B **535** (2002), 25-32 doi:10.1016/S0370-2693(02)01735-5 [arXiv:hep-ph/0202239 [hep-ph]].

[215] A. Pilaftsis and T. E. J. Underwood, "Resonant leptogenesis," Nucl. Phys. B **692** (2004), 303-345 doi:10.1016/j.nuclphysb.2004.05.029 [arXiv:hep-ph/0309342 [hep-ph]].

[216] S. K. Kang and C. S. Kim, "Extended double seesaw model for neutrino mass spectrum and low scale leptogenesis," Phys. Lett. B **646** (2007), 248-252 doi:10.1016/j.physletb.2006.12.071 [arXiv:hep-ph/0607072 [hep-ph]].

[217] H. Sung Cheon, S. K. Kang and C. S. Kim, “Low Scale Leptogenesis and Dark Matter Candidates in an Extended Seesaw Model,” JCAP **05** (2008), 004 [erratum: JCAP **03** (2011), E01] doi:10.1088/1475-7516/2008/05/004 [arXiv:0710.2416 [hep-ph]].

[218] J. D. Vergados, H. Ejiri and F. Simkovic, “Theory of Neutrinoless Double Beta Decay,” Rept. Prog. Phys. **75** (2012), 106301 doi:10.1088/0034-4885/75/10/106301 [arXiv:1205.0649 [hep-ph]].

[219] A. Faessler, M. González, S. Kovalenko and F. Šimkovic, “Arbitrary mass Majorana neutrinos in neutrinoless double beta decay,” Phys. Rev. D **90** (2014) no.9, 096010 doi:10.1103/PhysRevD.90.096010 [arXiv:1408.6077 [hep-ph]].

[220] A. Abada, Á. Hernández-Cabezudo and X. Marcano, “Beta and Neutrinoless Double Beta Decays with KeV Sterile Fermions,” JHEP **01** (2019), 041 doi:10.1007/JHEP01(2019)041 [arXiv:1807.01331 [hep-ph]].

[221] F. F. Deppisch, M. Hirsch and H. Pas, “Neutrinoless Double Beta Decay and Physics Beyond the Standard Model,” J. Phys. G **39** (2012), 124007 doi:10.1088/0954-3899/39/12/124007 [arXiv:1208.0727 [hep-ph]].

[222] S. Dell’Oro, S. Marcocci, M. Viel and F. Vissani, “Neutrinoless double beta decay: 2015 review,” Adv. High Energy Phys. **2016** (2016), 2162659 doi:10.1155/2016/2162659 [arXiv:1601.07512 [hep-ph]].

[223] M. Blennow, E. Fernandez-Martinez, J. Lopez-Pavon and J. Menendez, “Neutrinoless double beta decay in seesaw models,” JHEP **07** (2010), 096 doi:10.1007/JHEP07(2010)096 [arXiv:1005.3240 [hep-ph]].

[224] C. Hagedorn, J. Kriewald, J. Orloff and A. M. Teixeira, “Flavour and CP symmetries in the inverse seesaw,” Eur. Phys. J. C **82** (2022) no.3, 194 doi:10.1140/epjc/s10052-022-10097-3 [arXiv:2107.07537 [hep-ph]].

[225] P. D. Bolton, F. F. Deppisch and P. S. Bhupal Dev, “Neutrinoless double beta decay versus other probes of heavy sterile neutrinos,” JHEP **03** (2020), 170 doi:10.1007/JHEP03(2020)170 [arXiv:1912.03058 [hep-ph]].

[226] F. F. Deppisch, P. S. Bhupal Dev and A. Pilaftsis, “Neutrinos and Collider Physics,” New J. Phys. **17** (2015) no.7, 075019 doi:10.1088/1367-2630/17/7/075019 [arXiv:1502.06541 [hep-ph]].

[227] M. Mitra, G. Senjanovic and F. Vissani, “Neutrinoless Double Beta Decay and Heavy Sterile Neutrinos,” Nucl. Phys. B **856** (2012), 26-73 doi:10.1016/j.nuclphysb.2011.10.035 [arXiv:1108.0004 [hep-ph]].

[228] T. Li, J. A. Maxin and D. V. Nanopoulos, “Spinning no-scale $\mathcal{F}$-SU(5) in the right direction,” Eur. Phys. J. C **81** (2021) no.12, 1059 doi:10.1140/epjc/s10052-021-09835-w [arXiv:2107.12843 [hep-ph]].

[229] J. Ellis, J. L. Evans, N. Nagata, D. V. Nanopoulos and K. A. Olive, “Flipped SU(5) GUT phenomenology: proton decay and $\mathbf{g_\mu - 2}$,” Eur. Phys. J. C **81** (2021) no.12, 1109 doi:10.1140/epjc/s10052-021-09896-x [arXiv:2110.06833 [hep-ph]].

[230] T. Aaltonen *et al.* [CDF], “High-precision measurement of the W boson mass with the CDF II detector,” Science **376** (2022) no.6589, 170-176 doi:10.1126/science.abk1781

[231] S. Heinemeyer, W. Hollik and G. Weiglein, “Electroweak precision observables in the minimal supersymmetric standard model,” Phys. Rept. **425** (2006), 265-368 doi:10.1016/j.physrep.2005.12.002 [arXiv:hep-ph/0412214 [hep-ph]].

[232] K. Sakurai, F. Takahashi and W. Yin, “Singlet extensions and W boson mass in light of the CDF II result,” Phys. Lett. B **833** (2022), 137324 doi:10.1016/j.physletb.2022.137324 [arXiv:2204.04770 [hep-ph]].

[233] D. López-Val and T. Robens, “Δr and the W-boson mass in the singlet extension of the standard model,” Phys. Rev. D **90** (2014), 114018 doi:10.1103/PhysRevD.90.114018 [arXiv:1406.1043 [hep-ph]].

[234] E. Fernandez-Martinez, J. Hernandez-Garcia and J. Lopez-Pavon, “Global constraints on heavy neutrino mixing,” JHEP **08** (2016), 033 doi:10.1007/JHEP08(2016)033 [arXiv:1605.08774 [hep-ph]].

[235] M. Blennow, P. Coloma, E. Fernández-Martínez and M. González-López, “Right-handed neutrinos and the CDF II anomaly,” Phys. Rev. D **106** (2022) no.7, 073005 doi:10.1103/PhysRevD.106.073005 [arXiv:2204.04559 [hep-ph]].

[236] E. Bagnaschi, J. Ellis, M. Madigan, K. Mimasu, V. Sanz and T. You, “SMEFT analysis of m_W,” JHEP **08** (2022), 308 doi:10.1007/JHEP08(2022)308 [arXiv:2204.05260 [hep-ph]].

[237] M. Endo and S. Mishima, “New physics interpretation of W-boson mass anomaly,” Phys. Rev. D **106** (2022) no.11, 115005 doi:10.1103/PhysRevD.106.115005 [arXiv:2204.05965 [hep-ph]].

[238] A. M. Coutinho, A. Crivellin and C. A. Manzari, "Global Fit to Modified Neutrino Couplings and the Cabibbo-Angle Anomaly," Phys. Rev. Lett. **125** (2020) no.7, 071802 doi:10.1103/PhysRevLett.125.071802 [arXiv:1912.08823 [hep-ph]].

[239] A. Ghoshal, N. Okada, S. Okada, D. Raut, Q. Shafi and A. Thapa, "Type III seesaw with R-parity violation in light of mW (CDF)," Nucl. Phys. B **989** (2023), 116099 doi:10.1016/j.nuclphysb.2023.116099 [arXiv:2204.07138 [hep-ph]].

[240] J. J. Heckman, "Extra W-boson mass from a D3-brane," Phys. Lett. B **833** (2022), 137387 doi:10.1016/j.physletb.2022.137387 [arXiv:2204.05302 [hep-ph]].

[241] M. Ciuchini, E. Franco, S. Mishima and L. Silvestrini, "Electroweak Precision Observables, New Physics and the Nature of a 126 GeV Higgs Boson," JHEP **08** (2013), 106 doi:10.1007/JHEP08(2013)106 [arXiv:1306.4644 [hep-ph]].

[242] C. T. Lu, L. Wu, Y. Wu and B. Zhu, "Electroweak precision fit and new physics in light of the W boson mass," Phys. Rev. D **106** (2022) no.3, 035034 doi:10.1103/PhysRevD.106.035034 [arXiv:2204.03796 [hep-ph]].

[243] J. R. Ellis, J. S. Hagelin, S. Kelley and D. V. Nanopoulos, "Aspects of the Flipped Unification of Strong, Weak and Electromagnetic Interactions," Nucl. Phys. B **311** (1988), 1-34 doi:10.1016/0550-3213(88)90141-1

[244] G. K. Leontaris, "Gauge coupling unification in the SU(5) x U(1) string model," Phys. Lett. B **281** (1992), 54-58 doi:10.1016/0370-2693(92)90274-8

[245] F. Staub, "SARAH 4 : A tool for (not only SUSY) model builders," Comput. Phys. Commun. **185** (2014), 1773-1790 doi:10.1016/j.cpc.2014.02.018 [arXiv:1309.7223 [hep-ph]].

[246] J. H. Schwarz, "An SL(2,Z) multiplet of type IIB superstrings," Phys. Lett. B **360** (1995), 13-18 [erratum: Phys. Lett. B **364** (1995), 252] doi:10.1016/0370-2693(95)01405-5 [arXiv:hep-th/9508143 [hep-th]].

[247] A. Hebecker, P. Henkenjohann and L. T. Witkowski, "Flat Monodromies and a Moduli Space Size Conjecture," JHEP **12** (2017), 033 doi:10.1007/JHEP12(2017)033 [arXiv:1708.06761 [hep-th]].

[248] A. Font, L. E. Ibanez, D. Lust and F. Quevedo, "Strong - weak coupling duality and non-perturbative effects in string theory," Phys. Lett. B **249** (1990), 35-43 doi:10.1016/0370-2693(90)90523-9

[249] C. Vafa and E. Witten, "A Strong coupling test of S duality," Nucl. Phys. B **431** (1994), 3-77 doi:10.1016/0550-3213(94)90097-3 [arXiv:hep-th/9408074 [hep-th]].

[250] M. Dierigl and J. J. Heckman, "Swampland cobordism conjecture and non-Abelian duality groups," Phys. Rev. D **103** (2021) no.6, 066006 doi:10.1103/PhysRevD.103.066006 [arXiv:2012.00013 [hep-th]].

[251] C. Beasley, J. J. Heckman and C. Vafa, "GUTs and Exceptional Branes in F-theory - I," JHEP **01** (2009), 058 doi:10.1088/1126-6708/2009/01/058 [arXiv:0802.3391 [hep-th]].

[252] A. Font, "Yukawa couplings in string theory: the case for F-theory GUT's," J. Phys. Conf. Ser. **651** (2015) no.1, 012009 doi:10.1088/1742-6596/651/1/012009

[253] C. Beasley, J. J. Heckman and C. Vafa, "GUTs and Exceptional Branes in F-theory - II: Experimental Predictions," JHEP **01** (2009), 059 doi:10.1088/1126-6708/2009/01/059 [arXiv:0806.0102 [hep-th]].

[254] J. C. Callaghan, S. F. King, G. K. Leontaris and G. G. Ross, "Towards a Realistic F-theory GUT," JHEP **04** (2012), 094 doi:10.1007/JHEP04(2012)094 [arXiv:1109.1399 [hep-ph]].

[255] H. Georgi and C. Jarlskog, "A New Lepton - Quark Mass Relation in a Unified Theory," Phys. Lett. B **86** (1979), 297-300 doi:10.1016/0370-2693(79)90842-6

[256] V. Bouchard, J. J. Heckman, J. Seo and C. Vafa, "F-theory and Neutrinos: Kaluza-Klein Dilution of Flavor Hierarchy," JHEP **01** (2010), 061 doi:10.1007/JHEP01(2010)061 [arXiv:0904.1419 [hep-ph]].

[257] I. Esteban, M. C. Gonzalez-Garcia, M. Maltoni, T. Schwetz and A. Zhou, "The fate of hints: updated global analysis of three-flavor neutrino oscillations," JHEP **09** (2020), 178 doi:10.1007/JHEP09(2020)178 [arXiv:2007.14792 [hep-ph]].

[258] S. Antusch and V. Maurer, "Running quark and lepton parameters at various scales," JHEP **11** (2013), 115 doi:10.1007/JHEP11(2013)115 [arXiv:1306.6879 [hep-ph]].

[259] F. Björkeroth, F. J. de Anda, I. de Medeiros Varzielas and S. F. King, "Towards a complete $A_4\times$ SU(5) SUSY GUT," JHEP **06** (2015), 141 doi:10.1007/JHEP06(2015)141 [arXiv:1503.03306 [hep-ph]].

[260] H. Okada and M. Tanimoto, "Quark and lepton flavors with common modulus τ in A4 modular symmetry," Phys. Dark Univ. **40** (2023), 101204 doi:10.1016/j.dark.2023.101204 [arXiv:2005.00775 [hep-ph]].

[261] F. A. de Souza, M. Crispim Romão, N. F. Castro, M. Nikjoo and W. Porod, "Exploring parameter spaces with artificial intelligence and machine learning black-box optimization algorithms," Phys. Rev. D **107** (2023) no.3, 035004 doi:10.1103/PhysRevD.107.035004 [arXiv:2206.09223 [hep-ph]].

[262] J. C. Romão and M. Crispim Romão, "Combining evolutionary strategies and novelty detection to go beyond the alignment limit of the Z3 3HDM," Phys. Rev. D **109** (2024) no.9, 095040 doi:10.1103/PhysRevD.109.095040 [arXiv:2402.07661 [hep-ph]].

[263] cmaes : A Simple yet Practical Python Library for CMA-ES, M. Nomura, M. Shibata e-Print: 2402.01373